BIOGEOCHEMISTRY OF PARTICULATE ORGANIC MATTER ACROSS THE FRONTS IN THE INDIAN SECTOR OF THE SOUTHERN OCEAN

Thesis Submitted to the Goa University for the Degree of

DOCTOR OF PHILOSOPHY

In

MARINE SCIENCES

By

MELENA A. SOARES

(National Centre for Polar and Ocean Research)

School of Earth, Ocean and Atmospheric Sciences

GOA UNIVERSITY

MAY, 2021

STATEMENT OF THE CANDIDATE

I hereby state that the present thesis entitled "**Biogeochemistry of Particulate Organic Matter across the Fronts in the Indian Sector of Southern Ocean**" is my original contribution and the same has not been submitted on any other previous occasion, as required under the University ordinance OA-19.8 (v).

To the best of my knowledge, the present study is the first comprehensive work of its kind from the area mentioned. The literature related to the problem investigated has been cited and due acknowledgements have been made wherever facilities and suggestions have been availed.

MELENA A. SOARES

CERTIFICATE

This is to certify that the thesis entitled, "**Biogeochemistry of Particulate Organic Matter across the Fronts in the Indian Sector of Southern Ocean**", submitted by **Melena A. Soares** for the award of the Degree of Doctor of Philosophy in Marine Sciences (School of Earth, Ocean and Atmospheric Studies) is based on original studies carried out by her under my supervision. The thesis or any part thereof has not been previously submitted for any other degree, diploma, or any other fellowships, in any Universities or Institutions. This thesis represents independent work carried out by the student.

Dr. N. ANILKUMAR
Research Guide
Scientist F
National Centre for Polar and Ocean Research
Headland Sada,Vasco-da-Gama, Goa.

Dedicated

To

My Parents and Siblings

TABLE OF CONTENT

Acknowledgement **vi**

List of Tables **ix**

List of Figures **xii**

Abbreviations **xix**

CHAPTER-1

1. Introduction **1-15**

1.1 Ocean Carbon Cycle 1

1.2 Biological pump 3

1.3 Particulate Organic Matter (POM) 5

1.3.1 Composition of POM 5

1.3.2 Factors influencing the POM composition and transformation in Oceans 6

1.4 Importance of POM studies 8

1.4.1 Stable isotopes as a proxy for POM studies 9

1.5 Importance of studies in the Southern Ocean 9

1.6 Literature Review 11

1.6.1 POM studies in the Southern Ocean (SO) 11

1.6.2 Previous Studies in the Indian sector of the Southern Ocean (ISSO) 13

1.7 Objectives of the study 15

CHAPTER-2

2. Study Area and Methodology **16-28**

2.1 Study Area: Geographical Location and Hydrography 16

2.1.1 Southern Ocean 16

2.1.1.1 Indian sector of the Southern Ocean (ISSO) 17

2.1.2 Hydrography and biochemical characteristics of different Fronts 18

2.1.2.1 Mesoscale Eddies 19

2.2 Methods and Materials 19

2.2.1 Sampling Strategy 19

2.2.2 Sample Analysis 21

2.2.2.1 Hydrographic Data 22

2.2.2.2 Dissolved Oxygen (DO) 23

2.2.2.3 Total Carbon dioxide (tCO_2) 24

2.2.2.4 Nutrients 24

2.2.2.5 Particulate organic Carbon and Nitrogen (POC & PN) and stable isotopes of carbon and nitrogen ($\delta^{15}N$ and $\delta^{13}C$) in POM samples 25

2.2.2.6 Chlorophyll-a and Phytoplankton marker pigments 26

2.2.2.7 Zooplankton Abundance 26

2.2.3 Computation of Physical and Biochemical Variables 27

2.2.3.1 Euphotic Depth 27

2.2.3.2 Mixed Layer Depth 27

2.2.3.3 Apparent Oxygen Utilisation 27

2.2.3.4 Proxies for POM studies 27

2.2.4 Remote Sensing Data 28

2.2.5 Statistical Analysis 28

CHAPTER-3

3. Spatial distribution of Particulate organic matter and the factors controlling the POM characteristics in the surface waters **29-65**

3.1 Introduction 29

3.2 Results 31

3.2.1 Hydrography 31

3.2.2 tCO_2, Nutrients and Chl-a 35

3.2.3 Characteristics of POM 38

3.2.4 Statistical Analysis 41

3.3 Discussion

3.3.1 Spatial distribution of particulate organic carbon and nitrogen and the stable isotopic characteristics of carbon and nitrogen in the surface waters of the oceanic regimes of the Indian sector 49

3.3.1.1 Indian sector of the Southern Ocean 51

3.3.1.2 Tropical Indian Ocean 54

3.3.2 Factors controlling the stable isotopic composition of carbon and Nitrogen of POM in the surface waters across the fronts in the ISSO 59

3.3.2.1 Sea Surface Temperature (SST) 59

3.3.2.2 Total Carbon di oxide (tCO_2) concentration 60

3.3.2.3 Nutrient availability 61

3.3.2.4 Phytoplankton community 62

3.4 Salient Findings 64

CHAPTER-4

4. Influence of eddies on the variability of POM characteristics in the Subtropical Front of the ISSO **66-101**

4.1 Introduction 66

4.2 Results 68

4.2.1 Cyclonic Eddies 71

4.2.1.1 Hydrography and chemical variables 71

4.2.1.2 Chl-a and phytoplankton community 75

4.2.1.3 Characteristics of POM 76

4.2.2 Anticyclonic Eddies 79

4.2.2.1 Hydrography and chemical variables 79

4.2.2.2 Chl-a and phytoplankton community 80

4.2.2.3 Characteristics of POM 81

4.2.3 Statistical analysis 82

4.2.3.1 Cyclonic eddies 83

4.2.3.2 Anticyclonic eddies 86

4.3 Discussion

4.3.1 Eddy Characteristics and properties 89

4.3.2 Biochemical processes controlling POM characteristics at Cyclonic eddies 91

4.3.3 Biochemical processes controlling the POM characteristics at Anticyclonic eddies 96

4.4 Salient Findings 100

CHAPTER-5

5. Dynamics of POM in the upper water column across the fronts in the Indian sector of the Southern Ocean **102-145**

5.1 Introduction 102

5.2 Results 103

5.2.1 Hydrography and nutrients 103

5.2.2 Quality of POM 110

5.2.3 Chl-a and Phytoplankton community 114

5.3 Discussion

5.3.1 Upper water column variability of POM characteristics and the trophic dynamics across the fronts of the ISSO 115

5.3.1.1 POM biogeochemistry in the STFZ 115

5.3.1.2 POM biogeochemistry in the SAFZ 118

5.3.1.3 POM biogeochemistry in the PFZ 119

5.3.2 Factors influencing the distribution and transformation of POM characteristics in the upper water column of the ISSO 122

5.3.2.1 Role of nutrients 122

5.3.2.2 Influence of biological Processes 123

5.3.2.2.a Phytoplankton biomass, community and DCM 123

5.3.2.2.b Zooplankton abundance and community composition 125

5.3.2.2.c Heterotrophic activity 128

5.3.2.3 Influence of hydrographic factors on POM cycling 129

5.3.2.3.a Eddies 130
5.3.2.3.b MLD 130

5.3.3 Fate and cycling of POM across the fronts of the ISSO 132
5.3.3.1 Export fluxes of Particulate Organic Carbon (POC) 132
5.3.3.2 Remineralisation of POM within the upper water column 134

5.3.4 Inter-annual variability of POM characteristics and its fate in the ISSO 137
5.3.4.1 Temperature 137
5.3.4.2 Sea surface freshening and sea-ice 138
5.3.4.3 Influence of wind and MLD 139
5.3.4.4 Micro and macro nutrients 140
5.3.4.5 Phytoplankton community 142

5.4 Salient Findings 144

CHAPTER 6

6. Summary and Future Prospective **146-150**

7. References 151

List of Publications 190

Acknowledgement

I would like to express my heartfelt gratitude to all those who contributed and supported me through the journey of the PhD.

Firstly, I would like to extend my sincere thanks to my research guide Dr. N. Anilkumar (NCPOR) for his patience, motivation and continuous support during the work of my Phd and more importantly for believing in me as I progress through my PhD work.

I have been extremely fortunate to have Prof. G. N. Nayak (Goa University) and Dr. Aninda Mazumdar (National Institute of Oceanography) Department Research Committee members, and would like to acknowledge and thank them for their encouragement and support during my PhD. Also their thought provoking questions and insightful discussions helped me improve my research work at every step.

I am extremely thankful to Dr. S. Rajan (former Director) and Dr. M. Ravichandran (present Director), National Centre for Polar and Ocean Research (NCPOR), for providing me the facilities and support required for my thesis work.

I am grateful to Dr. Manish Tiwari for permitting me to complete my isotopic and elemental analysis at the

MASTIL laboratory (NCPOR), and am thankfuk to Mr. Siddesh Nagoaji for assisting me during the EA-IRMS analysis. I also express my heartfelt gratitude to Dr. V. Venkataramana, Dr. R. K. Naik for their help and support and also Dr. AshaDevi for their help in the generation of data for biological community. I would also like to express my thanks to Dr. Racheal Chacko, Dr. P. Sabu, for their continuous support. I would also like to acknowledge Dr. Jenson V. George, Dr. R.K. Mishra, Dr. P.V. Bhaskar, and Dr. S.C. Tripathy for their support during the various southern Ocean Expeditions.

I would also like to express my appreciation and thanks to all my friends... a few named above and some not mentioned here for their patience, motivation and continuous support during the tough times and the entire period of my PhD.

Most importantly, none of this would have been possible without the love and patience of my family. I would like to express my heartfelt gratitude to my parents, my brother and sister for their never-ending support and motivation that kept me going every time I strike a new hurdle in the journey of my PhD. I cannot thank them enough to stand by me firm and strong, giving the required push and positivity in my days of stress and hardships.

Above all I thank almighty God for granting health, strength and wisdom, to undertake and complete this research work successfully.

Melena A. Soares

List of Tables

Table 2.1: Frontal demarcation in the ISSO based on the criterion given in Anilkumar et al. (2006 & 2014).

Table 3.1: Average values of temperature, salinity, *t*CO_2, NO_3, NH_3, N:P, N:Si (N= NO_3+NO_2+NH_3), POC, PN, C:N, $\delta^{13}C_{(POM)}$ and $\delta^{15}N_{(POM)}$ POC:Chl *a* and dominating phytoplankton community (% abundance) in surface samples along the cruise transect, during austral summer 2012. Range is in parentheses.

Table 3.2: Average values of temperature, salinity, tCO_2, NO_3, NH_3, N:P, N:Si (N= NO_3+NO_2+NH_3), POC, PN, C:N, $\delta^{13}C_{(POM)}$ and $\delta^{15}N_{(POM)}$ POC:Chl *a* and dominating phytoplankton community (% abundance) in surface samples along the cruise transect, during austral summer 2013. Range is in parentheses.

Table 3.3: Pearson's correlation matrix for SO region during austral summer 2012. All values in bold imply significant correlation between the variables (significance level of alpha=0.05).

Table 3.4: Pearson's correlation matrix for SO region during austral summer 2013. All values in bold imply significant correlation between the variables (significance level of alpha=0.05).

Table 3.5: Pearson's correlation matrix for TIO region during austral summer 2012. All values in bold imply significant correlation between the variables (significance level of alpha=0.05).

Table 3.6: Pearson's correlation matrix for TIO region during austral summer 2013. All values in bold imply significant correlation between the variables (significance level of alpha=0.05).

Table 3.7: Correlations between variables and factors after Varimax rotation: Factor loading for ISSO region, during austral summer.

Table 3.8: Correlations between variables and factors after Varimax rotation: Factor loading for TIO region, during this study.

Table 4.1: The sampling locations of eddies along with the eddy type, date of origin, front of origin, approximate age of the eddy and the Mixed Layered Depth (MLD), surface PAR and the Deep Chlorophyll Maxima (DCM) at the locations during 2012 and 2013 austral summer.

Table 4.2: Range and column average (in parentheses) of temperature (temp), salinity, DO, tCO_2, NO_3, NO_2, NH_3, PO_4, SiO_4, N:P, N:Si (N= NO_3+NO_2+NH_3), POC, PN, C:N(m/m), $\delta^{13}C_{(POM)}$, $\delta^{15}N_{(POM)}$ and POC/Chl-*a* at the eddy locations during austral summer 2012 and 2013.

Table 4.3: Pearson's correlation matrix for bio-chemical variables at Cyclonic eddy (CE) locations during 2012 and 2013. All values in bold imply significant correlation between the variables (significance level alpha=0.05).

Table 4.4: Principle factor Analysis for bio-chemical variables at Cyclonic eddy (CE) locations during 2012 and 2013.

Table 4.5: Pearson's correlation matrix for bio-chemical variables at Anticyclonic eddy (ACE) locations during 2012 and 2013. All values in bold imply significant correlation between the variables (significance level alpha=0.05).

Table 4.6: Principle factor Analysis for bio-chemical variables at Anticyclonic eddy (ACE) locations during 2012 and 2013.

Table 5.1: The range and average (in parenthesis is the column average) of temperature, salinity, DO, NO_3, PO_4, SiO_4, NH_3, N:P, N:Si, Chl-*a*, POC, PN, $\delta^{13}C_{(POM),}$ $\delta^{15}N_{(POM)}$, C:N (M/M), POC:Chl-*a*, and AOU within the upper water column at the different fronts during austral summer 2012.

Table 5.2: The range and average (in parenthesis is the column average) of temperature, salinity, DO, NO_3, PO_4, SiO_4, NH_3, N:P, N:Si, Chl-*a*, POC, PN, $\delta^{13}C_{(POM),}$ $\delta^{15}N_{(POM)}$, C:N (M/M), POC:Chl-a, and AOU within the upper water column at the different fronts during austral summer 2013.

Table 5.3: The Euphotic Depth (ED), Mixed Layer Depth (MLD), and the depth of the Deep Chlorophyll Maxima (DCM), identified at the different locations across the fronts during the two consecutive austral summer studies in the ISSO.

List of Figures

Figure 1.1: Ocean carbon cycle, representation of the biological and physical (solubility) pump in the ocean (Adapted and modified; from Bopp et al., 2002).

Figure 1.2: Schematic depiction of the carbon cycling via the biological pump in the ocean. The linkage of Microbial Loop and Microbial Carbon Pump (MCP) in the Biological Carbon Pump (BCP) and the time scale representing the return of respired CO_2 to the surface, from the different depths of the ocean (adapted from Zhang et al., 2018).

Figure 2.1: Illustrates the study area, with the frontal structure encompassing the Antarctic continent, also demarcating the zones and the surrounding continents (figure plotted using Quantarctica).

Figure 2.2: Study area map with station locations overlaid on the sea surface temperature (monthly average SST, derived from MODIS aqua); black circles with white border are sampling locations during austral summer: (a) 2012 and (b) 2013.

Figure 2.3: Schematic representation of the sample processing and analytical techniques used for this study.

Figure 3.1: Latitudinal variation of (a)Temperature, (b) Salinity and (c) tCO_2 in the surface waters, of the TIO and across the fronts of the ISSO during austral summer 2012 (**Blue**) and austral summer 2013(**Red**).

Figure 3.2: Latitudinal variation of (a) Nitrate, (b) Phosphate and (c) Silicate in the surface waters, of the TIO and across the fronts of the ISSO during austral summer 2012 (**Blue**) and austral summer 2013(**Red**).

Figure 3.3: Latitudinal variation of (a) Chlorophyll-*a (*Chl-*a)*, (b)POC and (c) PN in the surface waters, of the TIO and across the fronts of the ISSO during austral summer 2012 (**Blue**) and austral summer 2013(**Red**).

Figure 3.4: Latitudinal variation of (a) $\delta^{13}C_{(POM)}$, (b) $\delta^{15}N_{(POM)}$ and (c) C:N (M/M) in the surface waters, of the TIO and across the fronts of the ISSO during austral summer 2012 (**Blue**) and austral summer 2013 (**Red**).

Figure 3.5: PCA analysis illustrating separate clusters for TIO, and ISSO, based on the governing factors across the two oceanic regimes, during the study.

Figure 3.6: A comparative analysis of the range of POC (µg/L) concentration, in different regions especially, high latitude waters and the current study.

Figure 3.7: Variation of the dominant phytoplankton community across the fronts in the ISSO during austral summer (a) 2012 and (b) 2013.

Figure 3.8: Spearman's correlation of POC with PN (a) ISSO, (b) TIO; and $\delta^{13}C_{(POM)}$ with $\delta^{15}N_{(POM)}$, (c) ISSO, (d)TIO during austral summer 2012 and 2013

Figure 3.9: Spearman's correlation of (a) $\delta^{13}C_{(POM)}$ and POC; (b)$\delta^{15}N_{(POM)}$ and PN in the TIO surface waters during 2012 and 2013.

Figure 3.10: Spearman's correlation of (a) Temperature with $\delta^{13}C_{(POM)}$; (b) temperature with tCO_2 and (c)$\delta^{13}C_{(POM)}$ with tCO_2 across the fronts in the ISSO during austral summer 2012 and 2013.

Figure 3.11: Spearman's correlation of (a) $\delta^{13}C_{(POM)}$ and Nitrate, (b)$\delta^{15}N_{(POM)}$ and Nitrate across the fronts in the ISSO during austral summer 2012 and 2013.

Figure 4.1: Sea Surface Temperature (SST) variability from the AVHRR data (a) ACE1, (b) CE1, (c) ACE2, (d) CE2, (e) ACE3 and (f) CE3 during the observation period.

Figure 4.2: Vertical distribution of temperature during (a) 2012 and (b) 2013; salinity during (c) 2012 and (d) 2013.

Figure 4.3: T-S diagram showing various water masses at the eddy locations during the study.

Figure 4.4: Vertical distribution of (a) DO, (b) Nitrate, (c) Silicate and (d) Phosphate at the Cyclonic eddies (**Blue**) and anticyclonic eddies (**Red**), during the study.

Figure 4.5: Vertical distribution of Chlorophyll a (Chl-*a*) at cyclonic eddies (CE) and anticyclonic eddies (ACE) during (a) 2012 and (b) 2013.

Figure 4.6: Dominant phytoplankton community at the surface (0 m), DCM and 120 m at the cyclonic (CE1, CE2, CE3) and anticyclonic (ACE1, ACE2, ACE3) eddies observed during this study.

Figure 4.7: POM variability (a) POC, (b) PN, (c) C:N, (d) $\delta^{13}C_{(POM)}$, (e) $\delta^{15}N_{(POM)}$ and (f) POC/Chl-*a* at the cyclonic (CE) and anticyclonic (ACE) eddies during this study.

Figure 4.8: Vertical distribution of POM characteristics in the upper 120 m water column: (a) POC, (b) PN, (c) $\delta^{13}C_{(POM)}$, (d) $\delta^{15}N_{(POM)}$, at the CEs and ACEs.

Figure. 4.9: Hierarchical cluster analysis of the eddy waters (at Surface, DCM and 120m), calculated from water physico-chemical variables and POM isotopic characteristics $\delta^{13}C_{(POM)}$ and $\delta^{15}N_{(POM)}$.

Figure 4.10: OSCAR (5-day average) surface currents variability in the study region during (a)2012 and (b)2013 during the study period.

Figure 4.11: Sea Surface Height (SSH) variability and the trajectory of eddies (a) ACE1, (b) CE1, (c) ACE2, (d) CE2, (e) ACE3 and (f) CE3.

Figure 4.12: Spearmen's correlation of (a) $\delta^{13}C_{(POM)}$ and ammonium, (b) $\delta^{15}N_{(POM)}$ and ammonium at CE1.

Figure 4.13: Weekly (6th to 13th January 2012) mean surface chlorophyll imagery derived from MODIS Aqua.

Figure 4.14: Spearmen's correlation of (a) $\delta^{15}N_{(POM)}$ with nitrate, (b) $\delta^{15}N_{(POM)}$ with chlorophyll and (c) Nitrate with chlorophyll at ACE3.

Figure 5.1: The variability of Temperature (a, b); Salinity (c, d) and the concentration of dissolved oxygen (DO) (e, f) in the upper 120 m water- column, across the different fronts of the ISSO during austral summer 2012 and 2013.

Figure 5.2: The variability in the concentration of nitrate (a, b); Silicate (c, d) and phosphates (e, f) in the upper 120 m water-column, across the different fronts of the ISSO during austral summer 2012 and 2013.

Figure 5.3: The variability in the concentration of POC and PN in the upper 120 m water-column, across the different fronts of the ISSO during austral summer 2012 (a, c) and 2013 (b, d).

Figure 5.4: The upper (120 m) water-column variability of $\delta^{13}C_{(POM)}$ and the the $\delta^{15}N_{(POM)}$ across the different fronts of the ISSO during austral summer 2012 (a, c) and 2013 (b, d).

Figure 5.5: The variation in the C:N ratio and the POC:Chl-*a* ratios in the upper water-column (120m), across the different fronts of the ISSO during austral summer 2012 (a, c) and 2013 (b, d).

Figure 5.6: The distribution Chlorophyll-*a* (Chl-*a)* in the upper 120 m water-column across the different fronts of the ISSO during austral summer 2012 (a) and 2013 (b).

Figure 5.7: The distribution of percentage abundance of the dominant communities of phytoplankton, in the upper water column (120m), at the different frontal regions of the ISSO during austral summer 2012 (a, b, c) and 2013 (d, e, f).

Figure 5.8: Spearman's correlation of (a) depth of Deep Chlorophyll maxima (DCM) and Mixed Layer Depth (MLD); (b) Column Integrated (IC) Chl-*a* upto the DCM and the depth of DCM; (c) Column Integrated (IC) Chl-*a* upto the MLD and depth of MLD

Figure 5.9: The distribution of percentage abundance of the dominant groups of zooplankton, in the upper mixed layer (ML) and below mixed layer (BML) at the different frontal regions of the ISSO during austral summer 2012 (a) and 2013 (b).

Figure 5.10: The variation in the Zooplankton biomass at the three frontal regions of the ISSO during austral summer 2012 (a), and 2013 (b).

Figure 5.11: Spearman's correlation of AOU with POC (a); AOU with $\delta^{13}C_{(POM)}$ (b) and POC with $\delta^{13}C_{(POM)}$ (c) , at the STFZ during austral summer 2012.

Figure 5.12: Particulate organic carbon (POC) flux out of the euphotic depth (green) and out of 120m (red), at the frontal regions of the ISSO, during austral summer 2012(a) and 2013 (b).

Figure 5.13: Variation of regenerated phosphate (P) and regenerated nitrogen (N), above the euphotic depth (0-PD) and below the Euphotic depth (PD-120m), at the frontal regions of the ISSO during austral summer 2012 (a, c) and 2013 (b, d).

Figure 5.14: Spatial variability of Sea Surface Temperature (SST) across the fronts of the ISSO during January 2012(a) and 2013 (b).

Figure 5.15: Variability of sea ice cover in the ISSO, during January 2012 (a) and 2013 (b).

Figure 5.16: Variability of Sea Surface Salinity (SSS) across the fronts of the ISSO, during January 2012(a) and 2013(b).

Figure 5.17: Variability of the Mixed layer depth (a & b) and Wind speed (c & d) across the fronts of the ISSO, during January 2012 and 2013.

Figure 5.18: Spatial distribution of dissolved Iron, in the study region of the ISSO for the period of Jan-Feb in 2012(a) and 2013(b), (re-analysis data derived from NOBM).

Figure 5.19: Spatial distribution of different phytoplankton communities, across the fronts of the ISSO for the period of Jan-Feb in 2012(a) and 2013(b), (re-analysis data derived from NOBM).

Figure 5.20: Spatial distribution of Chl-*a* in the study region of the ISSO, for the period of Jan-Feb 2012 (a) and 2013 (b), (re-analysis data derived from NOBM).

Figure 5.21: Spatial distribution of POC in the study region of the ISSO, for the period of January 2012 (a) and 2013 (b), (re-analysis data derived from MODIS).

Abbreviations

$\delta^{13}C_{(POM)}$	Stable isotopic ratio of Carbon
$\delta^{15}N_{(POM)}$	Stable isotopic ratio of Nitrogen
AAIW	Antarctic Intermediate Waters
AASW	Antarctic Surface Waters
ACC	Antarctic Circumpolar Current
ACE	Anticyclonic Eddy
AOU	Apparent Oxygen Utilisation
ARC	Agulhas Return Current
ARF	Agulhas Return Front
C:N	Carbon to Nitrogen ratio
$CaCO_3$	Calcium Carbonate
CE	Cyclonic Eddy
Chl-*a*	Chlorophyll a
CO_2	Carbon di oxide
COM	Colloidal Organic Matter
DCM	Deep Chlorophyll Maxima
DIC	Dissolved inorganic carbon
DO	Dissolved Oxygen
DOC	Dissolved Organic Carbon
DOM	Dissolved organic matter
HNLC	High Nutrient Low Chlorophyll
ISSO	Indian sector of the Southern Ocean
Kd	Downwelling irradiance

LC	Leeuwin Current
MLD	Mixed Layer Depth
N:P	dissolved inorganic nitrogen to phosphate ratio
PAR	Photosynthetically active radiation
PCA	Principle Component Analysis
PEPC	Phosphoenolpyruvate Carboxylase
PEPCK	Phosphoenolpyruvate Carboxykinase
PF	Polar Front
PF-I	Polar Front-I
PF-II	Polar Front -II
PFZ	Polar Frontal Zone
PIC	Particulate inorganic carbon
POC	Particulate organic carbon
POM	Particulate organic matter
SAF	SubAntarctic Front
SAFZ	SubAntarctic Frontal Zone
SB	Southern Boundary
SO	Southern Ocean
SOE-06	Southern Ocean Expedition six (2012)
SOE-07	Southern Ocean Expedition seven (2013)
SSH	Sea Surface Height
SSS	Sea Surface Salinity
SST	Sea Surface Temperature
STF	Subtropical Front
STFZ	Subtropical Frontal Zone
STSW	Subtropical Surface Waters

$t(CO_2)$	total carbon di oxide
TIO	Tropical Indian Ocean

1. Introduction

1.1 Ocean Carbon Cycle

Carbon is an important element in various biogeochemical cycles and plays a significant role in the biotic and abiotic processes in the ocean. Oceans act as a massive storage system for carbon, substantially greater than the atmospheric and terrestrial systems. Oceanic carbon can exist in various forms, mainly, dissolved inorganic carbon (DIC), dissolved organic carbon (DOC), particulate inorganic carbon (PIC) and particulate organic carbon (POC), and sometimes in Colloidal forms. Studies have revealed that these organic and inorganic forms mostly exists in an approximate ratio of DIC:DOC:POC = 2000:38:1 [about 37,000 GtC DIC (Falkowski et al., 2000; Sarmiento and Gruber, 2006): 685 GtC DOC (Hansell and Carlson, 1998) and 13 to 23 GtC POC (Eglinton and Repeta, 2004)]. Ever since the industrial revolution, the global oceans are considered to have drawn down nearly 40% of the anthropogenically produced carbon dioxide (CO_2) and so, oceans are regarded to be the major sink of atmospheric CO_2 (Khatiwala et al., 2013). The Southern Ocean (SO) alone, is estimated to account for nearly 20-40% of this oceanic CO_2 uptake (Gruber et al., 2009; Takahashi et al., 2012; Khatiwala et al., 2013) thereby playing a significant role in global carbon cycle and climate change. The transfer of CO_2 from the atmosphere to the oceans and ultimately into the sediments, involves the combined effect of two major mechanisms, namely the solubility pump/physical pump and the biological pump and the efficiency of these two pumps determine the long term storage and export of carbon in the ocean depths (Sarmiento and Toggweiler, 1984; Volk and Hoffert, 1985). While the solubility pump concentrates on the drawdown of atmospheric carbon via air-sea exchange by

dissolution of gases into the oceanic system and is strongly influenced by the hydrographic features and physical processes in the region. On the other hand, the biological pump regulates the CO_2 fixation by phytoplankton and the conversion of inorganic carbon to organic carbon and its transfer to the ocean interior. There is always a continuous exchange of CO_2 between the atmosphere-ocean-biosphere system, during dissolution, photosynthesis, upwelling and degassing processes. Strong winds can favour divergence causing upwelling that brings DIC and nutrient rich waters to the surface, and to an extent support degassing of CO_2 to the atmosphere. The upwelled waters may be aged/ older waters and have higher DIC, a result of remineralisation of organic matter and dissolution of biogenic $CaCO_3$ (Sarmiento and Gruber, 2006; Bopp et al., 2017) (Fig. 1.1).

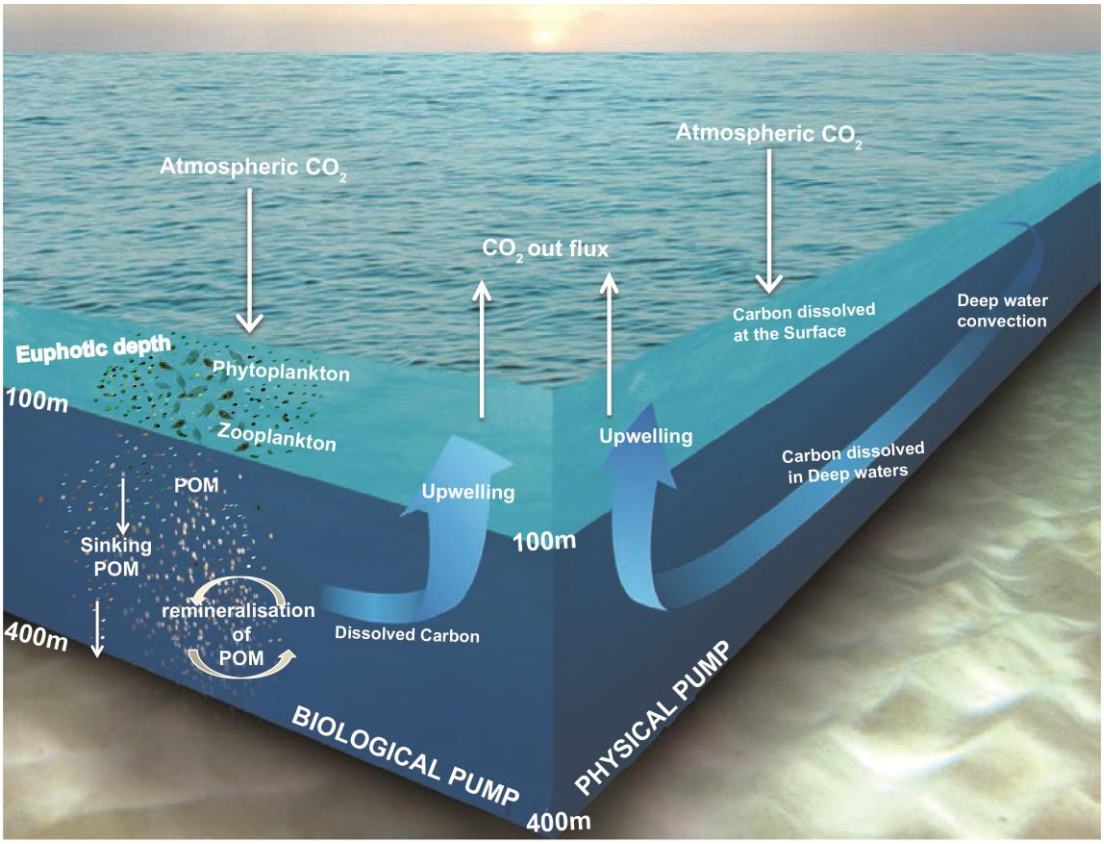

Figure 1.1: Ocean carbon cycle, representation of the biological and physical (solubility) pump in the ocean (Adapted and modified; from Bopp et al., 2002).

However, the increase in atmospheric CO_2 has led to a question as to "Will the ocean continue to drawdown atmospheric CO_2 at the same rate?" and also "How will this continuous CO_2 drawdown influence the biological pump efficiency?"

1.2 Biological Pump

The term pump was coined decades ago, with reference to the movement of carbon from the surface to the ocean bottom against the concentration gradient (Volk and Hoffert, 1985). A major fraction of the CO_2 that enters the deep ocean is through phytoplankton input pathways, and hence 'biological pump' plays a major role in the process of sequestration of atmospheric CO_2 (Smith and Comiso, 2008; Arrigo et al., 2008). From the fixation of inorganic carbon into particulate organic matter (POM) during photosynthesis to its transformation via trophic processes in the ocean, a suite of physical processes like circulation, mixing, upwelling, etc., assist the transport of organic matter, along with the gravitational settling of POM aggregates that act collectively to sequester carbon into the ocean (Ducklow et al., 2001; Siegel et al., 2016).

The first and foremost step of the biological pump is the synthesis of the organic (soft tissue) and inorganic carbon (hard skeleton) compounds by phytoplankton in the photic waters of the ocean water column. Primary productivity is the main process by which CO_2 is fixed into organic matter (OM) through photosynthesis, by phytoplankton, in the presence of light and nutrients.

$106CO_2 + 122H_2O + 16HNO_3 + H_3PO_4 \rightarrow (CH_2O)\ 106(NH_3)16H_3PO_4 + 138O_2$

Photosynthetic production by phytoplankton is the base of oceanic food-web, and plays a significant role in the carbon cycle by partitioning carbon between the ocean and atmosphere, thus disconnecting it from direct air-sea interaction (Behrenfeld et

al., 2006; Mcgillicuddy et al., 2007). The efficiency of the oceanic biological carbon pump is largely dependent on the trophic structure of the marine food-web comprising of phytoplankton, zooplankton and the microbial loop that takes part in mobilizing the carbon in the oceanic system (Azam et al., 1983; Smetacek, 1999). Carbon in its organic form and the respiratory CO_2, produced in deep waters, can remain away from contact with the atmosphere for varied time periods, from months to several years, depending on the chemical form of carbon and the depth of its existence in the ocean (Zhang et al., 2018) (Fig. 1.2).

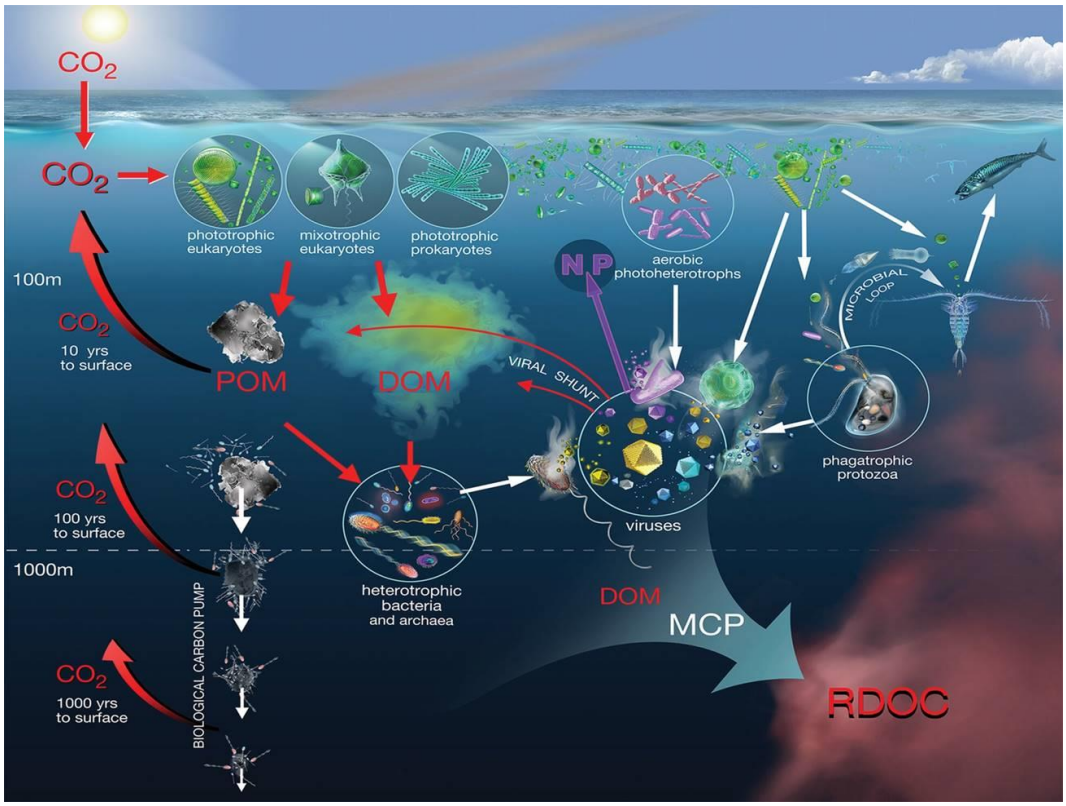

Figure 1.2: Schematic depiction of the carbon cycling via the biological pump in the ocean. The linkage of Microbial Loop and Microbial Carbon Pump (MCP) in the Biological Carbon Pump (BCP), and the time scale representing the return of respired CO_2 to the surface, from different depths of the ocean (adapted from Zhang et al., 2018).

The POM formed via photosynthesis is a fundamental component of the biosphere, it is ubiquitous, abundant and forms an essential component of the biogeochemical cycles. POM acts as a crucial link between the classic food-web and the microbial loop in oceanic systems, thus a vital component in the carbon export to the ocean depths, as well as other elemental cycles (Gordon and Goñi, 2003; Duforet-Gaurier et al., 2010).

1.3 Particulate Organic Matter (POM)

POM accounts for a very small fraction of the total organic matter in the oceans, but it is a very important fraction in transporting organic components from the surface/source of formation to the deeper waters and finally sinking to the sediments (Volk and Hoffert, 1985; Boyd and Trull, 2007). On an average, almost 97-99% of the POM is remineralized by grazing or decomposition in the upper water column (mesopelagic) and a very small portion (1-3%) reaches the bottom sediment (Buesseler, 1998; Honjo et al., 2008). The quality, composition and transformation of POM determine the efficiency of export of carbon through the water column.

1.3.1 Composition of POM

POM constitutes of diverse components of different sizes and can include living organisms like phytoplankton, bacteria, virus, to fecal pellets of grazers (zooplankton) and other larger organisms, as well as dead and detritus matter (Valkman and Tanoue, 2002; Lee et al., 2004). POM varies in its physical structure and biochemical composition depending on the source of formation, ambient conditions and the transformation process altering the POM characteristics (Menzel

and Goering, 1966). Biochemical composition of POM in ocean waters mainly comprise of carbohydrates, proteins, lipids formed from the combinations of monosaccharaides, amino acids and fatty acids respectively, along with other uncharacterised organic matter. The chemical composition of POM in oceans is highly variable, and studies have reported various factors like light intensity, nutrient availability, the phytoplankton community, and also the grazing community have an influential role in determining the composition of POM (Kuenzler and Ketchum, 1962; Menzel and Ryther, 1964), and further modulate the transformation and export of carbon.

1.3.2 Factors influencing the POM composition and transformation in oceans

Several processes like repackaging, degradation, aggregation, interaction between the suspended and sinking POM, are responsible for the transformation of POM and determining the quality and quantity of POM exported to the depths of the ocean (Lee, et al., 2004; Tsukasaki and Tanoue, 2010). Some of the controlling factors are as mentioned below.

Phytoplankton community: The biomass and community of the phytoplankton determines the chemical composition of the initial POM formed in the photic waters. However, the biomass and phytoplankton community is determined by the environmental conditions (light, temperature, nutrients, etc.) of the ambient waters. The phytoplankton community being the base of the marine food web, the size and the nutritional value of the phytoplankton community, determines the type of trophic structure, especially the grazing community and also contributes by influencing the carbon export flux of the oceanic regime (Finkel et al., 2010; Deppler and Davidson, 2017; Basu and Mackey, 2018).

Zooplankton Grazing: Studies have indicated that zooplankton grazing is the initial stage of transformation of POM by the consumption of phytoplankton in the marine systems. The community selective grazing and partial breakdown or complete engulfment of organism determines the resultant organic compounds (Cowie and Hedges 1994; Wakeham et al., 1997; Lee et al., 2000). Zooplankton also contributes to aggregation/repackaging of POM by the uptake of smaller particles, and further excreted as sinking fecal pellets. Zooplankton is also responsible for the vertical transport of POM below the mixed layer, during the process of its vertical migration within the water column. A change in the zooplankton biomass and composition can regulate the composition and sinking rate of the fecal pellets.

Microbial action: Microbial activity significantly contributes to POM transformation by breakdown/degradation of dead organisms (Legendre and Le Fèvre, 1995; Ewart et al., 2008). Microbial colonies can also be responsible for the formation of new POM by colonising the particles and aggregation of DOC (King and White, 1977, Burd and Jackson, 2009), resulting in altering the POM composition.

Aggregation and disaggregation: Exchange between sinking material, suspended particle and dissolved organic matter via aggregation /disaggregation and solution/dissolution alter the POM composition. The magnitude of particle aggregation and disintegration control the particle size and in-turn the settling velocity of POM. This process has a significant impact on the residence time and composition of organic matter in the water column and thus the efficiency of remineralisation during the transit (Hill, 1998; Sheridan et al. 2002). Studies have revealed that the particle size have a role to play in the level of degradation and the particle flux (Abramson et al., 2010; Rontani et al., 2011), as larger particles will exit the water

column as sinking particles with higher settling rate, thus exposed to the ambient environmental conditions for a shorter time period.

1.4 Importance of POM studies

It is of utmost importance to study the biochemical characteristics of POM as it play a significant role in understanding the extent of transformation that the OM can undergo due to heterotrophy and associated transformation processes prior to reaching the sediments, as the quality and size have a major role in determining the extent of carbon exported to the ocean depths and sediments (Hayes, 1993; Guo et al. 2003). Also, the elemental composition of POM in the water column varies based on remineralisation of POM by various factors/ processes, resulting in a difference in the C:N and N:P which are often used to understand the remineralisation of POM (Redfield, 1958; Li and Peng, 2002; Martiny et al., 2013). More recently, the study of organic matter to its molecular level and knowing its isotopic composition has been a useful tool to determine and elucidate pathways of the resultant POM and understand the ambient conditions at the time of formation of POM (Wada et al., 1987; Lara et al., 2010). Secondly, since POM is heterogenous in nature it would lead to selective preservation and altering its chemical composition (Cowie and Hedges 1994; Wakeham et al. 1997), thus the chemical characteristics of the remnant POM will give an idea of the dominant biogeochemical processes (degradation/remineralisation) in the oceanic regime. The isotopic ratios are not much affected by processes like photochemical degradation or structural modification as other biomarker molecules and therefore are useful in POM studies in the marine systems (Hedges, 1992; Raymond and Bauer, 2001).

1.4.1 Stable isotopes as a proxy for POM studies

Stable isotopes are often used as a tool to understand the biogeochemical cycling of POM and to deduce the source, transport, transformation and the processes controlling the distribution and fate of OM in the marine environment (Gordon and Goňi, 2003; Zhang et al., 2014). Stable isotopic ratio of carbon ($\delta^{13}C_{(POM)}$) is largely influenced by the conditions prevailing at the time of carbon fixation, as various factors including temperature, pCO_2, availability of nutrients, phytoplankton community structure, etc., determine the isotopic fractionation of carbon in POM (Popp et al., 1989; Laws et al., 1995; Bidigare et al., 1997; Gruber et al, 1999). The source of carbon and the varied forms of carbon utilized by the phytoplankton community during primary production also influence the $\delta^{13}C_{(POM)}$, as the existence of mixotrophic and heterotrophic plankton may support the assimilation of dissolved organic compounds unlike autotrophs which would prefer CO_2(aq) and other inorganic forms (Hayes, 1993; Bentaleb et al., 1998). On the other hand, $\delta^{15}N_{(POM)}$ is used to study nitrogen related processes involved in production and cycling of organic matter, like the form of nitrogen uptake (Liu and Kaplan, 1989; Reynolds et al., 2007) organic matter remineralisation (Wada et al., 1987; Macko et al., 1994) and other processes associated with the nitrogen cycle.

1.5 Importance of studies in the Southern Ocean

The SO, has often been considered as a sink of carbon (Gruber et al., 2009; Takahashi et al., 2009). However studies have implied that certain regions in the SO can also act as the source of carbon, via CO_2 outgassing (Takahashi et al., 2009; Lenton et al., 2013). Also, the efficiency of SO as a sink is weakening, and is

influenced by the seasonal effect (Meltz, 1991; Meltz et al., 2009). The efficiency of the Indian sector of the SO (ISSO), as a strong or weak sink is strongly dependent on the environmental factors at a particular time instance (Prasanna et al., 2015; Shetye, 2015). The complexity in the environmental setting of the ISSO, suggests that physical factors have a significant role in a change of the biological community structure and the biogeochemical cycles. The hydrographic features like fronts, gyres and eddies in the ISSO, stimulate the ejection of nutrients and can trigger phytoplankton blooms or a change in the phytoplankton community (Soares et al., 2020). These hydrography stimulated changes in the biological processes play a role in the POM formation and also influence the vertical transport of particles out of the euphotic waters (McGillycuddy et al., 1998; Sweeney et al., 2003; Gorsky et al., 2002).

Although the ISSO is a region of great importance for its role in the global carbon cycle and climate change, and studies carried out with respect to the air-sea exchange and the physical pump, the region is yet understudied with regard to the carbon dynamics and biological pump. One of the main reasons is likely the logistic difficulties in approaching the region for sample acquisition. In the last decade the studies in this region are increasing on a gradual scale. However, the region is understudied and needs a better understanding, especially with regard to the biological pump, and its response to the changing environmental conditions, influencing the carbon export, etc.

1.6 Literature Review

Identifying the characteristics and distribution of POM in ocean is a key component in the study of ocean carbon cycle and other biogeochemical processes. Several studies on POM have been carried out in the global waters using different tracers as tools. The SO being a complex, dynamic system the variability in the biogeochemical processes and the carbon dynamics strongly influences the global climate changes. Some of the studies in the other sectors of the SO and the ISSO are mentioned below.

1.6.1 POM studies in the Southern Ocean

Studies using the natural abundance of stable isotopes of carbon and nitrogen in POM were initiated decades ago. This proxy was used to address the biogeochemical structure of the food web in Antarctic waters by Wada et al. (1987). Later Fischer (1991), studied the variation of stable isotopic composition in phytoplankton, surface sediments and sinking particles from sediment traps, and implied high respiration in the benthic waters responsible for enrichment in ^{13}C at the sediment-water boundary.

Kennedy et al. (2002) carried out POM studies in Antarctic sea ice, over a wide area in the Weddell sea. The study suggested POM is highly variable in sea ice, also the nutrient supply and demand play a major role on biomass, and has a critical role in the complex sea ice ecosystem.

A study by Lara et al. (2010) was carried out to understand the characteristics of suspended POM in South West Atlantic using stable isotopes of carbon and nitrogen. This study implied that different oceanic regions across the south west

Atlantic waters have different factors, like temperature, nutrients and community structure, influence the POM isotopic characteristics of the region.

Berg et al. (2011) tried to understand the variation in the isotopic composition of carbon and nitrogen in an iron fertilized eddy in the Antarctic Polar Front of the Atlantic sector of SO. The study speculated that carboxylation, nitrogen assimilation, substrate pool enrichment and community composition could have been the contributing factors to the gradual increase in $\delta^{13}C_{(POM)}$ associated with phytoplankton biomass.

Stable isotopic ratio of carbon ($\delta^{13}C_{(POM)}$), has been used as a tool to understand the factors influencing the composition of surface and sediment trap derived POC (Henley et al., 2012), and proposed a shift in the diatom assemblage influence the isotopic composition. The study also suggested the influence of a seasonal effect on the POM composition.

Studies on POM in ocean surface waters of Prydz Bay, Antarctica (Yin et al., 2014, Zhang et al, 2014) have indicated that the dissolved CO_2 concentration, nutrients and biological properties including ice cover and sea ice melting have a role to play in POM dynamics and in determining the isotopic composition of POM.

In general, the POM studies in SO have suggested that isotopic ratios of carbon in POM ($\delta^{13}C_{(POM)}$) are sensitive to different environmental variables like temperature, CO_2, nutrients availability, as well as phytoplankton variables like cell size, shape and growth rate (Popp et al., 1998; 1999; O'Leary et al., 2001; Lourey et al., 2004).

1.6.2 Previous studies in the Indian sector of the SO

Previous studies in the Indian sector of SO (ISSO) have indicated that, the different fronts have distinct hydrographic features (Anilkumar et al., 2006) and different food web dynamics (Jasmine et al., 2009). Studies also illustrated the variability in the nutrient concentration, nutrient uptake rates and biological productivity (Pavithran et al., 2012; Gandhi et al., 2012) are significantly different across the different oceanic fronts and zones including a few studies addressing the cross frontal variability of carbon dioxide in the ISSO (Shetye et al., 2012; 2015). Although POM is an important component in the biogeochemical cycles, and more so in the global carbon cycle, very little is known about the nature, distribution and fate of POM, especially the ISSO which include limited studies on the POM dynamics.

Earlier isotopic studies of POM in the ISSO were restricted to the Crozet basin, the Subantarctic regions (Kaehler et al., 2000), the Southern Ocean south of Australia, (Lourey et al., 2004) and Leeuwin Current (LC), off Western Australia (Waite et al., 2007). These studies largely focussed on the trophic structure, food web structure and influence of total CO_2 (tCO_2), eddies and nutrients on the isotopic composition of POM. Moreover, to the best of our knowledge, there is very little information about the distribution of $\delta^{13}C_{(POM)}$ and $\delta^{15}N_{(POM)}$ in the ISSO (Francois et al., 1993). However, most of the previous studies in ISSO, were restricted to the surface waters or involved sediment traps (Henley et al., 2012) and very few address the water-column dynamics of POM.

As an attempt to fill in the void of lacking POM studies in the ISSO, the present doctoral research has attempted to study POM biogeochemistry in the ISSO with the objectives as mentioned below. This study was also an attempt to gain a

better understanding of the variability of POM across the different fronts in the SO, as well as the factors influencing the chemical and isotopic composition of POM and the transformation of POM within the upper water column.

1.7 Objectives

- **Characterisation of particulate organic matter in the water column of oceanic regimes.**

- **Factors influencing the variability of chemical and isotopic composition of particulate organic matter in the ocean.**

- **To understand the fate of particulate organic matter its decomposition/remineralisation within the water column.**

2. Study area and Methodology

2.1 Study Area: Geographical location and hydrography

2.1.1 Southern Ocean

Southern Ocean (SO) has a significant role in the global ocean circulation and climate change. It accounts upto nearly 21% of the world ocean surface. The SO encompasses the Antarctic continent (Fig. 2.1), and forms the largest water body that spans globally connecting the three major oceanic basins (Séférian et al., 2012).

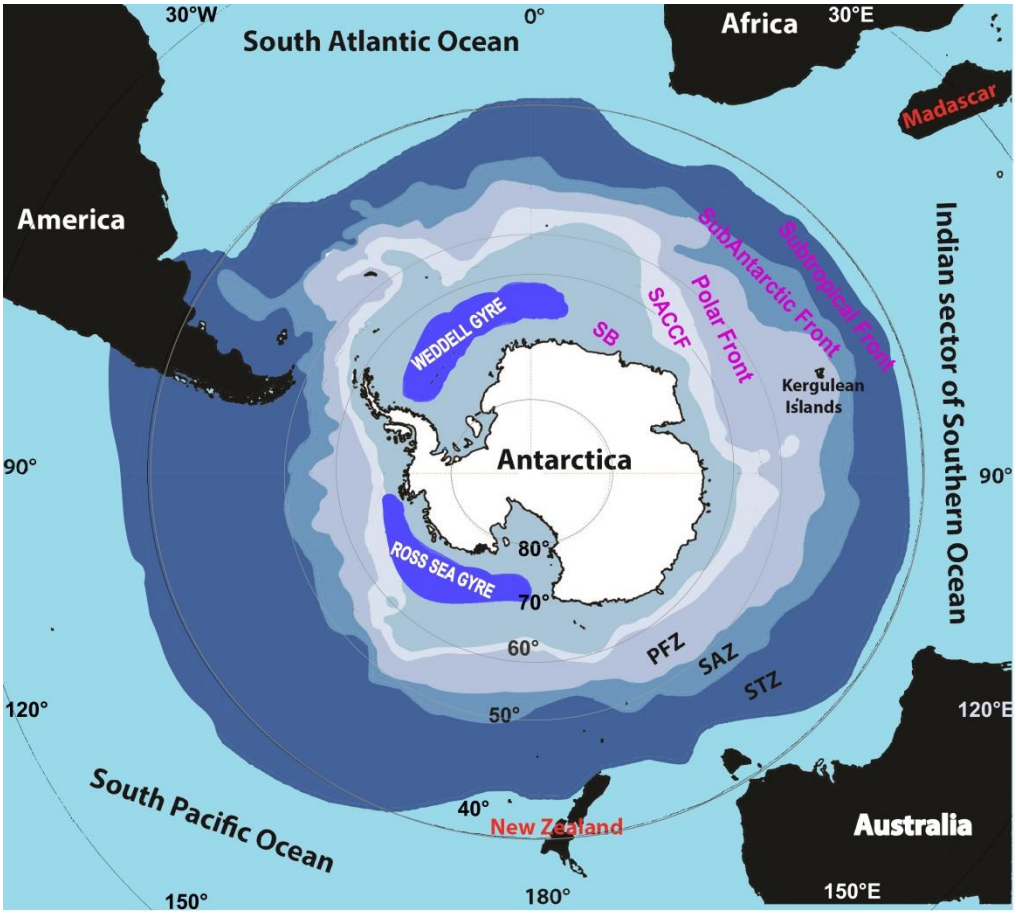

Figure 2.1: Illustrates the study area, with the frontal structure encompassing the Antarctic continent, also demarcating the zones and the surrounding continents (figure plotted using Quantarctica).

The SO also includes the largest oceanic current, the Antarctic Circumpolar Current (ACC) driven by the strong westerlies, and play a crucial role in transporting volumes of water, heat, nutrients and salts, globally and influencing the global biogeochemical cycles (Deacon, 1933; Pollard et al., 2002; Boyd and Ellwood, 2010). The SO is influenced by diverse physical processes, including sharp temperature gradient, strong ocean currents, high wind speeds, and extensive sea ice cover, making the region highly dynamic (Rintoul and Naveira Garabato, 2013). This region experiences strong seasonal changes like sea-ice formation and ice-melt, causing freshening of waters and further influencing the biological productivity of the region. The SO is a region for the formation of different water masses, and contribute to the thermohaline circulation, and associated transport of various components.

2.1.1.1 Indian sector of the Southern Ocean

The Indian sector of the Southern Ocean (ISSO) is defined as a region between 40°S to the Antarctic coast (~69°S) and 20°E to 150°E. Unlike the Atlantic sector, the ISSO is bound by landmasses in the north. Further, the ISSO include two major islands, the Crozet Island and the Kerguelen Island, which play a significant role in influencing the biogeochemistry of the region. Also, the strong wind and current induced mixing and northward transport of both seawater and solutes from its source in the Antarctic shelf and are the key features to the supply of nutrient and oxygen rich waters from the south to the mid-latitudes (Deacon, 1933; Jacob et al., 1996). Moreover, SO shows large scale meridional changes in temperature and salinity, resulting in the formation of various oceanic fronts including the Subtropical Front (STF), Sub Antarctic Front (SAF) and Polar Front (PF) (Orsi et al., 1995; Belkin and Gordan, 1996) (Fig. 2.1). Additionally, the unique features of the ISSO include: the PF split into two, namely the PF-I and the PF-II and it also includes the

Agulhas Return Front (ARF), fed by the Agulhas current that is retroflexed by the ACC and merge with the STF at some locations in the ISSO (Lutjeharms and van Ballegooyen, 1988; Anilkumar et al., 2006 & 2014). The different oceanic fronts are characterised by specific hydrographical features that regulate the biochemical process and food-web dynamics of these frontal regions (Sokolov and Rintoul, 2002; Jasmine et al., 2009).

2.1.2 Hydrography and biochemical characteristics of different Fronts

The STF is a zone of transition from warm, nutrient depleted subtropical waters to cold, nutrient rich Subantarctic waters, with the oligotrophic subtropical gyre, north of the STF. This region is highly influenced by mesoscale eddies, responsible for the redistribution of nutrients and other inorganic and organic components (Boyd et al., 1999; Jullion et al., 2010). Another feature of the STF is the high, but patchy, primary productivity, and the abundance of micro and mesozooplankton (Llido et al., 2005; Jasmine et al., 2009). South of STF is the SAF, this is a region of significant temperature stratification (Pollard et al., 2002). The stratification influenced nutrient gradient in this region is responsible for a succession in phytoplankton community (Deppeler and Davidson, 2017). The physico-chemical conditions of the SAF, favours the growth of smaller size phytoplankton and microzooplankton (Jasmine et al., 2009; Boyd et al., 2016). The PF, mostly extends beyond 50°S to the Southern boundary (SB), associated with low temperature. The PF is nutrient replete, known to become more productive during the austral summer, which is likely due to the availability of sunlight, the influx of micro and macro nutrients, contributed by ice melt (Gandhi et al., 2012; Sabu et al., 2014; Triparthy et al., 2015). The environmental conditions of this region mostly support larger

phytoplankton like the diatoms, which is the dominant phytoplankton community during austral summer (Naik et al, 2015; Mishra et al., 2017).

2.1.2.1 Mesoscale Eddies

The SO, especially the ARF and the STF is highly dynamic in-terms of the existence of ubiquitous feature like mesoscale eddies. The ARF is a region subject to enhanced eddy shedding and meandering (Machu and Garçon, 2001; Machu et al., 2005), resulting in the presence of numerous eddies in the ARF and STF region. Mesoscale eddies are often associated with exchange of various biochemical components like nutrients, salts, etc. due to associated hydrographic processes like upwelling and downwelling (McGillicuddy et al., 1998; Llido et al., 2005; George et al., 2018). Furthermore, the nutrient influx into the euphotic water column influence the phytoplankton community and biogeochemical processes of the eddy influenced regions (Kolasinski et al., 2012; Wang et al., 2018).

2.2 Methods and Materials

2.2.1 Sampling Strategy

The major focus of this study is in the ISSO. Based on the hydrographic properties the study region beyond 40°S was divided into different fronts and zones namely: the Subtropical Frontal Zone (STFZ), Subantarctic Frontal Zone (SAFZ) and Polar Frontal Zone (PFZ). The ISSO is yet understudied due to logistic constraints and need more investigations for a better understanding of the biogeochemical processes of the region.

For the current study seawater samples were collected from 7 discrete depths (0, 10, 30, 50, 75, 100, 120) using Niskin bottles mounted on a CTD rosette. Surface

water samples were also collected from the Tropical Indian Ocean (TIO) for a comparative understanding of the two contrasting oceanic regimes of the Indian sector; one being the warm, saline TIO waters and the other regime characterized as the cold, less saline SO waters. Samples were collected across the fronts in the ISSO during austral summer 2012 and 2013 during two different SO expeditions as below:

Austral summer 2012

Seawater samples were collected on-board *RV Sagar Nidhi* during the SO expedition (SOE-06) in December 2011-January 2012. Samples were collected from 9 locations from 40°S to 53°S. Six locations at the STFZ, one location at the SAFZ and two locations at the PFZ (Fig. 2.2). Additionally at 11 locations, surface samples were collected in the TIO.

Austral summer 2013

Seawater samples were collected on-board *RV Sagar Nidhi* during the SO expedition (SOE-07) in January-February 2013. Samples were collected from 11 locations from 40°S to 56°S. Three locations at the STFZ, one location at the SAFZ and seven locations at the PFZ (Fig. 2.2). Also, surface samples were collected from 12 locations in the TIO.

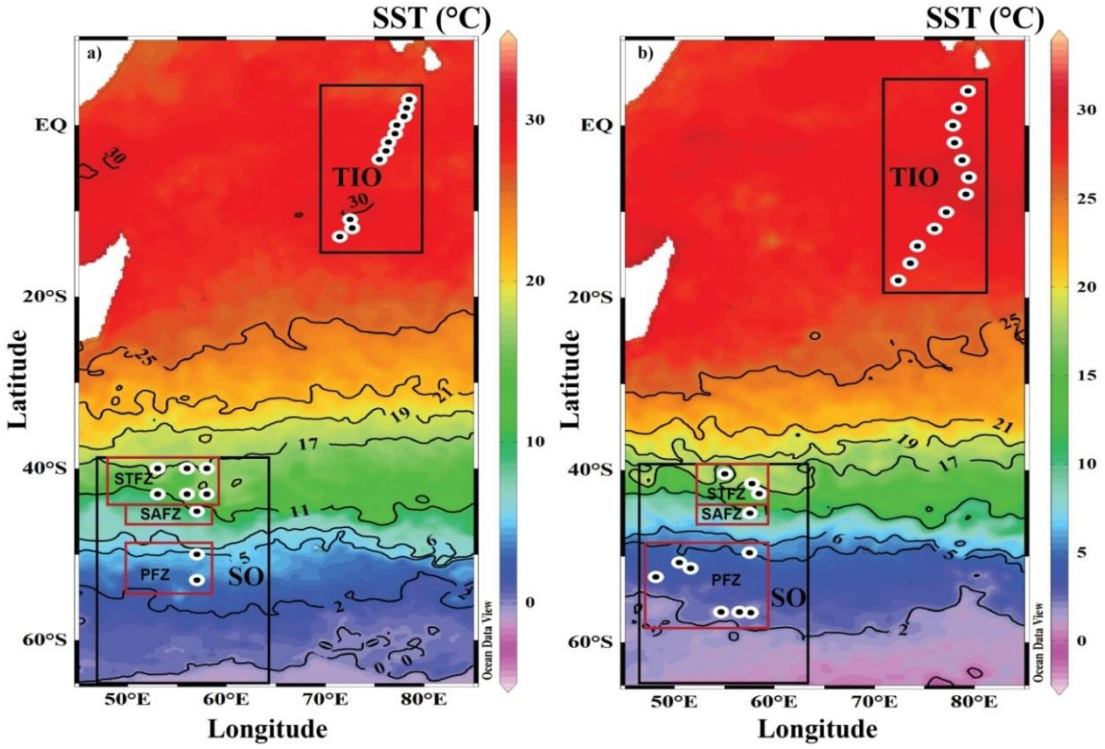

Figure 2.2: Study area map with station locations overlaid on the sea surface temperature (monthly average SST, derived from MODIS aqua); black circles with white border are sampling locations during austral summer: (a) 2012 and (b) 2013.

2.2.2 Sample Analysis

The samples for this study were collected with utmost precaution to avoid any contamination during sample collection, transport and storage of samples. An overview of the scientific methods, techniques and the instruments used for this study is illustrated as a schematic flowchart (Fig. 2.3).

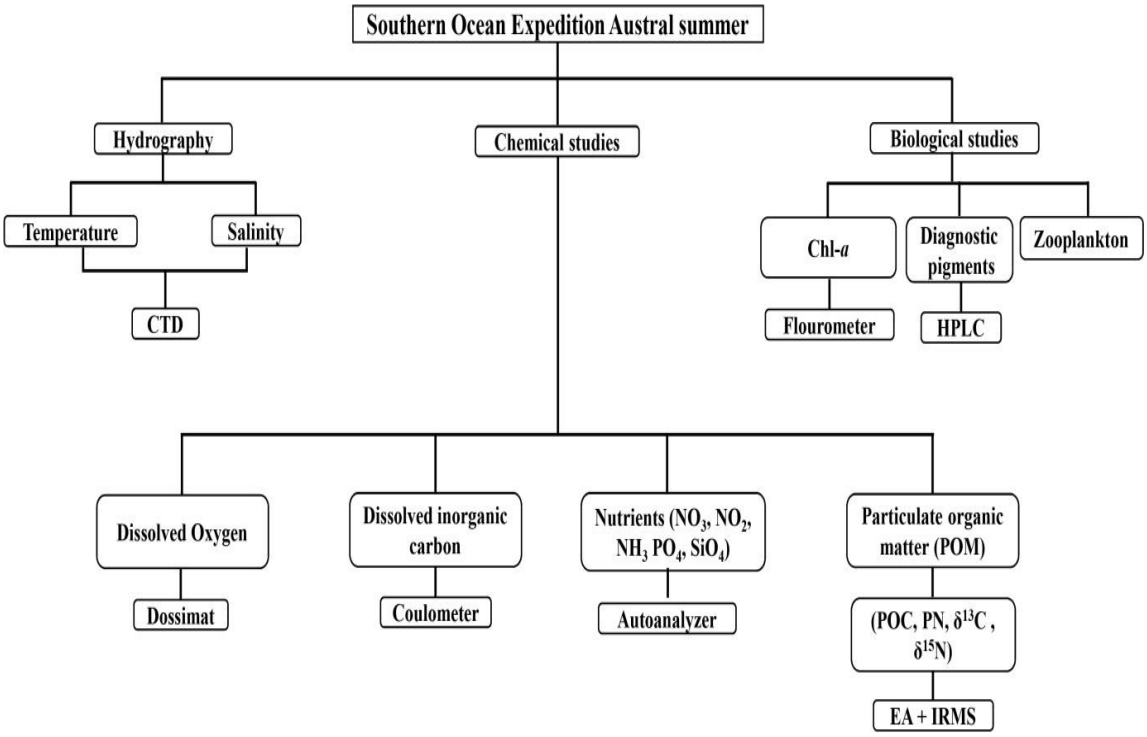

Figure 2.3: Schematic representation of the sample processing and analytical techniques used for this study.

2.2.2.1 Hydrographic Data

Hydrographic data, mainly the temperature and salinity, at all the sampling depths and locations were obtained from CTD (Seabird Electronics Sea Cat 21) mounted on a CTD rosette. The different fronts were demarcated based on the temperature, salinity indicators as described in Anilkumar et al. (2006 & 2014) (Table 2.1).

Front	Temperature	Salinity
Agulhas Return Front (ARF)	19-17°C, at the surface	35.54-35.39 at surface
Subtropical Front (STF)	17-11°C, at surface	35.35-34.05 at surface
SubAntarctic Front (SAF)	SAF1: 11-10°C, at surface SAF2: 7-6°C, at surface	SAF1: 34.0-33.85 at surface SAF2: ~33.85 at the surface south of SAF1
Polar Front-I (PF-I)	5-4°C, at the surface	33.8-33.9 at the surface
Polar Front-II (PF-II)	3-2°C at the surface	33.8-33.9, at the surface
Southern Antarctic Circumpolar Current Front (SACCF)	Temperature maximum >1.8°C	Salinity Maximum >33.74
Southern Boundary of ACC (SB)	1.5°C isotherms	

Table 2.1: Frontal demarcation in the ISSO based on the criterion given in Anilkumar et al. (2006 & 2014).

2.2.2.2 Dissolved Oxygen (DO)

Sub-samples for DO were collected carefully, directly from Niskin sampler, into a 125 ml glass bottles before any other samples being collected. Care was taken to avoid any air bubbles while sampling, and the bottle was allowed to overflow to avoid bubble trapping. The samples were quickly fixed with Winkler's A and Winkler's B. The precipitate was allowed to settle and later, acidified with 50% sulphuric acid, and 50 ml of the acidified sample was accurately measured and titrated against sodium thiosulphate following Winkler's method (Grasshoff et al., 1983) using an auto-titrator (Metrohm 865- Dosimat Plus, Switzerland).

2.2.2.3 Total Carbon dioxide (tCO_2)

Sub-samples were collected in 60 ml glass bottles and treated with 0.3 ml of saturated mercuric chloride. Later, 25 ml of the sample was injected into the Coulometer-acidification module system and acidified with 3 ml of 8.5% orthophosphoric acid. The gaseous CO_2 released was trapped into the reaction cell containing ethanolamine and photometrically back-titrated using a coulometer (Model 5015, U.I.C. Inc., USA). Calibrations were carried out using a certified reference material (CRMs, Batch #104) supplied by A. Dickson (SIO, University of California, USA) and also using pre-weighed and dried Na_2CO_3. Also acid blanks were carried out prior to analysis and deducted from the samples. The overall precision and accuracy of the analyses were ≤ 2 μM.

2.2.2.4 Nutrients

250 ml of seawater sample were collected for the analysis of Nutrients (nitrate, nitrite, ammonia, phosphate, silicate). The samples were preserved at -20°C until analysis. Prior to analysis, the samples were thawed and analysed at room temperature, following the standard colorimetric analysis procedure by Grasshoff et al. (1983). The seawater samples were analysed using autoanalyser (Model: Skalar Analytical San++ 8505 Interface v3.05, Netherland). Specific standards as defined in Grasshoff et al. (1983) were used to calibrate the auto-analyzer for each nutrient (nitrate, nitrite, ammonia, phosphate, silicate). Frequent baseline checks were made and the drift during analysis also considered using standard. The standard deviation for all nutrients analysed was ±1%.

2.2.2.5 Particulate organic carbon (POC), Nitrogen (PN) and the stable isotopes of carbon ($\delta^{13}C$) and nitrogen ($\delta^{15}N$) in Particulate organic matter samples

Five liters of seawater subsamples was collected in acid-cleaned plastic carboys and filtered through 0.7 μm pore size Whatman GF/F filters. The filter papers used for POM studies were pre-combusted at 450°C for 4 hrs. Post filtration, the filter paper samples were stored at -20°C until analysis. Prior to analysis the filters were decarbonated by exposing to fumes of HCl for 12 h in a desiccators, to remove the inorganic carbon component and dried completely to remove all the moisture before being packed tightly in tin cups for the analysis of POC, PN and stable isotopic ratios ($\delta^{15}N$ and $\delta^{13}C$) of POM. Analysis were carried out using, Isoprime Stable Isotope Ratio Mass Spectrometer in continuous-flow mode coupled with an Elemental Analyser (Isoprime, Vario Isotope Cube) (Owens and Rees, 1989). $\delta^{13}C$ values are reported with respect to V-PDB and $\delta^{15}N$ values are reported with respect to air N_2. The reference standard used for normalizing to V-PDB and air N_2 scale are Cellulose (IAEA-CH-3) & Ammonium sulphate (IAEA-N1). The ratios are expressed in per mil notation as follows:

$$\delta^{15}N \text{ or } \delta^{13}C(‰) = [(R \text{ sample}/R \text{ standard}) - 1] \times 1000,$$

$$\textit{where, } R = {}^{15}N/{}^{14}N \textit{ or } {}^{13}C/{}^{12}C.$$

The external precisions for $\delta^{13}C$ and $\delta^{15}N$ are ±0.05 ‰ and ±0.08 ‰ (1σ standard deviation) respectively, and for %C and %N are ±0.29% and ±0.35% (1σ standard deviation) respectively, obtained by repeated measurements of IAEA-CH-3 & IAEA-N1 (n = 27). The obtained %C and %N values were later converted to POC (μg/L) and PN (μg/L) using the dry weight of the particulate sample collected on the filterpaper.

2.2.2.6 Chlorophyll-a and Phytoplankton marker pigments

Three litres of seawater were filtered through GF/F Whatman filters Chlorophyll-a (Chl-*a*). The samples were stored at -20°C until analysis. For analysis of Chl-*a*, the samples (filter paper) were placed in 15 ml scintillation vials and extracted in 10 ml of 90% acetone, at 4°C overnight. And measured by fluorometry in a 10 cm cuvette, using Turner's AU 10 Fluorometer (Turner Designs Inc., USA). Calibration was carried out using standard chlorophyll-*a* pigment (DHI, Denmark).

The pigment analyses were carried out following the method of van Heukelem (2002) using High Performance Liquid Chromatography (HPLC). According to the standard practice, chemotaxonomically similar marker pigments were grouped together and pigment indices were calculated following the method of Barlow et al. (2007). This Diagnostic pigment (DP) index was used to assess the community structure by confirming the significant relationship between DP and total Chl-*a* ($r=0.871$, $n=15$, $p<0.0001$), as given in Naik et al. (2015).

2.2.2.7 Zooplankton Abundance

Zooplankton samples (vertical hauled) were collected in the upper water column using a Multi Plankton Sampler (MPS: mouth area of 0.25 m^2 and mesh size of 200-µm, Hydro-Bios, Germany) during the day. The MPS was hauled up at a speed of 0.8 m/ s, upon recovery of the samples, the catch was immediately preserved in 5% buffered formaldehyde/ seawater solution for the species counts and identification. In the laboratory, large and fragile zooplankton (krill and jellyfish etc.) were sorted from the rest of the specimens. Zooplankton biomass was measured by the volume

displacement method (ICES 2000) and expressed in ml/m^3. Samples were analysed at the laboratory at NCPOR and CMLRE.

2.2.3 Computation of physical and biochemical variables

2.2.3.1 Euphotic Depth

The vertical profiles of Photosynthetically active Radiation (PAR) were collected using a biospherical QSP-2300 underwater PAR sensor attached to the CTD. These profiles were used to estimate the coefficient of downwelling irradiance (Kd). The Euphotic depth was calculated by using beer-Lambert's equation (Kirk, 1996).

2.2.3.2 Mixed Layer Depth

The Mixed Layer Depth (MLD) in the ISSO was based on the density gradient method. It is defined as the shallowest depth at which density gradient is greater than 0.03 kg/m^3 from 10m depth (Dong et al., 2008).

2.2.3.3 Apparent oxygen utilization

The apparent oxygen utilization (AOU) was calculated as the difference of oxygen gas solubility ($O_{2(sat)}$) and the measured oxygen concentration (O_2) in the ocean. Oxygen gas solubility was calculated as a function of in situ temperature and salinity and one atmosphere of total pressure (Benson and Krause, 1984) assuming that the surface waters are near saturation.

$$Apparent\ Oxygen\ Utilization\ (AOU) = O_{2(sat)} - O_{2.}$$

2.2.3.4 Proxies for POM studies

Various proxies associated with POM were used to understand the state of POM, like C:N ratio, a ratio of POC/PN, was used to estimate the contribution from fresh and old organic matter. Also, the POC:Chl-*a* ratio was used to understand the

contribution of autotrophic and heterotrophic processes to the transformation of POM across the fronts in the ISSO.

2.2.4 Remote sensing Data

To understand the variability in SST over the study region during the study periods, Advanced Very High Resolution Radiometer data during the observation period was used (http://apdrc.soest.hawaii.edu). The eddies were identified using Sea Surface Height (SSH) data derived from the delayed time Maps of absolute dynamic topography (MADT) for the periods between November 2011 and January 2012 and November 2012 to January 2013 from the Copernicus Marine Environment Monitoring Service (http://marine.copernicus.eu). Geostrophic velocities were downloaded from AVISO (http://www.aviso.oceanobs.com). Weekly mean chlorophyll data from the satellite MODIS Aqua (https://coastwatch.pfeg.noaa.gov) was used to understand the chlorophyll and POC variability during the study.

2.2.5 Statistical Analysis

To understand the factors controlling the POM characterization and variation across the fronts, statistical analysis were carried out using Principal Component Analysis (PCA) and Factor analysis. Pearson's and Spearman's correlation analysis was also carried out to understand the influence of various environmental variables and biochemical parameters. Statistical analyses were carried out using EXCEL and XLSTAT.

3. Spatial distribution of Particulate organic matter and the factors controlling the POM characteristics in surface waters.

3.1 Introduction

In the Indian sector, the oceanic regime extends from the cold SO waters, more often addressed as the ISSO, to the warm Tropical Indian Ocean (TIO) waters towards the north, also including the oligotrophic subtropical gyre. As discussed earlier, the ISSO extends from south of 40°S to the Antarctic coast, and experiences large scale meridional changes in temperature and salinity, resulting in the formation of various oceanic fronts and zones (Belkin and Gordan, 1996; Holliday and Read, 1998; Anilkumar et al., 2006), governed by different biogeochemical processes. This oceanic regime is often considered as high nutrient low chlorophyll (HNLC) region. These waters being relatively nutrient rich, supports diverse food-webs, including an active microbial loop and strong microzooplankton grazing (Deacon, 1933; Jacob et al., 1996; Jasmine et al., 2009). The strong winds and currents, and the influence of eddies in this region favours the redistribution of nutrients and salts along with other dissolved and particulate components in and across the fronts (Huang and Xu, 2018; Zhang et al., 2018).

On the other hand, the TIO is fed by various water masses, like the Arabian Sea high saline waters, Bay of Bengal waters, Indonesian through flow, tropical surface waters, etc. (Prasanna Kumar and Narvekar, 2005; Sardessai et al., 2010). The TIO is also bound by land masses, namely the Asian continent and the African continent on the north and west, respectively, which influence the ocean current patterns, nutrient redistribution and biological productivity of these waters (Burkill et

al., 1993). The TIO also includes the south-western Indian Ocean gyre, and lies between 10°S to 35°S that extends from Madagascar to Australia. These waters are also known for its oligotrophic growth conditions with low and patchy biological productivity (Jena et al., 2013).

There is limited information about the characteristics of POM and its isotopic composition in relation to biological processes and physico-chemical changes, across the two hydrographically different oceanic regimes of the Indian Ocean sector namely the ISSO and TIO. The spatial variability of the elemental composition of POM and the stable isotopic composition of carbon and nitrogen of POM across the two oceanic regimes is discussed in this section **3.3.1**.

Furthermore, the POM characteristics and the natural abundance of stable isotopic ratio of carbon and nitrogen in the surface waters are strongly influenced by the conditions prevailing at the time of carbon fixation. Numerous factors including sea surface temperature, the abundance of dissolved CO_2, availability of nutrients, phytoplankton community structure and other phytoplankton related features like cell size, determine the isotopic fractionation of carbon in POM (Popp et al., 1989; Laws et al., 1995; Bidigare et al., 1997; Zhang et al., 2014). An understanding of the driving forces controlling the variability of POM characteristics across the fronts in the ISSO are important to improve the knowledge of carbon and nitrogen dynamics in such scarcely studied regions like ISSO, especially with respect to POM dynamics. Section **3.3.2**, addresses some of the key factors influencing the surface variability of isotopic characteristics of POM in the highly dynamic frontal region of the ISSO.

3.2 Results

3.2.1 Hydrography

In the ISSO a significant drop in the sea surface temperature (SST) was noted with a decreased from 19.25 to 2.32 °C (Fig. 3.1a). The sea surface salinity (SSS) values decreased by 1.79 meridionally (Fig.3.1b), whereas zonally the decline was ~1 (at 40 and 43°S) during 2012. However the gradient in SSS was less (0.26) during 2013. Moreover, significant variability was noted within the STF during both the study seasons (Table 3.1 & Table 3.2) and this was mainly a result of the influence of eddies on the hydrography of this region. In contrast, the TIO surface waters did not show much variation in temperature and salinity and ranged from 27.66 to 29.37 °C and 33.77 to 35.50, respectively (Fig 3.1a & b). The SSS, declined by ~0.59 across the equator. A comparison between the two years showed that there was no significant difference in the variability trends and the range of temperature and salinity during the two consecutive years of study (Table 3.1 & Table 3.2)

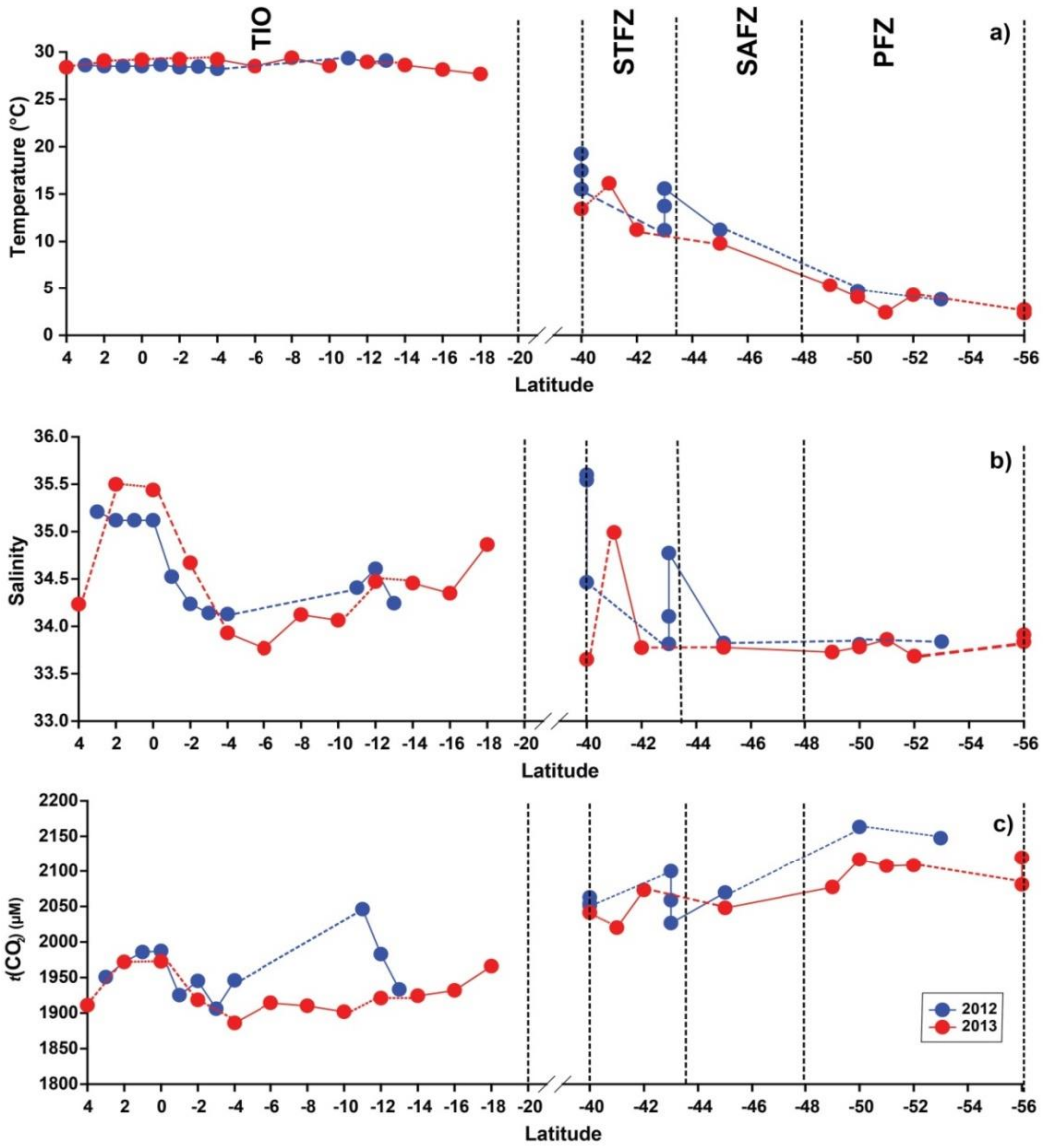

Figure 3.1: Latitudinal variation of (a) Temperature, (b) Salinity and (c) tCO_2 in the surface waters, of the TIO and across the fronts of the ISSO during austral summer 2012 (**Blue**) and austral summer 2013(**Red**).

Region	Latitude	SST (°C)	Salinity	tCO_2 (µM)	NO_3 (µM)	NH_3 (µM)	N:P	N:Si	Chl-*a* (µg/L)	POC (µg/L)	PN (µg/L)	C:N (m/m)	$\delta^{13}C_{(POM)}$ (‰)	$\delta^{15}N_{(POM)}$ (‰)	POC/Chl-*a*	Dominant phytoplankton community * (%abundance)
TIO	3°N-13°S	28.65 (28.21 - 29.33)	34.56 (34.13-35.21)	1961 (1905-2045)	0.28 (0.07-0.61)	1.89 (1.49-2.13)	2.01 (1.73-2.30)	1.34 (1.11-1.80)	0.47 (0.29-0.71)	30.50 (18.93-45.72)	4.27 (3.15-6.97)	8.46 (5.18-12.66)	-26.28 (-26.82 to -25.52)	-0.88 (-5.09 to 2.45)	70.17 (35.05-168.40)	Prokaryotes (46%)
STFZ	40°S-43°S	15.44 (11.18-19.25)	34.72 (33.81-35.60)	2058 (2026-2099)	5.24 (0.61-10.58)	1.90 (1.29-2.30)	4.08 (1.90-7.24)	5.44 (1.46-12.14)	0.46 (0.11-1.13)	51.70 (36.88-71.33)	10.35 (4.64-14.88)	6.75 (3.79-14.83)	-22.81 (-24.55 to -21.40)	2.05 (0.68 to 4.09)	156.74 (62.94-324.47)	Flagellates (93%)
SAFZ	45°S	11.21	33.82	2069	2.73	1.82	3.19	3.71	0.81	31.44	7.54	4.86	-24.81	2.89	38.97	Diatoms (59%)
PFZ	50°S-53°S	4.26 (3.79-4.73)	33.82 (33.81-33.84)	2155 (2146-2163)	23.18 (23.00-23.35)	2.25 (1.85-2.64)	8.97 (7.05-10.89)	4.80 (3.04-6.57)	0.48 (0.34-0.62)	48.45 (41.97-54.94)	9.30 (7.49-11.11)	6.15 (5.77-6.53)	-25.82 (-25.99 to -25.65)	0.29 (0.26 to 0.32)	106.34 (88.04-124.65)	

Table 3.1: Average values of temperature, salinity, tCO_2, NO_3, NH_3, N:P, N:Si (N= NO_3+NO_2+NH_3), POC, PN, C:N(m/m), $\delta^{13}C_{(POM)}$ and $\delta^{15}N_{(POM)}$ POC/Chl-*a* and dominating phytoplankton community (% abundance) in surface samples along the cruise transect, during austral summer 2012. Range is in parentheses.

*Dominant phytoplankton community is based on diagnostic pigment index.

Region	Latitude	SST (°C)	Salinity	tCO_2 (µM)	NO_3 (µM)	NH_3 (µM)	N:P	N:Si	Chl-*a* (µg/L)	POC (µg/L)	PN (µg/L)	C:N (m/m)	$\delta^{13}C_{(POM)}$ (‰)	$\delta^{15}N_{(POM)}$ (‰)	POC/Chl-*a*	Dominant phytoplankton community * (%abundance)
TIO	4°N-18°S	28.73 (27.66-29.37)	34.49 (33.77-35.50)	1927 (1885-1972)	0.21 (0.09-0.35)	2.52 (1.94-3.11)	4.34 (2.86-5.15)	1.09 (0.90-1.35)	0.22 (0.05-1.11)	30.45 (15-54.43)	4.68 (2.77-8.42)	7.54 (6.32-8.65)	-24.21 (-25.24 to -22.26)	1.06 -2.00 to 4.35	271.24 (46.98-598.26)	Prokaryotes (53%)
STFZ	40°S-43°S	13.60 (11.24-16.13)	34.14 (33.65-34.99)	2045 (2020-2073)	10.10 (0.78-15.40)	1.71 (0.99-2.37)	7.25 (3.17-10.15)	3.38 (1.68-4.46)	0.26 (0.20-0.33)	92.93 (61.31-113.05)	10.25 (8.30-12.89)	10.63 (8.62-13.82)	-24.58 (-25.45 to -24.05)	0.32 (-3.07 to 3.77)	364.37 (314.40-439.58)	Flagellates (51%)
SAFZ	45°S	9.77	33.78	2047	12.22	2.55	9.12	4.38	0.67	56.53	8.65	7.62	-24.68	-0.53	84.92	Mixed (29% Diatoms+ 39%Flagellates+ 32%prokaryotes)
PFZ	49°S-56.5°S	3.52 (2.32-5.32)	33.80 (33.69-33.91)	2101 (2077-2119)	21.47 (12.34-27.06)	2.61 (2.07-3.10)	13.30 (11.49-17.21)	2.57 (0.98-5.31)	0.38 (0.31-0.46)	51.71 (42.24-69.95)	7.76 (5.34-8.51)	7.86 (6.25-9.90)	-26.20 (-26.77 to -25.35)	-1.19 (-2.53 to 0.15)	142.85 (102.39-222.30)	Diatoms (61%)

Table 3.2: Average values of temperature, salinity, tCO_2, NO_3, NH_3, N:P, N:Si (N= NO_3+NO_2+NH_3), POC, PN, C:N (M/M), $\delta^{13}C_{(POM)}$ and $\delta^{15}N_{(POM)}$ POC:Chl-*a* and dominating phytoplankton community (% abundance) in surface samples along the cruise transect, during austral summer 2013. Range is in parentheses.

*Dominant phytoplankton community is based on diagnostic pigment index

3.2.2 tCO_2, Nutrients and Chl-a

The concentrations of tCO_2 increased from TIO to PF and ranged from 1885 µM to 2162 µM (Table 3.1 & 3.2). In the ISSO waters, the concentrations showed a steady increase from 2020 µM to 2163 µM (Fig 3.1c) from STF to PF. However, in the TIO, tCO_2 concentrations increased towards equator and further declined sharply across the equator and further increased.

The ISSO surface waters displayed a strong gradient in the concentration of nitrate across the fronts, with the lowest nitrate in STF (0.61 µM) and maximum in PF (27.06 µM) (Table 3.1 & 3.2), especially during 2012. However the variability within the STF was high during both the study periods (Fig. 3.2a). Unlike nitrate, the phosphate gradient across fronts was very small (Fig 3.2b), and ranged from 1.24 µM to 3.65 µM (Table 3.1 & 3.2). Also, the silicate concentration increased gradually by a small magnitude from the STF to the PF (Fig. 3.2c), with a maximum at 56.5 °S often considered as the PF-II. The variability was quite similar for both 2012 and 2013 (Table 3.1 & 3.2). However, ammonium did not show much change in the ISSO waters and varied from 0.99 to 3.1 µM.

In contrast to the ISSO, surface nutrients in the TIO were considerably low. This region being considered as oligotrophic, the observed nutrient concentrations are fairly justified. The nitrate was low and ranged from 0.07 to 0.61 µM (Fig 3.2a). However, the phosphates varied from 0.70 to 1.51 µM, although a small range was comparatively higher in 2012 (Fig. 3.2b). The silicates were also low (1.28 to 3.43 µM) in these waters (Fig. 3.2c). Unlike other nutrients, ammonium showed a wider

variation and ranged from 1.49 to 3.11µM, and was on an average higher in 2013 (Table 3.1 & 3.2).

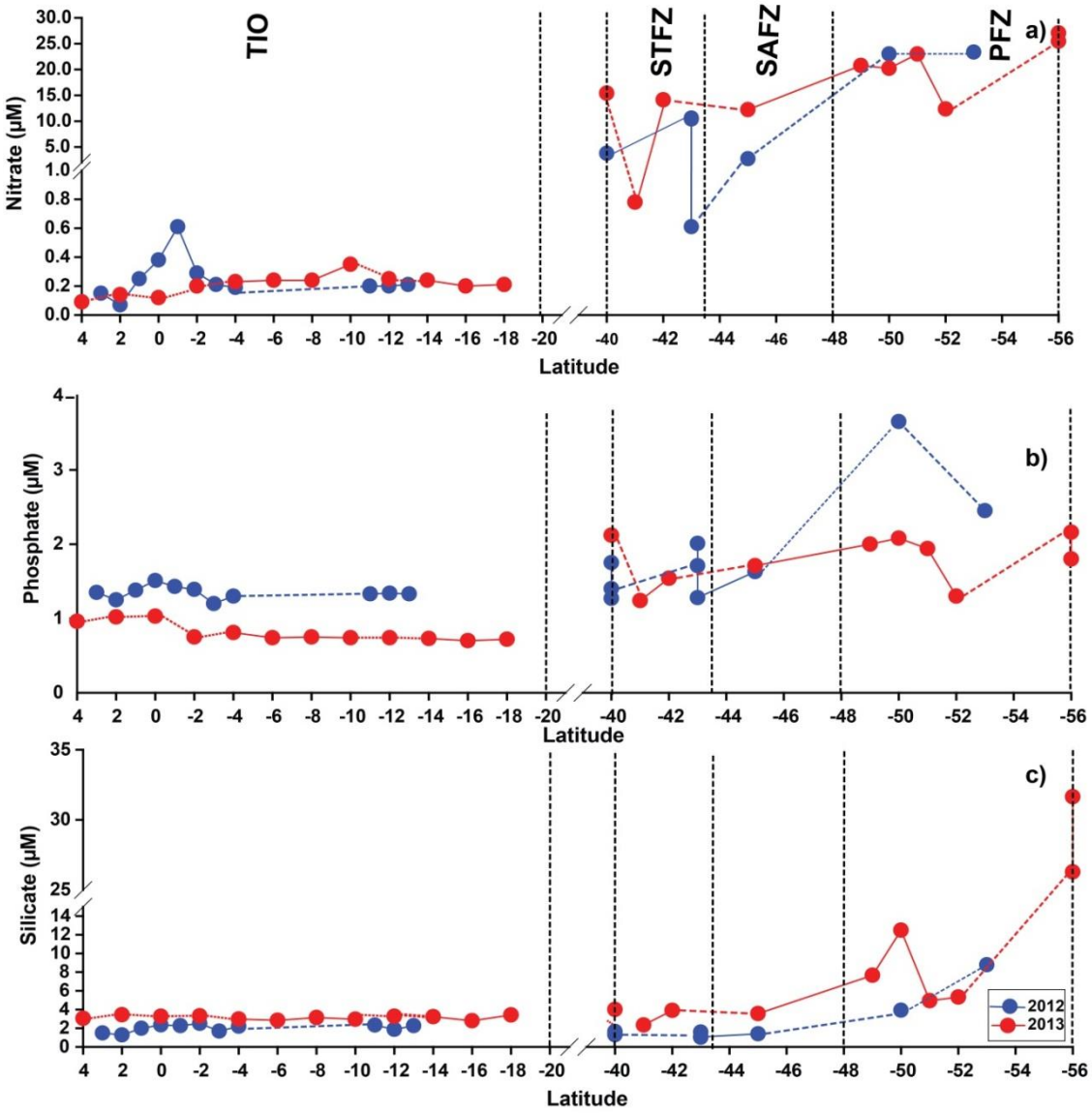

Figure 3.2: Latitudinal variation of (a)Nitrate, (b)Phosphate and (c)Silicate in the surface waters, of the TIO and across the fronts of the ISSO during austral summer 2012 (**Blue**) and austral summer 2013(**Red**).

The N:P ratio increased from 4.08 in the STF to 8.97 in the PF in 2012, but was comparatively higher during 2013 (Table 3.1). Moreover, in the TIO the N:P ratio was 2.01 on an average, in 2012, but was comparatively higher in 2013 (4.34) which is likely a result of higher contribution of ammonium to the dissolved inorganic nitrogen. Also, the N:Si, showed a greater variation across the fronts from 1.46 to 12.14 in the STF and 3.04 to 6.57 in the PF (Table 3.1), especially during 2012, unlike 2013 which had an overall range of 0.98-5.31 across the fronts (Table 3.2). Although the ratio was closer to 1 in the TIO with an average of 1.34 and 1.09, during 2012 and 2013 respectively, this was mainly due to the nitrate limitation in these waters.

The overall Chl-*a* concentration was considerably higher in 2012 throughout the study section (Fig. 3.3a), and ranged from 0.04 to 1.13 µg/L with no specific distribution pattern. In the ISSO, higher concentration of Chl-*a* was observed at STF and SAF (Fig. 3.3a), and varied from 0.11 to 1.13 µg/L. Further north in the TIO, the concentration remained between 0.05 to 1.11 µg/L with a maximum Chl-*a* concentration of 0.71 µg/L at 4°S, during 2012. However in 2013 the Chl-*a* concentration was comparatively low in both the oceanic regimes. Chl-*a* decreased from 4°N towards equator beyond which it remained constantly low (≤ 0.2) within the TIO (Fig. 3.3a). Also, in the ISSO the Chl-*a* observed was low at STF, especially in 2013, however, moderately higher in the SAF and PF (Fig. 3.3a).

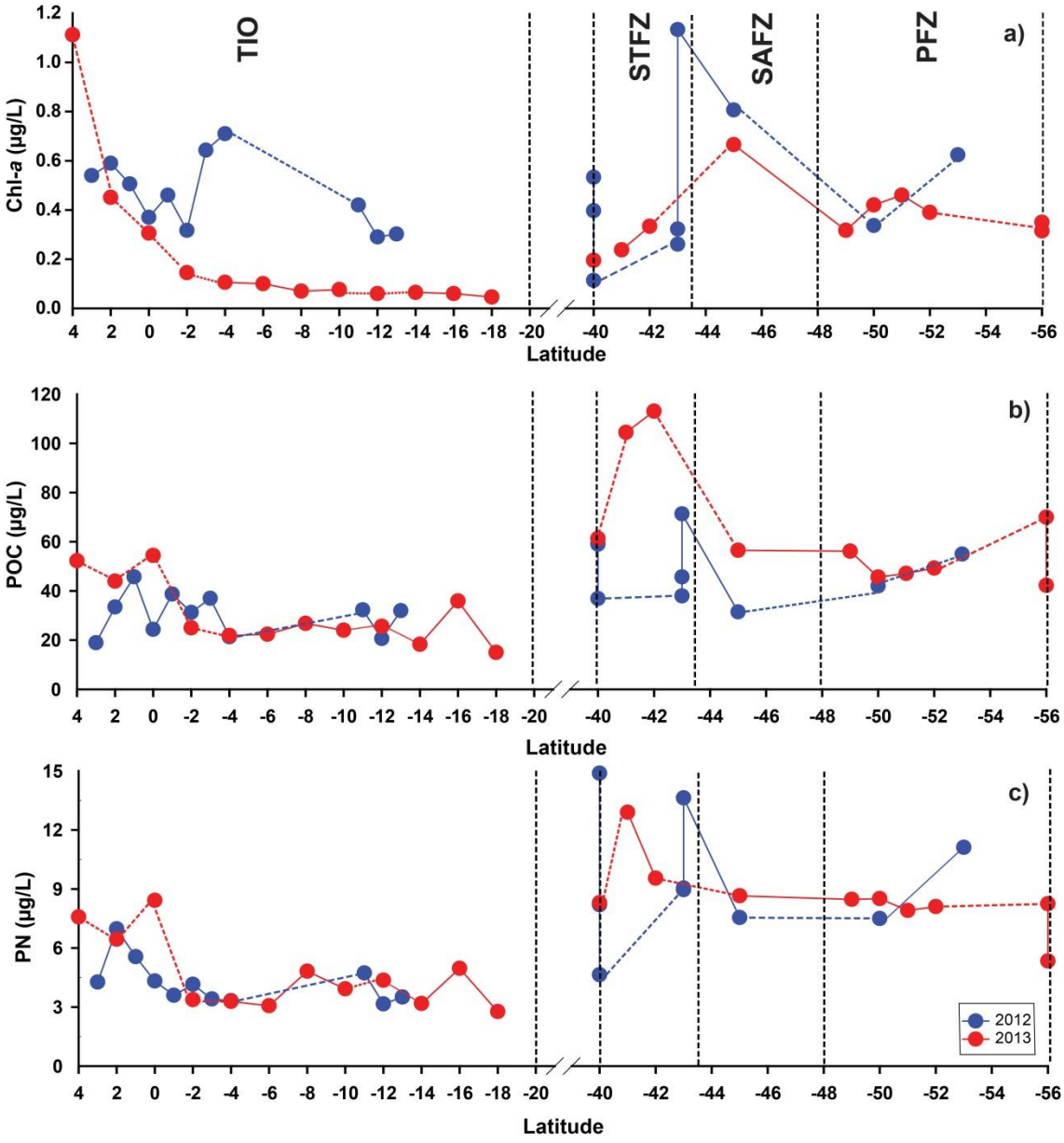

Figure 3.3: Latitudinal variation of (a) Chlorophyll-*a* (Chl-*a*), (b) POC and (c) PN in the surface waters, of the TIO and across the fronts of the ISSO during austral summer 2012 (**Blue**) and austral summer 2013(**Red**).

3.2.3 Characteristics of POM

POC ranged from 15 to 113 µg/L during the entire study period. Also, POC showed a significant variation during the two study periods within the ISSO (Fig.

3.3b). The average POC in the TIO waters was 30.50 µg/L, which increased to 51.70 µg/L in the STF and dropped to 48.45 µg/L in PF (Table 3.1) during 2012. Although the POC concentration in TIO was similar in 2013, with an average of 30.45 µg/L, and decreased towards the equator and remained moderately low, especially in 2013. The POC concentration was significantly different in ISSO (Fig. 3.3b), and varied from 92.93 µg/L in in STF, and decreased towards SAF (56.53 µg/L) and 51.71 µg/L in the PF (Table 3.2). Also, a large scale variation was observed at STF during both the periods (2012 & 2013), ranging from 36.88 to 113 µg/L (Table 3.1 & 3.2). The POC contribution to POM decreased at SAF and PF during both the years of study. The spatial variation of PN in the surface waters was similar to POC (Fig. 3.3b) during both the periods.

Overall, in the TIO, the PN ranged from 2.77 to 8.42 µg/L (Table 3.1 & 3.2), while in ISSO it ranged from 4.64 to 14.88 µg/L, across the fronts. Likewise, the PN concentration was a notch higher in 2013; however, the distribution pattern remained similar, with a higher variability in the STF and a slight decrease towards PF (Fig 3.3c).

$\delta^{13}C_{(POM)}$ was lower (depleted) in TIO with an average of -26.28 ‰ during 2012, however the POM was comparatively enriched during 2013, with an average of -24.21 ‰. Likewise in the ISSO waters $\delta^{13}C_{(POM)}$ ranged from -21.40 to -26.77 ‰ (Fig. 3.4a), during both the consecutive years. Within ISSO, the $\delta^{13}C_{(POM)}$ average in STF (-22.81 ‰) was higher by ~3 ‰, compared to PF (-25.82 ‰) (Table 3.1) during 2012. However, the variability was comparatively less during 2013, with a gradual depletion of 1.6 ‰ from the average $\delta^{13}C_{(POM)}$ STF (-24.58 ‰) towards the PF (-26.20‰). Unlike $\delta^{13}C_{(POM)}$, the $\delta^{15}N_{(POM)}$ showed large variations ranging from (-5.09 ‰ to 4.35 ‰) during the two study periods. $\delta^{15}N_{(POM)}$ in TIO was lower, ranged from

-5.09 to 1.08‰ and -2.00 to 4.35 ‰, during 2012 and 2013, respectively, and did not show any specific pattern (Fig. 3.4b). While, in the ISSO, $\delta^{15}N_{(POM)}$ values were higher and more variable in the STF (2012: 0.68 to 4.09 ‰; 2013: -3.04 to 3.77 ‰) which decreased in PF waters (2012: 0.26 to 0.32 ‰; 2013: -2.53 to 0.15 ‰), implying more depletion in 2013 (Table 3.2; Fig 3.4b).

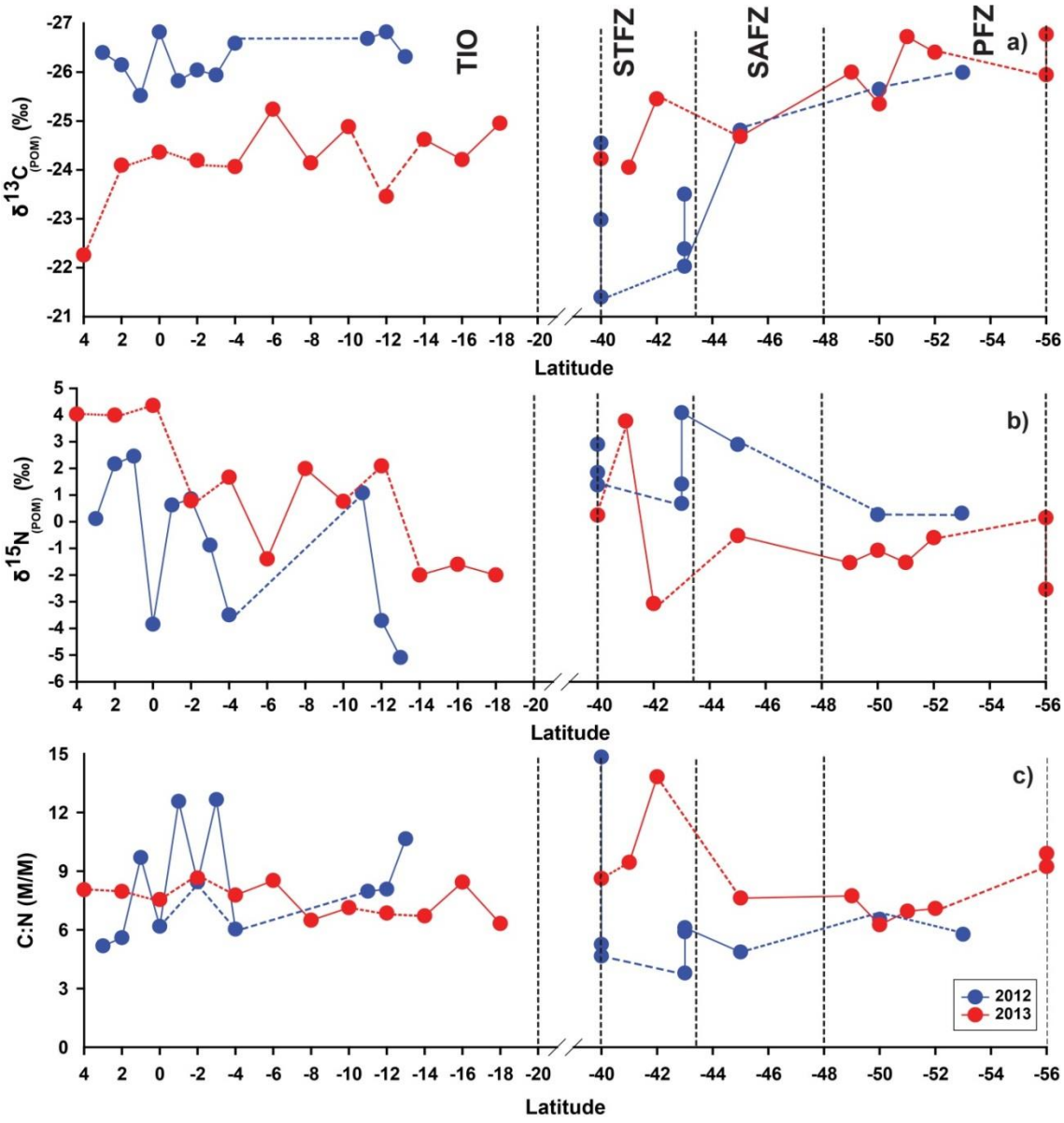

Figure 3.4: Latitudinal variation of (a) $\delta^{13}C_{(POM)}$, (b) $\delta^{15}N_{(POM)}$ and (c) C:N (M/M) in the surface waters, of the TIO and across the fronts of the ISSO during austral summer 2012 (**Blue**) and austral summer 2013 (**Red**).

The overall C:N ratio in the ISSO, displayed a wide range, with the maximum variability from 3.79 to 14.83 in the STF (Fig. 3.4c) during both the years. Beyond STF, the C:N variability was comparatively less during both the periods, and the ratios observed (Table 3.1 & 3.2) were mostly closer the reported C:N ratio of phytoplankton. In the TIO, the average C: N ratio was 8.46, and showed a wide variation from 5.18 to 12.66, and an average of 7.54 with a smaller range from 6.32 to 8.65 in 2013 (Fig. 3.4c) in TIO surface waters.

3.2.4 Statistical analyses

3.2.4.1 Pearson's Correlations

The Pearson's Correlation analysis of various physical and biochemical variable for the ISSO was carried out during both the periods (2012 and 2013). During both the years, SST showed a significant inverse correlation with tCO_2 and nitrate. Also, $\delta^{13}C_{(POM)}$ had a linear positive relation with temperature and an inverse correlation with tCO_2 and nitrate. Also an inverse correlation was observed between $\delta^{15}N_{(POM)}$ and nitrate as shown below (Table 3.3 and 3.4).

In TIO, the Pearson's correlations of various physico-chemical and biological variables is illustrated in Table 3.5 and 3.6. The observed correlations among many biochemical variables were not as significant in the TIO as in the ISSO. However, a significant correlation was observed between $\delta^{13}C_{(POM)}$ and POC, and also $\delta^{15}N_{(POM)}$ with PN, especially during 2012, along with an influence of nutrients on the POM characteristics during 2013 (Table 3.5 & 3.6). Additionally, a significant linear correlation between POC and PN and also $\delta^{13}C_{(POM)}$ $\delta^{15}N_{(POM)}$ was observed in the entire study area indicating common source and the POM is of allochthonous origin.

Variables	Temperature	Salinity	$t(CO_2)$	Nitrate	Ammonia	Phosphate	Silicate	Chl-*a*	POC	PN	$\delta^{13}C_{(POM)}$	$\delta^{15}N_{(POM)}$	C:N(m/m)
Temperature	**1**												
Salinity	**0.818**	**1**											
***t*(CO_2)**	**-0.901**	**-0.587**	**1**										
Nitrate	**-0.928**	**-0.699**	**0.923**	**1**									
Ammonia	-0.263	-0.075	0.135	0.326	**1**								
Phosphate	**-0.828**	**-0.605**	**0.869**	**0.890**	0.215	**1**							
Silicate	**-0.763**	-0.368	**0.746**	**0.787**	**0.644**	**0.563**	**1**						
Chl-*a*	-0.100	-0.173	-0.258	-0.175	0.168	-0.209	0.029	**1**					
POC	0.182	0.315	-0.309	-0.150	0.441	-0.193	0.078	**0.528**	**1**				
PN	0.001	-0.180	-0.251	-0.006	0.392	-0.112	0.071	0.488	0.868	**1**			
$\delta^{13}C_{(POM)}$	**0.680**	0.328	**-0.787**	**-0.619**	-0.048	**-0.555**	**-0.686**	0.178	**0.534**	0.443	**1**		
$\delta^{15}N_{(POM)}$	**0.574**	0.426	**-0.730**	**-0.792**	-0.278	**-0.703**	**-0.576**	**0.681**	0.423	0.123	**0.507**	**1**	
C:N(m/m)	0.264	0.567	-0.088	-0.228	0.070	-0.117	-0.052	-0.080	0.367	**-0.557**	0.099	0.282	**1**

Table 3.3: Pearson's correlation matrix for SO region during austral summer 2012. All values in bold imply significant correlation between the variables (significance level of alpha=0.05).

Variables	Temperature	Salinity	$t(CO_2)$	Nitrate	Ammonia	Phosphate	Silicate	Chl-*a*	POC	PN	$\delta^{13}C_{(POM)}$	$\delta^{15}N_{(POM)}$	C:N(m/m)
Temperature	**1**												
Salinity	**0.511**	**1**											
***t*(CO$_2$)**	**-0.900**	**-0.508**	**1**										
Nitrate	**-0.836**	**-0.618**	**0.723**	**1**									
Ammonia	**-0.504**	0.083	0.406	0.252	**1**								
Phosphate	-0.418	**-0.539**	0.246	**0.748**	0.060	**1**							
Silicate	**-0.617**	-0.132	**0.509**	**0.724**	0.373	0.393	**1**						
Chl-*a*	-0.313	-0.290	0.239	0.093	0.309	-0.033	-0.102	**1**					
POC	**0.710**	**0.531**	**-0.627**	**-0.601**	**-0.738**	-0.471	-0.344	-0.381	**1**				
PN	**0.749**	**0.734**	**-0.729**	**-0.846**	-0.360	-0.498	**-0.623**	-0.238	**0.753**	**1**			
$\delta^{13}C_{(POM)}$	**0.897**	0.426	**-0.872**	**-0.727**	-0.349	-0.145	**-0.511**	-0.189	**0.510**	**0.703**	**1**		
$\delta^{15}N_{(POM)}$	**0.561**	**0.758**	**-0.678**	**-0.669**	0.070	-0.304	-0.271	-0.304	0.312	**0.730**	**0.653**	**1**	
C:N(m/m)	0.393	0.147	-0.301	-0.135	**-0.760**	-0.241	0.070	-0.365	**0.811**	0.227	0.147	-0.162	**1**

Table 3.4: Pearson's correlation matrix for SO region during austral summer 2013. All values in bold imply significant correlation between the variables (significance level of alpha=0.05).

Variables	Temperature	Salinity	*t*(CO_2)	Nitrate	Ammonia	Phosphate	Silicate	Chl-*a*	POC	PN	$\delta^{13}C_{(POM)}$	$\delta^{15}N_{(POM)}$	C:N(m/m)
Temperature	**1**												
Salinity	-0.108	**1**											
***t*(CO_2)**	**0.507**	0.359	**1**										
Nitrate	-0.057	-0.095	-0.222	**1**									
Ammonia	0.274	-0.179	0.215	**0.622**	**1**								
Phosphate	0.009	0.356	0.249	**0.676**	**0.765**	**1**							
Silicate	0.175	-0.478	0.136	**0.574**	**0.876**	**0.596**	**1**						
Chl-*a*	**-0.563**	0.007	-0.272	-0.267	**-0.615**	**-0.548**	**-0.500**	**1**					
POC	0.014	-0.035	-0.079	0.288	-0.005	-0.087	0.073	0.072	**1**				
PN	-0.090	**0.641**	0.424	-0.351	-0.264	-0.092	-0.442	0.195	**0.558**	**1**			
$\delta^{13}C_{(POM)}$	-0.345	0.035	-0.438	0.239	-0.182	-0.145	-0.136	0.255	**0.836**	0.288	**1**		
$\delta^{15}N_{(POM)}$	-0.137	0.339	0.202	-0.014	-0.274	-0.127	-0.294	0.277	**0.574**	**0.681**	**0.628**	**1**	
C:N(m/m)	0.172	-0.498	-0.466	**0.515**	0.083	-0.113	0.253	-0.123	**0.675**	-0.386	**0.574**	0.032	**1**

Table 3.5: Pearson's correlation matrix for TIO region during austral summer 2012. All values in bold imply significant correlation between the variables (significance level of alpha=0.05).

Variables	Temperature	Salinity	*t*(CO_2)	Nitrate	Ammonia	Phosphate	Silicate	Chl-*a*	POC	PN	$\delta^{13}C_{(POM)}$	$\delta^{15}N_{(POM)}$	C:N(m/m)
Temperature	**1**												
Salinity	0.126	**1**											
***t*(CO_2)**	-0.188	**0.903**	**1**										
Nitrate	-0.059	**-0.556**	**-0.508**	**1**									
Ammonia	0.294	-0.213	-0.360	**0.650**	**1**								
Phosphate	0.340	**0.623**	0.471	**-0.757**	-0.408	**1**							
Silicate	0.189	**0.770**	**0.629**	-0.302	0.140	0.329	**1**						
Chl-*a*	-0.034	0.164	0.072	**-0.733**	**-0.611**	**0.704**	0.049	**1**					
POC	0.204	0.485	0.383	**-0.777**	**-0.701**	**0.855**	0.037	**0.742**	**1**				
PN	0.236	**0.519**	0.417	**-0.732**	**-0.664**	**0.856**	0.121	**0.700**	**0.978**	**1**			
$\delta^{13}C_{(POM)}$	0.175	0.026	-0.176	**-0.563**	-0.322	0.426	0.055	**0.768**	**0.572**	**0.565**	**1**		
$\delta^{15}N_{(POM)}$	**0.604**	0.403	0.141	**-0.530**	-0.193	**0.838**	0.277	**0.624**	**0.764**	**0.801**	**0.628**	**1**	
C:N(m/m)	0.115	-0.065	-0.115	-0.351	-0.322	0.225	-0.408	0.305	0.375	0.182	0.144	0.116	**1**

Table 3.6: Pearson's correlation matrix for TIO region during austral summer 2013. All values in bold imply significant correlation between the variables (significance level of alpha=0.05).

3.2.4.2 Principle Component Analysis (PCA)-Factor Analysis

PCA-Factor analysis was carried out for the analysed environmental variables to identify the major governing factors/processes in the two oceanic regimes.

In the ISSO the factors influencing POM characterisation was summed up into four major factors: 1) the environmental factor or the hydrography influenced factor, that include temperature, and availability of nutrients; 2) The tCO_2 abundance and variability that influence the $\delta^{13}C_{(POM)}$ of surface waters; 3) Primary productivity; 4) Nutrient (Silicate) dependent shift in phytoplankton community. The first two strongly controlled by physico-chemical parameters and the other two are biological factors. A minor contribution from regenerative production and phosphate driven production. This sum up to 70% of the factors influencing in the ISSO (Table 3.7).

Variables	F1	F2	F3	F4
Temperature	**0.912**	-0.190	0.056	-0.327
Salinity	**0.748**	-0.053	-0.078	0.076
***t*(CO_2)**	**-0.708**	**0.503**	-0.187	-0.074
Nitrate	**-0.946**	0.042	-0.184	0.103
Ammonia	-0.303	0.192	0.034	**0.720**
Phosphate	**-0.604**	0.403	0.021	-0.337
Silicate	**-0.525**	-0.072	-0.283	**0.505**
Chl-*a*	0.112	0.173	**0.540**	0.159
POC	0.075	**-0.888**	0.200	-0.120
PN	0.198	-0.325	**0.862**	-0.046
$\delta^{13}C_{(POM)}$	**0.697**	0.021	0.438	-0.243
$\delta^{15}N_{(POM)}$	**0.719**	0.224	0.412	-0.051
Eigenvalue	**5.52**	**1.08**	**1.00**	**0.82**
Variability (%)	**45.96**	**8.98**	**8.30**	**6.80**
Cumulative %	**45.96**	**54.94**	**63.24**	**70.04**

Table 3.7: Correlations between variables and factors after Varimax rotation: Factor loading for ISSO region, during austral summer.

Within the TIO, biological processes were the major contributing processes followed by hydrographical factor responsible for 74% of the factor loading. One of the major factors being the regenerative production that is phytoplankton productivity based on ammonia that regulates the Chl-*a* biomass and the POM characteristics; second being the heterotrophic activity altering the POM concentration and variability; third is

hydrography driven process and the forth significant contributing process is the nitrate driven phytoplankton community productivity (Table 3.8).

Variables	F1	F2	F3	F4
Temperature	**0.228**	0.204	0.154	0.168
Salinity	-0.117	0.369	**0.659**	-0.056
***t*(CO_2)**	-0.315	0.081	**0.884**	-0.013
Nitrate	0.024	-0.307	-0.152	**0.532**
Ammonia	**0.953**	-0.119	-0.114	0.184
Phosphate	**-0.823**	0.032	0.358	0.399
Silicate	**0.834**	0.168	-0.118	-0.018
Chl-*a*	**-0.695**	0.463	-0.120	-0.110
POC	-0.195	**0.864**	-0.006	0.088
PN	-0.076	**0.924**	0.259	-0.190
$\delta^{13}C_{(POM)}$	**0.653**	0.546	-0.458	-0.211
$\delta^{15}N_{(POM)}$	0.251	**0.804**	0.007	0.012
Eigenvalue	**3.99**	**3.16**	**1.07**	**0.63**
Variability (%)	**33.26**	**26.35**	**8.89**	**5.26**
Cumulative %	**33.26**	**59.61**	**68.50**	**73.76**

Table 3.8: Correlations between variables and factors after Varimax rotation: Factor loading for TIO region, during this study.

3.3 Discussion

3.3.1 Spatial distribution of particulate organic carbon, nitrogen and the stable isotopic characteristics of carbon and nitrogen in the surface waters of the oceanic regimes of the Indian sector

The two oceanic regimes are governed by different contributing factors and processes. This is also ascertained from the PCA analysis (Table 3.7 & Table 3.8, Fig. 3.5) which displayed 2 large clusters for the ISSO and TIO observations. These governing factors are the major variables and processes responsible in determining the POM characteristics in the two oceanic regimes.

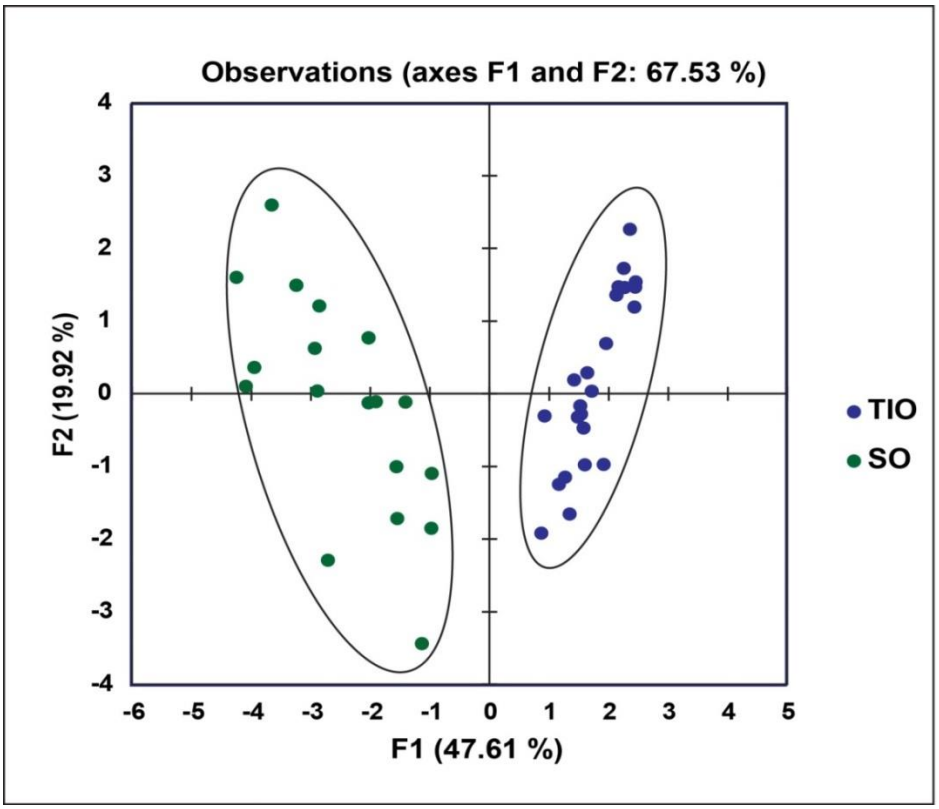

Figure 3.5: PCA analysis illustrating separate clusters for TIO, and ISSO, based on the governing factors across the two oceanic regimes, during the study.

The POC concentration observed in the surface waters during this study was well within the range of the earlier POC studies carried out in the different regions globally. Some of the earlier studies in the high latitude waters including other sectors of SO, namely Southern Pacific Ocean (Kennedy and Robertson, 1995), Southern Atlantic Ocean (Lara et al., 2010), Southern Indian Ocean (Bentaleb et al., 1996), Arctic Ocean (Zhang et al., 2011), Prydz Bay (Zhang et al., 2014) were compared with the POC observed in the current study, and was similar, except for the high POC observed south of SB in some of the earlier studies (Fig. 3.6).

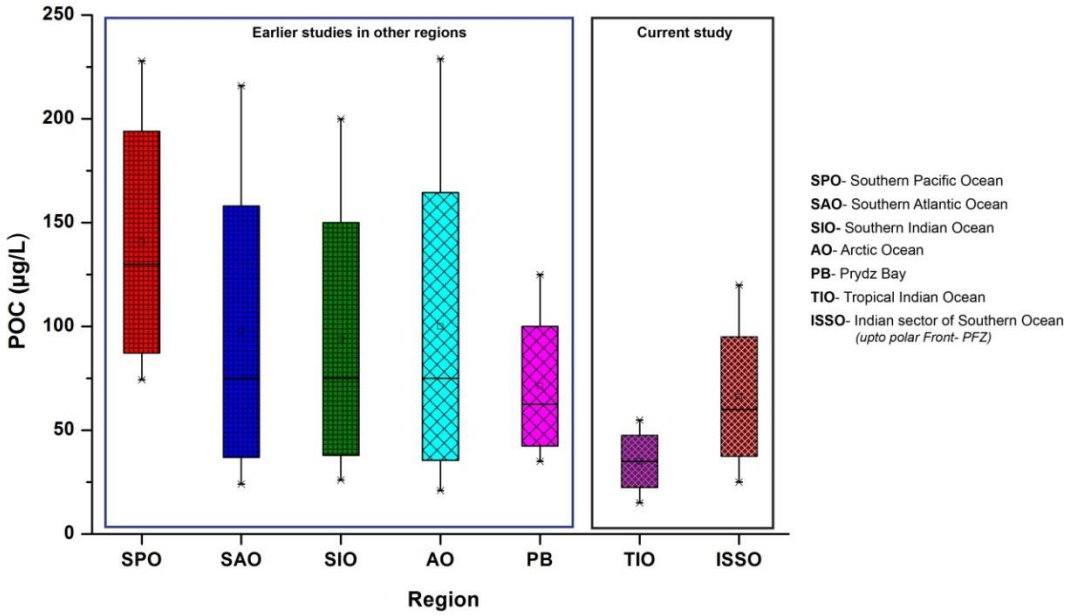

Figure 3.6: A comparative analysis of the range of POC (µg/L) concentration, in different regions especially, high latitude waters and the current study.

3.3.1.1 Indian sector of the Southern Ocean (ISSO)

The prevalence of high wind speeds in the ISSO and the decrease in temperature favours strong wind driven mixing, thereby supporting higher dissolution and increase in the concentration of dissolved gasses like tCO_2. The colder ISSO waters were also nutrient rich, especially with nitrates and silicates. A general trend with a southward lowering/depletion of $\delta^{13}C_{(POM)}$ was observed from 40°S onwards, as observed in most of the high latitude regions. The isotopic values observed in ISSO were comparable to that observed in other high latitude studies like the South Pacific (-27.89 to -24.47 ‰), Arctic (-28.5 to -21.1 ‰) and Prydz Bay, Antarctica (-27.4 to -19.0 ‰) (Kennedy and Robertson, 1995; Zhang et al., 2011; Zhang et al., 2014). This was mostly associated with the uptake of isotopically lighter carbon by phytoplankton resulting in the low $\delta^{13}C_{(POM)}$ in surface waters (Rau et al., 1992; Georicke and Fry, 1994, Gruber et al, 1999).

Within the ISSO, maximum variability in the biochemical components of the surface waters, from nutrients to the isotopic composition of POM ($\delta^{13}C_{(POM)}$ and $\delta^{15}N_{(POM)}$) was observed at the STF. The STF (40°S-43°S) is an eddy prone region (Sabu et al., 2015, George et al., 2018), causing hydrographical changes in this region, responsible for the redistribution of nutrients and other components present in the water. The high $\delta^{13}C_{(POM)}$ and $\delta^{15}N_{(POM)}$ in the STF region coincided with the eddy (cyclonic eddy) influenced locations in in this region. This was similar to an earlier study by Kolasinski et al. (2012), that attributed this enrichment to the upwelling of deep water nitrate. However, the $\delta^{15}N_{(POM)}$ values did not match exactly with the typical $\delta^{15}N$ of nitrate from deep waters or new production. Furthermore, the high variability of the available nutrients within the STF and the phytoplankton biomass

(Chl-*a*) was largely responsible for the highly variable elemental and isotopic composition (POC, PN, $\delta^{13}C_{(POM)}$ and $\delta^{15}N_{(POM)}$) of POM in these waters. The low environmental conditions prevailing in the STF surface waters favoured the dominance of flagellates (Fig. 3.7) during both the study periods. Flagellates, especially the dinoflagellates, are phytoplankton known to be less discrimination towards the available carbon species during the uptake and utilisation of carbon, thereby making the $\delta^{13}C_{(POM)}$ heavier (Bentaleb et al., 1996; Bentaleb et al., 1998; Gaul et al., 1999; Lara et al., 2010). The higher C:N ratios observed at certain locations in STF surface waters was mostly associated with high macrozooplankton abundance of mostly salp, pyrosoma and the mesozooplankton biomass was mostly dominated by copepods.

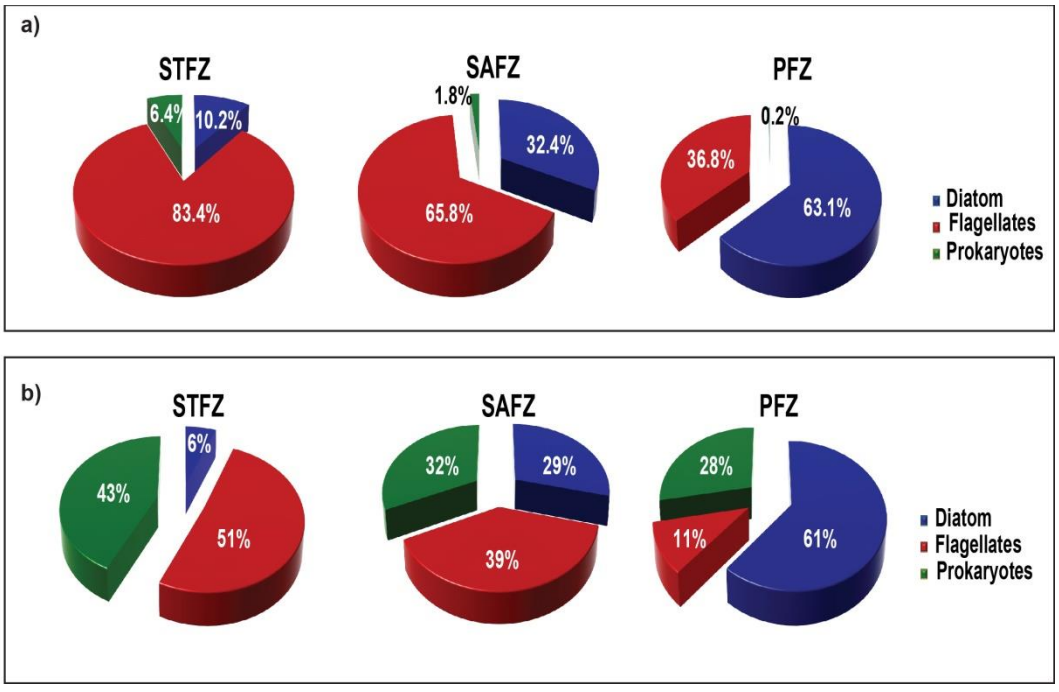

Figure 3.7: Variation of the dominant phytoplankton community across the fronts in the ISSO during austral summer (a) 2012 and (b) 2013

The PF surface waters were rich in nutrients; yet, the high nutrient availability did not match well with the moderate phytoplankton biomass, reported in terms of the Chl-*a* concentration. However, the reported Chl-*a*, matched with the earlier reports in the PF waters of the ISSO (Jasmine et al., 2009; Gandhi et al., 2012; Naik et al., 2015). The N:Si ratio < 1 generally favours the dominance of diatoms community. Although the N:Si ratio was higher, the silicate concentration was not limiting, and favoured the growth of diatoms in these waters which is also reflected from the diagnostic pigment study (Table 3.1 & 3.2). The low $\delta^{13}C_{(POM)}$ and $\delta^{15}N_{(POM)}$ observed in PF waters was attributed to the increased availability of tCO_2 and nitrates, favouring the uptake of lighter tCO_2 and nutrients (Popp et al., 1989; Lourey et al., 2004) during photosynthetic fixation of carbon and nutrients by the phytoplankton (diatoms) community. Furthermore, the C:N ratio of POM was closer to the Redfield ratio of plankton, especially during 2012. Moreover, the POC:Chl-*a* ratio in these waters indicated the existence of fresh organic matter and the prevalence of autotrophy (Bentaleb et al. 1998, Savoye, et al. 2003). Unlike 2012, in the consequent year of study (2013), the C:N ratio ($\geq$ 6.63) was a little higher than the Redfield ratio of living plankton reported by Redfield (1993), and this was supported by a significant contribution of prokaryotic phytoplankton to the system dominated by dinoflagellates and diatoms. Also, during this period the POC:Chl-*a* was >100 but mostly <200, suggesting a contribution from the heterotrophic activity (Savoye, et al. 2003) to the region and the zooplankton contribution (Venkataramana et al., 2020) in these waters also implied from the factor analysis.

3.3.1.2 Tropical Indian Ocean (TIO)

Unlike the ISSO, the warm (avg. 28.65 °C) TIO waters, showed a moderate variations in SSS (~ 1 psu). This decline in salinity was noted immediately below the equator. This drop in salinity is possibly due to the effect of an increased localized precipitation associated with presence of Inter Tropical Convergence Zone (Tiwari et al., 2013). These waters were oligotrophic with low nutrients (Fig. 3.2a, b, & c) especially, nitrates. However, the region witnessed moderate biological productivity, evident from the Chl-*a* concentration (Fig. 3.3a) and decreased across the equatorial waters to a minimum in the subtropical oligotrophic gyre. The major governing processes in these waters were the biological processes, implied from the PCA, factor loading analysis (Table 3.8). These biological processes are highly responsible for the variation of the POM composition in this region. This is also evident from a significant relation of POC with PN (Fig. 3.8b), $\delta^{13}C_{(POM)}$ with $\delta^{15}N_{(POM)}$ and (Fig. 3.8d) and also a considerably significant correlation of $\delta^{13}C_{(POM)}$ with POC (Fig. 3.9a) and $\delta^{15}N_{(POM)}$ with PN (Fig. 3.9b).

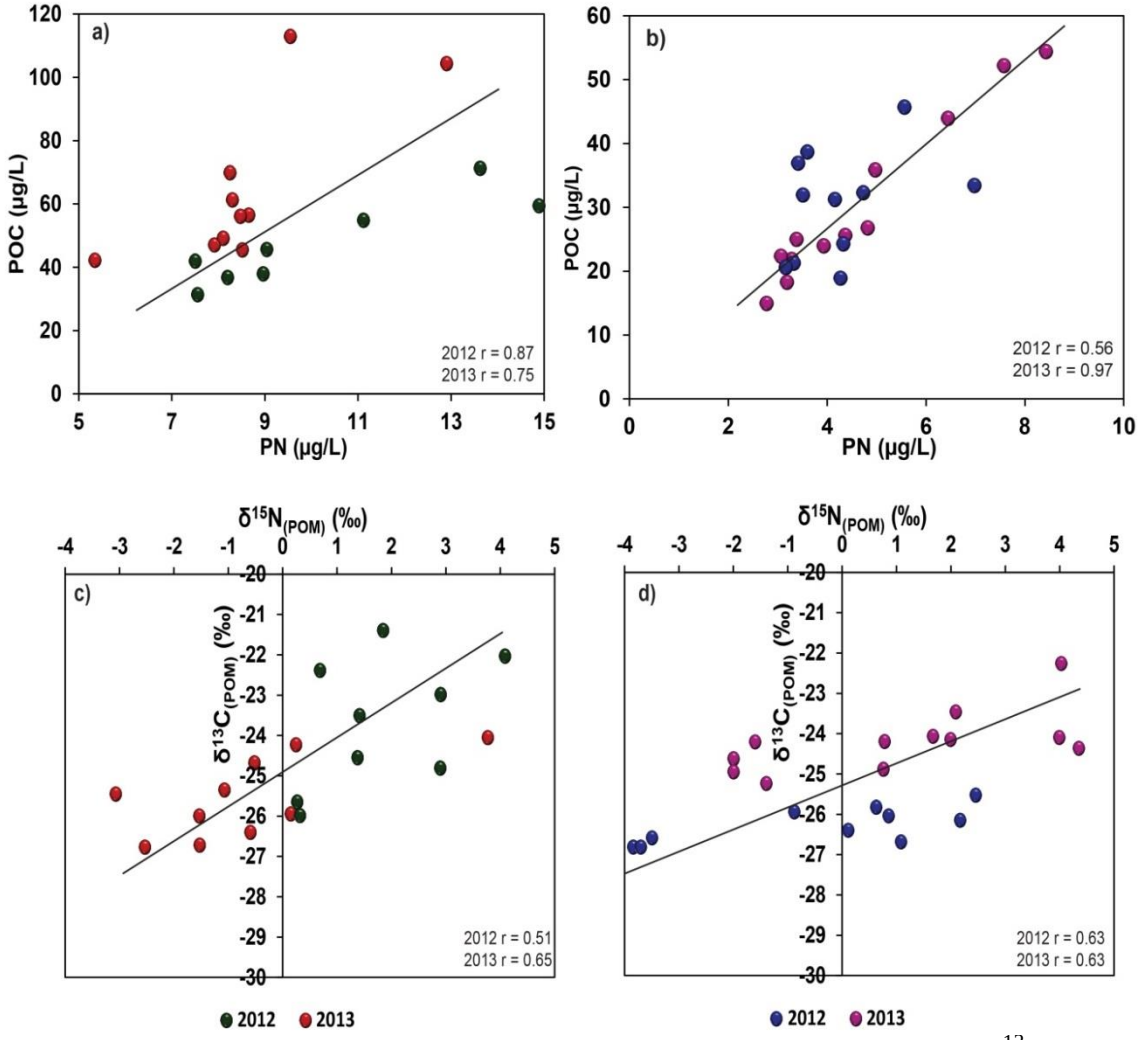

Figure 3.8: Spearman's correlation of POC with PN (a)ISSO, (b)TIO; and $\delta^{13}C_{(POM)}$ with $\delta^{15}N_{(POM)}$ (c) ISSO, (d)TIO, during 2012 and 2013.

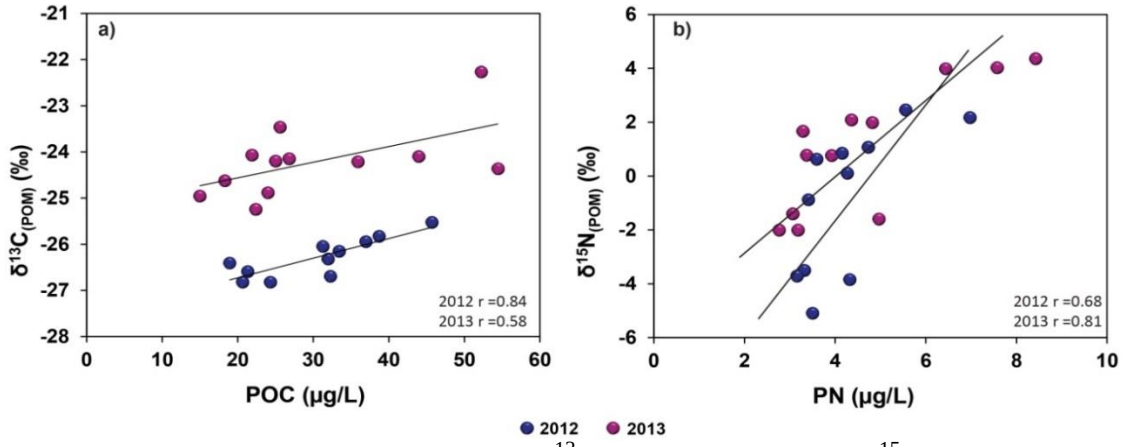

Figure 3.9: Spearman's correlation of (a) $\delta^{13}C_{(POM)}$ and POC; (b) $\delta^{15}N_{(POM)}$ and PN in the TIO surface waters during 2012 and 2013.

The average elemental composition of POM in the TIO waters was moderately low and comparable, during the two consecutive years (Fig. 3.3b & 3.3c). However, it was an irregular pattern in 2012, which matched well with the Chl-*a* pattern. The $\delta^{13}C_{(POM)}$ values in TIO waters, were within the $\delta^{13}C$ reported for marine phytoplankton and matched well with the $\delta^{13}C$ values of picoplankton as reported earlier (Rau et al.,1990; Hansman and Sessions, 2016). The surface waters of the TIO, displayed a dominance of prokaryotic picoplankton (Table 3.1 & 3.2), which again justifies the observed $\delta^{13}C_{(POM)}$ values in this region. Picoplankton biomass is a major contributor to the total biomass in warm, low nutrient (NO_3 + NO_2 <1µM) (Agawin et al., 2000), oligotrophic TIO waters. Furthermore, prokaryotic picoplankton is known to have a small isotope fractionation during carbon fixation (Popp et al., 1998) but preferentially incorporate lighter carbon molecules during lipid biosynthesis (Sakata et al., 1997). However, even though the dominant community between both the years was prokaryotic picoplankton, the ~1 ‰ variation within the two consecutive years of study could likely be associated with the difference in the metabolism, and difference in the carbon source as suggested in some of the earlier studies (Estep et al., 1978; Goericke and Fry, 1994).

Unlike $\delta^{13}C_{(POM)}$, $\delta^{15}N_{(POM)}$ showed large scale variations during both 2012 (-5.09 to +2.45 ‰) and 2013 (-5 to +4 ‰) (Fig. 3.4b). The $\delta^{15}N_{(POM)}$ in TIO was significantly lower than those of marine organic matter range (3 to 12 ‰) (Wada and Hattori 1991; Maksymowska et al., 2000). However, it was apparently in the range (-4 to +5 ‰) observed by Altabet and Francois (2001) and (-3 to +7 ‰) reported by Lourey et al. (2003), in the SO region. To an extent the higher variability of $\delta^{15}N_{(POM)}$ can be explained by the dominance of prokaryotic picoplankton. The high surface to volume ratio of these small organism support efficient nutrient uptake even in nutrient

deficient conditions (Veldhuis et al., 2005). Moreover, the picoplankton community is capable to take up different nitrogen species from nitrate to dissolved organic nitrogen (Zubkov et al., 2003; Gracia-Fernandez et al., 2004) and also ammonia (Moore et al., 2002), this explains the high $\delta^{15}N_{(POM)}$ variability in the TIO surface waters. The simultaneous uptake of nitrate and ammonia is responsible for a higher variation in the $\delta^{15}N_{(POM)}$ depending on the relative uptake ammonia over nitrate which causes large changes in the $\delta^{15}N_{(POM)}$ (Waser et al., 1998). These depleted $\delta^{15}N_{(POM)}$, could be attributed to the uptake of ^{14}N enriched ammonium (Altabet, 1988; Waser et al. 1999) by picophytoplankton in low nitrate waters. The $\delta^{15}N_{(POM)}$ values closer to zero was attributed to nitrogen fixation (Saino and Hattori, 1987).

The C:N ratio has often been used as an indicator of freshness of organic matter. The average C:N ratios were mostly being >6.63, however it was mostly <9 at most of the locations, except for a few stations. This imply that although low in productivity, the surface waters in this region was mostly autotrophic and the POM dominated by fresh organic matter especially during 2012. It is also indicated from the POC:Chl-*a* ratios that during 2012 the study locations of TIO were comparatively having a higher contribution from autotrophic activity than in 2013, when the heterotrophic processes had a significant contribution to the POM characterisation. Additionally, the dominance of picoplankton in oligotrophic waters is also an indicator of an active microbial loop as an alternate carbon pathway and heterotrophic bacteria an important contributor to the organic carbon pool (Azam et al., 1983; Marañón et al., 2003). Previous studies in the oligotrophic equatorial Indian Ocean waters have suggested the contribution of heterotrophic bacterial production to the biological production (Fernandes et al. 2008, Ramaiah et al., 2009). Selective mineralization of POM resulting in preferential removal of nitrogen by heterotrophic

bacteria is fairly well-known in marine environments (Eadie and Jeffrey, 1973; De Niro and Esptin, 1977). The reported greater bacterial productivity in TIO coupled with selective N-removal is likely responsible for the higher C:N ratio at some locations in these waters.

3.3.2 Factors controlling the stable isotopic composition of carbon and nitrogen of POM in the surface waters across the fronts in the Indian sector of Southern Ocean

The highly dynamic environmental settings of the ISSO imply that the hydrodynamics of the region has a significant role in the biogeochemical processes regulating the POM characteristics of surface waters. The ISSO observes a significant gradient in temperature, dissolved gases and nutrients across the different fronts. Also, the nutrient dynamics in this region influence the phytoplankton community structure. These factors individually and/or in combination have a critical role in modulating the POM characteristics in surface waters at different fronts and zones in the ISSO. The major attributes controlling the isotopic composition of POM in the ISSO are discussed in this section.

3.3.2.1 Sea Surface Temperature (SST)

The SST, displayed a strong gradient across the fronts and reflected a significant correlation with $\delta^{13}C_{(POM)}$. Although there was a correlation between temperature and $\delta^{13}C_{(POM)}$, the magnitude to significance was different in the consecutive years (Fig. 3.10a). Initial studies on $\delta^{13}C_{(POM)}$ in surface waters had related the latitudinal variability of the stable isotopic composition of POM to temperature (Eadie and Jeffrey, 1973; Fontugne and Duplessy, 1981). However, later it was revealed that in the surface waters, SST has an indirect effect on the isotopic composition of POM, as it controls the dissolved CO_2 and the phytoplankton carbon, thus subsequently influencing the $\delta^{13}C_{(POM)}$ (Rau et al., 1992). This relation is mainly because the southward drop in the SST, favours higher CO_2 saturation in the colder surface waters (Fig. 3.10b). This is also supported by the kinetic fractionation of carbon at the air-sea

interface, during CO_2 dissolution into the surface waters. The increased abundance of isotopically light CO_2 (CO_2 rich with ^{12}C) in the upper ocean is more likely to result in a decrease in the $\delta^{13}C$ of the available tCO_2 (Quay et al., 2003) and consequently influence the phytoplankton uptake and the resultant $\delta^{13}C$ of POM (Francois et al., 1993; Cullen et al., 2001).

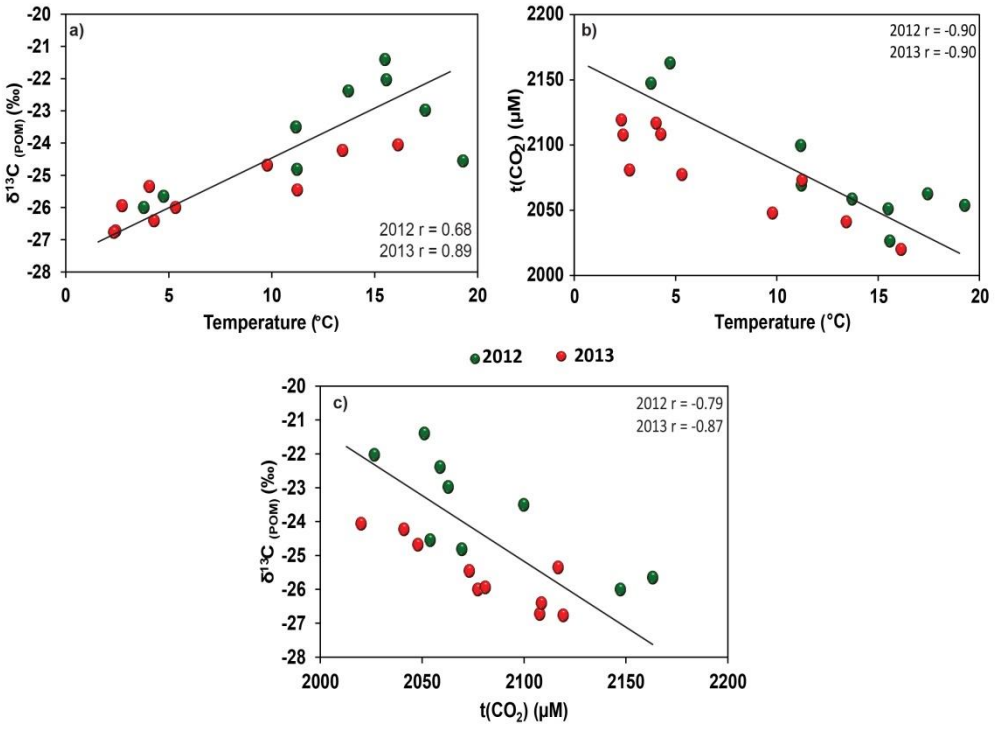

Figure 3.10: Spearman's correlation of (a) Temperature with $\delta^{13}C_{(POM)}$; (b) Temperature with tCO_2; (c) $\delta^{13}C_{(POM)}$ with tCO_2 across the fronts in the ISSO during austral summer 2012 and 2013

3.3.2.2 Total Carbon di oxide (tCO_2) concentration

The availability and abundance of dissolved CO_2 is one of the major factors controlling the isotopic composition of carbon phytoplankton and the resultant $\delta^{13}C_{(POM)}$ in the SO surface waters (Rau et al., 1992; François et al., 1993). The SO favoured by strong winds and wind driven mixing, that supports higher dissolution

resulting in higher concentration of the dissolved fraction of CO_2. A significant relation between $\delta^{13}C_{(POM)}$ and tCO_2 (Fig. 3.10c), imply the dependence of isotopic composition of carbon in POM on the concentration and isotopic composition of tCO_2 in the surface waters. Similar correlations ($\delta^{13}C_{(POM)}$ and tCO_2), have been reported earlier in the Southern Ocean (Kennedy and Robertson, 1995; Lourey et al., 2004), Atlantic Ocean (Rau et al., 1992), Arctic waters (Zhang et al., 2011), Prydz Bay (Zhang et al., 2014). This relation is mainly a result of the isotopic fractionation during photosynthetic uptake by phytoplankton. Furthermore, the comparatively weaker relation in 2012 austral summer implied that availability of dissolved CO_2 was not the only major controlling factor in determining the $\delta^{13}C_{(POM)}$ but also included significant contribution from biological factors.

3.3.2.3 Nutrient Availability

The gradient in nutrients especially nitrates and silicates across the fronts in the ISSO, is to a certain extent an attribute of temperature in the SO (Table 3.3 & 3.4). During this study, a strong relation observed between $\delta^{13}C_{(POM)}$ and nitrate (Fig. 3.11a) reflected a depletion in $\delta^{13}C_{(POM)}$ with an increase in the nutrients, especially nitrates, across the fronts towards the PF. The relatively enriched values in low nitrate, warmer waters reveal that, some locations were controlled by a regenerative, nitrate depleted system (Lara et al., 2010).

Also a significant negative correlation of $\delta^{15}N_{(POM)}$ and nitrate (Fig. 3.11b) suggest the noteworthy contribution of nitrate concentration in determining the isotopic characteristics of carbon and nitrogen in POM via biological productivity and nitrogen uptake by the organism (Wada and Hattori, 1978). Similar relations were reported earlier in the PF waters of SO (Altabet and Francois, 1994) and the Atlantic

waters (Lara et al., 2010) and was attributed to the isotopic ratio of nitrate and the fraction of unutilized substrate in the system. This is mostly a consequence of isotopic fractionation during nitrogen assimilation, and the preferential uptake of the lighter nitrate ($^{14}NO_3$) resulting in decrease in $\delta^{15}N_{(POM)}$ in nitrate replete conditions (Montoya, 1994; Kolasinski et al., 2012).

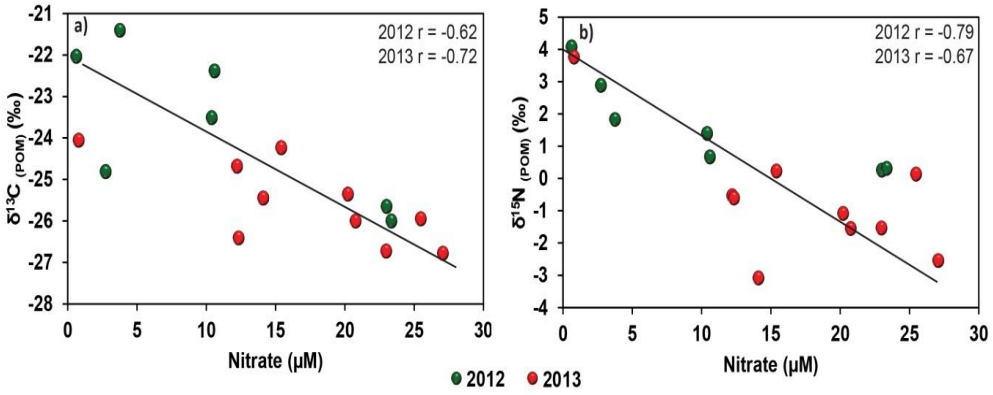

Figure 3.11: Spearman's correlation of (a) $\delta^{13}C_{(POM)}$ and Nitrate, (b) $\delta^{15}N_{(POM)}$ and Nitrate across the fronts in the ISSO during austral summer 2012 and 2013.

3.3.2.4 Phytoplankton community

The surface water POM gets its major contribution from living organisms, mainly the phytoplankton biomass. Therefore, the cell morphology and phytoplankton community have a prominent role in determining the stable isotopic composition of carbon in POM (Law et al., 1995; Popp et al., 1998). Also, the source (species) of carbon and nitrogen taken up by the phytoplankton and the isotopic fractionation during the metabolic process, influenced by the environmental conditions (Savoye et al., 2003) contribute to the shaping of isotopic characteristics of POM. Fig. 3.7, clearly indicated a shift in the dominant phytoplankton community across the fronts. It is also illustrated that regions with low nutrients is dominated by flagellates,

especially the STF. An earlier study by Lara et al (2010) associated the isotopically heavier POM in the Atlantic surface waters to the dominance of flagellates. Moreover in the present study, the observed flagellates were mostly dinoflagellates that were the dominant phytoplankton in the STF and the SAF, and are noted to be a mixotropic community. This phytoplankton community have assimilatory enzymes like the phosphoenolpyruvate carboxylase and phosphoenolpyruvate carboxykinase, that is responsible for lesser (smaller) isotopic discrimination during carbon uptake and assimilation, resulting in heavier $\delta^{13}C_{(POM)}$ (Bentaleb et al., 1998; Gaul et al., 1999) that was evident in this study. Further down south in the PF, the abundance of nutrients and other environmental conditions favour the flourishing of diatoms (Table 3.1 & 3.2). The depletion of isotopic signatures in diatom dominated PF waters, can be attributed to the higher fractionation by diatoms due to the abundance of CO_2 and the associated photosynthetic pathway (Descolas-Gros and Oriol, 1992; Law et al., 1997). Also, the growth rate of diatoms and associated carbon demand that favour higher fractionation during carbon uptake (Sommer, 1989; Fischer, 1991) in the colder nutrient rich high latitude waters. Further, diatoms have the ability synthesise lipids depleted in ^{13}C and stored in its cell (Degens et al., 1968; Sinninghe Damsté et al., 2003). The high accumulation of lipids is a mechanism mainly for self-maintenance and repair by the organism, especially in colder Polar Regions (Fahl and Kattner, 1993; Thomas and Dieckmann, 2002; Sackett et al., 2013). Fucoxanthin is a major diatom pigment, and this can contribute to the $\delta^{13}C$ depletion of diatoms and is subsequently reflected in $\delta^{13}C_{(POM)}$ (Sinninghe Damsté et al., 2003; Henley et al., 2012). During this study, the dominance of *Fragilariopsis* spp., followed by *Thalassiosira* spp., and *Cheatoceros* spp. was indicated from the microscopic

analysis in the PFZ waters. This explains the depletion of $\delta^{13}C_{(POM)}$ in diatom dominated PFZ waters in this study.

3.4 Salient Findings

Overall, in both the regimes the POM produced was from autochthonous sources, evident from the relation of POC with PN and $\delta^{13}C_{(POM)}$ with $\delta^{15}N_{(POM)}$. Also it is ascertained from the diagnostic pigment observations that the dominant phytoplankton community has a critical role in shaping the POM characteristics in-terms of the qualitative, quantitative and isotopic composition of carbon and nitrogen of the POM in surface waters across the fronts, as well as, the two distinct oceanic regimes. It is evident from the illustrated results that physical factors like SST, wind driven mixing and eddies play a major role in determining the isotopic characteristics of POM in ISSO. Higher $\delta^{15}N_{(POM)}$ and $\delta^{13}C_{(POM)}$ in the surface waters of the STF, implied a significant influence of the eddies in this front. Also, the dominance of flagellates in these waters influenced the $\delta^{13}C_{(POM)}$, which was attributed to their non-discriminative uptake of C and N species available in the system. The increasing availability of nutrients and tCO_2 towards the PF, favoured the growth of diatoms beyond 50°S. As a result, enhanced isotopic fractionation during photosynthesis resulting in the depletion of $\delta^{13}C$ and $\delta^{15}N$ of POM in polar waters.

Contrastingly, in the warm oligotrophic TIO waters, small scale depletion in $\delta^{13}C_{(POM)}$ and a wide variation of $\delta^{15}N_{(POM)}$ was explained by the dominance of picophytoplankton, that are less discriminative towards the uptake of nitrogen substrate. This regenerative production is predominantly responsible for sustaining the picoplankton biomass in these nitrate depleted waters. The role of heterotrophy in

this region is evident from earlier studies and contributes to the variability is POM characteristics during the two consecutive years.

From this study, the role of hydrography, nutrient dynamics and the predominant phytoplankton community in shaping the isotopic signature of POM in the surface waters of the two different oceanic regimes, and the variability across the fronts in the ISSO is elucidated.

4. Influence of Eddies on the Characteristics and Variability of Particulate Organic Matter in the Upper Water Column of the Subtropical Front.

4.1 Introduction

Eddies are an ubiquitous feature in the ocean that influences the ocean circulation and the marine biogeochemical processes (Marshal and Radke, 2003; Bakun, 2006). The SO, especially the STF region is highly dynamic with frequent eddy activity (Lutjeharms & Valentine, 1988; Jullion et al, 2010; Sabu et al, 2015). Eddies influence the vertical structure of the water column, and supports the transfer of heat, salt, nutrients and other components both vertically and laterally (Sallée et al., 2008; Ito et al., 2010). Eddies are important for nutrient transport and re-distribution, resulting in an increase of the phytoplankton productivity and phytoplankton blooms prompting the accumulation of chlorophyll in the overlying waters (Falkowski et al., 1991; Allen et al., 2005; Bibby et al., 2008) and further influencing the recycling and transport of organic matter (Bakun, 2006; Waite et al., 2007; Huang et al., 2010) in eddy influenced regions.

Mesoscale eddies are mainly of two types; cyclonic eddies and anticyclonic eddies. In the ISSO Cyclonic eddies (CE) are cold core and the clock-wise flow of currents displace the isopycnals upwards inducing upwelling, consequently supporting the influx of nutrients along with colder subsurface/deep waters into the euphotic zone, thus promoting increased primary productivity at the center (Bidigare et al., 2003; McGillicuddy et al., 2003; Bakun et al., 2006). In contrast, anticyclonic eddies (ACE) are warm core, with an anticlock-wise flow of currents and depress the

isopycnals downwards, triggering convergence of surface waters, thus causing downwelling (Bakun, 2006). The CE and ACE behave differently and have significantly diverse implications on the chemical variability and biological community by altering the hydrography and associated processes (McGillicuddy and Robinson, 1997, Bidigare et al., 2003). Studies have also indicated that eddy dynamics mediate changes in the zooplankton community structure and behavior (Beckmann et al., 1987; Hernández-león et al., 2001; Verdeny et al., 2008).

Sweeney et al. (2003) proposed seven stages of an eddy life cycle, from eddy intensification to the eddy decay stage, during which the eddy influenced regions are dominated by different processes due to eddy dynamics. Commencing with the flux of nutrients to the sustained presence of elevated macronutrients resulting in a shift of phytoplankton community, and favor a change in the zooplankton and the export food web (Li and Hansell, 2008; Eden et al., 2009) or the functioning of oligotrophic food webs over time (Buesseler et al., 2008). Furthermore, in such eddy influenced regions, heterotrophic activities play a significant role in determining the fate of the eddy induced biological production. Higher bacterial activity, responsible for the remineralisation of POM and DOM, may result in a reduced export flux of carbon due to regeneration of POM within the upper water column (Legendre and Le Fèvre, 1995; Coppola et al., 2005).

These mesoscale features are responsible for significant changes in the ocean dynamics, especially, the prevalence of eddies in nutrient depleted STF waters are largely responsible for influencing the biogeochemical processes due to an alteration in the nutrient dynamics of the STF waters (Soares et al., 2020). This chapter discusses the role of the source of origin and the eddy dynamics over its life span on

the POM characteristics and isotopic composition of POM in eddy influenced waters of STF in ISSO.

4.2 Results

During both the periods of study, the vertical distribution of temperature and salinity showed large undulations at STFZ. To understand the reason for the undulations, satellite SST was analyzed and it was found that, a total of six eddies were encountered in the observation regions during the study period (Fig. 4.1; Table 4.1).

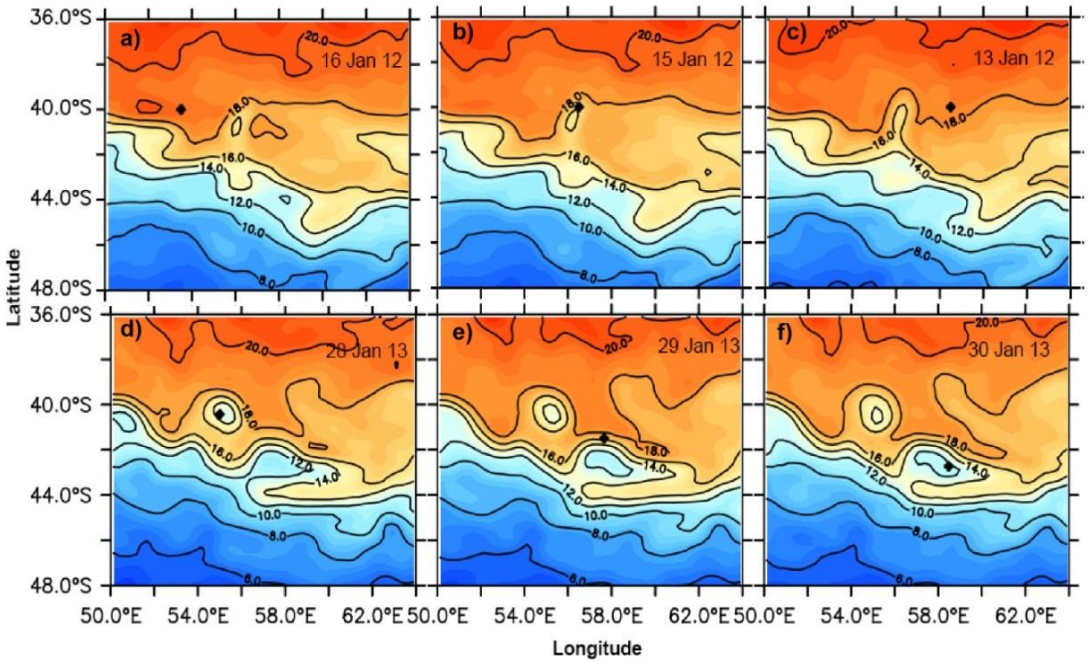

Figure 4.1: Sea Surface Temperature (SST) variability from the AVHRR data (a) ACE1, (b) CE1, (c) ACE2, (d) CE2, (e) ACE3 and (f) CE3 during the observation period.

During 2012, observations were inside and at peripheral regions of the three eddies that included one CE (CE1; 40°S; 56.30°E), with a diameter of ~200 km and two ACEs, ACE1 (40°S; 53.5°E) and ACE2 (40°S; 58.5°E) with diameters of ~250 km and 300 km, respectively (Fig. 4.1).

Similarly during 2013, the observations were carried out in CEs located at 40.26°S; 55.03°E (CE2) and 42.44°S; 58°S (CE3) having diameters of >300 km and ~250 km, respectively (Fig. 4.1), also an ACE was observed at 41.35°S; 57.45°E (ACE3) with a diameter of ~250 km. For a better understanding and differentiate the characteristics between CE and ACE in the STF, we combined the CEs (CE1, CE2, CE3) and ACEs (ACE1, ACE2 and ACE3) together for discussion in the subsequent sections.

Year	Eddy type (Code)	Latitude	Longitude	Date of Origin	Front of origin	Age of Eddy (months)	MLD (m)	PAR (Einstein/m^2/D)	DCM (m)
2012	Anticyclonic Eddy (ACE1)	40°S	53.30°E	26/09/2011	STF	~ 4	23	66	73
2012	Cyclonic Eddy (CE1)	40°S	56.30°E	15/11/2011	PF	~ 2	18	62	50
2012	Anticyclonic Eddy (ACE2)	40°S	58.30°E	6/11/2011	STF	~ 2	37	~65	75
2013	Cyclonic Eddy (CE2)	40.26°S	55.03°E	15/12/2012	STF	~ 1	24	19	53
2013	Anticyclonic Eddy (ACE3)	41.35°S	57.45°E	03/01/2013	ARF	<1	63	~27	15
2013	Cyclonic Eddy (CE3)	42.44°S	58°E	08/01/2013	STF	<1	41	62	50

Table 4.1: The sampling locations of eddies along with the eddy type, date of origin, front of origin, approximate age of the eddy and the Mixed Layered Depth (MLD), surface PAR and the Deep Chlorophyll Maxima (DCM) at the eddy locations during 2012 and 2013 austral summer.

4.2.1 Cyclonic Eddies

4.2.1.1 Hydrography and chemical parameters

In general, the temperature in the upper 120 m at the CEs ranged from 5.03 to 15.36 °C (Table 4.2). During 2012, CE was found to be comparatively warmer (13.63±2.32 °C) than that in 2013 (9.44±2.71 °C). Also, during both the years, a prominent shift was noticed in the position of isotherms and isohalines in the CE regions. At CE1, the 12 °C isotherm was displaced from deeper depths (>120 m) to ~100 m, and at CE2 and CE3, the 12 °C isotherm was displaced from deeper depths to ~30 m and surface respectively (Fig. 4.2a, b). The salinity at the CEs ranged from 33.65 to 34.90 (Table 4.2). The isohalines also showed similar variability as observed for isotherms (Fig. 4.2c & d). The CE locations were characterized by colder and less saline waters.

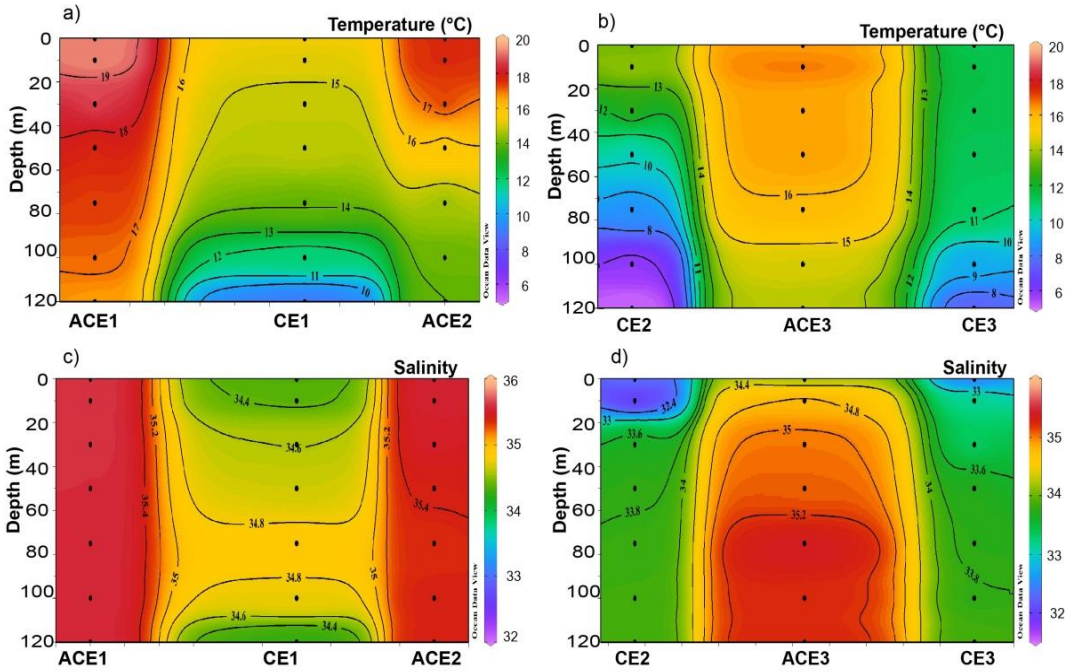

Figure 4.2: Vertical distribution of temperature during (a) 2012 and (b) 2013; salinity during (c) 2012 and (d) 2013.

Eddy type	year	Temp (° C)	Salinity	DO (µM)	tCO_2 (µM)	NO_3 (µM)	NO_2 (µM)	NH_3 (µM)	PO_4 (µM)	SiO_4 (µM)	N:P	N:Si	Chl-*a* (mg/m^3)	POC (µg/L)	PN (µg/L)	C:N (m/m)	$\delta^{13}C_{(POM)}$ (‰)	$\delta^{15}N_{(POM)}$ (‰)	POC/Chl-*a*
CE1	2012	**13.63** (9.14 - 15.36)	**34.56** (34.25 - 34.90)	**257.1** (243.5 - 279.9)	**2071.9** (2043.1 - 2140.7)	**5.16** (2.29 - 11.84)	**0.79** (0.67 - 1.17)	**2.52** (2.05 - 3.25)	**1.85** (1.70 - 2.31)	**1.80** (1.23 - 3.29)	**4.47** (3.42 - 6.91)	**4.97** (3.20 - 6.13)	**0.41** (0.21 - 0.75)	**40.12** (29.62 - 59.42)	**7.79** (4.68 - 14.89)	**6.31** (4.66 - 7.63)	**-23.14** (-25.51 To -21.40)	**1.51** (-0.31 To 3.90)	**104.9** (75.4 - 148.2)
CE2	2013	**9.38** (5.03 - 13.43)	**33.77** (33.65 - 33.86)	**285.9** (265.9 - 298.2)	**2068.9** (2041 - 2101.6)	**14.10** (11.53 - 17.69)	**0.65** (0.58 - 0.72)	**1.79** (1.47 - 2.21)	**1.50** (0.94 - 2.20)	**4.01** (3.39 - 6.13)	**11.64** (6.46 - 19.14)	**3.51** (0.54 - 4.66)	**0.22** (0.09 - 0.35)	**86.89** (49.72 - 123.71)	**11.89** (7.81 - 16.67)	**8.43** (7.29 - 10.04)	**-24.49** (-25.11 To -24.06)	**-0.84** (-5.20 To 3.66)	**389.4** (194.4 - 527.2)
CE3	2013	**9.51** (6.62 - 11.24)	**33.81** (33.76 - 33.91)	**286.3** (276.9 - 296.8)	**2074.7** (2050.3 - 2101.6)	**13.89** (11.51 - 17.75)	**0.60** (0.49 - 0.70)	**1.68** (0.81 - 2.80)	**1.69** (1.37 - 1.90)	**4.02** (3.39 - 5.80)	**10.86** (7.79 - 19.14)	**3.48** (0.63 - 4.43)	**0.38** (0.16 - 0.75)	**93.95** (36.03 - 194.19)	**8.56** (4.64 - 10.96)	**12.17** (7.14 - 22.45)	**-25.66** (-26.60 To -24.89)	**1.53** (-3.07 To 5.46)	**274.4** (98.6 - 577.9)
ACE1	2012	**18.01** (16.67 - 19.28)	**35.58** (35.56 - 35.60)	**239.46** (225.9 - 288.8)	**2072.7** (2049.9 - 2090.6)	**0.39** (0.09 - 1.89)	**0.62** (0.56 - 0.68)	**1.78** (1.36 - 2.09)	**1.34** (1.26 - 1.46)	**2.37** (1.65 - 3.09)	**2.05** (1.60 - 2.92)	**1.18** (1.03 - 1.46)	**0.40** (0.11 - 0.91)	**31.89** (23.21 - 40.19)	**6.34** (4.24 - 8.20)	**5.88** (4.67 - 6.74)	**-25.80** (-27.86 To -24.12)	**2.32** (0.40 - 4.16)	**151.4** (27.20 - 335.3)
ACE2	2012	**15.86** (14.02 - 17.58)	**35.45** (35.37 - 35.53)	**243.3** (233.9 - 252.7)	**2075.2** (2045.2 - 2091.1)	**1.99** (0.25 - 5.60)	**0.51** (0.41 - 0.70)	**2.01** (1.78 - 2.34)	**1.42** (1.34 - 1.61)	**2.29** (1.58 - 3.76)	**3.11** (1.89 - 4.94)	**1.94** (1.44 - 2.22)	**0.49** (0.28 - 0.79)	**34.20** (15.10 - 58.94)	**3.53** (1.47 - 7.83)	**13.37** (4.28 - 22.88)	**-24.95** (-26.36 To -22.98)	**3.21** (1.22 To 4.39)	**84.9** (22.9 - 148.6)
ACE3	2013	**15.74** (14.40 - 16.32)	**35.14** (34.99 - 35.42)	**234.7** (216.9 - 244.2)	**2055.7** (2020.0 - 2098.3)	**2.81** (0.78 - 6.86)	**0.80** (0.77 - 0.87)	**2.18** (1.97 - 2.54)	**1.12** (1.02 - 1.24)	**3.58** (2.34 - 5.73)	**5.17** (3.17 - 8.65)	**1.62** (1.23 - 1.91)	**0.26** (0.04 - 0.46)	**53.83** (29.54 - 104.44)	**7.43** (3.33 - 12.89)	**9.16** (6.52 - 11.69)	**-24.15** (-25.18 To -22.50)	**0.51** (-3.62 To 3.77)	**249.8** (93.5 - 448.3)

Table 4.2: Column average and range of temperature (temp), salinity, DO, tCO_2, NO_3, NO_2, NH_3, PO_4, SiO_4, N:P, N:Si (N= NO_3+NO_2+NH_3), POC, PN,C:N(m/m), $\delta^{13}C_{(POM)}$, $\delta^{15}N_{(POM)}$ and POC/Chl-*a* at the eddy locations during austral summer, 2012 and 2013. Range is in parentheses.

The water mass analysis showed that the CE2 and CE3 had similar water mass properties in the upper water column (Fig. 4.3). However at CE1, the upper water column was comparatively warmer than the CE2 and CE3. The analysis further confirms that the upper water column in the CEs did not show any characteristics of Subtropical Surface Waters (STSW). However, the deeper water of all the three CEs showed the characteristics of Antarctic Intermediate Water (AAIW). Also, the upwelling in the CE regions resulted the shallowing of MLD which was <18 m at CE1 ~25 at CE2 and ~40 m at CE3.

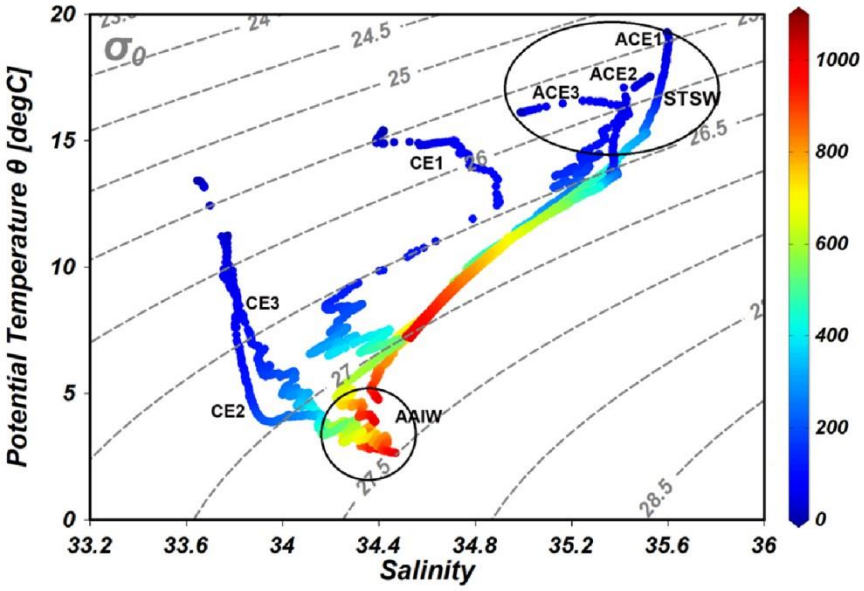

Figure 4.3: T-S diagram showing various water masses at the eddy locations during the study.

The variation of the thermohaline structure at the CEs was also reflected in the various chemical variables. In general, CE regions were rich in oxygen with a range of 243.5 to 298.2 µM (Table 4.2). The concentration of DO in CE2 and CE3 was higher (Fig. 4.4a) with an average of 285.9±13 µM and 286.3±8 µM, respectively, compared to 257.0±12 µM at CE1. Likewise, the concentration of nitrate was also

high at CE regions and ranged from 2.29 to 17.75 µM (Table 4.2). However, higher nitrate concentration was observed at the CE2 and CE3 than CE1 (Fig. 4.4b). Overall the concentration of silicates ranged from 1.23 to 6.13 µM at the CE locations (Table 4.2), with an increase below 80 m (Fig. 4.4c). The concentration of silicate was low at CE1 with an average of 1.8±0.9 µM, whereas it was observed to be more than double (av. 4.01±0.8 µM) at CE2 and CE3. In the CE regions, the phosphate concentration ranged from 0.94 to 2.31 µM (Table 4.2), and the distribution showed a subsurface minimum at ~60 m in CE2 and CE3, whereas an increase in concentration was noticed below 80 m in CE1 (Fig. 4.4d).

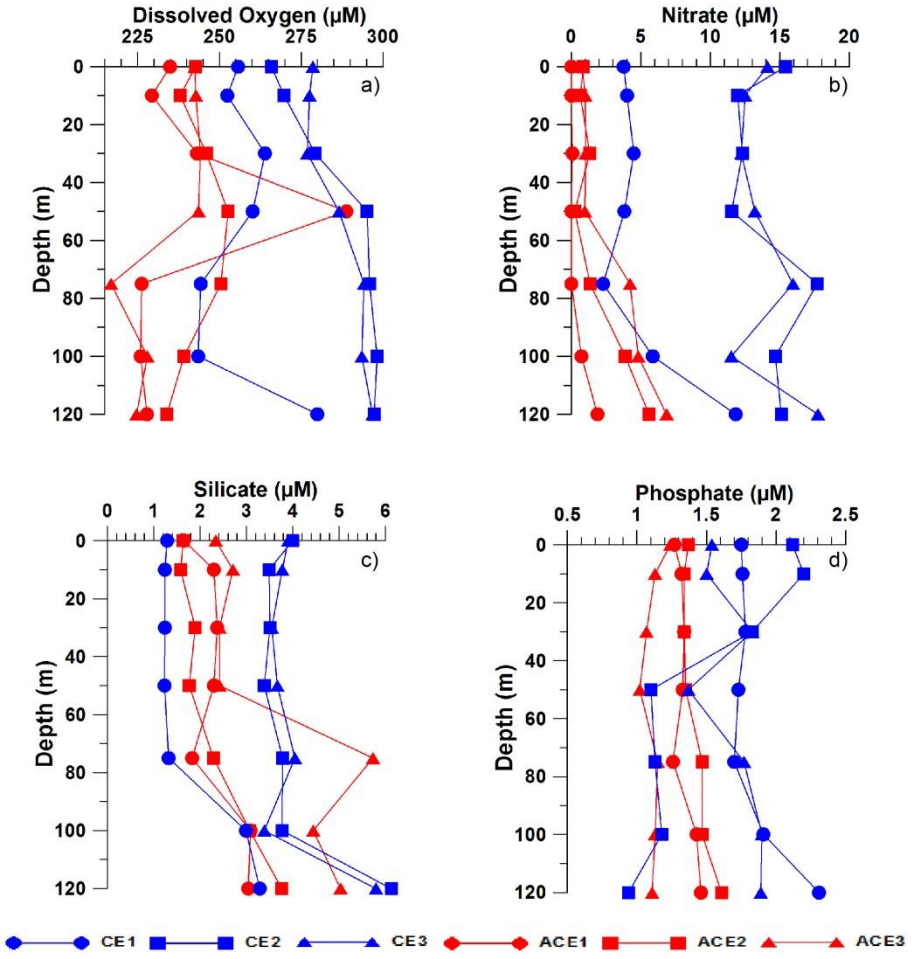

Figure 4.4: Vertical distribution of (a) DO, (b) Nitrate, (c) Silicate and (d) Phosphate at the Cyclonic eddies (**Blue**) and anticyclonic eddies (**Red**), during the study.

4.2.1.2 Chl-a and phytoplankton community

The water column variability due to CEs in the STF was reflected in the distribution of Chl-*a* and phytoplankton. The overall Chl-*a* concentration ranged from 0.09 to 0.75 µg/L (Table 4.2), with a lower concentration at CE2 (0.09 to 0.35 µg/L). A Deep Chlorophyll maxima (DCM) was observed at ~50 m at all the CEs, however the DCM was more sharp and prominent at CE1 and CE3 (Fig. 4.5).

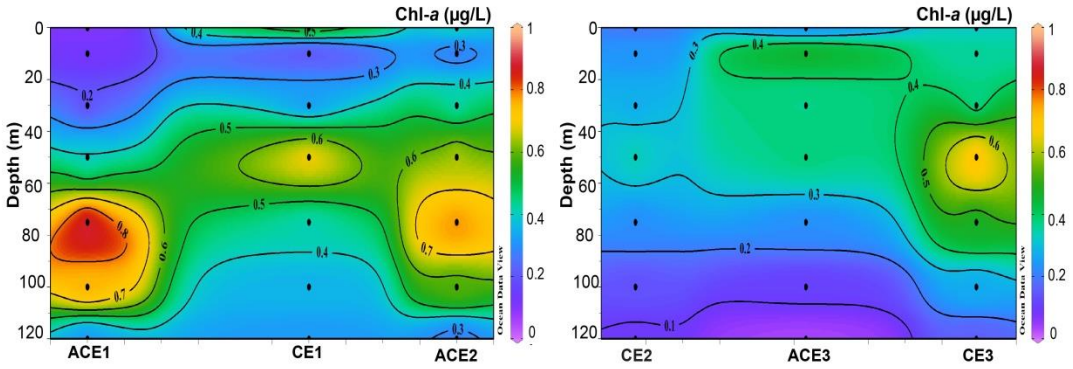

Figure 4.5: Vertical distribution of Chlorophyll a (Chl-*a*) at cyclonic eddies and anticyclonic eddies during (a) 2012 and (b) 2013.

Further, it was noted that the phytoplankton community distribution was markedly different between the CEs. At CE1 >80 % contribution to the phytoplankton community was from flagellates and the remaining contribution was from other groups such as diatoms and prokaryotes (Fig. 4.6). Also, the contribution of diatoms showed an increase with depth at this location (Fig. 4.6). At CE2, flagellates contributed more than 50 % at the surface and the DCM depth, and prokaryotes were the second major contributor to the phytoplankton community. However, the contribution of prokaryotic phytoplankton was negligible below DCM (~ 120 m) and the major contributing communities were the flagellates (~70 %) and diatoms (~30 %), at these depths (Fig. 4.6). Further at CE3, the flagellates contribution was ~65%

at the surface but was negligible at DCM, and again increased to ~ 29 % at 120 m. Contrary to flagellates, the contribution of diatoms was less (5 %) at the surface and it increased to ~ 50 % at the DCM and again decreased to 34% at 120 m (Fig. 4.6). In general, the Chl-*a* and the phytoplankton showed contrasting variability in all the CEs.

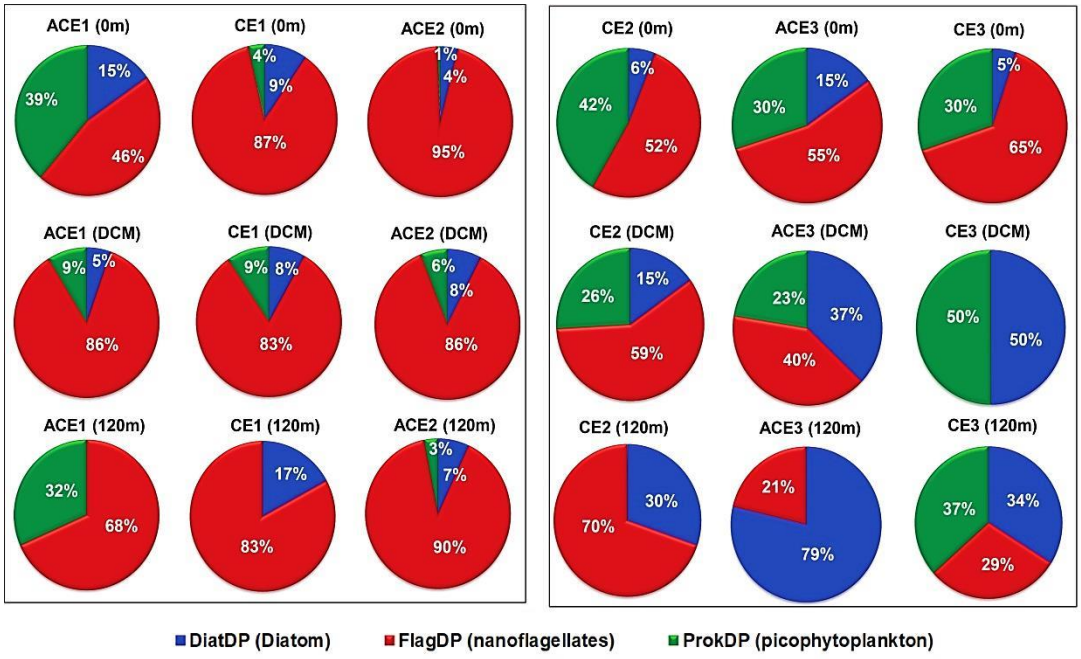

Figure 4.6: Dominant phytoplankton community at the surface (0 m), DCM and 120 m at the cyclonic and anticyclonic eddies observed during this study

4.2.1.3 Characteristics of POM

Like the other variables, the POC concentration was markedly different in the CEs. Although the overall range of POC was between 29.62 to 194.19 µg/L (Fig. 4.7a), and POC decreased with depth at CE1 and CE3, unlike CE2 where the distribution with depth was highly variable (Fig. 4.8a). Also, the concentration of POC was lower at CE1, with no prominent variability with depth. At CEs, the PN varied between 4.64 and 16.67 µg/L (Table 4.2). Similar to POC, the concentration of

PN also showed a gradual decrease with depth (Fig. 4.8) at CE1 and CE3 whereas at CE2 showed a larger variation (Fig. 4.7a & b). The $\delta^{13}C_{(POM)}$, was highly variable between the CEs and ranged from -26.6 to -21.4‰ (Table 4.2). The $\delta^{13}C_{(POM)}$ was most enriched at CE1 (Fig. 4.7c) with a significant decrease with depth from -21.4‰ at the surface to -25.5 ‰ at 120 m (Fig.4.8c). However, at CE2 (-25.11 to -24.06 ‰) and CE3 (-26.60 to -24.89 ‰) the $\delta^{13}C_{(POM)}$ was depleted with smaller variability with depth. Similarly, the $\delta^{15}N_{(POM)}$ ranged from -5.2 to 5.46 ‰ (Table 4.2), and a wide variation was observed with depth, especially at CE2 and CE3. In contrast to the variability at CE2 and CE3, the $\delta^{15}N_{(POM)}$ decreased with depth at CE1 (Fig. 4.8d). Additionally, at CE3 a subsurface maxima of $\delta^{15}N_{(POM)}$ was observed at 50 m, and coincided with the DCM.

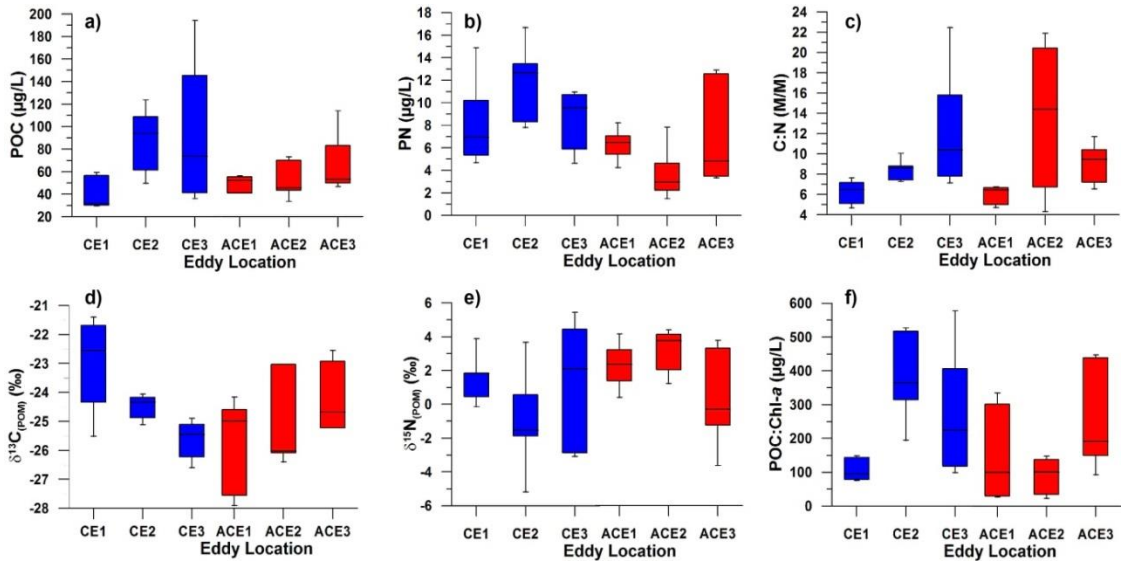

Figure 4.7: POM variability (a) POC, (b) PN, (c) C:N, (d) $\delta^{13}C_{(POM)}$, (e) $\delta^{15}N_{(POM)}$ and (f) POC/Chl-*a* at the cyclonic and anticyclonic eddies during this study

Further, C:N ratios were examined in the CEs and observed that the overall C:N ratio was highly variable and ranged from 4.66 to 15.8 (except for the abrupt

high of 22.4 at CE3). The lower C:N ratios were observed at CE1 (4.66 to 7.63) and the higher C:N values were noted at CE3 (7.14 to 22.45) (Fig. 4.7e) with a high variability within the upper water column. The POC:Chl-*a* ranged from 75 to 577, with the higher values at CE2 and CE3 (Table 11). At CE1, the POC:Chl-*a* ratio, was mostly <200, while at CE2 and CE3, the POC:Chl-*a* ratio of POM were mostly >200 and showed high variability with a minimum value (<200) (Fig. 4.7f).

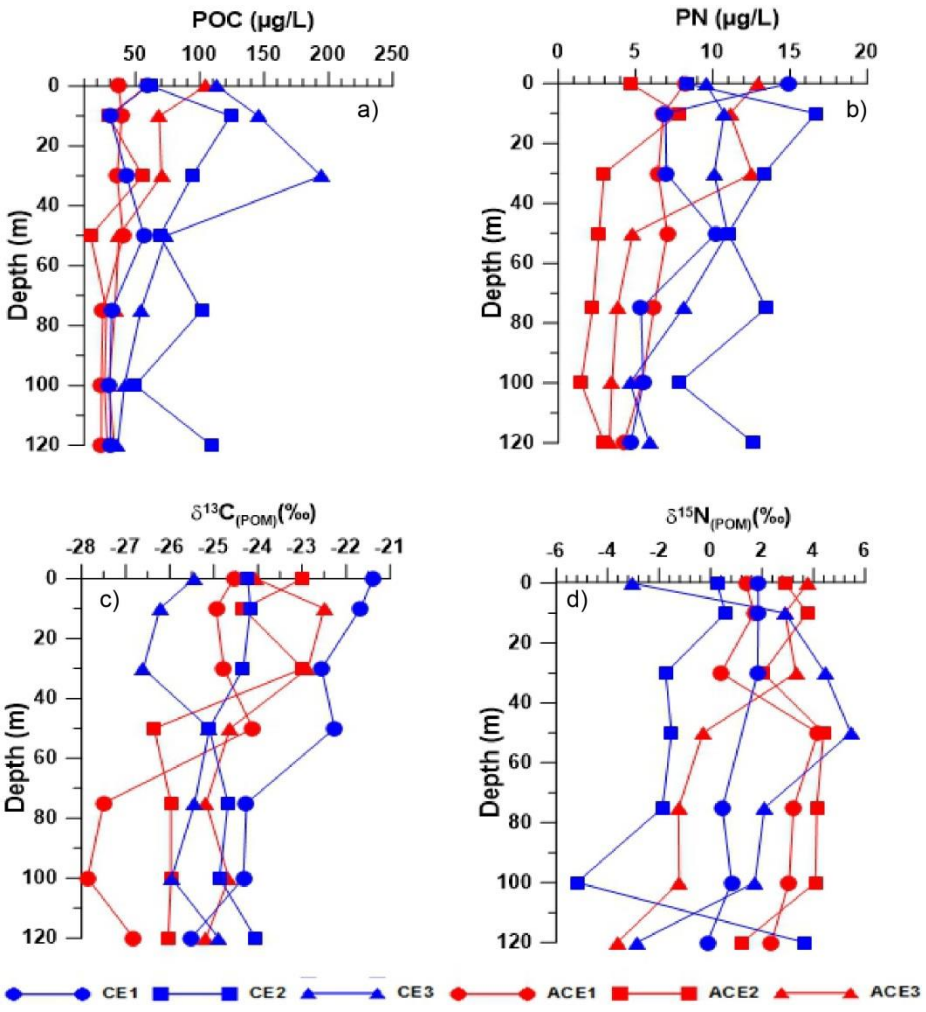

Figure 4.8: Vertical distribution of POM characteristics in the upper 120 m water column: (a) POC, (b) PN, (c) $\delta^{13}C_{(POM)}$, (d) $\delta^{15}N_{(POM)}$, at the CEs and ACEs.

4.2.2 Anticyclonic Eddies

4.2.2.1 Hydrography and chemical parameters

The temperature in the ACE regions ranged from 14.02 °C to 19.28 °C (Table 4.2) with a downward displacement of isotherms. The 16 °C isotherm was pushed down to >120 m at the ACE1, while at ACE2 and ACE3 it was displaced to ~50 m and ~70 m respectively (Fig. 4.2a, b). The salinity at ACEs ranged from 35.0 to 35.6 (Table 4.2), and showed a downward displacement of isohalines (Fig. 4.2c, d). It was observed that the warmer and saline waters were pushed to deeper depths in the ACE regions. The water mass analysis showed the presence of STSW in the upper water column (200 m) in the ACEs. The AAIW was observed below 900 m in all the ACE regions. The downward movement of STSW in the ACE regions was also evident in the water column (Fig. 4.3). It was also observed that the MLD was deeper at ACE3 (~63 m) compared to ACE1 (~23 m) and ACE2 (~37 m).

In ACE regions, the DO concentration ranged from 216.9 to 288.8 µM (Table 4.2) and a subsurface maxima (260 µM) was observed at ~50 m at the ACE1 and ACE2 (Fig. 4.4a). However, at ACE3 the subsurface maximum was not observed and the concentration of DO decreased with depth (Fig. 4.4a). The concentration of nitrate ranged from 0.09 to 6.86 µM in ACEs (Table 4.2), with the lowest concentration observed at ACE1 (0.09 to 1.89 µM), However, at the ACE2 and ACE3 the nitrate concentration was higher below ~75 m (Fig. 4.4b). Likewise, the silicate concentration in the ACEs ranged from 1.58 to 5.73 µM (Table 4.2) and increased with depth below ~75 m (Fig. 4.4c). It was noticed that the silicate concentration at ACE3 (2.34 to 5.73 µM) was comparatively higher than ACE1 (1.65 to 3.09 µM) and ACE2 (1.58 to 3.76 µM). The phosphate ranged from 1.02 to 1.61 µM (Table 4.2) in the ACEs with a minor increase (~0.2 µM) within the upper waters at ACE1 and

ACE2 (Fig. 4.4d), compared to ACE3, however, within the column the phosphate distribution was uniform.

4.2.2.2 Chl-a and phytoplankton community

The Chl-*a* concentration at ACEs was reported in the range of 0.04 to 0.91µg/L (Table 4.2), and was lower at ACE3. A well-defined DCM was observed at ~75-80 m at ACE1 and ACE2, however it was not very prominent at ACE3 (Fig. 4.5).

The diagnostic pigment analysis, showed a strong variation in the phytoplankton community in the upper 120 m. At ACE1, the contribution of flagellates was ~46 % at surface and ~86 % at DCM and decreased thereafter to ~68 % at 120 m. Conversely, the contribution from the prokaryotes showed an opposite trend with a decrease from surface to DCM with contribution of ~39 % and ~9 % respectively, and further increased to ~ 32 % at 120 m. However, the contribution of diatoms in the ACE1 was small (~15 %) at surface and decreased to 120 m (negligible) (Fig. 4.6). At ACE2, the contribution of flagellates was consistent within the upper 120 m, with an abundance of >85 %. The contribution of diatoms was higher than the prokaryotes at all the observational depths (0 m, DCM, 120 m) of ACE2 (Fig. 4.6). Contrastingly at ACE3, a shift in the dominant phytoplankton community was observed with the dominance of flagellates (55 %) at the surface, to the dominance of diatoms (79 %) at 120 m. It was also observed that the contribution of flagellates and prokaryotes decreased with depth and the contribution of prokaryotes was negligible at 120 m, converse to the diatoms that increased with depth (Fig. 4.6).

4.2.2.3 Characteristics of POM

The overall range of POC concentration in the ACEs was from 15.1 to 104.4 µg/L (Table 4.2; Fig 4.7), and the POC concentration decreased with depth (Fig. 4.8). Unlike ACE1 and ACE2, the column variability of POC at ACE3 was much higher, with a sharp decrease from 104.4 µg/L (surface) to 29.5 µg/L (120 m). Similarly, the concentration of PN decreased with depth at all the ACEs, with a range of 1.47 to 12.89 µg/L. The PN concentration was lower at ACE2 (avg. 3.53±2.13 µg/L) with a larger variability within the upper 120 m (Fig. 4.7b). The $\delta^{13}C_{(POM)}$ at ACEs ranged from -27.86 to -22.50 ‰ (Table 4.2) and decreased with depth. The $\delta^{13}C_{(POM)}$ was comparatively depleted (-25.80±1.55 ‰) at ACE1 (Fig. 4.7c) than ACE3 (-24.15±1.08 ‰). Unlike $\delta^{13}C_{(POM)}$, the $\delta^{15}N_{(POM)}$ was highly variable at all the ACEs and it ranged from -3.62 to 4.39 ‰. The maximum enrichment of $\delta^{15}N_{(POM)}$ was noted at ACE2 with large variability with depth. Further, the column distribution at ACE1 and ACE2 were similar (Fig. 4.7d) and showed an increase in ^{15}N contribution to POM possibly responsible for an enrichment of $\delta^{15}N_{(POM)}$ with increase in depth (Fig 4.8).

Additionally, the observation of POM characteristics showed that the C:N ratios were between 4.28 to 14.83 (with high values of 21.88 at ACE2) (Fig. 4.7e). At ACE1, the column distribution was uniform with an average of 5.88±0.87 and comparatively lower than the C:N ratio observed at ACE2 (13.37±6.6 having high variability) and ACE3 (9.5±1.8). Additionally, the observed POC:Chl-*a*, at ACEs varied from 22.9 to 448.3 (Fig. 4.7; Table 4.2) and showed a decrease with depth at ACE1 and ACE2. The observed POC:Chl-*a*, was also consistently <200 at these two regions, in contrast to the ACE3.

4.2.3 Statistical Analysis

Based on factor analysis and principle component analysis using Physico-chemical parameters and the POM characteristics it was derived that although all the six eddies were significantly different in the factors controlling the POM characteristics. Furthermore, a similarity matrix analysis based on Pearson's correlation coefficient was classified by a hierarchical agglomerative clustering based on the major physico-chemical variables and the stable isotopic composition of carbon and nitrogen, showed the ACE and CE clustered out as separate branches at ~97 % (Fig. 4.9). While the surface waters displayed a significant difference in the characteristics of CEs and ACEs with separate branches (87 %), DCM and 120 waters shared considerable similarity.

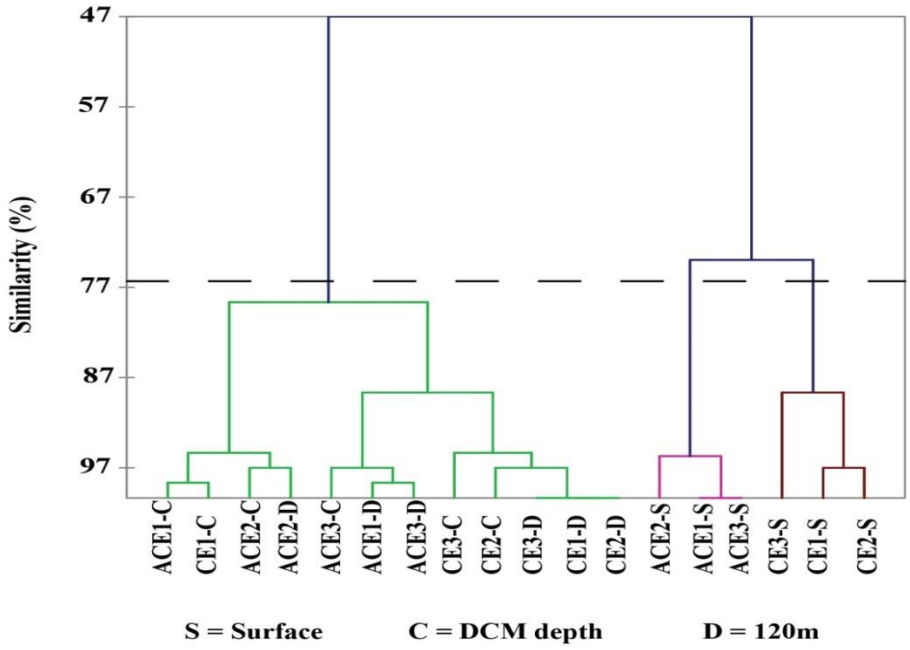

Figure 4.9: Hierarchical cluster analysis of the eddy waters at Surface, DCM and 120m, calculated from water physico-chemical variables and POM isotopic characteristics $\delta^{13}C_{(POM)}$ and $\delta^{15}N_{(POM)}$.

Also, significant grouping of the surface waters separate from the other depths (DCM and 120m) was at ~76 % similarity level (0.76). Further, the dendrogram displayed the CE3 and ACE2, branch out separately from the CE surface water and ACE surface water clusters respectively, implying that these two locations share distinct features different from that noted at the other two CEs and ACEs respectively (Fig. 4.9).

4.2.3.1 *Cyclonic eddies*

Statistical analysis using Pearson's correlation coefficient, suggested that overall temperature, nutrients and phytoplankton community had a significant role along with heterotrophic activity on the POM characteristics in CE influenced waters. This was implied from the positive linear correlation of $\delta^{13}C_{(POM)}$ with temperature and salinity (Table 4.3) and an inverse correlation with nitrates and silicates and C:N ratio (Table 4.3). Also, $\delta^{15}N_{(POM)}$ displayed a positive linear correlation with Chl-*a*, suggesting the role of phytoplankton biomass and community on the $\delta^{15}N_{(POM)}$ signatures (Table 4.3).

Moreover, the factor analysis implied that at CE upwelling driven hydrographic changes, especially the role temperature in influencing the chemical variables, like dissolved gases (DO, tCO_2) was one of the main factors at the CEs. The second important factor was regeneration of inorganic nutrients like ammonium, phosphate and nitrites. Additionally, the influx of nitrates and silicates that regulate the biological productivity and essentially the prevailing phytoplankton community structure was another contributing factor that had a significant role in controlling the POM dynamics at the CE locations (Table 4.4).

	Temperature	Salinity	DO	NO_3	Nitrite	Ammonia	Phosphate	Silicate	Chl-*a*	POC	PN	$\delta^{13}C_{(POM)}$	$\delta^{15}N_{(POM)}$	C:N	POC:Chl-*a*	AOU
Temperature	1															
Salinity	**0.517**	1														
DO	**-0.872**	**-0.745**	1													
NO_3	**-0.658**	**-0.717**	**0.750**	**1**												
Nitrite	0.073	**0.568**	-0.438	-0.278	**1**											
Ammonia	-0.047	**0.607**	-0.199	-0.198	**0.642**	**1**										
Phosphate	0.457	0.198	**-0.463**	-0.147	0.350	0.356	**1**									
Silicate	**-0.811**	**-0.714**	**0.746**	**0.743**	-0.180	-0.287	-0.257	**1**								
Chl-*a*	0.424	0.305	-0.286	-0.221	-0.110	-0.101	0.048	**-0.462**	**1**							
POC	-0.069	**-0.568**	0.235	0.221	**-0.488**	-0.717	-0.207	0.329	-0.062	**1**						
PN	0.112	-0.429	0.130	0.078	-0.373	**-0.570**	-0.293	0.104	0.105	**0.606**	**1**					
$\delta^{13}C_{(POM)}$	**0.611**	**0.564**	**-0.565**	**-0.578**	0.213	0.251	0.059	**-0.616**	0.158	-0.429	0.185	**1**				
$\delta^{15}N_{(POM)}$	0.330	0.176	-0.267	-0.194	-0.095	-0.114	0.080	-0.217	**0.540**	0.233	0.112	0.121	**1**			
C:N	-0.162	-0.450	0.230	0.224	-0.382	**-0.507**	-0.051	0.327	-0.109	**0.847**	0.107	**-0.663**	0.222	**1**		
POC:Chl-*a*	-0.320	**-0.654**	0.391	0.326	-0.365	-0.524	-0.262	**0.543**	**-0.539**	**0.830**	**0.546**	-0.363	-0.115	**0.652**	**1**	
AOU	-0.326	0.379	-0.153	-0.116	**0.661**	**0.495**	-0.034	0.217	-0.367	-0.380	-0.471	-0.033	-0.192	-0.20	-0.105	**1**

Table 4.3: Pearson's correlation matrix for bio-chemical variables at Cyclonic eddy (CE) locations during 2012 and 2013. All values in bold imply significant correlation between the variables (significance level alpha=0.05).

Variables	F1	F2	F3	F4
Depth	**0.936**	0.343	-0.039	-0.018
Temperature	**-0.887**	0.119	0.411	0.173
Salinity	-0.095	0.549	**0.595**	0.412
DO	**0.807**	-0.324	-0.327	-0.261
***t*CO_2**	**0.709**	0.454	-0.096	-0.339
Nitrate	0.393	-0.218	**-0.663**	-0.515
Nitrite	0.016	**0.970**	-0.053	0.182
Ammonia	0.214	**0.960**	0.082	0.160
Phosphate	-0.368	**0.748**	-0.006	-0.293
Silicate	0.605	-0.221	**-0.674**	-0.227
Chl-*a*	-0.271	-0.178	**0.942**	0.087
$\delta^{13}C_{(POM)}$	-0.394	0.180	0.251	**0.866**
$\delta^{15}N_{(POM)}$	0.085	-0.161	**0.490**	0.405
C:N	0.048	-0.400	-0.371	**-0.445**
Eigen value	**6.32**	**3.51**	**1.59**	**0.75**
Variability (%)	**45.11**	**25.06**	**11.37**	**5.36**
Cumulative %	**45.11**	**70.17**	**81.53**	**86.89**

Table 4.4: Principle factor Analysis for bio-chemical variables at Cyclonic eddy (CE) locations during 2012 and 2013.

Although the major controlling factors/processes were common at the CE influenced locations, the intensity of the impact of these factors are likely to vary at the three CE locations that were considerably different from each other. Especially, CE1 was significantly different from CE2 and CE3, that were considerably similar in the

dominant biological processes influencing the POM characteristics and the variability of $\delta^{13}C_{(POM)}$ and $\delta^{15}N_{(POM)}$ at these locations.

4.2.3.2 *Anticyclonic eddies*

Statistical analysis using Pearson's correlation coefficient displayed significant positive relation between $\delta^{13}C_{(POM)}$ and POC, PN, ammonium and also an inverse correlation with Chl-*a* (Table 4.5). Likewise, $\delta^{15}N_{(POM)}$ displayed a positive correlation with DO and Chl-*a*. It also had an inverse correlation with nitrate and silicate (Table 4.5). Also, the POC and PN correlation was comparatively more significant than that observed at the CEs. These features suggest the role of heterotrophic activity and regenerated production on the POM characteristics at the ACE influenced regions.

Moreover, the factor analysis performed on POM characteristic variables like $\delta^{13}C_{(POM)}$, $\delta^{15}N_{(POM)}$, POC, PN, C:N ratio and other physico-chemical properties at the ACE influenced locations implied four major factors influencing the POM dynamics at the ACE. One of the main factors was the hydrographic change due to eddy currents, which influence of inorganic components mainly the nitrates and silicate and tCO_2. Secondly, the heterotrophic activity in the ACE influenced waters. Another important factor to be considered is the influence of advective mixing, implied from the salinity and nutrients association and lastly the role of phytoplankton biomass and community variability in influencing the POM characteristics at the ACEs (Table 4.6).

Variables	Temperature	Salinity	DO	Nitrate	Nitrite	Ammonia	Phosphate	Silicate	Chl-*a*	POC	PN	$\delta^{13}C_{(POM)}$	$\delta^{15}N_{(POM)}$	C:N	POC:Chl-*a*	AOU
Temperature	**1**															
Salinity	**0.498**	**1**														
DO	0.084	-0.048	**1**													
Nitrate	**-0.731**	-0.172	-0.429	**1**												
Nitrite	-0.343	**-0.602**	-0.302	0.351	**1**											
Ammonia	-0.303	**-0.495**	0.050	0.195	0.305	**1**										
Phosphate	-0.054	**0.596**	0.107	-0.024	**-0.655**	-0.252	**1**									
Silicate	**-0.519**	-0.158	**-0.494**	**0.846**	**0.606**	0.198	-0.221	**1**								
Chl-*a*	-0.181	0.063	0.187	-0.349	-0.163	-0.200	0.314	-0.361	**1**							
POC	0.109	**-0.588**	0.192	-0.203	0.243	**0.509**	-0.364	-0.182	-0.245	**1**						
PN	0.383	**-0.440**	0.150	**-0.471**	0.251	0.140	-0.425	-0.317	-0.188	**0.739**	**1**					
$\delta^{13}C_{(POM)}$	0.194	-0.415	0.356	-0.125	0.031	**0.499**	**-0.460**	-0.183	**-0.460**	**0.713**	**0.488**	**1**				
$\delta^{15}N_{(POM)}$	0.124	0.079	**0.518**	**-0.640**	-0.424	-0.107	**0.468**	**-0.717**	**0.639**	0.151	0.256	-0.041	**1**			
C:N	-0.422	-0.052	0.059	0.405	-0.094	0.311	0.221	0.138	0.059	0.113	**-0.519**	0.218	-0.046	**1**		
POC:Chl-*a*	0.124	-0.256	-0.217	0.242	0.347	0.313	**-0.446**	0.253	**-0.771**	**0.525**	0.404	0.406	**-0.514**	-0.045	**1**	
AOU	**-0.599**	-0.077	**-0.665**	**0.842**	**0.522**	0.032	-0.055	**0.871**	-0.127	-0.311	-0.370	**-0.451**	**-0.550**	0.099	0.122	**1**

Table 4.5: Pearson's correlation matrix for bio-chemical variables at Anticyclonic eddy (ACE) locations during 2012 and 2013. All values in bold imply significant correlation between the variables (significance level alpha=0.05).

Variables	F1	F2	F3	F4
Depth	**0.880**	-0.387	0.101	0.164
Temperature	**-0.892**	-0.349	0.161	-0.237
Salinity	-0.118	-0.462	**0.847**	0.005
DO	-0.319	**0.803**	-0.087	0.339
***t*CO_2**	**0.720**	-0.261	0.530	0.078
Nitrate	**0.906**	0.046	0.058	-0.399
Nitrite	0.081	-0.224	**-0.905**	-0.090
Ammonia	-0.043	**0.958**	-0.093	-0.080
Phosphate	0.208	0.111	**0.721**	0.349
Silicate	**0.913**	-0.078	-0.150	-0.371
Chl-*a*	-0.136	-0.092	0.136	**0.786**
$\delta^{13}C_{(POM)}$	-0.403	**0.701**	-0.082	-0.583
$\delta^{15}N_{(POM)}$	-0.508	0.189	0.297	**0.680**
C:N	0.342	**0.841**	0.210	-0.005
Eigenvalue	**4.82**	**3.51**	**2.78**	**1.45**
Variability (%)	**34.40**	**25.05**	**19.83**	**10.37**
Cumulative %	**34.40**	**59.46**	**79.29**	**89.65**

Table 4.6: Principle factor Analysis for bio-chemical variables at Anticyclonic eddy (ACE) locations during 2012 and 2013.

Similar to CEs, even though the major factors/ processes responsible for changes in the POM characteristics were common at the ACE influenced regions, there was a

considerable difference at the ACE1, ACE2 and ACE3, implied from the statistical analysis of different physico-chemical and biological variables and the POM characteristics.

4.3 Discussion

4.3.1 Eddy characteristic features

The analysis of OSCAR data showed the presence of six eddies in the STF during the years 2012 and 2013. Also, the eddies observed in 2013 were found to be stronger than 2012 as evident from the magnitude of the surface currents in the study region. The detachment of CEs from the mean flow was evident at ~ 40°S during both the years and 42° 44′S & 58°E in 2013 (Fig. 4.10).

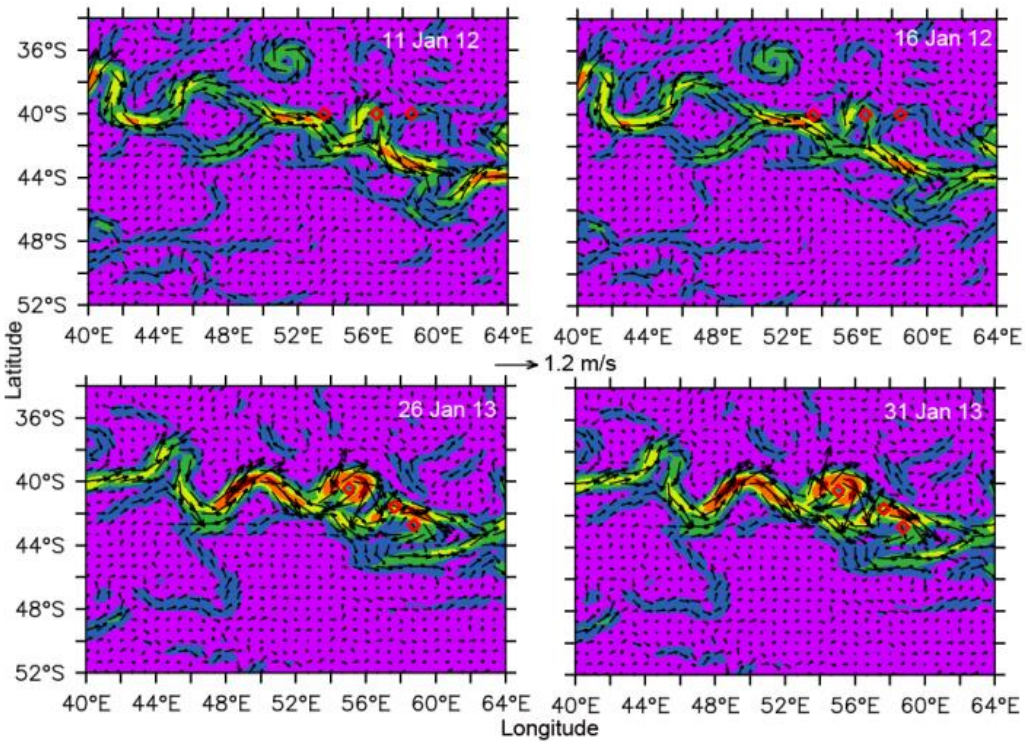

Figure 4.10: OSCAR (5-day average) surface currents variability in the study region during 2012 and 2013 during the study period.

The magnitude of the surface current at the CE2 and CE3 was strong (> 1 m/s) than the CE1 (<0.5 m/s). Likewise, the surface current at ACE2 and ACE3 was stronger (> 1 m/s) than ACE1 (<1 m/s). The ARC and STF merged region has been identified as the highest mesoscale variability in the entire SO (Lutjeharms & van Ballegooyen, 1988) due to the baroclinic instability of the mean currents at this region (Wells et al., 2000). Also, Zhu et al. (2018) reported that the region around the ARF is an area where the eddy kinetic energy transfer, from the mean flow to the eddies is most prominently. The eddy generation due the instability of the mean flow was visible in the surface current data during our period of study (Fig. 4.10).

Further, based on daily SSH, it was confirmed that the observation of CE1 was carried out at the eddy center. Also, the tracking of CE1 suggested that this eddy was ~ 3 months old at the time of sampling (Table 4.1) and had evolved from the south of STF (Fig. 4.11b). Similarly, CE2 sampling was done at the center of the eddy. However, this was a newly generated eddy, approximately 1 month old (Table 4.1) and originated in the STF (Fig. 4.11d). Compared to CE1 and CE2, the CE3 was <1 month old, with its origin in the STF, however this sampling location was at the eddy periphery (Fig. 4.11f).

The ACEs observed in 2012 were much older at the time of observation compared to the ACE observed in 2013. The SSH analysis showed that the ACE1 and ACE2 were ~ 3 to 4 months old at the time of study (Table 4.1), evolved within the STF (Fig. 4.11). However, the observation locations, ACE1 and ACE2 were made at the center and periphery respectively. Whereas, ACE3 was originated in the ARF (39°S) and evolved, moving towards the STF (Table 4.1) and noted to be <1 month, at the time of observation (Fig. 4.11).

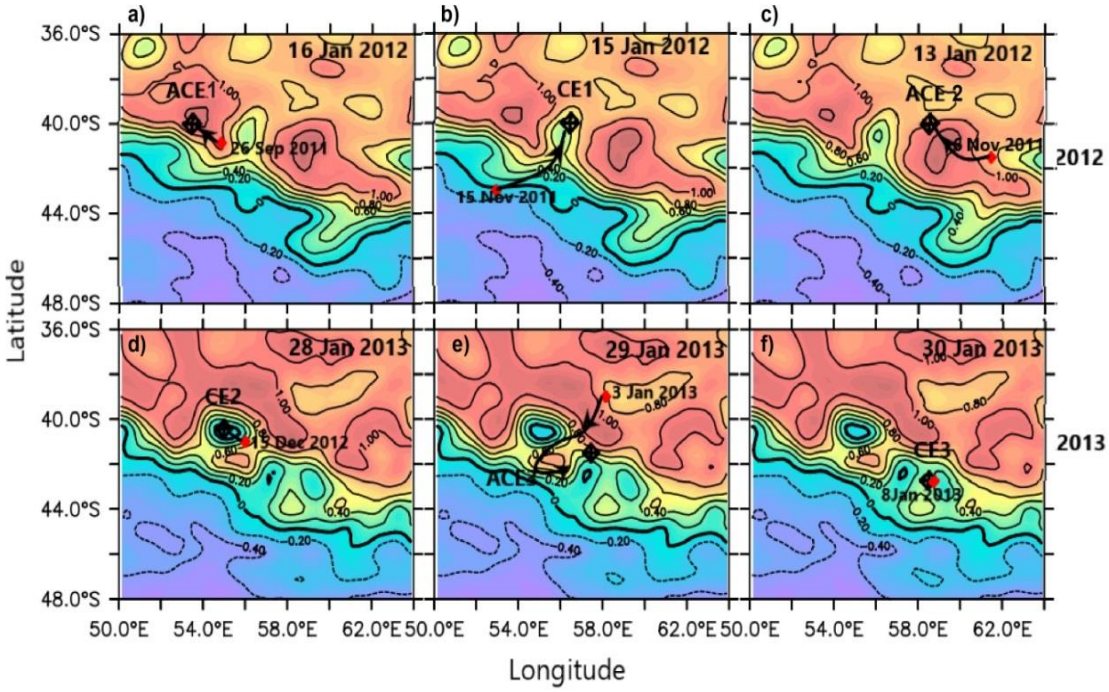

Figure 4.11: SSH variability and the trajectory of (a) ACE1, (b) CE1, (c) ACE2, (d) CE2, (e) ACE3 and (f) CE3.

The observed MLD at the CE locations was shallower compared to the ACEs during the period of study (Table 4.1). This was due to the eddy driven upwelling and downwelling process occurred in the study region (Bakun, 2006).

4.3.2 Biogeochemical processes controlling the POM characteristics at cyclonic eddies

The observed lower temperature in the CEs mostly coincided with higher nutrient concentration, which was due to the upward flux of cold, nutrient rich subsurface/deeper waters into the surface layer (McGillicuddy et al., 1998; Bidigare et al., 2003; Kolasinski et al., 2012), influencing the biological productivity and POM characteristics. During this study, it was observed that the POC concentration and the $\delta^{13}C_{(POM)}$ characteristics were considerably different at the three CEs. The influx of

nutrients to the euphotic waters played a significant role in the variability of $\delta^{13}C_{(POM)}$ in the STF. The higher $\delta^{13}C_{(POM)}$ were generally associated with warmer temperature and lower nutrient concentration indicated from the significant correlations of $\delta^{13}C_{(POM)}$with nutrients and temperature at this region (Table 4.3).

The $\delta^{13}C_{(POM)}$ at CE1 was enriched in ^{13}C (-22 ‰), especially upto the DCM depth (Fig. 4.8). This was likely due to the increase in primary productivity, as a result of supply of nutrients due to eddy pumping to the euphotic waters. The enhanced productivity is often associated with an increase in the CO_2 demand, and smaller fractionation (Canuel et al., 1995) during phytoplankton uptake which favors the enrichment of $\delta^{13}C_{(POM)}$ at CE1. Moreover, these waters were dominated by nanoflagellates (mostly dinoflagellates) (Fig. 4.6), which contains the enzymes PEPC (phosphoenolpyruvate carboxylase) and PEPCK (phosphoenolpyruvate carboxykinase), that can result in higher $\delta^{13}C_{(POM)}$ (Descolas-Gros and Oriol, 1992). The smaller fractionation and lesser discrimination among the available carbon forms during photosynthetic uptake (Bentaleb, et al., 1998) contribute to the high $\delta^{13}C_{(POM)}$ observed. Additionally, this enrichment of $\delta^{13}C_{(POM)}$ may be a response of regenerative processes and available ammonium supporting the biological productivity in low nitrate waters (Lara et al., 2010). It was evident from the biochemical variables that the CE1, was a region with contribution from regenerative processes. Also, the concentration of ammonium was higher at this location and showed a significant inverse correlation with $\delta^{13}C_{(POM)}$ and $\delta^{15}N_{(POM)}$ (Fig. 4.12a & b).

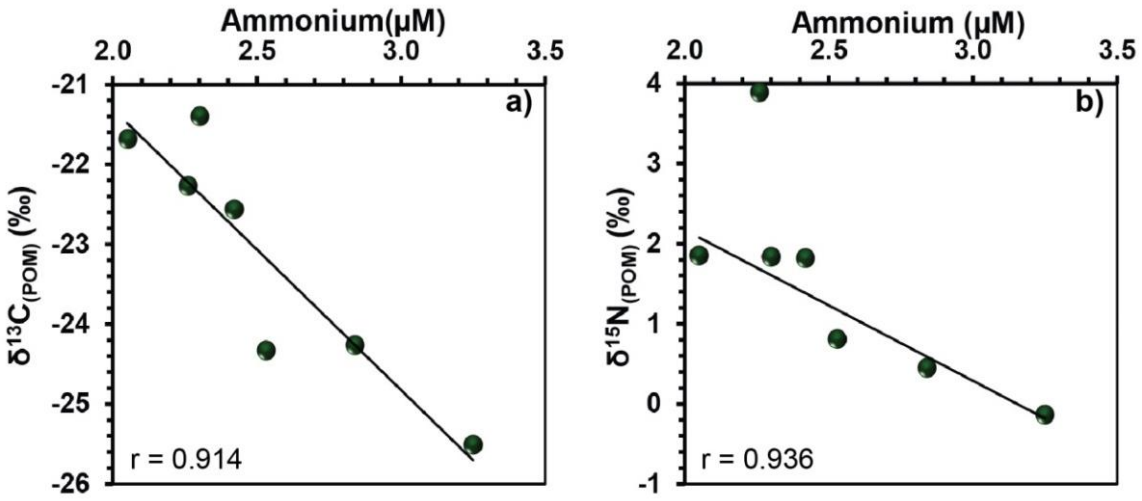

Figure 4.12: Spearmen's correlation of (a) $\delta^{13}C_{(POM)}$ and ammonium, (b) $\delta^{15}N_{(POM)}$ and ammonium at CE1.

This suggests the role of ammonium concentration to the biological productivity and thus the POM characteristics, at this location with low nitrates. Furthermore, the average of C:N ratio at CE1 (6.3), was closer to the Redfield's ratio (6.63) of fresh and growing phytoplankton cells (Laws et al., 2001), suggesting the presence of phytoplankton growth at CE1, which was evident in the satellite Chl-*a* (Fig. 4.13). Further, the CE1 was approximately 3 months old at the time of observation (Fig. 4.11) which suggests that this eddy was at a decaying phase during which the biological response is moderate with a sustained column production. The observed age of the CE1 and the governing biochemical processes implied that a recycling/ regenerative system prevailed in the CE1, also indicated from the factor analysis.

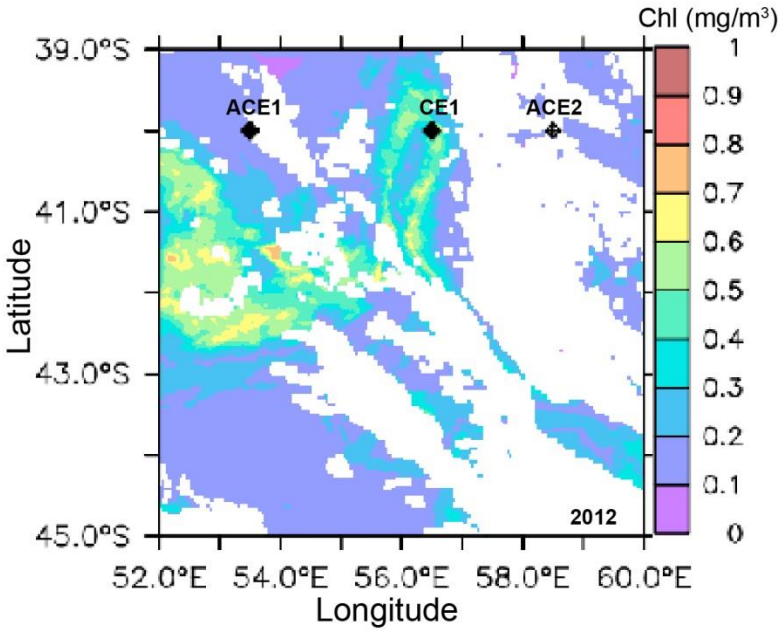

Figure 4.13: Weekly (6th to 13th January 2012) mean surface chlorophyll imagery derived from MODIS Aqua.

In the case of CE2 and CE3, the influx of nutrients due to eddy pumping was much higher than CE1, however, it was not reflected in the distribution of Chl-*a*. In the present study the low response of phytoplankton was probably due to a time lag between the initial influx of nutrients to the euphotic zone and its uptake. It was observed that CE2 and CE3 were newly generated with an approximate age of one month. This indicates that these eddies were at the initial stage of its life cycle, dominated by strong upwelling of subsurface/deeper waters (Sweeney et al., 2003). Further, the surface waters at CE2 and CE3, were dominated by nanoflagellates similar to CE1, but the contribution from picophytoplankton was considerably higher than at CE1. The observed low Chl-*a* and phytoplankton biomass has been attributed to the dominance of small sized phytoplankton at these eddies (Jasmine et al., 2009; Mishra et al., 2020; Venkataramana et al., 2020). Also the $\delta^{13}C_{(POM)}$, at the CE2 and CE3 was depleted (avg. -24.5 ‰) compared to CE1. The lower $\delta^{13}C_{(POM)}$ was possibly due to the strong upwelling of subsurface waters which can also bring partially

degraded POM from deeper waters to the surface layer. Additionally, the higher C:N ratio and higher POC:Chl-*a* (Fig. 4.7), suggested the presence of older, partially degraded refractory POM, rich in ^{13}C or probably a contribution from heterotrophic processes (Çoban-Yildiz et al., 2006) in the water column. This explains the higher (~twice) concentration of POC and PN observed at the CE2 and CE3, even though the Chl-*a* concentration was lower at these regions.

However, the surface waters at CE3 were comparatively colder than CE2, and also a prominent DCM was observed at ~ 50 m of CE3, unlike CE2. This increase in phytoplankton biomass at ~50 m could be due to a shift in the phytoplankton community at the DCM depth which comprised of nearly equal contribution from diatoms and picophytoplankton (Fig. 4.6). Further, even though the POM attributes (C:N ratio, POC:Chl-*a* ratio and $\delta^{15}N_{(POM)}$ values) were more variable and a notch higher compared to CE2 (Fig. 4.7), these properties affirmed the observation at CE3 was at an early phase (Kolasinski et al., 2012). Even though CE2 and CE3 were almost similar in age and origin, there are differences in the biological processes/activity. This may since the CE3 was at the periphery of the eddy while CE2 location was at the centre (Fig. 4.1). The strong currents at the outer periphery of the eddies favours higher biological production (Sabu et al., 2015; Brannigan, 2016) hence the variability of POM characteristics.

Overall the POM properties (C:N, POC:Chl-*a*) at the DCM was similar to fresh POM, suggesting higher autotrophic activity at this depth (Hoffmann et al., 2006). Further, the $\delta^{15}N_{(POM)}$ at the DCM depth was also enriched, with the maximum enrichment at CE3 and a significant positive correlation of $\delta^{15}N_{(POM)}$ and Chl-*a*, further ascertains the prevalence of growing phytoplankton cells at the DCM.

In general, the three CEs observed at STF in the present study were different in their biogeochemical responses and POM characteristics which can be attributed to the significant difference in the age of these eddies at different phases of its life cycle. Previous studies have revealed that the origin and stage of the eddy life cycle have a significant role in the biological pattern (Sweeney et al., 2003; Josè et al., 2014). This study implied that the eddy dynamics also influence the POM dynamics in the photic waters. Hence it can be postulated that the physical processes such as age, intensity and origin of the eddy at the STF, may play a significant role in influencing the local biogeochemical processes and the POM characteristics

4.3.3 Biogeochemical processes controlling the POM characteristics at Anticyclonic eddies

The observed ACEs in the present study were low in nutrients and increased gradually below ~75 m. Also, the ACEs were associated with comparatively lower POC and PN than the CEs. In spite of the low nutrients, a prominent DCM was observed at ~75 m, especially in ACE1 and ACE2. Also, the euphotic depths at ACE1 and ACE2 were deeper and observed at ~85 m and ~80 m respectively; unlike at ACE3. This suggested that the depth of the DCM at these locations was dependent on the nutrient concentration and the light availability. Earlier studies have explained the relation between the light and the DCM (Liu et al., 2018) due to the adaptation of phytoplankton to increased nutrients and the light intensity (Gieskes et al., 1978; Hickman et al., 2012).

The $\delta^{15}N_{(POM)}$ was enriched at ACE1 and ACE2, especially at DCM which was attributed to an increase in phytoplankton productivity. The $\delta^{15}N_{(POM)}$ is primarily

dependent on the isotopic ratio of the nitrate present and the degree of its uptake in the water column (Altabet and François, 1994; Montoya, 1994). At the DCM, the presence of actively growing phytoplankton and low nitrates, could result in the dominance of ^{15}N rich nitrate available for uptake, which favors the enrichment of $\delta^{15}N_{(POM).}$ This was indicated from the significant positive correlation of $\delta^{15}N_{(POM)}$ with Chl-*a* and inverse correlation with nitrates (Table 4.5). Further, the $\delta^{13}C_{(POM)}$ depleted gradually with depth below the DCM at these two ACEs suggesting the role of degradation in altering the POM properties responsible for the lower $\delta^{13}C_{(POM)}$ below the DCM (Eadie and Jeffrey, 1973; Harvey et al., 1995; Kolasinski et al., 2012).

Additionally, the ACE1 was warmer with least concentration of nitrates than the other ACEs, this resulted in the low Chl-*a* concentration with significant contribution from prokaryotic picophytoplankton (~30 %) above the DCM. Similar scenario has been reported in nutrient depleted warm oligotrophic waters (Agawin et al., 2000). Also, the POC:Chl-*a* ratio above DCM was >200, suggesting the contribution from heterotrophic processes (Savoye et al., 2003). However, at the DCM the C:N ratio (~6) and POC:Chl-*a* ratio (<100) suggested a major contribution from fresh organic matter and phytoplankton to the POC which also indicates the dominance of autotrophic processes at this depth (Maksymowska et al., 2000; Savoye et al., 2003).

Moreover, the C:N ratio was higher than the Redfield's ratio of phytoplankton, and was highly variable at ACE2 (Fig. 4.7). This was likely due to the abundance of macrozooplankton like Pyrosoma and Salps in the surface waters of this region, implying the effect of grazing. This also suggests a significant contribution

from the fecal matter of this grazing community to the POM (Caron et al., 1989), responsible for the higher C:N ratios observed at ACE2. Another possible factor contributing to the high variability in POM characteristics at ACE2 was, that this location was at the periphery of an aged ACE (Fig. 4.1; Table 4.1), and under the influence of eddy-wind interactions. The higher variability of C:N within the upper water column was due to the complex dynamics of ACE2 location (Soares et al., 2020) altering the POM characteristics.

Furthermore, at ACE3 the $\delta^{13}C_{(POM)}$ was the most enriched compared to the other two ACEs (Fig. 4.7), and also showed lower Chl-*a*. However, the correlation of $\delta^{13}C_{(POM)}$ with nitrate and Chl-*a* (Table 4.5), implied the nitrate dependent phytoplankton growth at ACE3. Additionally, the correlations of $\delta^{15}N_{(POM)}$ with nitrates and Chl-*a* (Fig. 4.14a & b), and the inverse relation of nitrate with Chl-*a* (Fig. 4.14c), suggests the sustenance of phytoplankton biomass under low nutrient conditions (Chen et al., 2004). It was also noted, that the contribution of the diatom community was higher at ACE3.

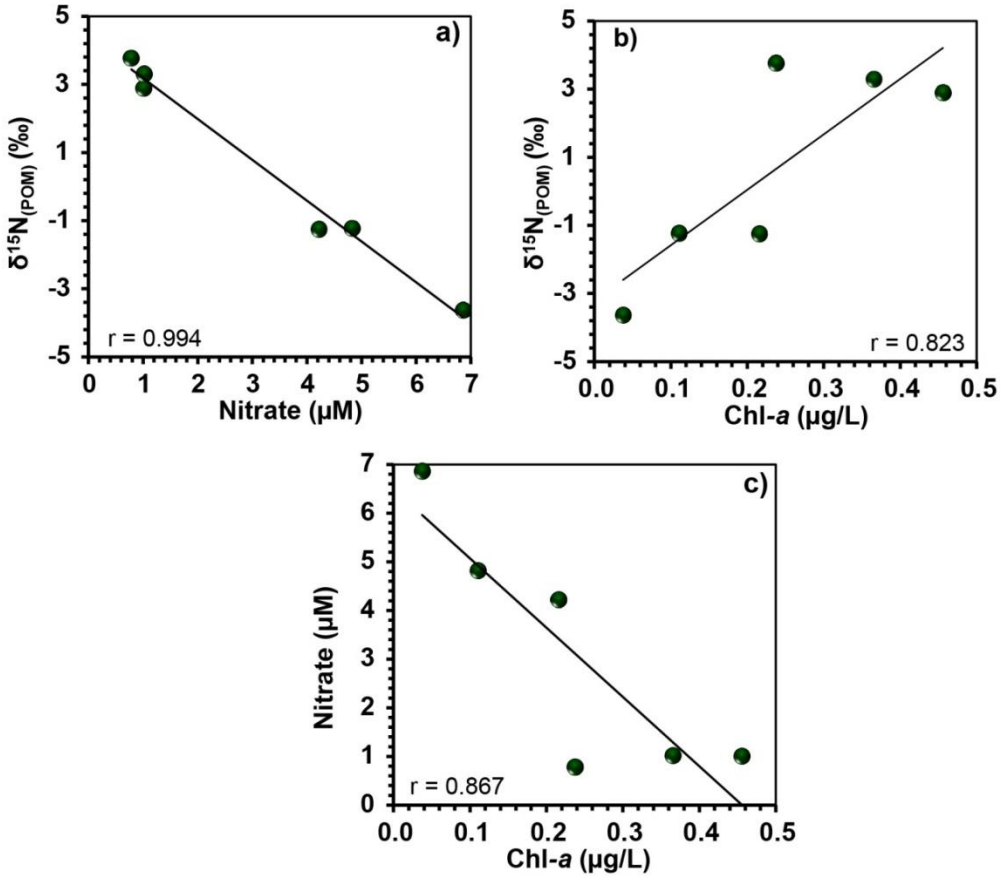

Figure 4.14: Spearmen's correlation of (a) $\delta^{15}N_{(POM)}$ with nitrate, (b) $\delta^{15}N_{(POM)}$ with chlorophyll and (c) Nitrate with chlorophyll at ACE3.

Additionally, it was observed that the C:N ratio and POC:Chl-*a* ratio increased with depth and was accompanied with a decrease in POC, implying a contribution of detrital matter to POM or the prevalence of heterotrophic processes (Savoye et al., 2003; Coppola et al., 2005) relative to autotrophy below the DCM. This is also supported by a positive correlation of $\delta^{13}C_{(POM),}$ with POC, and an increase in AOU corresponding to the decrease in POC at this region, implying the impact of increase in respiration/heterotrophic activity (Omand et al., 2015) beyond the DCM.

Overall, although, the hydrographic features and chemical variables at CE3 and ACE2 were quite distinct and different, there was a little similarity in the column

variability of POM properties, at CE3 and ACE2. Perhaps this could be because both these sampling locations were at the eddy periphery of CE and ACE, respectively. Although the age and origin of these two eddies were different, these sampling locations were associated with the dynamics of eddy boundary processes. The CE3 had a significant influence from the eddy-eddy interaction and supported by submesoscale mixing at the edge of the eddy (Gaube et al., 2015; Brannigan 2016). While, ACE2 was associated with eddy-wind mixing that cause undulations and changes in the nutrient dynamics, impacting the biology (McGillicuddy, 2016; Soares et al., 2020) and POM characteristics at eddy periphery.

4.4 Salient Findings

The prevalence of eddies had a significant influence on the thermohaline properties, and the nutrient availability in these regions. Further, the nutrient variability and column stability influenced the dominant phytoplankton community, and POM characteristics.

The POM characteristics, its isotopic signatures ($\delta^{13}C_{(POM)}$ & $\delta^{15}N_{(POM)}$) were significantly different at the CEs and ACEs and also at the centre and periphery of the eddy. Overall, the enrichment of $\delta^{13}C_{(POM)}$ at the CEs was the most at CE1 surface waters, unlike the $\delta^{15}N_{(POM)}$ that was most enriched at the DCM of ACEs. Although, the hydrographical features at CE3 and ACE2 were different, the similarity in the POM properties was attributed to the eddy-eddy interaction and eddy-wind interaction that influenced the nutrient dynamics and the POM characteristics via the response of the biological community.

Further, the observed eddies were at different stages of the eddy-cycle. In 2012 the eddies were at a later phase, mainly at a maturity phase, unlike 2013 when the eddies were at its initial phase of the eddy life cycle, that was responsible for a shift in the phytoplankton community and the variability in POM characteristics. This study ascertains that the origin/source of the eddy, its age and the different phases of the eddy life cycle are very critical in determining the POM characteristics in the STF. This also have an important role in determining the functional food web structure and the fate of POM at the eddy influenced regions like STF.

5. Dynamics of POM in the upper ocean across the Fronts in the Indian sector of the Southern Ocean

5.1 Introduction

Oceans contain large amount of OM and exists as, DOM and POM forms that play an important role in the global carbon. The quality and quantity of POM in oceans are largely dependent on the column stratification, light intensity, nutrient availability, phytoplankton community (Kuenzler and Ketchum, 1962; Menzel and Ryther, 1964; Menzel and Goering, 1966). Heterotrophic organisms including the zooplankton also play a crucial role in determining the elemental composition of POM (Crawford et al., 2015; Talmy et al., 2016). The different biogeochemical processes can alter the carbon and nitrogen content of POM (Schneider et al., 2003). The ISSO being a dynamic region due to seasonal changes and short-term events, which may greatly impact the qualitative and quantitative properties of POM (George et al., 2018; Huang et al, 2018; Soares et al., 2020).

Studies in the ISSO have shown that the composition and transformation of POM vary largely across the fronts (Soares et al., 2020a) due to changes in the environmental conditions leading to its export or remineralisation (Omand et al., 2020). The depth of remineralisation is also important in the sequestration and redistribution of carbon and nutrients in the upper water column (Kwon et al., 2009; Segschneider and Bendtsen, 2013). Hence, the changes in the POM characteristics produced in the surface waters, is significantly related to its origin and the alterations in the water column (Tremblay, et al., 2014).

Understanding the variability of POM across the different fronts is very important to quantify the biogenic carbon fluxes in the oceanic environment, as addressed in this chapter. Since there are limited studies on POM dynamics with the column of the ISSO, section **5.3.1** of this chapter address the upper column variability across the fronts of the ISSO and the dominant trophic process in these frontal regions. Further the next section (**5.3.2**) attempts to understand the major factors contributing to the column transformation of POM and the frontal variability of POM characteristics. This chapter also address the possible fate of POM, with respect to POC-fluxes and the remineralisation of POM in section **5.3.3**, in an attempt to understand the efficiency of the oceanic biological pump. And the next section (**5.3.4**) tries to elucidate the driving forces responsible for the inter-annual variability of POM dynamics across the frontal regions of the ISSO.

5.2 Results

5.2.1 Hydrography and nutrients

There was a sharp gradient (~19 to 2 °C) in the water-column temperature from STFZ to SAFZ and PFZ with an increased cooling (0.4 °C) in the PFZ water column, especially during 2013 (Fig. 5.1a & b; Table 5.1 & 5.2). The upper water column was comparatively warmer during 2012 than 2013. Further, the isotherms within the STFZ showed undulations during both the years of study, and were more intense during 2013 (Fig. 5.1b), probably due to the fact that this region is prone to frequent formation of both cyclonic and anti-cyclonic eddies. Likewise, the gradient in salinity also showed a decrease from the STFZ (avg. 34.60±0.71) to the PFZ (avg. 33.84±0.07), (Table 5.1 & 5.2).

Similar to isotherms, undulations in the isohalines was observed at the STFZ during both the years (Fig. 5.1c & d). It was also observed that the waters were fresher at SAFZ (33.8) and almost similar to PFZ (33.7-33.9) (Fig. 5.1d) during 2013. Overall the water column was fresher during 2013 compared to 2012. Also, the observed MLD deepened towards the PFZ (Table 5.3). Dissolved oxygen generally ranged from 217 to 339 µM (Table 5.1 & 5.2) during the study periods. In the STFZ, DO (217 to 304 µM) exhibited a large variation (Fig 5.1e & f), especially during 2013. Also, DO increased gradually southwards along SAFZ (241 to 292 µM) where the DO within the water-column was more uniform than the other regions, beyond which, the oxygen levels became highly saturated (306 - 339 µM) at the PFZ (Fig. 5.1e & f). Further, the AOU increased with depth and was higher below the euphotic depth across all the frontal regions. It was also observed that the AOU was a notch higher during 2013 austral summer (Table 5.1 & 5.2)

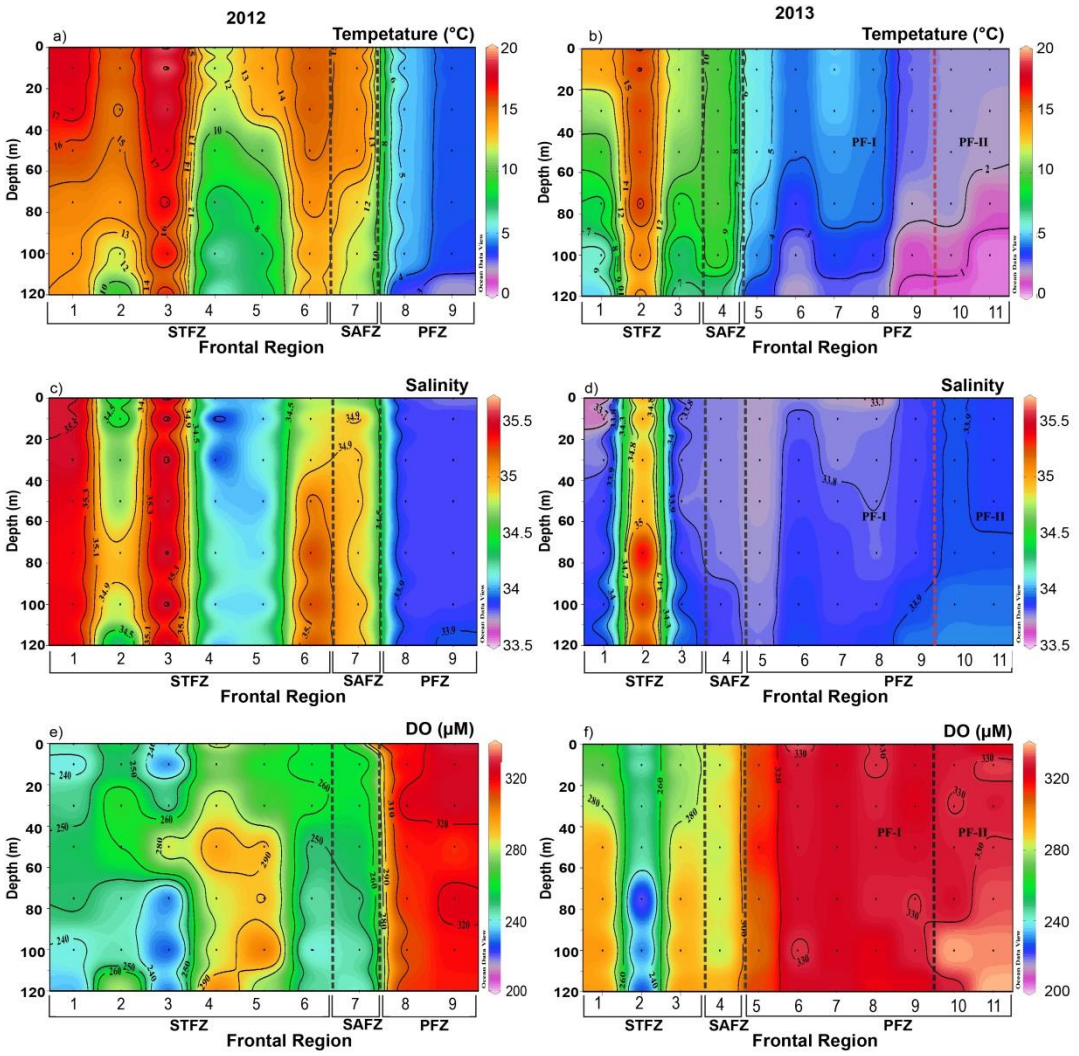

Figure 5.1: The variability of Temperature (a, b); Salinity (c, d) and the concentration of dissolved oxygen (DO) (e, f) in the upper 120 m water-column, across the different fronts of the ISSO during austral summer 2012 and 2013.

Region	Temperature (°C)	Salinity	DO (µM)	NO_3 (µM)	PO_4 (µM)	SiO_4 (µM)	NH_3 (µM)	N:P	N:Si	Chl-*a* (µg/L)	POC (µg/L)	PN (µg/L)	$\delta^{13}C_{(POM)}$ (‰)	$\delta^{15}N_{(POM)}$ (‰)	C:N	POC:Chl-a	AOU (µM)
Sub-Tropical Frontal Zone (STFZ)	**5.8 - 19.3** (13.6 ±3.7)	**33.82 - 35.60** (34.78 ±0.66)	**225 - 304** (259 ±22)	**0.09 - 20.10** (6.80 ±5.81)	**1.18 - 2.56** (1.67 ±0.37)	**0.88 - 5.49** (2.35 ±1.29)	**0.85 - 3.25** (1.94 ±0.47)	**1.6 - 9.0** (4.8 ±2.3)	**1.0 - 14.0** (4.3 ±3.3)	**0.05 - 1.19** (0.48 ±0.31)	**15.1 - 74.6** (63.0 ±15.5)	**1.5 - 16.6** (6.7 ±3.6)	**-27.8 to -21.4** (-24.5 ±1.8)	**-0.7 to 4.4** (1.8 ±1.5)	**3.1 - 21.8** (7.2 ±3.8)	**22 - 366** (108 ±80)	**-10.6 to 28.2** (4.9 ±11.2)
Sub Antarctic Frontal Zone (SAFZ)	**11.6 - 14.5** (13.4 ±1.39)	**34.66 - 34.96** (34.89 ±0.10)	**241 - 256** (249 ±6)	**2.03 - 11.37** (5.68 ±3.97)	**1.18 - 1.75** (1.15 ±0.24)	**1.19 - 4.92** (2.67 ±1.65)	**1.65 - 2.30** (2.03 ±0.27)	**3.2 - 8.1** (5.3 ±1.2	**2.7 - 3.8** (3.3 ±0.5)	**0.07 - 0.81** (0.48 ±0.29)	**21.3 - 36.8** (31.9 ±5.0)	**4.02 - 7.55** (6.3 ±1.1)	**-26.2 to -24.8** (-25.5 ±0.6)	**2.9 To 4.1** (3.4 ±0.4)	**4.2 - 5.6** (5.1 ±0.5)	**26 - 202** (78 ±70)	**-0.1 To 31.2** (13.7 ±13.9)
Polar Frontal Zone (PFZ)	**2.2 - 5.3** (4.2 ±0.8)	**33.73 - 33.92** (33.80 ±0.05)	**306 - 328** (316 ±5)	**15.01 - 28.46** (20.47 ±3.54)	**1.79 - 3.65** (2.37 ±0.45)	**2.80 - 25.81** (7.76 ±5.0)	**1.12 - 3.60** (2.02 ±0.62)	**7.0 - 12.7** (9.9 ±1.7)	**1.19 - 7.18** (3.8 ±1.8)	**0.07 - 0.67** (0.45 ±0.17)	**31.2 - 54.9** (41.3 ±7.3)	**5.8 - 16.7** (9.2 ±3.1)	**-28.3 to -24.0** (26.5 ±1.0)	**-2.9 to 2.2** (-0.0 ±1.4)	**3.3 - 10.2** (6.1 ±1.4)	**59 - 269** (109 ±51)	**-3.2 to 24.1** (7.7 ±7.6)

Table 5.1: The range and average (in parenthesis is the column average) of temperature, salinity, DO, NO_3, PO_4, SiO_4, NH_3, N:P, N:Si, Chl-*a*, POC, PN, $\delta^{13}C_{(POM)}$, $\delta^{15}N_{(POM)}$, C:N (M/M), POC:Chl-*a*, and AOU within the upper water column at the different fronts during austral summer 2012.

Region	Temperature (°C)	Salinity	DO (µM)	NO_3 (µM)	PO_4 (µM)	SiO_4 (µM)	NH_3 (µM)	N:P	N:Si	Chl-*a* (µg/L)	POC (µg/L)	PN (µg/L)	$\delta^{13}C_{(POM)}$ (‰)	$\delta^{15}N_{(POM)}$ (‰)	C:N	POC:Chl-a	AOU (µM)
Sub-Tropical Frontal Zone (STFZ)	**5.0 - 16.3** (11.5 ±3.8)	**33.65 - 35.42** (34.24 ±27.2)	**217 - 298** (269 ±27)	**0.78 - 17.75** (10.27 ±5.8)	**0.94 - 2.20** (1.44 ±0.40)	**2.34 - 6.13** (3.87 ±1.07)	**0.81 - 2.80** (1.88 ±0.52)	**3.2 - 18.7** (9.1 ±4.3)	**1.2 - 5.4** (3.3 ±1.3)	**0.04 - 0.75** (0.28 ±0.16)	**29.5 - 194.2** (78.2 ±42.9)	**3.3 - 16.7** (9.3 ±3.8)	**-26.6 to -22.5** (-24.8 ±0.9)	**-5.2 to 5.4** (0.4 ±2.9)	**6.5 - 22.4** (9.9 ±3.6)	**93 - 517** (285 ±148)	**-5.7 to 31.9** (6.5 ±11.6)
Sub Antarctic Frontal Zone (SAFZ)	**7.0 - 9.7** (9.3 ±1.0)	**33.78 - 33.83** (33.79 ±0.02)	**281 - 292** (284 ±4)	**12.22 - 16.78** (14.45 ±1.4)	**1.64 - 2.07** (1.89 ±0.17)	**3.56 - 4.65** (4.01 ±0.34)	**1.07 - 3.40** (2.29 ±0.85)	**8.4 - 10.4** (9.3 ±0.7)	**4.1 - 4.6** (4.4 ±0.2)	**0.29 - 0.67** (0.44 ±0.14)	**20.9 - 121.4** (53.2 ±25.7)	**3.6 - 11.5** (8.9 ±2.7)	**-25.7 to -23.8** (-24.5 ±0.6)	**-4.1 to -0.5** (-2.7 ±1.2)	**5.1 - 13.5** (7.2 ±2.8)	**79 - 212** (108 ±47)	**1.5 to 11.4** (4.5 ±3.4)
Polar Frontal Zone (PFZ)	**0.4 - 4.9** (3.0 ±1.3)	**33.69 - 33.97** (33.84 ±0.06)	**319 - 339** (327 ±4)	**11.46 - 27.04** (21.74 ±4.5)	**1.30 - 2.30** (1.89 ±0.31)	**3.73 -** 40.27 (18.6 ±11.6)	**1.87 - 3.52** (2.62 ±0.49)	**10.5 - 14.9** (13.3 ±1.0)	**0.69 - 6.20** (2.2 ±1.7)	**0.08 - 1.11** (0.43 ±0.31)	**24.8 - 80.5** (52.4 ±14.4)	**4.2 - 14.7** (8.8 ±2.8)	**-27.3 to -24.8** (-25.8 ±0.72)	**-4.9 to 1.5** (-2.0 ±1.7)	**5.6 - 11.9** (7.1 ±1.5)	**54 - 374** (152 ±96)	**-7.3 to 33.2** (6.7 ±10.2)

Table 5.2: The range and average (in parenthesis is the column average) of temperature, salinity, DO, NO_3, PO_4, SiO_4, NH_3, N:P, N:Si, Chl-*a*, POC, PN, $\delta^{13}C_{(POM),}$ $\delta^{15}N_{(POM)}$, C:N (M/M), POC:Chl-*a*, and AOU within the upper water column at the different fronts during austral summer 2013.

Station No.	Front	Latitude (°S)	Longitude (°E)	ED (m)	MLD (m)	DCM (m)		Station No.	Front		Latitude (°S)	Longitude (°E)	ED (m)	MLD (m)	DCM (m)
2012 austral summer								**2013 Austral summer**							
1.	STFZ	40	58.5	50	37	62		1.	STFZ		40.4	55.06	63	24	55
2.		40	56.5	46	18	45		2.			41.6	57.7	59	63	50
3.		40	53.5	76	23	68		3.			42.7	58.5	54	41	55
4.		43	53.5	54	36	50		4.	SAFZ		45.0	57.6	43	86	60
5.		43	56.5	58	29	30		5.	PFZ	PF-I	49.6	57.5	54	57	65
6.		43	58.5	34	39	35		6.			50.7	50.5	56	66	70
7.	SAFZ	45	58.5	40	48	52		7.			51.4	51.6	56	106	100
8.	PFZ	50	57.5	53	105	82		8.			52.4	48.1	74	76	75
9.		53	57.5	44	90	88		9.		PF-II	56.6	57.7	55	71	70
								10.			56.5	54.7	74	100	98

Table 5.3: The Euphotic Depth (ED), Mixed Layer Depth (MLD), and the depth of the Deep Chlorophyll Maxima (DCM), identified at the different locations across the fronts during the two consecutive austral summer studies in the ISSO.

All the macronutrients (nitrate, silicate, phosphate) remained low in the STFZ, which increased gradually towards PFZ. Overall, the nutrients were comparatively higher during 2013 than 2012 (Fig. 5.2 a-f). Nitrate showed a patchy distribution in STFZ (0.09 - 20.10 µM), and SAFZ (2.03 to 16.78 µM), but there was a ~10-fold increase in the PFZ waters (11.46 to 28.46 µM) (Fig 5.2 a & b; Table 5.1 & 5.2).

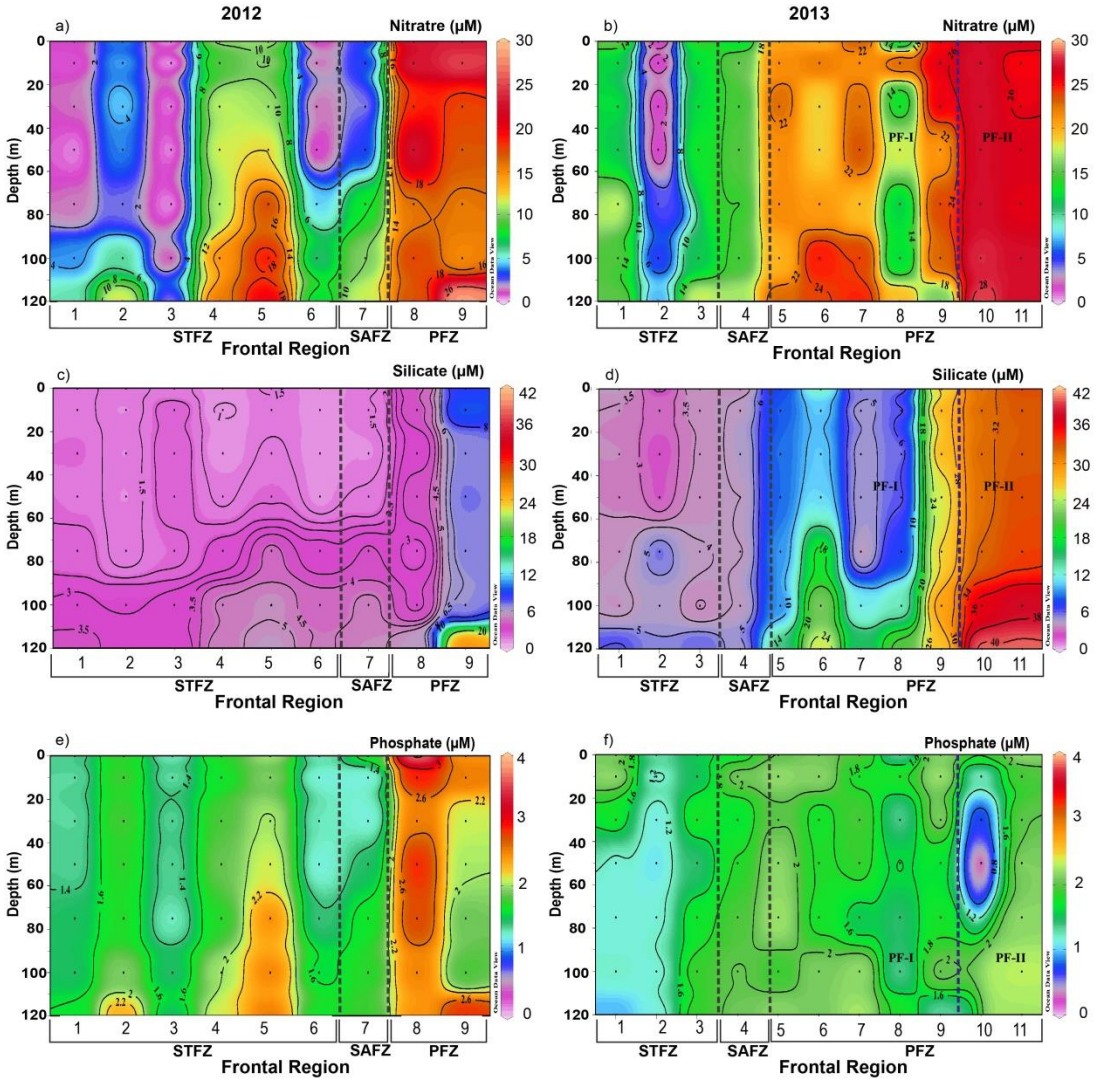

Figure 5.2: The column variability in the concentration of nitrate (a, b); silicate (c, d) and phosphates (e, f) in the upper 120 m water-column, across the different fronts of the ISSO during austral summer 2012 and 2013.

In general, the concentration of silicates increased from the STFZ with high variability (0.88 to 6.13 µM) and SAFZ (1.19 to 4.92 µM) to a maximum in the PFZ

(2.8 to 40.27 µM) during both the periods (Fig 5.2 c & d), especially during 2013. The concentration of phosphate, however, did not show any significant variation across these fronts. The average concentration of phosphate was 1.6± 0.4 µM; 1.7±0.3 µM and 2.0±0.5 µM at the STFZ, SAFZ and PFZ, respectively, indicating a small increasing gradient towards PFZ during this study (Fig. 5.2 e & f).

5.2.2 Quality of POM

The concentration of POC was lower (15.1 to 74.6 µg/L) during 2012 compared to 2013 (29.5 to 194.2 µg/L) in the STFZ (Table 5.1 & 5.2). Both POC and PN were highly variable during both years (Fig. 5.3a, b), though POC decreased below the depth of DCM.

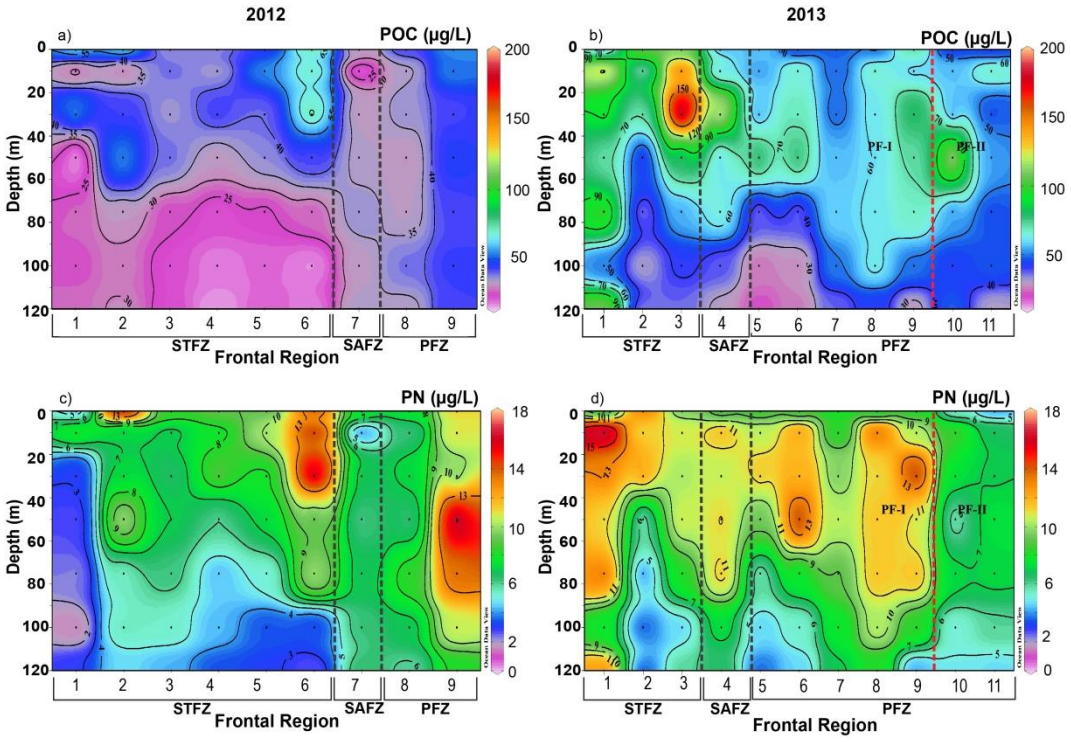

Figure 5.3: The column variability in the concentration of POC and PN in the upper 120 m water-column, across the different fronts of the ISSO during 2012 (a, c) and 2013 (b, d)

Further in the SAFZ, the POC was consistently low during both the years, with a range of 21.3 to 36.8 µg/L and 28.8 to 121.4 µg/L, respectively during 2012 and 2013. However, in the PFZ the POC ranged from 31.2 to 54.9 µg/L and showed very little column variability during 2012 (Fig. 5.3a) and varied from 24.8 to 80.5 µg/L during 2013 (Fig. 5.3b).

Similar to POC, the overall concentration of PN ranged from 1.5 to 16.7 µg/L and 3.3 to 16.7 µg/L across the fronts during 2012 and 2013, respectively, with maximum variability in the STFZ (Table 5.1 & 5.2). Although the overall range of PN was quite similar during both the periods, it was noted that the overall PN was higher during 2013 and the concentration decreased with depth in the upper water column (Fig. 5.3c & d). It was observed that during 2012, PN concentration was higher in the PFZ (Fig. 5.3c), but during 2013 the higher PN was observed at the STFZ, and the low concentration at PF-II in the PFZ (Fig. 5.3d).

During this study, the overall $\delta^{13}C_{(POM)}$ ranged from -28.3 ‰ to -21.4 ‰ in 2012 and -27.3 ‰ to -22.5 ‰ in 2013 indicating its relative enrichment during 2012 (Fig 5.4a & b). $\delta^{13}C_{(POM)}$ showed maximum variability in STFZ (-27.8 to -21.4 ‰) followed by SAFZ (-26.2 to -24.8 ‰) and PFZ (-28.3 to -24.0 ‰) during 2012 (Table 1). During 2013, $\delta^{13}C_{(POM)}$ was almost consistent with 2012, and the concentration was higher at STFZ (-26.6 to -22.5 ‰), it was depleted towards the south from SAFZ (-25.7 to -23.8 ‰) and PFZ (-27.3 to -24.8 ‰). (Table 5.2). Additionally, $\delta^{13}C_{(POM)}$ showed a gradual decrease with depth (Fig 5.4a & b).

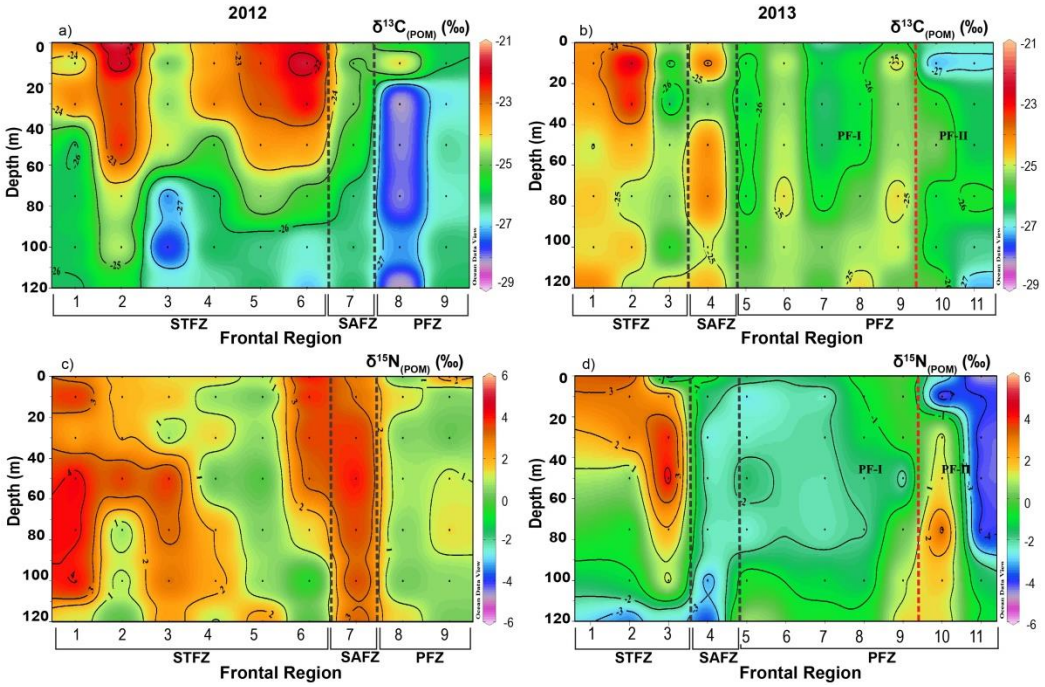

Figure 5.4: The upper (120 m) water column variability of $\delta^{13}C_{(POM)}$ and the $\delta^{15}N_{(POM)}$ across the different fronts of the ISSO during 2012 (a, c) and 2013 (b, d)

The overall variability of $\delta^{15}N_{(POM)}$ was comparatively lower during 2012 (-0.7 to 4.4 ‰) than 2013 (-5.2 to 5.4 ‰) and showed a decreasing gradient towards PFZ (Fig 5.4c & d). The maximum variability of $\delta^{15}N_{(POM)}$ was observed in STFZ (-5.2 to 5.4 ‰), also the enrichment of $\delta^{15}N_{(POM)}$ was higher at the STFZ during 2012. $\delta^{15}N_{(POM)}$ showed a consistent depletion from STFZ (1. 4±2.2 ‰) to SAFZ (0.4 ±3.3 ‰) and PFZ (-1.1 ±2.1 ‰), and the lowest $\delta^{15}N_{(POM)}$ was observed during 2013 at the PF-II (~56°S). High $\delta^{15}N_{(POM)}$ values were observed at DCM depths especially, within the STFZ (Fig. 5.4c), which decreased below DCM.

The C:N ratio showed wide variability in STFZ (3.1 to 22.4) followed by SAFZ (4.2 to 13.5) and PFZ (3.3 to 11.9). The C:N ratio was generally high during 2013 (Fig 5.5a, b), especially in STFZ water column.

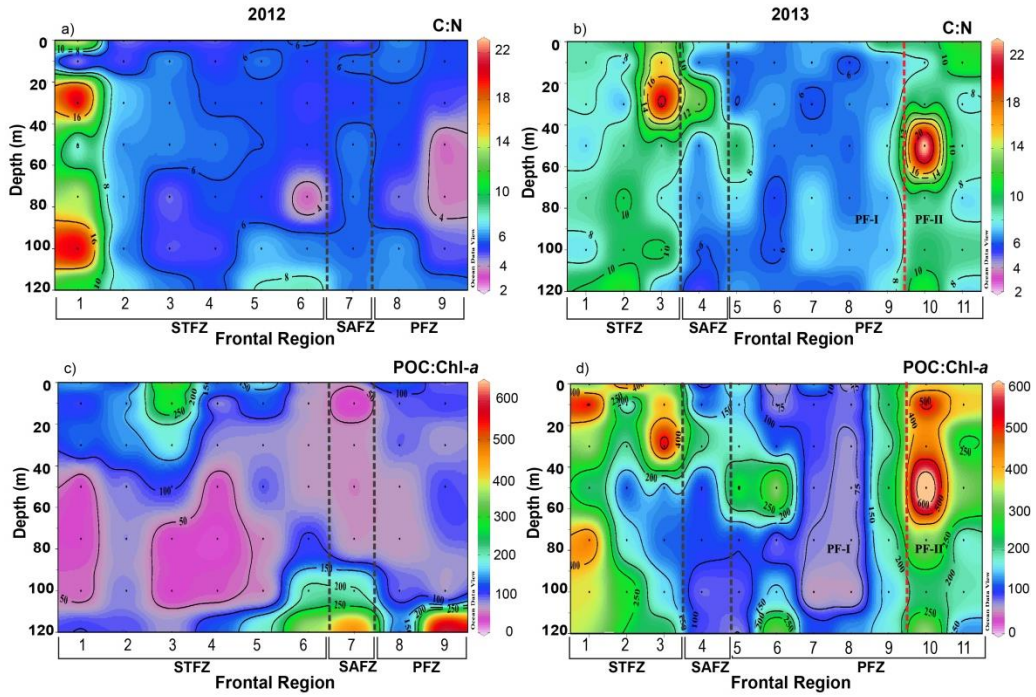

Figure 5.5: The variation in the C:N ratio and the POC:Chl-*a* ratios in the upper water-column (120m), across the different fronts of the ISSO during 2012 (a, c) and 2013 (b, d).

Further, the POC:Chl-*a* ratio was also higher during 2013 (54 to 517) compared to 2012 (22 to 366), except for some exceptional vales. POC:Chl-*a* ratio showed high variation within the STFZ (22 to 517) compared to the other two frontal (SAFZ and PFZ) regions (Fig. 5.5c, d). In the STFZ, the POC:Chl-*a* ratio was low at the DCM depth. Additionally, the higher POC:Chl-*a* ratios observed in PFZ were mainly the locations sampled beyond 56°S, which is referred as PF-II in the ISSO.

5.2.3 Chl-a and Phytoplankton Community

The Chl-*a* concentration varied from 0.04 to 1.19 µg/L and was comparatively higher during 2012 than 2013 (Fig. 5.6a & b). Chl-*a* exhibited significantly high variability in the STFZ (0.04 to 1.19 µg/L), during 2012 (Fig. 5.6a). Further south, it varied from 0.07 to 0.81µg/L at SAFZ and 0.07 to 1.1 µg/L at PFZ and showed a prominent DCM at STFZ and SAFZ between ~ 50 - 75 m, especially during 2012 (Fig. 5.6a) and was mostly relative to the MLD (Table 5.3). In general, Chl-*a*,was higher at the PFZ, especially during 2013 (Fig.5.6b), except at PF-II (~56°S).

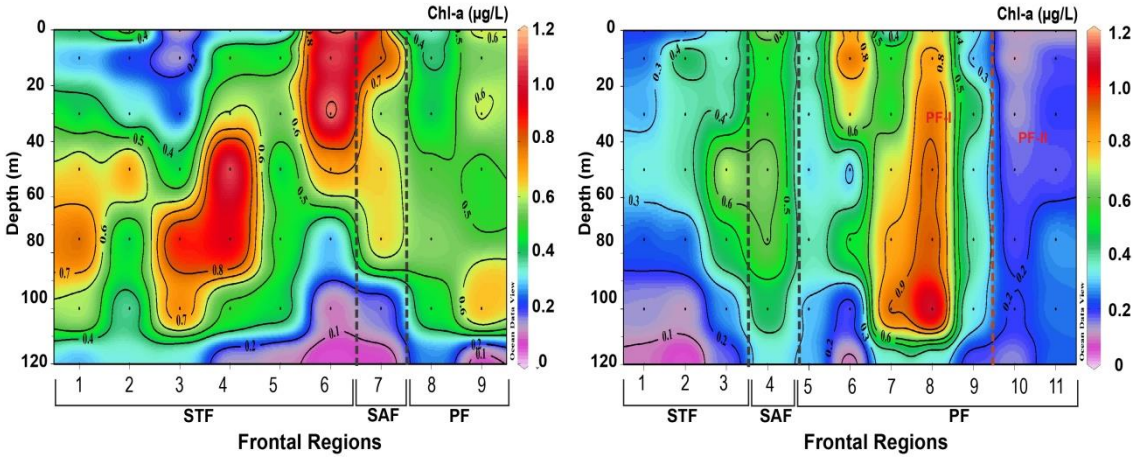

Figure 5.6: The distribution Chlorophyll-*a* (Chl-*a*) in the upper 120 m water-column across the different fronts of the ISSO during austral summer 2012 (a) and 2013 (b).

Based on the Pigment analysis, it was noted that there was a significant shift in the phytoplankton community across the fronts from the STFZ to the PFZ. Nanoflagellates were the dominant community in STFZ a small contribution from the diatom and picophytoplankton community during 2012 (Fig. 5.7a), though diatoms contributed in the deeper depths was considerably higher during 2013 (Fig. 5.7d). At the SAFZ, the flagellates dominated, with an increase in the contribution from the diatoms with depth, during 2012 (Fig. 5.7b). However during 2013, flagellates

dominated only in the surface waters, beyond which, a mixed community appeared with substantial contribution from diatoms and pico-phytoplankton (Fig. 5.7e). In the colder PFZ, diatoms were the dominant community throughout the water column during both years, though a significant contribution from picoplankton was indicative of a shift in the phytoplankton community during 2013 (Fig. 5.7 c & f).

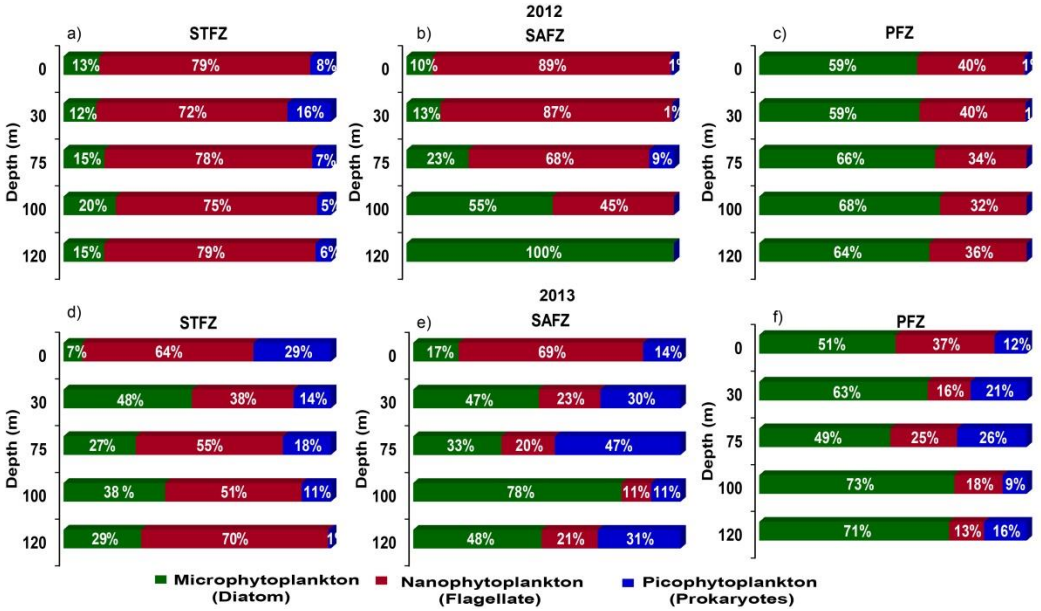

Figure 5.7: The distribution of percentage abundance of the dominant communities of phytoplankton, in the upper water column (120m), at the different frontal regions of the ISSO during 2012 (a, b, c) and 2013 (d, e, f)

5.3 Discussion

5.3.1 Upper water-column variability of POM characteristics and the trophic dynamics across the fronts of the ISSO

5.3.1.1 POM biogeochemistry in the STFZ

The STFZ is a warmer and low-nutrient region (Fig. 5.1 & 5.2) influenced by the subtropical gyre in the north. The oligotrophic subtropical gyre (Jena et al., 2013) combines with the nutrient rich cooler waters coming from the south (Boyd et al.,

1999) to bring in substantial variability in the POM characteristics and biogeochemical processes of STFZ (see Chapter 4).

During both years of study, the STFZ waters was enriched in $\delta^{13}C_{(POM)}$ (Fig. 5.4), probably as a result of the dominance of nanoflagellates (Fig. 5.7). Studies have suggested that this phytoplankton community is adapted to low-nutrient (nitrate and silicate) environment, leading to an enrichment of $\delta^{13}C_{(POM)}$ (Bentaleb et al., 1998; Gaul et al., 1999; Lara et al., 2010). The presence of flagellates, a mixotrophic phytoplankton community, suggests that a heterotrophic food web is operational in the STFZ (Archer et al., 1996; Sherr and Sherr, 2007). Furthermore, a contribution from picophytoplankton (Fig. 5.7) during 2013, also indicated the existence of a microbial loop in the region (Jasmine et al., Venkataramana et al., 2020). The high C:N ratio (~9.9) during 2013 could be indicative of the partially degraded organic matter rich in ^{12}C supporting heterotrophic activity (Çoban-Yildiz et al., 2006). This could also be a reason for the comparatively lower $\delta^{13}C_{(POM)}$ observed below the DCM during 2012. The POC:Chl-*a* ratios (100-200) observed in the STFZ (Fig. 5.5d) during 2013 could have been derived from detrital matter/partially degraded POM brought from the subsurface via eddies pumping (Zeitzchel, 1970; Maksymowska et al., 2000; Coppola et al., 2005).

The C:N ratios were high (8-16) with maximum variability at 40°S and 53.30°E of STFZ during 2012, higher than the Redfield's ratio for plankton/fresh organic matter (6.63). Although a direct explanation to this is not available, salps and pyrosoma were predominant at this location, suggesting grazing effect of the POM. The C:N ratios of salp faecal material, irrespective of the size and species of the organism may vary between 7.3 to 24.1 (Caron et al., 1989). This suggests the

possible contribution of these voracious grazers to the heterotrophy in these waters, signifying the role of grazing and repackaging in the alteration of POM composition in the upper water column, thus regulating the food web dynamics in STFZ (Perissinotto et al., 2007) and cycling of POM. Additionally, the higher POC:Chl-*a* ratio (100 - 200) indicated the prevalence of heterotrophic activity in this region (Leblanc et al., 2002; Savoye et al., 2003). Moreover, the abundance of microzooplankton with dinoflagellates and ciliates in these waters, suggest the dominance of heterotrophs supporting the co-existence of a microbial loop along with the classical food web in this region, as proposed by Jasmine et al (2009).

The POM characteristics showed a distinct inter-annual variability in the STFZ with significant increase in the POC:Chl-*a* ratio and corresponding reductions in the POC, PN and the $\delta^{13}C_{(POM)}$ values below DCM, that was just above the base of the photic depth. This coincided with an increase in AOU below the DCM depth, suggesting that an increase in respiration/remineralisation consequently was responsible for the changes in the POM quality (Omand et al., 2015) below DCM. This also indicate that partial degradation has led to the depletion of $\delta^{13}C_{(POM)}$ in POM due to the removal of ^{13}C rich compounds (Eadie and Jeffrey, 1973; Harvey et al., 1995; Kolasinski et al., 2012) below DCM in STFZ. All the above observations confirm the predominance of heterotrophic processes in the STFZ, especially in the eddy influenced regions and below the DCM, whereas autotrophic processes were still dominant in the waters above the DCM, upto the euphotic depth.

5.3.1.2 POM biogeochemistry in the SAFZ

The SAFZ, is a region located between warm STF and cold PF, and is often considered as a transition zone exhibiting distinct gradients in temperature and nutrients. However, at times, SAFZ behaves as an HNLC region, due to the lack of solar irradiance and low iron content (Martin et al., 1990; Dubischar and Bathmann, 1997). During the current study also, the nutrients in SAFZ (nitrates and silicates) were higher than in the STFZ, which supported an enhanced growth and a shift in the phytoplankton community structure. Although the dominant phytoplankton community was flagellates in the top of the mixed layer, the contribution of diatoms increased with depth, and was the dominant phytoplankton community in the subsurface during 2012. However, it was not the case during 2013, when the surface waters were dominated by flagellates, while the subsurface had a mixed community composed of diatoms and picoplankton (Fig. 5.7). The nutrient concentrations in the mixed layer and light intensity could be the factors responsible for the shift in phytoplankton community as a result of adaptation of phytoplankton (Hickman et al., 2012), which can change the POM characteristics.

The distribution of nutrients and phytoplankton community followed considerably different patterns at SAFZ and STFZ. However, the POC and PN decreased with depth with increasing AOU below the euphotic depth, similar to that observed at the STFZ. Thus, indicating the role of photosynthesis in the upper water column and respiration in deeper depths (Omand et al., 2015). Additionally, the abundance of prokaryotic picoplankton and microzooplankton also indicate the existence of an active microbial loop, supported by secondary production (Marañón et al., 2003; Venkataramana et al., 2020), and contribute to the alteration of POM

characteristics (Azam et al., 1983; Fenchel, 2008) in SAFZ water column, during 2013. Furthermore, the higher $\delta^{13}C_{(POM)}$ during this period could also be attributed to the shift in the phytoplankton community in the region during the two years. The moderate decrease of $\delta^{13}C_{(POM)}$ and $\delta^{15}N_{(POM)}$ during both the years could possibly be a resultant of the respiration-remineralisation processes within the upper water column (Eadie and Jeffrey, 1973; Kolasinski et al., 2012). The more or less similar characteristics of POM in the SAFZ and STFZ imply that autotrophy was the major activity in the surface layers, whereas heterotrophy was dominant below the DCM at these frontal regions.

5.3.1.3 POM biogeochemistry in the PFZ

PFZ is a typical high nutrient zone, while the persistent winds might have favoured the deepening of the mixed layer in this region. There was a 5 to 10-fold increase in the nutrient concentrations (NO_3: 23.18 µM, SiO_4: 6.35 µM) during the present study. The strong winds further increased the oxygen levels and other dissolved gases in the surface waters via higher air-sea interactions, and the presence of Antarctic Surface Waters (AASW) in this region contribute to the presence of higher dissolved gases in the PFZ waters. However, the comparatively low $\delta^{13}C_{(POM)}$ values could be due to the increased uptake of lighter carbon isotope (^{12}C) by phytoplankton via fractionation during photosynthesis due to relatively higher nutrients and dissolved gases in the cold in polar waters (Checkley and Miller, 1989; Gruber et al., 1999; Mino et al., 2002). The $\delta^{13}C$ content of phytoplankton is often found to be lower than the $\delta^{13}C$ of the inorganic carbon assimilated by phytoplankton (Hayes, 1993). In the present study, the $\delta^{13}C$ content of DIC of surface waters was -

1.48 ±0.12 ‰, while its content in the source CO_2 was proposed to be 9.22 ±0.26 ‰ (Prasanna et al., 2015). The $\delta^{13}C_{(POM)}$ observed in the PFZ (-28.30 to -24.00 ‰) during the study was matching well with the $\delta^{13}C_{(POM)}$ values reported for higher latitudes (O'Leary et al., 2001; Lourey et al.,, 2004; Lara et al., 2010).

Studies have shown that the cell size and dominant phytoplankton community are the major factors determining the quality of POM $\delta^{13}C_{(POM)}$ signatures (Popp et al., 1998; 1999; Henley et al. 2012). Diatoms were identified as the dominant phytoplankton community during this study (Fig. 5.7). The $\delta^{13}C_{(POM)}$ values are found to be very low (depleted) in the diatom-dominated, cold, nutrient replete Antarctic waters, depending on the species abundance (Wada et al., 1987; Henley et al., 2012) and the growth rates in (Sommer, 1989; Fischer, 1991) and lipid accumulation (Sackett et al., 2013).

Moreover, the POM collected from the PFZ contained higher POC and PN compared to the STFZ and SAFZ, though Chl-*a* was highly variable and did not follow the same trend. Further, the $\delta^{13}C_{(POM)}$ and $\delta^{15}N_{(POM)}$ was comparatively more depleted along with low C:N and POC:Chl-*a* ratios, in the PFZ (except PF-II locations). These lower values can be attributed to the abundance of diatoms (>65%) in PFZ, which have an affinity for a higher uptake and storage of nutrients, mainly nitrates (Lomas and Glibert, 2000; Martiny et al., 2013), especially in nutrient rich regions like the PFZ. Conversely, the combined contribution of flagellates and prokaryotic picophytoplankton (~ 50%), and the uptake by these communities could be the reason for difference in the C:N ratios in the PFZ during 2013. However, the C:N and POC:Chl-*a* ratios observed during both the years were having signatures of freshly formed POM (except in PF-II, ~ 56°S), suggesting the predominance of

autotrophic processes prevailing in the PFZ (Zeitzchel, 1970; Maksymowska et al., 2000; Savoye et al., 2003). This evidently shows that PFZ is a region where autotrophic process plays a significant role in determining the POM characteristics during austral summer.

Overall the STFZ and the SAFZ showed a predominance of heterotrophic processes, especially below the DCM, while the prevalence of autotrophy in the euphotic depth was significant. However at the PFZ the predominance of autotrophy and the role of biological community in the upper 120 m water column was evident from this study.

5.3.2 Factors influencing the distribution and transformation of POM characteristics across the fronts of the ISSO

There are several hydrographical and biological processes that influence the POM composition and variability within the water column and across the fronts as mentioned in the earlier section. These factors/processes may eventually favour transformation the POM via repackaging, aggregation, degradation/remineralisation, and determine the fate of POM, with regard to its export to greater depths of the ocean (Lee at al., 2004; Tsukasaki et al., 2010). Some of the factors controlling these transformation processes are discussed below.

5.3.2.1 Role of Nutrients

As discussed in the earlier chapters, the influence of nutrients on the POM characteristics across the fronts is highly significant. The present study observed that the variations in nitrates and silicates was very high in the water column at the STFZ and SAFZ (Fig. 5.2 a-f). This influenced the POM quality via a change in the phytoplankton biomass and community structure (Martiny et al., 2013). Reduced light intensity and iron stress can influence the sensitivity to nitrate uptake (Glibert and Garside, 1992), further reflected in the isotopic signatures (δ^{13}Cand δ^{15}N) of phytoplankton and the POM (Altabet, 1988; Montoya et al., 1990; Lara et al., 2010). In nutrient limited waters like STFZ, where the nitracline was sharp, $\delta^{15}N_{(POM)}$ showed a higher variability in the upper water column. This can be due to less discrimination during nitrate uptake, and subsequent uptake of the residual nitrate (enriched in ^{15}N) in a nitrogen limited environment (Ostrom et al., 1997). It is also possible that under such low nitrate conditions, other forms of nitrogen like ammonia also contributed to the primary production, and the POM composition and its isotopic

characteristics (Zubkov et al., 2003; Gracía-Fernández et al., 2004), which was observed in the STFZ during this study.

5.3.2.2 Influence of biological processes

5.3.2.2. a. Phytoplankton biomass, community and DCM

The overall phytoplankton biomass (in terms of total Chl-*a*) was high in the PFZ (except for a low in PF-II) in 2013 (Fig. 5.6a & b) as compared to that in STFZ and SAFZ. A well-defined DCM, observed during this study, especially in the STFZ was an important factor determining the POM characteristics in the photic waters. This feature was mostly due to the adaptation of phytoplankton to optimum depths for maximum growth (Beinfang et al., 1982; Parslow et al., 2001). Factors like light intensity, nutrient availability and the dominant phytoplankton thriving in the region also contribute significantly towards maintenance of such a prominent DCM (Cullen, 1982; Parslow et al, 2001). During this study, the DCM was mostly located at the base of the euphotic zone (Table 5.3), where the light intensity was optimum for phytoplankton growth (Nielson and Hansen, 1959). Studies have shown that DCM can also be formed along the upper boundary of the temperature minimum layer (Tripathy et al., 2015). The present study ascertains the role of ML in determining the depth of DCM with a significant linear positive relation between the DCM depth and MLD (Fig. 5.8a), which was overlying the MLD in the PFZ (Table 5.3). Furthermore, the deepening of the DCM in the PFZ was probably caused by diffused light intensity and nutrient availability.

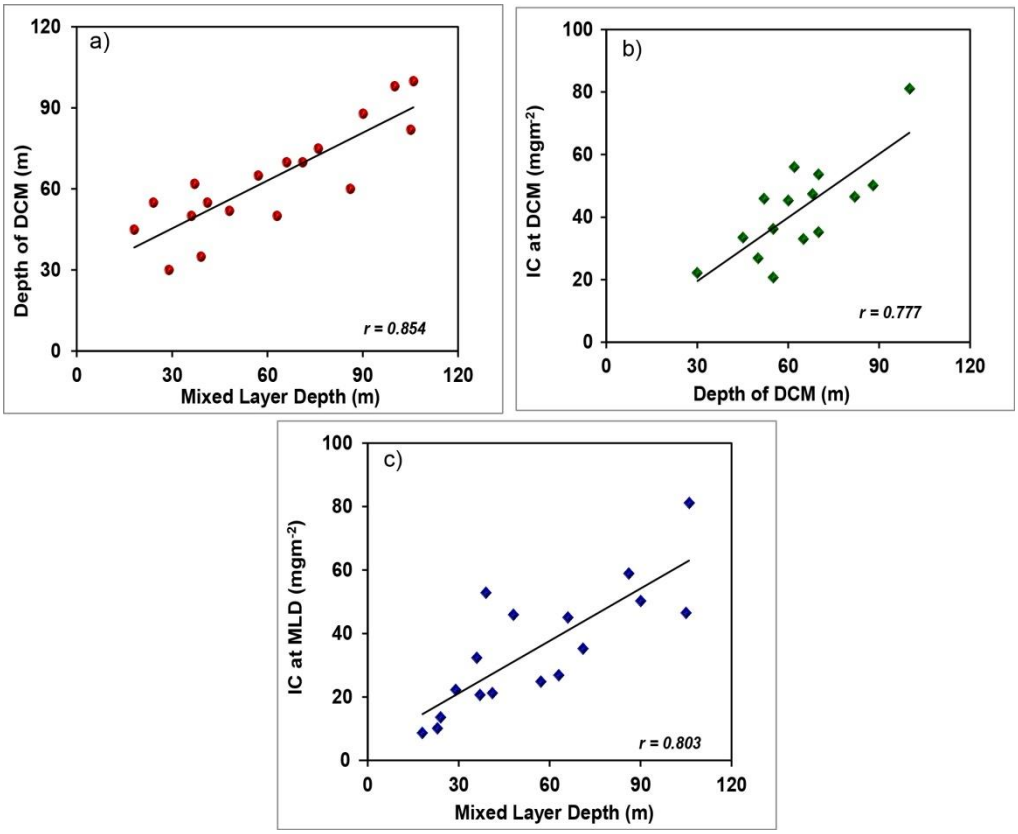

Figure 5.8: Spearman's correlation of (a) depth of Deep Chlorophyll maxima (DCM) and Mixed Layer Depth (MLD); (b) column Integrated Chl-*a* (IC) upto the DCM and the depth of DCM; (c) Column Integrated Chl-*a* (IC) upto the MLD and depth of MLD;

The integrated Chl-*a* (IC) was high when the DCM was deep (Fig. 5.8a), while POC peak was mostly coinciding with DCM or was just overlying the DCM depth (Fig. 5.3). The low (~50) POC:Chl-*a* ratio was suggestive of the presence of fresh OM (living plankton cells) at this depth. A similar finding from the frontal region of the NE Mediterranean Sea has been attributed to the phytoplankton size and its sinking rate in the upper water column (Edigar et al., 2005). Moreover, the POM, when retained in the DCM depths is susceptible to increased grazing and microbial remineralization (Abdel-Moati, 1990; Gomi et al., 2010) due to the higher residence time. The DCM can also act as a barrier in the vertical transport of POM under

stratified conditions, which decreased the POC and PN below DCM during the present study (Fig. 5.3). The POM accumulated in DCM is often released when the stratification breaks due to hydrographic events, consequently releasing nutrients and dissolved organic matter to the surrounding waters for utilisation (Abdel-Moati, 1990; Ediger and Yilmaz, 1996). This suggests the strong coupling of DCM-MLD (Fig. 5.8b) in regulating the POM composition, transformation and distribution in the upper water column.

Also, there was a shift in the phytoplankton community across the fronts. While STFZ and SAFZ were composed of mixed phytoplankton community, mostly dominated with flagellates, PFZ was always dominated by diatoms (Fig. 5.7). There were also wide variations in the contribution from the major contributing phytoplankton communities in these regions. The role of a shift in the phytoplankton community is evident in the significant variation in the POM characteristics and its isotopic composition as described in in the earlier chapter (3.3.2.4).

5.3.2.2. b. Zooplankton abundance and community composition

The size and community of zooplankton have great influence in the structuring of food web dynamics and can control the transformation and flux of POM via zooplankton grazing (Lee et al., 2000; Perissinotto et al., 2007) in the marine ecosystem. During this study, macro zooplankton (salp and pyrosoma) were present in the STFZ region during both the periods (Fig. 5.9a & b). The role of macro zooplankton in the cycling of POM has already been explained in the previous section (5.3.1.1). Further, copepod were the dominant contributors to the zooplankton community at all the three frontal regions and also during both the periods (Fig. 5.9).

However, the other contributing zooplankton groups were a little different during the two periods. While 2012 observed a contribution from chaetognath, pteropod, ostracod in addition to salp and copepod (Fig 5.9a), during 2013, there was a considerable contribution from appendicularians, with chaetognath, salp and copepod (Fig. 5.9b).

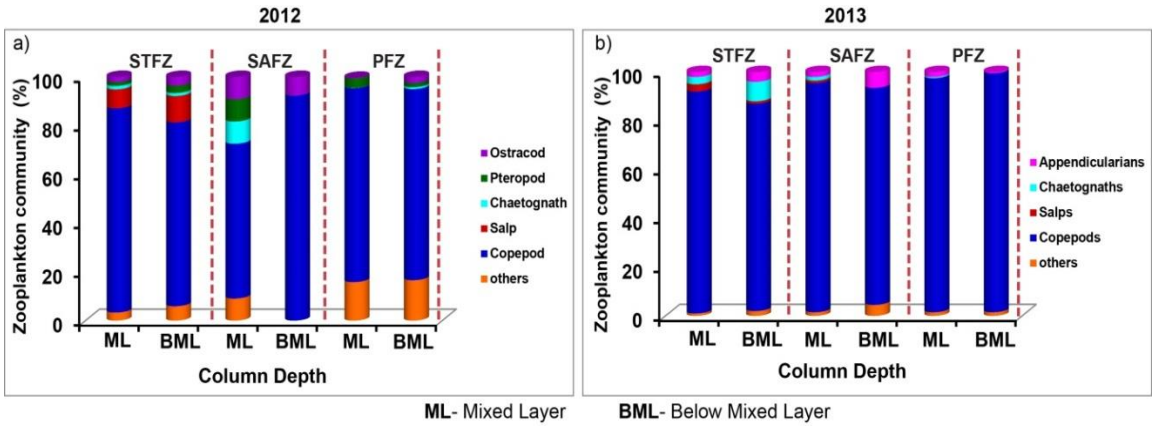

Figure 5.9: The distribution of percentage abundance of the dominant groups of zooplankton, in the upper mixed layer (ML) and below mixed layer (BML) at the different frontal regions of the ISSO during 2012 (a) and 2013 (b).

Additionally, it was noted that the STFZ also had a high abundance of small copepods (Venkataramana et al., 2020) along with a significant contribution from ciliates (AshaDevi et al., 2020) and pico-phytoplankton, indicating the presence of an active microbial loop, which was also evident from the POM characteristics, especially the POC:Chl-*a* values. Earlier studies have indicated that the STFZ is a region supporting the co-existence of a microbial loop and a classic food web (Jasmine et al., 2009; Venkataramana et al., 2020). A parallel study during the same period has also attributed the role of eddies in determining the dominant pathways that exist in this regime, and suggested the cross-linkage of a microbial loop and the

classic food web in the eddy influenced waters of the STFZ (AshaDevi et al., 2020). Further south, at the PFZ the zooplankton biomass was having mainly contribution from copepods (Fig.5.9), and a considerable contribution from numerous, identified and unidentified zooplankton groups. Earlier study (Venkataramana et al., 2020), has revealed that the size of copepods increased southwards and the PFZ composed of larger copepod species.

Moreover, the dominance of large size copepod may have been the reason for the high zooplankton biomass in the PFZ during the present study (Fig. 5.10a & b). This region was found to sustain increased grazing rates due to high zooplankton biomass contributed by the dominance of large copepods (Pavithran et al., 2011, Pillai et al., 2018). This implies that despite a major contribution from as autotrophic processes and the dominance of diatoms, the role of zooplankton grazing has a significant role in the cycling of POM in the PFZ.

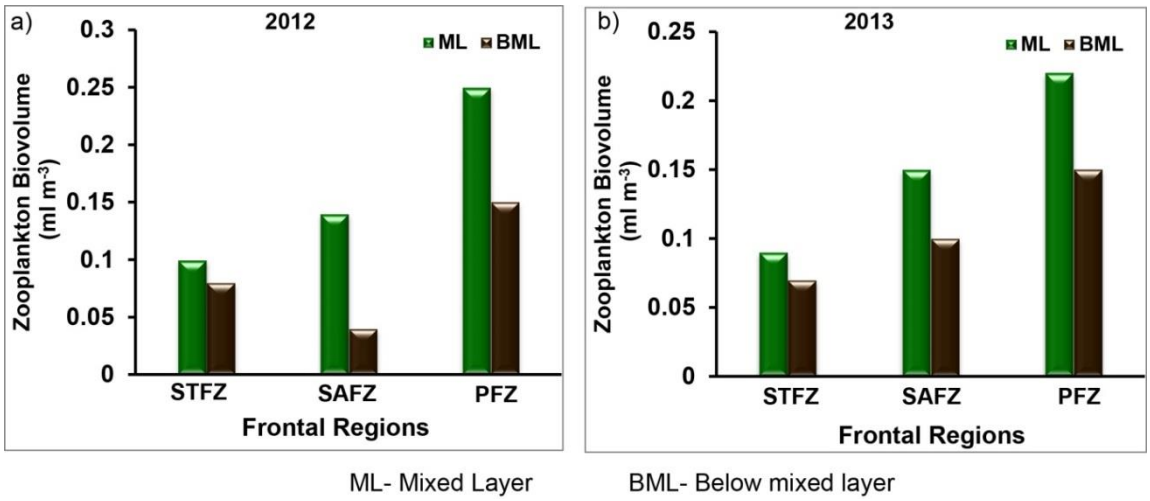

Figure 5.10: The variation in the Zooplankton biomass at the three frontal regions of the ISSO during austral summer 2012 (a), and 2013 (b).

5.3.2.2. c. Heterotrophic activity

Besides the contribution from mixotrophic dinoflagellates, and grazing effect of zooplankton, processes like microbial respiration also contribute significantly to the heterotrophic processes in the upper water column. POM degradation due to microbial respiration and remineralisation are important processes (Blain et al., 2002; Ewart et al., 2008) especially, below the photic depth. However, the microbial diversity was found to be influenced by eddies and currents in the SO (Venkatachalam et al., 2017). During this study, a significant correlations for AOU with POC and $\delta^{13}C_{(POM)}$ was found in the STFZ and SAFZ, especially below DCM during 2012 (Fig. 5.11 a & b), suggesting respiration to be an important process in the transformation of POM (Omand et al., 2015).

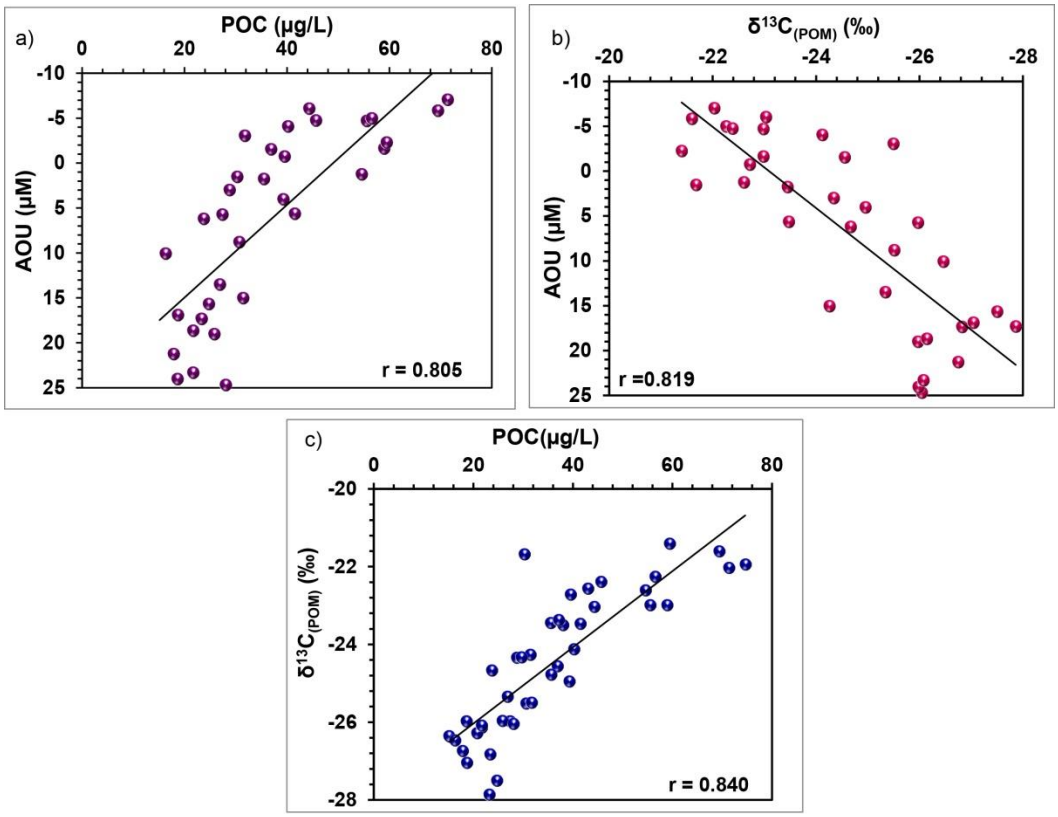

Figure 5.11: Spearman's correlation of AOU with POC (a); AOU with $\delta^{13}C_{(POM)}$ (b) and POC with $\delta^{13}C_{(POM)}$ (c) , at the STFZ during austral summer 2012

Additionally, Heterotrophic activity was evident from the high (> 200) POC:Chl-*a* ratio in the STFZ and also at the PF-II (~56°S) region (Fig. 5.5b) during 2013 (Maksymowska et al., 2000; Leblanc et al., 2002). This study ascertains the low export fluxes from STFZ were low due to an efficient remineralisation of OM in the upper water column (Coppola et al., 2005; Robinson and Ramaiah, 2011). These findings also suggest that the heterotrophic activity towards POM transformation processes was lower in the PFZ, except for the region around ~56°S in PF-II.

Collectively, it can be said from this study that factors such as nutrient availability, phytoplankton biomass and community, and the heterotrophic community (zooplankton and other heterotrophs) strongly influence the POM cycling (composition and transformation) in the photic water column across the fronts in the ISSO. Besides, the present study also found that hydrographical factors also have a critical role in determining the community structure in this frontal regime, which are addressed in the following section.

5.3.2.3 Influence of hydrography on the POM cycling across the fronts

One of the most significant hydrographical factors influencing the biogeochemical processes and POM cycling across the fronts in the ISSO is the strong thermal gradient (Fig. 5.1). The influence of temperature as a controlling factor has been described in the earlier chapter (Ch. 3) for surface waters. However, the thermal gradient down the water column also has remarkable influence on the phytoplankton community and other biogeochemical processes.

5.3.2.3. a. Eddies

Eddies, being an ubiquitous feature of the SO, especially the STFZ in the ISSO. The high variability in the POM composition in the STFZ during this study can be attributed to the numerous eddies formed and dissipated in the sampling region (Fig. 4.11). As discussed in the earlier chapter (Ch. IV), it is evident that most of the locations were at the core or the periphery of CEs and ACEs in the STFZ. Eddy driven upwelling and advection processes played a significant role in changing the hydrography and the nutrient levels in the STFZ (Sweeney et al., 2006, Sabu et al., 2015, Soares et al., 2020). These alterations were responsible for inducing a shift in the biological community (McGillicuddy et al., 1998; Kahru et al., 2007; Waite et al., 2007) that can be elucidated in the elemental composition and isotopic characteristics of POM in the STFZ (Berg 2011; Kolasinski et al., 2012). The present study also postulated the role of the age of the eddy and its eddy cycle stage along with its region of origin to play a significant role in the POM characterisation in the STFZ by altering the various biogeochemical processes in these waters (as explained in Ch. 4). Further south the influence of eddies was considerably low at the SAFZ, and almost negligible at the PFZ during the two periods.

5.3.2.3. b MLD

The shoaling and deepening of the MLD also play a significant role in influencing the productivity and community structure of phytoplankton (Riebesell et al., 2007; Li et al., 2012), which further determine the composition and fate of POM, especially in high latitude oceans. The deepening of MLD can have an adverse effect on the biological productivity at higher latitudes, as it reduces the availability of light for phytoplankton (Venables and Meredith, 2014), depending on the season and

location. However this study was carried out during austral summer, during which, there was sufficient availability of light and macronutrients for the phytoplankton growth. During the study, STFZ region was characterised by low nutrient concentrations, the deepening of the mixed layer at ACEs influenced regions may result in limitation of macronutrients over a longer time period. However, this low nutrient condition was favourable for the proliferation of nano and pico-phytoplankton (Ishikawa et al., 2002).

Furthermore, the strong winds and waves (turbulent mixing) are mainly responsible for the deepening of MLD in ISSO. During this study, wind induced MLD deepening was evident in PFZ (Table 5.3) leading to an increase in the integrated Chl-*a* in the mixed layer of the water column, and showed a linear positive correlation (Fig. 5.8c), corroborating the influence of MLD on the biological productivity, and more evidently the depth of DCM (Fig. 5.8b). Additionally, stratification and column stability also determine the type of phytoplankton that proliferates in the given oceanic condition (Clarke et al., 2008). The deeper MLD with abundant macronutrients and optimum light favoured the enhanced growth of siliceous diatoms in the PFZ during the study periods (Fig. 5.7).

Above mentioned are some of the major factors contributing to the variability and transformation of POM, in the upper water column across the fronts of the ISSO. These factors also play a significant role in determining the fate of POM and efficiency of the biological pump in these frontal regions.

5.3.3 Fate and cycling of POM across the fronts in the ISSO

The two major processes (other than the gravity based sinking) that determine the efficiency of the biological pump are the export and remineralisation of POM. Both processes can regulate CO_2 sequestration for a longer period and regeneration on a shorter time scales. Model studies have suggested higher transfer efficiency at low latitudes and a low transfer efficiency at high latitudes (Henson et al., 2012; Guidi et al., 2015), though there are contradictions to these postulations (Marsay et al., 2015; Weber et al., 2016). Studies suggest that factors such as temperature, stratification, oxygen and community structure play a significant role in determining the fate of POM (Devol et al., 2001; Klass and Archer, 2002; Francois et al., 2002) including its export of POM out of the water column and remineralisation of POM with the regeneration of nutrients and inorganic carbon to the water column.

5.3.3.1. Export fluxes of POC

It has been estimated that nearly 80% of the organic matter is exported from the euphotic zone via sinking (Hansell, 2002). POC flux for this study was estimated based on the empirical equations provided in earlier studies and depended on the primary productivity, POC concentrations and depth (Suess, 1980; Pace, 1987). Here, we have used VGPM data and in-situ data for flux estimates.

The estimated export fluxes of POC out of the euphotic waters were found to be high in SAFZ and showed a flux of ~160 mgC/m^2/day (2012) and 105 mgC/m^2/day (2013), followed by STFZ, ranging from 28 to 138 mgC/m^2/day, except for a high of 190 mgC/m^2/day observed at 43°S in 2012 (Fig. 5.12a), that is influenced by eddies and 40 to 60 mgC/m^2/day in 2013 (Fig. 5.12b). Further south at the PFZ the POC flux

estimates out of the euphotic depth ranged from 36 to 59 mgC/m^2/day during 2012 and 9.7 to 33 mgC/m^2/day during 2013. However, below 120 m, the estimates of export fluxes of POC were significantly different during both the periods. It was observed that the POC fluxes were high in PFZ (2012: 4 to 4.5 mgC/m^2/day and 2013:1.8 to 4.7 mgC/m^2/day) followed by SAFZ (3.0 mgC/m^2/day and 4.3 mgC/m^2/day, in 2012 and 2013, respectively). At the STFZ, the POC export flux estimates were comparatively higher during 2013 (4 to 4.5 mgC/m^2/day) unlike 2012 (0.8 to 2.4 mgC/m^2/day) (Fig. 5.12a & b).

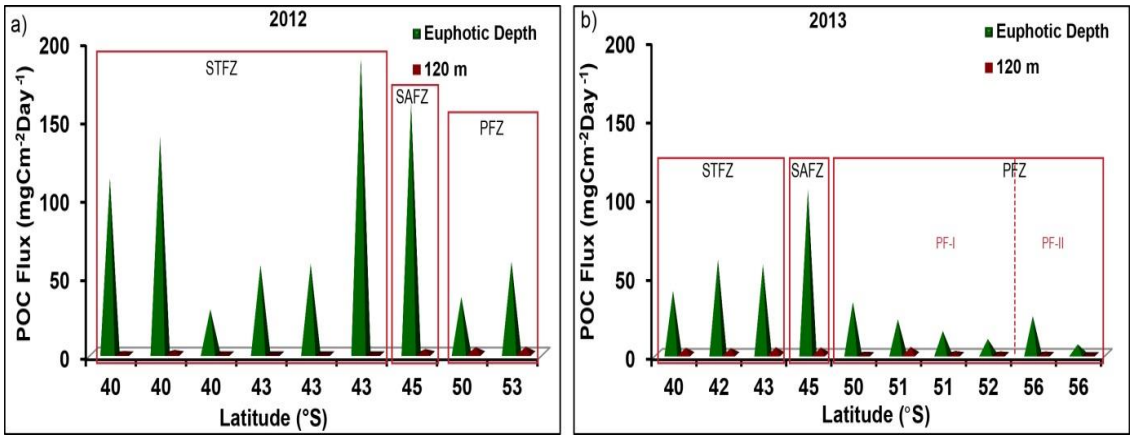

Figure 5.12: Particulate organic carbon (POC) flux out of the euphotic depth (green) and out of 120m (red) across the fronts of the ISSO, during austral summer 2012(a) and 2013 (b).

Overall the POC export flux out of the upper 120 m was < 10 % of that estimated in the euphotic waters. During 2012, higher POC export was at the PFZ, while during 2013, the POC export fluxes increased in the CE influenced locations and in PFZ (Fig. 5.12b), though it was lowest in PF-II. Earlier studies have reported the possibility of low export flux from STFZ (Coppola et al., 2005; DeVries and Weber, 2016), except the upwelling regions, which is also evident in this study. Further, model studies have suggested temperature, oxygen and phytoplankton size to

be important in determining the export fluxes and the transfer efficiency out of the water column (Van Mooy et al., 2002; Marsay et al., 2015; Weber et al., 2016). The low POC fluxes observed at the STFZ especially during 2012 were possibly due to the regenerative processes, below the euphotic depth. Also, the overall temperature in the water column was warmer in the STFZ especially during 2012. Additionally, the biological community structure was comparatively different during the two periods (Fig. 5.7 & 5.9). Studies have indicated that the structure of the food web is a crucial factor that determines the availability of labile organic matter (Lam et al., 2011; Wilson et al., 2012) that will control the long term sequestration of carbon into the ocean depths.

5.3.3.2 Remineralisation of POM within the upper water column

The remineralisation studies in the ocean depends on the regenerated nutrients, oxygen utilisation and nutrient stoichiometric ratios based on Redfield's equation (Redfield, 1958; Martiny et al., 2013). This Redfield's ratio of nutrients was used here to study the process of remineralisation in the region. The estimates suggest that the regenerated nutrients increased below the euphotic depth, also suggesting its negligible contribution in the surface layers (Fig. 5.13a-d).

During 2012, the regenerated nutrients (nitrogen and phosphorus) were high in SAFZ, followed by STFZ and PFZ (Fig. 5.13a-d), indicating a relatively higher regeneration via remineralisation at STFZ and SAFZ. However, during 2013 the regenerated nutrients increased at some locations in PFZ and STFZ (ACE influenced locations), with a least value at SAFZ (Fig. 5.13a-d).

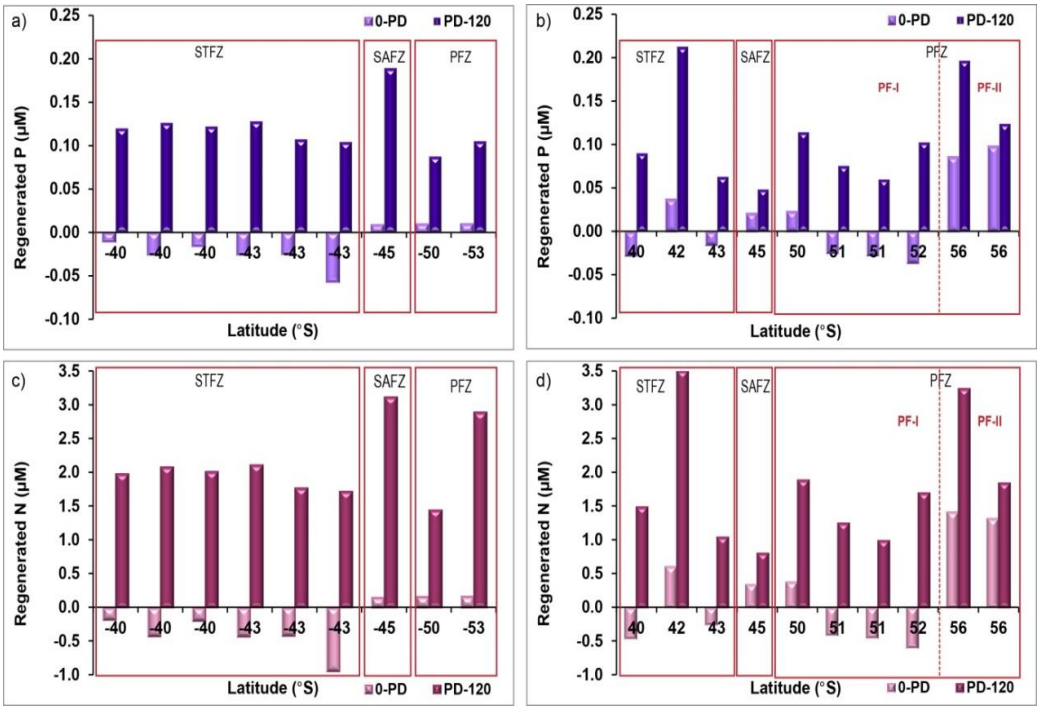

Figure 5.13: Variation of regenerated phosphate (P) and regenerated nitrogen (N), above the Photic depth (0-PD) and below the photic depth (PD-120m), across the fronts of the ISSO during austral summer 2012 (a,c) and 2013 (b,d).

The increased regenerated nutrients corresponding with high N:P ratios below euphotic depth supports an active remineralisation process in these waters. Further, the locations with high remineralised nutrients below the photic waters showed low POC export fluxes out of the 120 m water column, except at the SAFZ, this can possibly be attributed to the biological community structure, especially the phytoplankton community. Regenerated N was always higher than regenerated P and remained similar across the fronts, mainly due to the faster breakdown of nitrogenous compounds, also reflected in the C:N ratios. Further, there was a significant inverse correlation between the POC and the regenerated nutrients suggesting that breakdown of POC by the oxidation is a major process that release inorganic nutrients below euphotic depths.

Overall, the POC export flux estimates and the regenerated nutrients together suggest that the generally low export fluxes of POC in STFZ and at some locations in PFZ (PF-II, during 2013) were possibly due to high remineralisation below the euphotic depths during this study. Earlier studies have also shown that low export flux of POC in the STFZ may be caused by high remineralisation in the upper water column due to microbial activity (Robinson and Ramaiah, 2011). Recent studies have shown that temperature play an important role in determining the export fluxes, as warmer waters enhance the process of remineralisation to reduce the POC export levels (DeVries and Weber, 2016). This is evident in this study, where the high remineralisation in STFZ has resulted in a low POC flux below 120 m and the colder PFZ waters had higher POC fluxes.

5.3.4 Inter-annual variability of POM characteristics and fate in the ISSO

Inter-annual variability in the oceanic carbon cycling is found to have a significant global effect, mainly due to the thermohaline circulation and associated hydrography. The inter-annual variation in the biological productivity and the community structure influence the POM characteristics and the overall carbon cycle during the study. Some of the factors responsible for the inter-annual variability of POM are addressed in this section.

5.3.4.1 Temperature

A study by Johnston and Gabric (2010) postulated that SST and Southern Annular Mode (SAM) induced changes in the environmental conditions can lead to high growth of certain phytoplankton during consecutive years and thus indirectly have a role in the POM variability.

The state of SAM can favour strong winds that support enhanced vertical mixing, thus supplying subsurface nutrients to the surface waters and influence the biological response (Sengupta and England, 2006). These factors may have contributed to the inter-annual variability in primary productivity and the biological community structure, that directly influence the POM characteristics and variability (Popp et al., 1998; Lara et al., 2010). The AVHRR derived SST imagery and the *in-situ* data showed that the surface waters and the mixed layer was warmer during 2012 compared to 2013 (Fig. 5.14a & b).

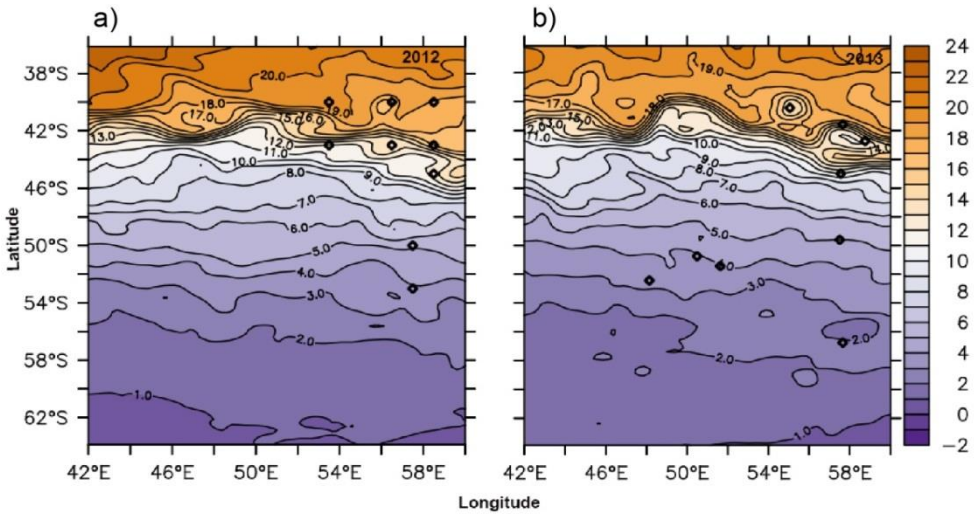

Figure 5.14: Spatial variability of Sea Surface Temperature (SST) across the fronts of the ISSO during January 2012(a) and 2013 (b).

5.3.4.2 Sea surface freshening by sea-ice

The sea-ice spread was comparatively higher during 2012 than 2013 (Fig. 5.15 a & b) suggesting that an increased ice melt may have led to the freshening of the waters in the study region during 2013.

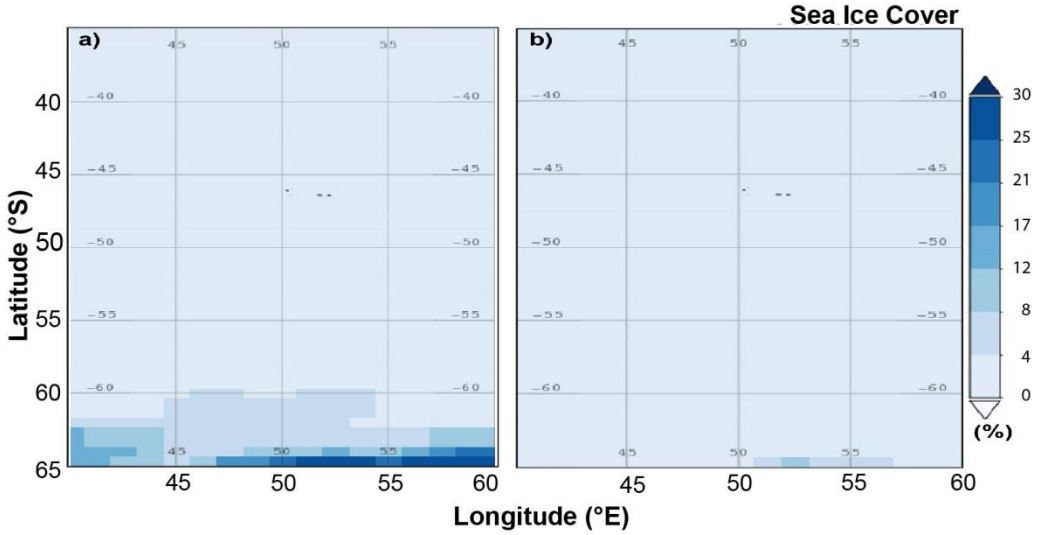

Figure 5.15: Variability of sea ice cover across the fronts of the ISSO, during January 2012 (a) and 2013 (b).

Satellite derived SSS (Fig. 5.16a & b) evidently shows that there was moderate freshening by low saline waters during 2013. This suggests the role of sea ice cover on the inter-annual variability in the productivity patterns (Johnston and Gabric, 2011), thus influencing the POM dynamics.

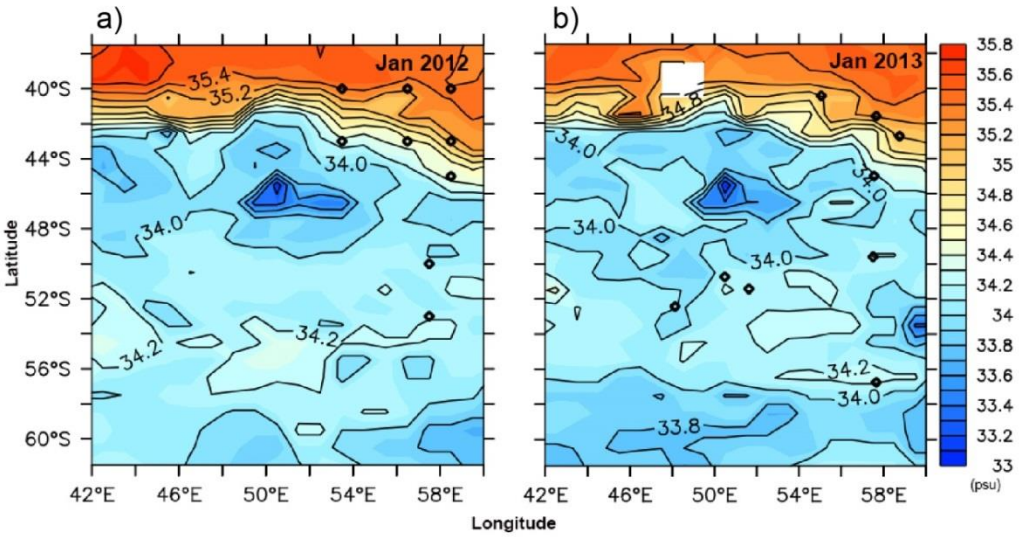

Figure 5.16: Variability of Sea Surface Salinity (SSS) across the fronts of the ISSO, during January 2012(a) and 2013(b)

5.3.4.3. Influence of winds and MLD

Both the re-analysis data and the *in-situ* data indicated a deepening of MLD towards the polar region during both the years (Table 5.3). The deep MLD has severe implications on the light intensity and can alter the Chl-*a* based biomass and phytoplankton community (Fauchereau et al., 2011) which influence the POM cycling (Lara et al., 2010; Soares et al., 2020). Further, the MLD in PFZ was relatively deeper during 2012 than 2013 (Fig. 5.17a & b), which probably lead to an inter-annual variability in the Chl-*a* (Fig. 5.6) and POC concentrations between the two consecutive years. In contrast, the MLD was deeper in STFZ during 2013. The

variability in the MLD was evidently a result of the stronger winds in the STFZ during 2013 and at the PFZ during 2012 which became more intense southwards (Fig. 5.17c & d).

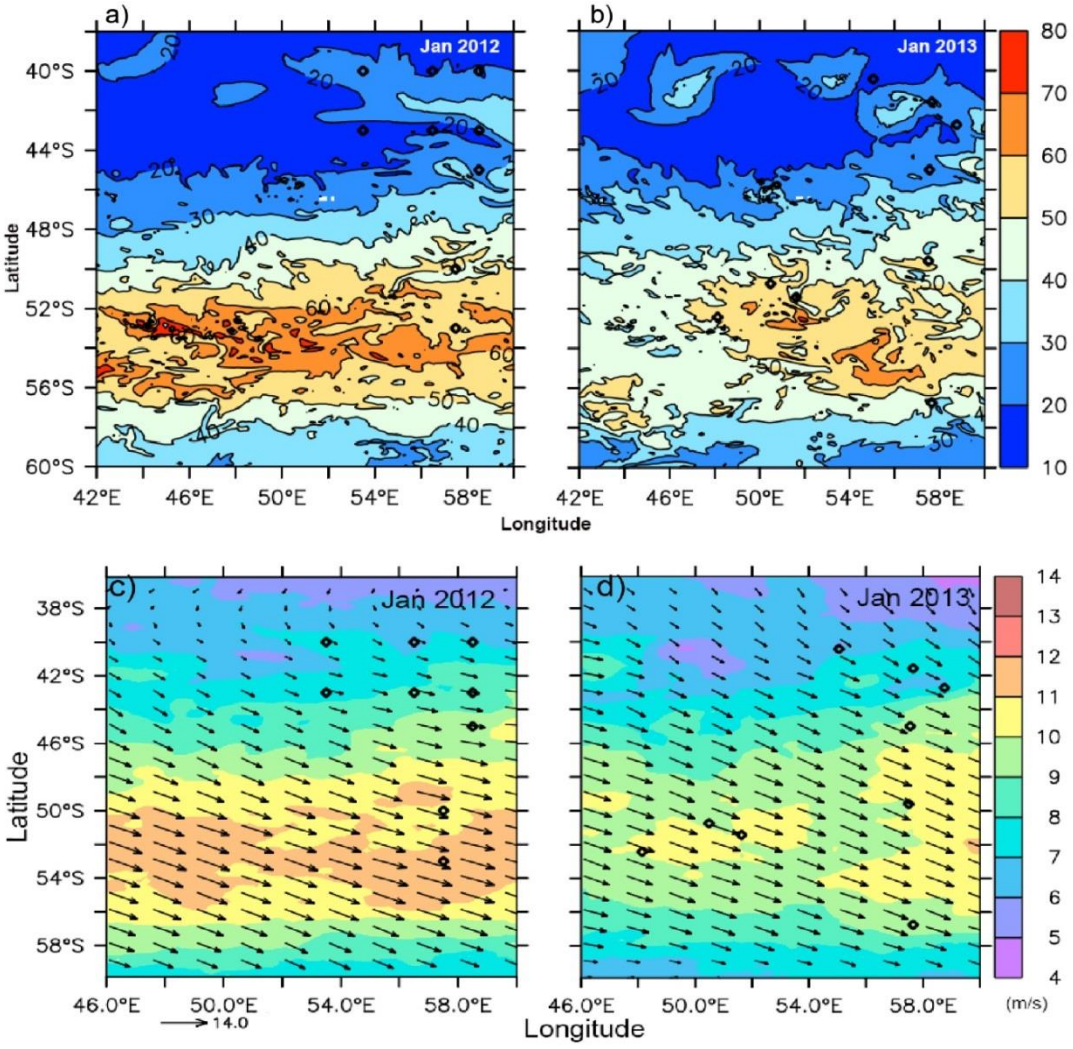

Figure 5.17: Variability of Mixed layer depth (a & b) and Wind speed (c & d) across the fronts of the ISSO, during January 2012 and 2013.

5.3.4.4. Micro and Macro nutrients

An essential micronutrient that controls the primary productivity and phytoplankton growth in the ISSO is iron (Moore et al., 2007). The freshening of the surface waters of PFZ in ISSO by sea-ice melt during 2013 possibly introduced

significant influx of iron, as evident from the NOBM derived re-analysis data (Fig. 5.18a & b).

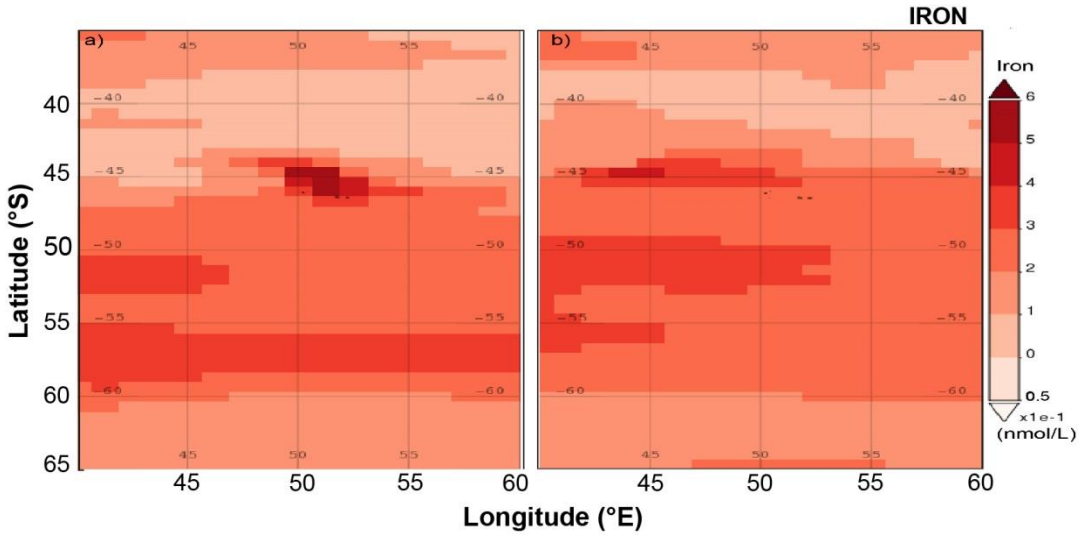

Figure 5.18: Spatial distribution of dissolved Iron, in the study region of the ISSO for the period of Jan-Feb in 2012(a) and 2013(b), (re-analysis data derived from NOBM).

It has been shown that iron limitation and low light intensities can substantially result in high sensitivity of the phytoplankton towards nitrate uptake (Glibert and Garside, 1992) influencing the primary productivity and further production of POM. Changes in the nutrient stoichiometry can also influence the quality of POM by supporting different phytoplankton community and/or causing a shift in the dominant phytoplankton community (Ho et al., 2003; Martiny et al., 2013). During the two years, there was a significant difference in the nutrient concentrations across the fronts. The high nutrients in the STFZ during 2013 were caused by the intense eddy pumping, which was weak during 2012, mainly a result of the age and different stages of the eddy during the two years (Sweeney et al., 2013). There was also a sharp nitracline in STFZ during 2012, which contributed to the increased biological production with different POM characteristics. However, although at the SAFZ the nutrient abundance did not vary much, the nutrient

concentrations increased in the PFZ during 2013, possibly due to strong wind-driven mixing.

5.3.4.5. Phytoplankton Community

The cumulative effect of environmental factors during the two study periods was responsible for the variation in the chlorophyll concentration and a shift in the phytoplankton community (Wright et al., 2010; Mishra et al., 2020). The re-analysis data from NOBM implied that although the dominant phytoplankton community did not vary much during both the years, there was significant difference in the abundance of the communities and the contribution from different phytoplankton groups. Thus, the contributions of Coccolitophore, Chlorophytes and Cyanobacteria were much higher in the STFZ during austral summer 2012 (Fig. 5.19a, b).

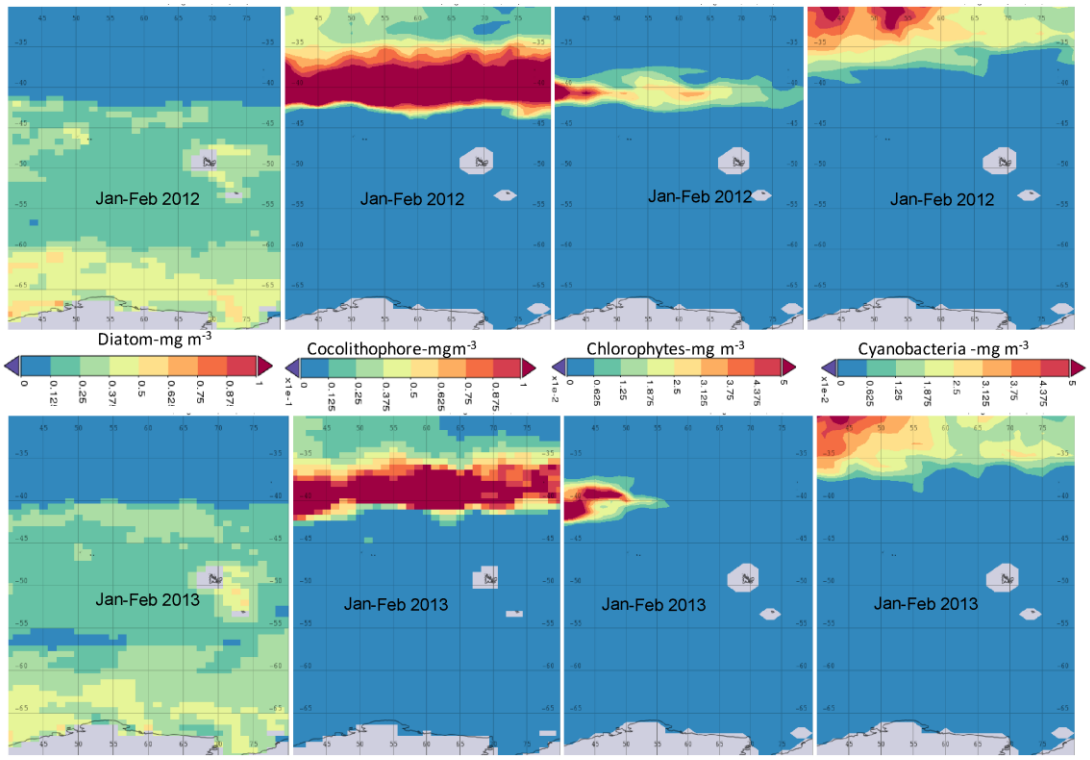

Figure 5.19: Spatial distribution of different phytoplankton communities, across the fronts of the ISSO for the period of Jan-Feb in 2012(a) and 2013(b), (re-analysis data derived from NOBM).

However, the mixed phytoplankton community in SAFZ remained almost identical during both years. Further in the PFZ, had a higher abundance of diatoms during 2013 likely due to the variability in the column stability and increase in nutrients. The variation in chlorophyll (Fig 5.20a & b) and a shift in phytoplankton community is reflected in the small scale variability in POM concentration (Fig. 5.21c & d).

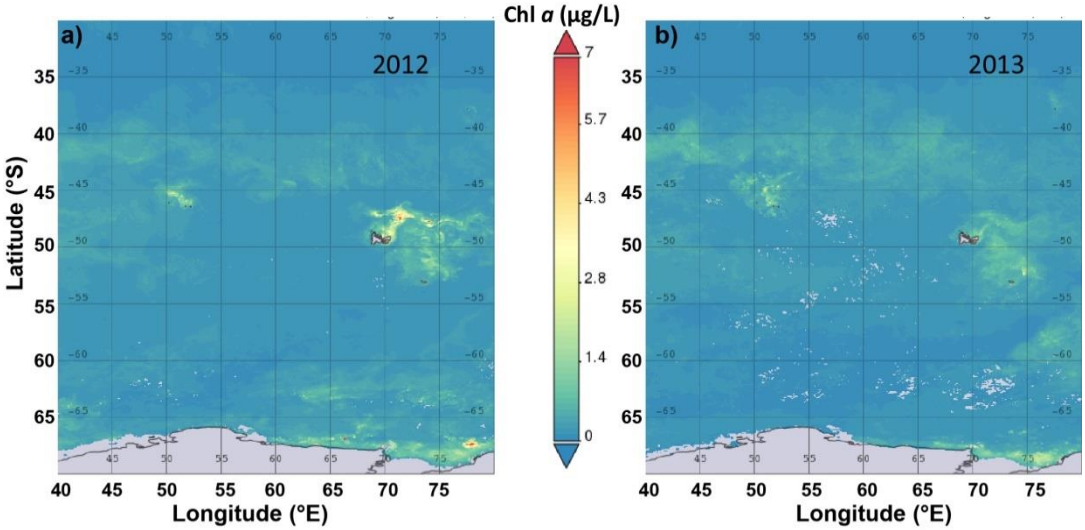

Figure 5.20: Spatial distribution of Chl-*a* in the study region of the ISSO, for the period of Jan-Feb 2012 (a) and 2013 (b), (re-analysis data derived from NOBM).

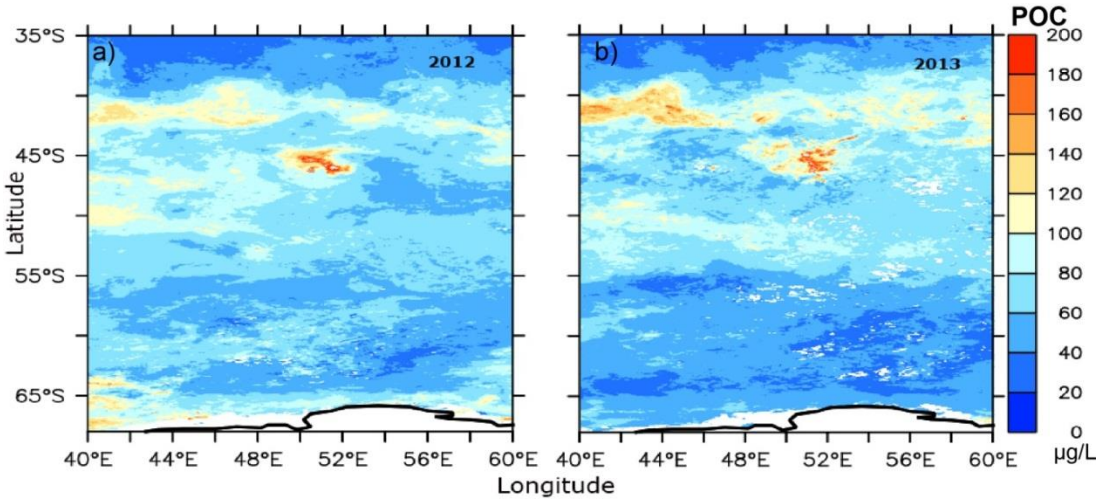

Figure 5.21: Spatial distribution of POC across the fronts of the ISSO, for the period of January 2012 (a) and 2013 (b), (re-analysis data derived from MODIS).

The above illustrations suggest that apart from the primary factors (biochemical processes), there are some secondary factors (hydrographical features), which together control the inter-annual variability of the POM characteristics and fate in the upper water column during the two consecutive periods of study.

5.4 Salient Findings

This chapter illustrates that heterotrophic processes were predominant in the STFZ were largely influencing the POM characteristics and cycling within the upper water column, especially during 2012. Further, the co-existence of a microbial loop and a classic food web in the STFZ has led to an increased remineralisation of POM and has considerably reduced the export fluxes of POC out of the upper 120 m in this frontal region.

The predominance of a mixed phytoplankton community in SAFZ supported autotrophy in the photic waters and heterotrophy below the euphotic depth. Even though, the POC flux out of the euphotic zone was the highest at the SAFZ, the efficiency of remineralisation varied during the two periods and substantially increased the export fluxes at SAFZ below 120 m, during 2013.

However, in PFZ, autotrophy was the dominant process, while the role of heterotrophy (regenerated nutrients) also was quite significant below the euphotic zone, especially during 2012 which reduced the POC export flux at 120 m. However, a comparison of the two periods showed that the POC export fluxes were maximum in the PFZ during 2013. Also, the POC export flux in the upper water column was considerably the highest at the PFZ among the three frontal regions studied.

Overall, the changes in POM characteristics, its transformation and fate across the fronts, were a result of the alterations in the nutrients, phytoplankton, zooplankton and heterotrophic activities in the ISSO. Additionally, some of the secondary factors like temperature, eddy, mixed layer, etc., also have indirect influence on the efficiency of biological pump across the frontal regions of ISSO, causing a considerable inter-annual variability in the POM characteristics and export fluxes, thus the efficiency of the biological pump in the highly dynamic ISSO.

6. Summary and Future Prospective

6.1 Summary

The SO is often considered as a sink of CO_2 and support the long-term sequestration of carbon out of contact with the atmosphere. However, due to the variability in the hydrography and biogeochemical processes across the frontal structure of the ISSO, only some regions of the ISSO act as a sink, while some other regions can act as a source of CO_2, which vary over different years (Shetye, et al., 2015; Prasanna et al., 2015).

This thesis tried to address the POM dynamics in context to the variability in the composition of POM, its flux or remineralisation at the different frontal regions of the ISSO, which are very important processes that determine the long term sequestration of carbon into the ocean. This study used *in-situ* data collected from the ISSO, a region from which sparse *in-situ* data of biochemical variables is available, due to the difficulty in accessibility of the region, also owing to the harsh conditions of the ISSO.

The elemental and isotopic composition of carbon and nitrogen, observed in the ISSO, matched with the earlier reports in the other sectors of the SO. However, the POM characteristics observed in the oceanic regime north of the ISSO, that is, the oligotrophic TIO waters, were considerably different and the region was dominated by heterotrophy and regenerated production. Further, it was indicated from this study that in the POM characteristics in the surface waters of the ISSO, varied across the fronts and the isotopic signatures of carbon and nitrogen depleted southwards from the STFZ to the PFZ. This variability in the isotopic signatures was mainly a result of

isotopic fractionation, during the uptake by phytoplankton, due to the higher availability of nutrients and tCO_2 towards the PF, and also a significant role of temperature and the dominant phytoplankton community.

This study also addressed the role of eddies in influencing the POM characteristics at the STFZ, which is an eddy prone region, with numerous cyclonic and anticyclonic eddies formed or meandered to the region. Moreover the eddy dynamics associated changes in the thermo-haline structure of the water-column had a considerable role in the redistribution of nutrients and other organic and inorganic components. This was responsible for a shift in the dominant phytoplankton community and the food-web structure. Overall, the isotopic signatures ($\delta^{13}C_{(POM)}$ & $\delta^{15}N_{(POM)}$) of POM, were more enriched in the surface waters at cyclonic eddies compared to anticyclonic eddies. It was further revealed from this study, that eddy properties like the type of eddy (cyclonic or anticyclonic), region of origin of the eddy and the age of the eddy which determines the phase of the eddy life cycle play a crucial role in determining the POM variability, transformation and fate of POM at the STFZ.

The POM characteristics observed, suggested the co-existence of microbial loop alongside a classic food-web and the predominant contribution of heterotrophic processes towards the transformation of POM characteristics within the upper water-column of the STFZ. Also, the role of autotrophy in the euphotic waters and heterotrophy below the photic waters was evident in the transformation of POM characteristics in the STFZ and SAFZ waters of the ISSO. Further south, at the PFZ the predominance of autotrophy resulting from the abundance of inorganic components and colder temperatures that favoured the dominance of diatoms,

contributed to the variability of POM characteristics and isotopic signatures in the upper water column.

Another important finding from this study revealed that the efficiency of the biological pump varied at the different fronts of the ISSO. Moreover, even though the atmospheric drawdown of carbon via primary productivity was high, and the amount of POC exported out of the euphotic waters was high at the STFZ and the SAFZ, the export of carbon out of the upper 120 m was very low, due to greater remineralisation, implied from the regenerated nutrients. However, at the PFZ the export flux out of the upper 120 m was considerably higher than the other two fronts (STFZ, and SAFZ), eventhough there was regeneration of nutrients below the euphotic waters of this region. However, the estimated export flux of POC at 120 m, was < 10% of the total POC flux at the euphotic depth of the water column.

This study also suggested significant inter-annual variability in the transformation and flux of POM out of the upper water column. Factors like the variability in temperature, sea-ice cover, depth of the mixed layer and column stability along with eddy and water-mass effect had a critical role in the interannual variability of POM in the ISSO. The afore mentioned factors are responsible in triggering a shift in the dominant phytoplankton community and influencing the biological process, the zooplankton community structure and the food-web dynamics across the fronts within the upper water column, during the two consecutive austral summers. All these factors collectively played a significant role in the variability of POM composition and the transformation and fate of the POM produced in the euphotic waters at these frontal regions of the ISSO.

The study provides important information on the biogeochemical processes across the fronts and the POM dynamics with regard to the biological pump. However, this region needs more detailed and long term *in-situ* studies for a better understanding of the efficiency of the biological pump and the remineralisation of POM for estimating the carbon sequestration and carbon cycle for a better predictability of the global climate variability and changes due to the processes in the ISSO.

6.2 Future Prospects and Scope for Further Studies

Future research for a better understanding of the transformation and fate of POM should include time series studies that would help to reveal the biogeochemical processes with higher clarity. Long-term monitoring of highly dynamic areas is of utmost importance for simplification of the complex inter-linked processes involved in the POM transformation, its sinking and long term sequestration. Long term time series studies, will also help to elucidate the process of remineralisation and formation of the inorganic and organic nutrients and carbon, and its exchange through the oceanic system. Also, the role of microbial processes in determining the efficiency of the biological pump needs to be given more importance, as the ISSO still have limited studies in this aspect.

Additionally, sediment trap studies are important for the estimation and understanding of the POM dynamics especially for the quantification of the flux of sinking particles. The success of these efforts of deployment of sediment traps and retrieval in the near future which will be a good means to achieve a better understanding of the POM dynamics throughout the year and also during different

seasons. As the ISSO is logistically unapproachable during winters, sediment traps are very important to give direct estimate of the downward POC flux in the ISSO, which cannot be estimated by models, which are mostly biased to short term events, and often overestimates, due to negligence of certain important links of the food web structure.

Also, a detailed study of the molecular and biochemical composition of POM of suspended and sinking particles will help to determine the extent of transformation within the water column. As the labiality and refractory property of POM depends on its molecular and biochemical composition, which would determine the period for which the carbon is sequestered away from contact with the atmosphere and consequent air-sea exchange that impact the global climatic changes.

7. References

Abdel-Moati, Alaa R., 1990. Particulate organic matter in the subsurface chlorophyll maximum layer of the Southeastern Mediterranean. Oceanologica Acta, 13, 307-315.

Abramson, L.C., Lee, Z., Liu, J., Szlosek, J., Wakeham, S.G., 2010. Exchange between suspended and sinking particles in the northwest Mediterranean as inferred from the organic composition of insitu pump and sediment trap samples. Limnology and Oceanography, 55, 725-739.

Agawin, N.S.R., Duarte, C.M., Agustí, S., 2000. Nutrient and temperature control of the contribution of picoplankton to phytoplankton biomass and production. Limnology and Oceanography, 45(3), 591-600.

Allen, J.T., Brown, L., Sanders, R., Moore, C.M., Mustard, A., et al. 2005. Diatom carbon export enhanced by silicate upwelling in the northeast Atlantic. Nature, 437, 728–32

Altabet, M.A., 1988. Variations in nitrogen isotopic composition between sinking and suspended particles: Implications for nitrogen cycling and particle transformations in the open ocean. Deep Sea Research 1, 35, 535–554.

Altabet, M.A., Francois, R., 1994. Sedimentary nitrogen isotopic ratio as a recorder for surface ocean nitrate utilization. Global Biogeochemical Cycles, 8(1), 103-116.

Altabet, M.A., Francois, R., 2001. Nitrogen isotope biogeochemistry of the Antarctic Polar Frontal Zone at 170 W. Deep Sea Research II, 48, 4247–4273.

Anilkumar, N., Alvarinho, L., Somayaluju, Y.K., Ramesh Babu, V., Dash, M.K., Pednekar, S.M., Babu, K.N., Sudhakar, M., Pandey, P.C., 2006. Fronts, water masses and heat content variability in the Western Indian sector of the Southern Ocean during austral summer 2004. Journal of Marine Systems, 63 (1–2), 20–34.

Archer, S.D., Leakey, R.J.G., Burkill, P.H., Sleigh, M.A., 1996. Microbial dynamics in coastal waters of East Antarctica: Herbivory by heterotrophic dinoflagellates. Marine Ecology Progress Series. 139, 239-255.

Arrigo K.R., van Dijken G.L., Bushinsky S., 2008. Primary production in the Southern Ocean, 1997-2006. Journal of Geophysical Research, 113, C08004, doi: 10.1029/2007JC004551.

Asha Devi, C.R., Sabu, P., Naik, R.K., Bhaskar, P.V., Achuthankutty, C.T., M. Soares, Anilkumar, N., Sudhakar, M.,2020. Microzooplankton concerning the plankton food web in subtropical frontal region of the Indian Ocean sector of the Southern Ocean during austral summer 2012. Deep sea Research-II (in press).

Azam, F, Fenchel, T, Field, J.G., Gray, J.S., Meyer Reil, L.A., Thingstad, F., 1983. The ecological role of water-column microbes in the sea. Marine Ecology Progress Series, 10, 257–63.

Bakun, A., 2006. Fronts and eddies as key structures in the habitat of marine fish larvae: opportunity, adaptive response and competitive advantage. Scientia Marina, 70, 105–122.

Barlow, R., Stuart, V., Lutz, V., Sessions, H., Sathyendranath, S., Platt, T., Kyewalyanga, M., Clementson, L.,Fukasawa, M., Watanabe, S., Devred, E., 2007.

Seasonal pigment patterns of surface phytoplankton in the subtropical southern hemisphere. Deep Sea Research I, 54, 1687–1703.

Basu S., Mackey K.R.M., 2018. Phytoplankton as key mediators of the biological carbon pump: Their responses to a changing climate. Sustainability, 10, 869.

Beckmann, W., Auras, A., Hemleben, C., 1987. Cyclonic cold-core eddy in the eastern North Atlantic. III. Zooplankton. Marine Ecology Progress Series 39, 165–173.

Behrenfeld, M.J., O'Malley, R.T., Siegel, D.A., McClain, C.R., Sarmiento, J.L., Feldman, G.C., Milligan, A.J., Falkowski, P.G., Latelier, R.M., Boss, E.S., 2006. Climate – driven trends in contemporary ocean productivity. Nature, 444, 752 – 755.

Belkin, I.M., Gordon, A.L., 1996. Southern Ocean fronts from the Greenwich Meridian to Tasmania. Journal of Geophysical Research, 101, 3675–3696.

Benson, B., Krause, D., 1984. The concentration and isotopic fractionation of oxygen dissolved in freshwater and seawater in equilibrium with the atmosphere. Limnology and Oceanography, 29(3), 620-632.

Bentaleb, I., Fontugne, M., Descolas-Gros, C., Girardin, C., Mariotti, A., Pierre, C., Brunet, C., Poisson, A., 1998. Carbon isotopic fractionation by plankton in the Southern Indian Ocean: relation between $\delta^{13}C$ of particulate organic carbon and dissolved carbon dioxide. Journal of Marine Systems, 17, 39-58.

Bentaleb, I., Fontugne, M., Descolas-Gros, C., Girardin, C., Mariotti, A., Pierre, C., Brunet, C., Poisson A., 1996. Organic carbon isotopic composition of phytoplankton

and sea-surface pCO_2 reconstructions in the Southern Indian Ocean during the last 50,000yr. Organic Geochemistry, 24, 399–410.

Berg, G.M., Mills, M.M., Long, M.C., Bellerby, R., Strass, V., Savoye, N., Rottgers, R., Croot, P.L., Webb, A., Arrigo, K.R., 2011. Variation in particulate C and N isotope compostion following iron fertilization in two successive phytoplankton communities in the Southern Ocean. Global Biogochemical Cycles, 25, GB3013, doi:10.1029/2010GB003824

Bibby, T.S., Gorbunov, M.Y., Wyman, K.W., Falkowski, P.G., 2008. Photosynthetic community responses to upwelling mesoscale eddies in the subtropical North Atlantic and Pacific oceans. Deep Sea Research II 55, 1310–1320.

Bidigare, R.R., Fluegge, A., Freeman, K.H., Hanson, K.L., Hayes, J.M., Hollander, D., Jasper, J.P., King, L.L., Laws, E.A., Milder, J., Millero, F.J., Pancost, R., Popp, B.N., Steinberg, P.A.,Wakeham, S.G., 1997. Consistent fractionation of 13C in nature and in the laboratory: growth-rate effects in some haptophyte algae. Global Biogeochemical Cycles. 11, 279–292.

Bidigare, R.R., Benitez-Nelson, C., Leonard, C. L., Quay, P.D., Parsons, M.L., Foley, D.G., Seki, M.P., 2003. Influence of a cyclonic eddy on microheterotroph biomass and carbon export in the lee of Hawaii.

Blain, S., Sedwick, P.N., Griffiths, F.B., Quequiner, B., Bucciarelli, E., Fiala, M., Pondaven, P., Treguer, P., 2002. Quantification of algal iron requirements in the Subantarctic Southern Ocean (Indian sector). Deep Sea Research II, 49, 3255-3273.

Bopp, L., Resplandy, L., Untersee, A., Le Mezo, P., Kageyama, M., 2017. Ocean (de)oxygenation from the last glacial maximum to the twenty-first century: insight from earth system models. Philosophical Transactions of the Royal Society A: Mathematical, Physical and Engineering Science, 375, 20160323. http://doi.org/10.1098/rsta.2016.0323.

Boyd, P. W., Dillingham, P. W., McGraw, C. M., Armstrong, E. A., Cornwall, C. E., Feng, Y. Y., Hurd, C. L., Gault-Ringold, M., Roleda, M. Y., Timmins-Schiffman, E., Nunn, B. L., 2016. Physiological responses of a Southern Ocean diatom to complex future ocean conditions. Nature Climate Change, 6, 207–213. doi: 10.1038/nclimate2811

Boyd, P., La Roche, J., Gall, M., Frew, R., McKay, R.M.L., 1999. Role of iron, light, and silicate in controlling algal biomass in subantarctic waters SE of New Zealand. Journal of Geophysical Research, 104, 13391–13404.

Boyd, P.W., and Trull, T.W., 2007. Understanding the export of biogenic particles in oceanic waters: Is there consensus?. Progress in Oceanography, 72, 276-312.

Boyd, P.W., Ellwood, M.J., 2010. The biogeochemical cycle of iron in the ocean. Nature Geoscience, 3, 675–682

Brannigan, L., 2016. Intense submesoscale upwelling in anticyclonic eddies. Geophysical Research Letters, 43, 3360–3369.

Buesseler, K.O., 1998. The decoupling of production and particulate export in the surface ocean. Global Biogeochemical Cycles, 12, 297 – 310.

Buesseler, K.O., Lamborg, C., Cai, P., Escoube, R., Johnson, R., Pike, S., Masque, P., McGillicuddy, D.J., Verdeny, E., 2008. Particle fluxes associated with mesoscale eddies in the Sargasso Sea. Deep Sea Research II, 55, 1426–1444.

Burd, A.B., Jackson, G.A., 2009. Particle aggregation. Annual Review in Marine Science, 1, 65-90.

Burkill, P.H., Mantoura, R.C.F., Owens, N.J.P., 1993. Biogeochemical cycling in the northwestern Indian Ocean: a brief overview. Deep Sea Research II, 40(3), 643-649.

Canuel, J.L., Dodson, S.I., Ringelberg, D.B., Guckert, J.B., Rau, G.H., 1995. Molecular and isotopic tracers used to examine source of organic matter and its incorporation into food webs of San Francisco Bay. Limnology and Oceanography. 40, 129–142.

Caron, D.A., Madin, P.L., Cole, J.J., 1989. Composition and degradation of salp fecal pellets: Implications for vertical flux in oceanic environments. Journal of Marine Research, 47, 829-850.

Checkley, D.M., Miller, C.A., 1989. Nitrogen isotope fractionation by oceanic zooplankton. Deep Sea Research A, 36, 1449–1456.

Chen Chentung Arthur, Wang Bingjye, Hsing Liyu, 2004. Upwelling and degree of nutrient consumption in the Nanwan Bay, Southern Taiwan. Journal of Marine Science and Technology, 12 (5), 442-447.

Clarke, A., Meredith, M.P., Wallace, M.I., Brandon, M.A., Thomas, D.N., 2008. Seasonal and interannual variability in temperature, chlorophyll and macronutrients in northern Marguerite Bay, Antarctica. Deep Sea Research II, 55, 1988-2006.

Çoban-Yildiz, Y., Altabet, M.A., Yilmaz, A., Tuğrul, S., 2006. Carbon and nitrogen isotopic ratios of suspended particulate organic matter (SPOM) in the Black Sea water column. Deep Sea Research II, 53, 1875-1892.

Coppola, L., Roy-Barman, M., Mulsow, S., Poninec, P., Jeandel, C., 2005. Low particulate organic carbon export in the frontal zone of the Southern Ocean (Indian sector) revealed by ^{234}Th. Deep Sea Research I, 52, 51-68.

Cowie, G.L., Hedges, J.I., 1994. Biochemical indicators of diagenetic alteration in natural organic matter mixtures. Nature, 369, 304–307.

Crawford, D.W., Wyatt, S.N., Wrohan, I.A., Cefarelli, A.O., Giesbrecht, K.E., Kelly, B., Varela, D.E., 2015. Low particulate carbon to nitrogen ratios in marine surface waters of the Arctic. Global Biogeochemical Cycles, 29, 2021–2033.

Cullen, J.J., 1982. The deep chlorophyll maximum: comparing vertical profiles of chlorophyll a. Canadian Journal of Fisheries and Aquatic Science, 39, 791-803.

Cullen, J.T., Rosenthal, Y., Falkowski, P.G., 2001. The effect of anthropogenic CO_2 on the carbon isotope composition of marine phytoplankton. Limnology and Oceanography, 46 (4), 996–998.

Deacon, G.E.R., 1933. A general account of the hydrology of the Southern Atlantic Ocean. Discovery Report. 7, 171–238.

Degens, E.T., Behrendt M., Gotthart B., Reppmann E., 1968. Metabolic fractionation of carbon isotopes in marine plankton. II: Data on samples collected off the coasts off Peru and Ecuador. Deep Sea Research, 15, 11-20.

DeNiro, M.J., Esptin, S., 1977. Mechanism of carbon isotope fractionation associated with lipid synthesis. Science, 197(4300), 261-263.

Deppeler, S.L., Davidson, A.T., 2017. Southern ocean phytoplankton in a changing climate. Frontiers in Marine Science, 4, 40, 1-28.

Descolas-Gros, Oriol, 1992. Variations in carboxylase activity in marine phytoplankton cultures. P-carboxylation in carbon flux studies. Marine Ecology Progress Series, 85: 163-169

Devol, A.H., Hartnett, H.E., 2001. Role of the oxygen-deficient zone in transfer of organic carbon to the deep ocean. Limnology and Oceanography, 46, 1684-1690.

DeVries, T., and Weber T., 2017. The export and fate of organic matter in the ocean: New constraints from combining satellite and oceanographic tracer observations. Global Biogeochemical Cycles, 31, 535–555, doi:10.1002/2016GB005551.

Dong, S., Garzoli, S.L., Baringer, M., 2009. An assessment of the seasonal mixed layer salinity budget in the Southern Ocean. Journal of Geophysical Research, 114, http://dx.doi.org/10.1029/2008JC005258.

Druffel, E.R.M., Griffin, S., Bauer, J.E., Wolgast, D., Wang, X., 1996. Distribution of particulate organic carbon and radiocarbon in the water column from the upper slope of the abyssal NE Pacific Ocean. Deep Sea Research II. 45, 667-687.

Dubischar, C.D., Bathmann, U.V., 1997. Grazing impact of copepods and salps on phytoplankton in the Atlantic sector of the Southern Ocean. Deep Sea Research II, 44, 415-433.

Ducklow, H.W., Steinberg, D.K., Buesseler, K.O., 2001. Upper ocean carbon export and the biological pump. Oceanography, 14 (4), 50-58.

Duforet-Gaurier, L., Loisel, H., Dessailly, D., Nordkvist, K., Alvain, S., 2010. Estimation of particulate organic carbon over the euphotic depth from in situ measurements. Application to satellite data over the global ocean. Deep Sea Research I, 57, 351-367

Eadie, B.J., Jeffrey L.M., 1973. ^{13}C analyses of ocean particulate organic matter. Marine Chemistry, 1, 199–209.

Eden, C., Dietze, H., 2009. Effects of mesoscale eddy/wind interactions on biological new production and eddy kinetic energy. Journal of Geophysical Research. 114:C05023.

Ediger, D., Tuğrul, S., Yilmaz, A., 2005.Vertical profiles of particulate organic matter and its relationship with chlorophyll-a in the upper layer of the NE Mediterranean Sea. Journal of Marine Systems, 55, 311-326.

Ediger, D., Yilmaz, A., 1996. Characteristics of deep chlorophyll maxima in the Northeastern Mediterranean with respect to environmental conditions. Journal of Marine Systems, 9, 291-303

Eglinton, T.I., Repeta, D.J., 2004. Organic matter in the contemporary ocean. In: Treatise on Geochemistry. [Holand, H.D., and Turekian K.K., (eds)]. The Oceans and Marine Geochemistry, Elsevier Pergamon, Amsterdam, 6, 145-180.

Estep, M.F., Tabita, F.R., Parker, P.L., Van Baalen, C., 1978. Carbon isotope fractionation by ribulose 1, 5 biphosphate carboxylase from various organisms. Plant Physiology, 61, 680-687.

Ewart, C.S., Meyers, M.K., Waller, E.R., McGillicuddy, D.J. Jr., Carlson, C.A., 2008. Microbial dynamics in cyclonic and anticyclonic mode water eddies in the north-western Sargasso Sea. Deep Sea Research II, 55, 1334-1347.

Fahl, K., Kattner, G., 1993. Lipid content and fatty acid composition of algal communities in sea-ice and water from the Weddell Sea (Antarctica). Polar Biology, 13: 405–409.

Falkowski, P., Scholes, R.J., Boyle, E., Canadell, J., Canfield, D., Elser, J., Gruber, N., Hibbard, K., Högberg, P., Linder, S., Mackenzie, F.T., Moore, B., Pedersen, T., Rosenthal, Y., Seitzinger, S., Smetacek, V., Steffen, W., 2000. The global carbon cycle: a test of our knowledge of Earth as a system. Science, 290: 291–6.

Falkowski, P.G., Ziemann, D., Kolber, Z., Bienfang, P.K., 1991. Role of eddy pumping in enhancing primary production in the ocean. Nature 352, 55–58.

Fauchereau, N., Tagliabue, A., Monteiro, P., Bopp, L, 2011. The response of phytoplankton biomass to transient mixiing events in the Southern Ocean. Geophysical Research Letter 38, L17601.

Fenchel, T., 2008. The microbial loop – 25-years later, Journal of Experimental Marine Biology and Ecology, 366, 99-103,

Fernandes, V., Rodrigues, N., Ramaiah, N., Paul, J.T., 2008. Relevence of Bacterioplankton abundance and production in the oligotrophic equatorial Indian Ocean. Aquatic Ecology, 42, 511-519.

Finkel, Z.V., Beardall, J., Flynn, K.J., Quigg, A., Rees, T.A.V., and Raven, J.A. 2010. Phytoplankton in a changing world: cell size and elemental stoichiometry. Journal of Plankton Research, 32, 119–137.

Fischer, G., 1991. Stable carbon isotope ratios of plankton carcon and sinking organic matter from the Atlantic sector of the Southern Ocean. Marine Chemistry, 35, 581-596.

Fontugne, M.R., Duplessy, J.C., 1981. Organic carbon isotopic fractionation by marine plankton in the temperature range -1 to 31°C. Oceanologica Acta. 4(1), 85-90.

Francois, R., Altabet, M.A., Goericke, R., McCorkle, D.C., Brunet, C., Poisson, A., 1993. Changes in the $\delta^{13}C$ of surface water particulate organic matter across the subtropical convergence in the SW Indian Ocean. Global Biogeochemical Cycles, 7(3), 627–644.

Francois, R., Honjo, S., Krishfield, R., Manganini, S., 2002. Factors controlling the flux of organic carbon to the bathypelaic zone of the ocean, Global Biogeochem. Cycles, 16, 1087, doi:10.1029/2001GB001722.

Gandhi, N., Ramesh, R., Laskar, A.H., Sheshshayee, M.S., Shetye, S., Anilkumar, N., Patil, S.M., Mohan, R., 2012. Variability in primary production and nitrogen uptake rates in the southwestern Indian Ocean and the Southern Ocean. Deep Sea Research I, 67, 32–43.

Gaube, P., Chelton, D.B., Samelson, R.M., Schlax, M.G., O'Neill, L.W., 2015. Satellite observations of mesoscale eddy-induced Ekman pumping. Journal of Physical Oceanography 45, 104–132.

Gaul, W., Anita, N.A., Koeve, W., 1999. Microzooplankton grazing and nitrogen supply of phytoplankton growth in the temperate and subtropical North east Atlantic. Marine Ecology Progress Series, 189, 93–104.

George, J.V., Anilkumar, N., Nuncio, M., Soares, M.A., Naik, R.K., Tripathy, S.C., 2018. Upper layer diapycnal mixing and nutrient flux in the subtropical frontal region of the Indian sector of the Southern Ocean. Journal of Marine Systems, 187, 197-205.

Gieskes, W.W.C., Kraay, G.W., and Tijssen, S.B., 1978. Chlorophylls and their degradation products in the deep pigment maximum layer of the tropical North Atlantic, Netherlands. Journal of Sea Research, 12, 195–204.

Glibert, P.M., Garside, C., 1992. Diel variability in nitrogenous nutrient uptake by phytoplankton in the Chesapeake Bay plume. Journal of Plankton Research, 14,271-288.

Goericke, R., Fry, B., 1994. Variations of marine plankton $\delta^{13}C$ with latitude, temperature, and dissolved CO_2 in the world Ocean. Global Biogeochemical Cycle, 8, 85–90.

Gomi, Y., Fukuchi, M., Taniguchi, A., 2010. Diatom assemblages at subsurface chlorophyll maximum layer in the eastern Indian sector of the Southern Ocean in summer. Journal of Plankton Research, 32(7), 1039-1050.

Gordon, E.S., Goñi, M.A., 2003. Source and distribution of terrigenous organic matter delivered by the Atchafalaya River to sediments in the northern Gulf of Mexico. Geochimica et Cosmochimica Acta, 67, 2359-2375.

Gorsky, G., Prieur, L.M., Taupier-Letage, I., Stemmann, L., Picheral, M., 2002. Large particulate matter in the Western Mediterranean – I.LPM distribution related to mesoscale hydrodynamics. Journal of Marine Systems, 33-34, 289 – 311.

Gracía-Fernández, J.M., de Marsa, N.T., Diez J., 2004. Streamlined regulation and gene loss as adaptive mechanisms in Prochlorococcus for optimised nitrogen utilization in oligotrophic environments. Microbiology and Molecular Biology Review, 68(4), 630-638

Grasshoff, K., Ehrhardt, M., Kremling, K., 1983. Methods of Seawater Analysis, 2nd eds. Verlag Chemie, Weinheim, Germany.

Gruber, N., Gloor, M., Mikaloff Fletcher, S.E., Doney, S.C., Dutkiewicz, S., Follows, M.J., Gerber, M., Jacobson, A.R., Joos, F., Lindsay, K., Menemenils, D., Mouchet, A., Muller, S.A., Sarmiento, J.L., Takahashi, T., 2009. Oceanic sources, sinks, and transport of atmospheric CO_2. Global Biogeochemical Cycles, doi.org./10.1029/2008GB003349.

Gruber, N., Keeling, C.D., Bacastow, R.B., Guenther P.R., Lueker, T. J., Wahlen, M., Meijer, H.A.J., Mook, W.G., Stocker, F.T., 1999. Spatiotemporal patterns of carbon-13 in the Global surface oceans and the oceanic Suess effect. Global Biogeochemical Cycles, 13 (2), 307-335.

Guidi, L., Legendre, L., Reygondeau, G., Uitz, J., Stemmann, L., Henson, S.A., 2015. A new look at ocean carbon remineralization for estimating deep water sequestration. Global Biogeochemical Cycles, 29, 1044-1059

Guo, L.N., Tanaka, N., Schell, D.M., Santschi, P.H., 2003. Nitrogen and carbon isotopic composition of HMW dissolved organic matter in marine environments. Marine Ecology Progress Series, 252, 51 – 60.

Hansell, D.A., 2002. Chapter 15 - DOC in the global ocean carbon cycle, in Biogeochemistry of Marine Dissolved Organic Matter, edited by D. A. Hansell and C. A. Carlson, pp. 685–715, Academic Press, San Diego, Calif., doi:10.1016/B978-012323841-2/50017-8.

Hansman, R.L., Sessions, A. L., 2016. Measuring the in situ carbon isotopic composition of distinct marine plankton populations sorted by flow cytometry. Limnology and Oceanography: Methods, 14, 87–99.

Harvey, H.R., Tuttle, J.H., Bell, J.T., 1995. Kinetics of phytoplankton decay during simulated sedimentation-changes in biochemical composition and microbial activity under oxic and anoxic conditions. Geochimica et Cosmochimica Acta, 59, 3367–3377.

Hayes, J.M., 1993. Factors controlling 13C contents of sedimentary organic compounds: principles and evidence. Marine Geology, 113, 111–125.

Hedges, J.I., 1992. Global biogeochemical cycles: Progress and problems. Marine Chemistry, 39, 67-93.

Henley, S.F., Annett, A.L., Ganeshram, R.S., Carson, D.S., Weston, K., Crosta, X., Tait, A., Dougans, J., Fallick, A.E., Clarke, A. 2012. Factors influencing the stable carbon isotopic composition of suspended and sinking organic matter in the coastal Antarctic sea ice environment. Biogeosciences, 9, 1137–1157.

Henson, S.A., Sanders, R., Madsen, E., 2012. Global patterns in efficiency of particulate organic carbon export and transfer to the deep ocean. Global Biogeochemical Cycles, 26, GB1028, doi:10.1029/2011GB004099.

Hernández-León, S., Almeida, C., Gomez, M., Torres, S., Montero, I., Portillo-Hahnefeld, A., 2001. Zooplankton biomass and indices of feeding and metabolism in island-generated eddies around Gran Canaria. Journal of Marine Systems. 30, 51–66.

Hickman, A.E., Moore, C.M., Sharples, J., Lucas, M.I., Tilstone, G.H., Krivtsov, V., and Holligan P., 2012. Primary production and nitrate uptake within the seasonal thermocline of a stratified shelf sea. Marine Ecology Progress Series, 463, 39– 57.

Hill, P.S., 1998. Controls on floc size in the sea. Oceanography, 11: 13–18.

Ho, T.Y., Quigg, A., Finkel, Z.V., Milligan, A.J., Wyman, K., Falkowski, P.G., Morel, F.M.M., 2004. The elemental composition of some marine phytoplankton. Journal of Phycology, 39, 1145–1159.

Hoffmann, L.J., Peeken, I., Lochte, K., Assmy, P., and Veldhuis, M. , 2006. Different reactions of Southern Ocean phytoplankton size classes to iron fertilization. Limnology and Oceanography, 51, 1217–1229.

Holliday, N.P., Read, J.F., 1998. Surface oceanic fronts between Africa and Antarctica. Deep Sea Research I, 45, 217–238.

Honjo, S., Manganini, S.J., Krishfield, R.A., Francois, R., 2008. Particulate organic carbon fluxes to the ocean interior and factors controlling the biological pump: A synthesis of global sediment trap programs since 1983. Progress in Oceanography, 76, 217 – 285.

Huang, B., Hu, J., Xu, H., Cao, Z., Wang, D., 2010. Phytoplankton community at warm eddies in the northern South China Sea in winter 2003/2004. Deep Sea Research II, 57, 1792–1998.

Huang, J., Xu, F., 2018. Observational evidence of subsurface chlorophyll response to mesoscale eddies in the North Pacific. Geophysical Research Letters, 45, 8462–8470.

ICES 2000. Zooplankton methodology manual. California, CA: Academic Press, 684.

Ishikawa, A., Wright, S.W., van den Enden, R., Davidson, A.T., Marchant, H.J., 2002. Abundance, size structure and community composition of phytoplankton in the Southern Ocean in the austral summer 1999/2000. Polar Bioscience, 15, 11–26.

Ito, T., Woloszyn, M., Mazloff, M., 2010. Anthropogenic carbon dioxide transport in the Southern Ocean driven by Ekman Flow. Nature. 463, 80–83.

Jacobs, S.S., Hellmer, H.H., Jenkins, A., 1996. Antarctic ice sheet melting in the Southeast Pacific. Geophysical Research Letters, 23 (9), 957-960.

Jasmine, P., Muraleedharan, K.R., Madhu, N.V., Asha Devi, C.R., Alagarsamy, R., Achuthankutty, C.T., Jayan, Z., Sanjeevan, V.N., Sahayak, S., 2009. Hydrographic and production characteristics along 45°E longitude in the southwestern Indian Ocean and Southern Ocean during austral summer 2004. Marine Ecology Progress Series, 389, 97–116.

Jena, B., Sahu, S., Avinash, K., Swain, D., 2013. Observation of oligotrophic gyre variability in the south Indian Ocean: environmental forcing and biological response. Deep Sea Research I, 80, 1–10.

Johnston, B.M., Albert, J. Gabric, A.J., 2010. Long-term trends in upper ocean structure and meridional circulation of the Southern Ocean south of Australia derived from the SODA reanalysis. Tellus A: Dynamic Meteorology and Oceanography, 62(5), 719-736, DOI: 10.1111/j.1600-0870.2010.00462.x

Johnston, B.M., Albert, J. Gabric, A.J., 2011. Interannual variability in estimated biological productivity in the Australian sector of the Southern Ocean in 1997-2007. Tellus B: Chemical and Physical Meteorology, 63(2) 266-286, DOI: 10.1111/ j.1600-0889.2011.00526.x

Jośe, Y.S., Aumont, O., Machu, E., Penven, P., Moloney, C.L., Maury, O., 2014. Influence of mesoscale eddies on biological production in the Mozambique Channel: Several contrasted examples from a coupled ocean-biogeochemistry model. Deep Sea Research II, 100, 79-93.

Jullion, L., Heywood, K.J., Naveira Garabato, A.C., Stevens, D.P., 2010. Circulation and water mass modification in the Brazil–Malvinas Confluence. Journal of Physical Oceanography, 40, 845–864.

Kaehler, S., Pakhomov, E.A., Mcquaid, C.D., 2000. Tropical structure of the marine food web at the Prince Edward Islands (Southern Ocean) determined by $\delta^{13}C$ and $\delta^{15}N$ analysis. Marine Ecology Progress Series, 208, 13-20.

Kahru, M., Mitchell, B.G., Gille, S. T., Hewes, C.D., Holm-Hansen, O., 2007. Eddies enhance biological production in the Weddell-Scotia Confluence of the Southern Ocean. Geophysical Research Letters, 34, L14603, doi:10.1029/2007GL030430

Kennedy, H., Robertson, J., 1995. Variations in the isotopic composition of particulate organic carbon in surface waters along an 88 W transect from 67°S to 54°S. Deep Sea Research II, 42, 1109–1122.

Kennedy, H., Thomas, D.N., Kattner, G, Haas C, Dieckmann, G.S., 2002. Particulate organic matter in Antarctic summer sea ice: concentrations and stable isotopic composition. Marine Ecology Progress Series, 283, 1 – 13.

Khatiwala, S., Tanhua, T., Mikaloff Fletcher, S., Gerber, M., Doney, S.C., Graven, H.D., Gruber, N., McKinley, G.A., Murata, A., Ríos, A.F., Sabine, C.L., 2013. Global ocean storage of anthropogenic carbon. Biogeosciences, 10, 2169 – 2191.

King, J.D, White, D.C., 1977. Muramic acid as a measure of microbial biomass in estuarine and marine samples. Applied and Environmental Microbiology, 33, 777–783

Kirk, J.T.O., 1996. Light and photosynthesis in Aquatic Ecosystems. Cambridge University press.

Klaas, C., Archer D.E., 2002. Association of sinking organic matter with various types of mineral ballast in the deep sea: Implications for the rain ratio, Global Biogeochemical Cycles, 16(4), 1116, doi:10.1029/2001GB001765.

Kolasinski, J., Kaehler S., Jaquemet, S., 2012. Distribution and sources of particulate organic matter in a mesoscale eddy dipole in the Mozambique Channel (South-

western Indian Ocean): Insites of C and N stable isotopes. Journal of Marine Systems, 96-97, 122-131.

Kuenzler, F.J., Ketchum, B. H., 1962. Rate of uptake of phosphorus by Phaeodactylum tricornutum. Biological Bulletin, 123, 134-145.

Kwon, E.Y., Primeau, F., Sarmiento, J.L., 2009. The impact of remineraliszation depth on the air-sea carbon balance. Nature Geoscience Letters, 2, 630-635.

Lam, P.J., Doney, S.C., Bishop J.K.B., 2011. The dynamic ocean biological pump: Insights from a global compilation of particulate organic carbon, $CaCO_3$, and opal concentration profiles from the mesopelagic. Global Biogeochemical Cycles, 25, GB3009, doi:10.1029/2010GB003868.

Lara, R.J., Alder, V., Franzosi, C.A., Kattner, G., 2010. Characteristics of suspended particulate organic matter in the southwestern Atlantic: influence of temperature, nutrient and phytoplankton features on the stable isotope signature. Journal of Marine Systems. 79, 199–209.

Laws, E. A., R. R. Bidigare, and B. N. Popp. 1997. Effect of growth rate and CO_2 concentration on carbon isotopic fractionation by the marine diatom Phaeodactylum tricornutum. Limnology and Oceanography, 42: 1552–1560. doi:10.4319/ lo.1997.42.7.1552

Laws, E.A., Popp, B.N., Bidigare, R.R., Kennicutt, M.C., Macko, S.A., 1995. Dependence of phytoplankton carbon isotopic composition on growth rate and $[CO_2]$aq: theoretical considerations and experimental results. Geochimica et Cosmochimica Acta. 59 (6), 1131–1138.

Laws, E.A., Popp, B.N., Bidigare, R.R., Riebesell, U., Burkhardt, S., Wakeham, S.G., 2001. Controls on the molecular distribution and carbon isotopic composition of alkenones in certain haptophyte algae. Geochemistry, Geophysics, Geosystems, 2. doi:10.1029/ 2000GC000057.

Leblanc, K., Queguiner, B., Fiala, M., Blain, S., Morvan, J., Corvaisier, R., 2002. Particulate biogenic silica and carbon production rates and particulate matter distribution in the Indian sector of the Subantarctic Ocean. Deep Sea Research II, 49, 3189-3206.

Lee, C. Wakeham, S., Arnosti, C., 2004. Particulate organic matter in the Sea: the composition conundrum. Ambio, 33, 565-575.

Lee, C., Wakeham, S.G., Hedges, J.I., 2000. Composition and flux of particulate amino acids and chloropigments in equatorial Pacific seawater and sediments. Deep Sea Research I 47, 1535–1568.

Legendre, L., Le Fèvre, J., 1995. Microbial food webs and the export of biogenic carbon in the oceans. Aquatic Microbial Ecology, 9, 69–77.

Lenton, A, Tilbrook, B, Law, RM, Bakker, D, Doney, SC, et al. 2013. Sea–air CO_2 fluxes in the Southern Ocean for the period 1990–2009. Biogeosciences, 10:4037–54.

Li, Q.P., Hansell, D.A., 2008. Nutrient distributions in baroclinic eddies of the oligotrophic North Atlantic and inferred impacts on biology. Deep-Sea Research II, 55, 1291–1299.

Li, Y.H., and Peng, T.H., 2002. Latitudinal change of remineralization ratios in the oceans and its implication for nutrient cycles. Global Biogeochemical Cycles, 16, 77-1-77-16.

Li,W., Gao, K.S., Beardall, J., 2012. Interactive effects of ocean acidification and nitrogen-limitation on the diatom phaeodactylum tricornutum. PLoS ONE , 7, e51590.

Liu, F., Yin, K., He, L., Tang, S., Yao, J., 2018. Influence on phytoplankton of different developmental stages of mesoscale eddies off eastern Australia. Journal of Sea Research, 137, 1-8.

Liu, K.K., Kaplan, I.R., 1989. The eastern tropical Pacific as a source of ^{15}N-enriched nitrate in seawater off southern California. Limnology and Oceanography, 34, 820 – 830.

Llido, J., Garçon, V., Lutjeharms, J.R.E., Sudre, J., 2005. Event-scale blooms drive enhanced primary productivity at the subtropical convergence. Geophysical Research Letters, 32, L15611. http://dx.doi.org/10.1029/2005GL022880

Lomas, M.W., Glibert, P.M., 2000. Comparisons of nitrate uptake, storage, and reduction in marine diatoms and flagellates. Journal of Phycology, 36, 903-913.

Lourey, M.J., Trull, T.W, Sigman, D.M, 2003. Sensitivity of delta N-15 of nitrate, surface suspended and deep sinking particulate nitrogen to seasonal nitrate depletion in the Southern Ocean, Global Biogeochemical Cycles, 17 (3), 1081, doi:10.1029/2002GB001973.

Lourey, M.J., Trull, T.W., Tilbrook, B., 2004. Sensitivity of $\delta^{13}C$ of Southern Ocean suspended and sinking organic matter to temperature, nutrient utilization, and atmospheric CO_2. Deep Sea Research I, 51(2), 281–305.

Lutjeharms, J.R.E., and van Ballegooyen, R.C., 1988. The retroflection of the Agulhas current. Journal of Physical Oceanography, 18 (11), 1570-1583

Lutjeharms, J.R.E., Valentine, H.R., 1988. Eddies at subtropical convergence south of Africa. Journal of Physical Oceanography, 31,1461–1475.

Machu, E., Biastoch, A. Oschlies, A. Kawamiya, M. Lutjeharms, J.R.E. Garçon, V., 2005. Phytoplankton distribution in the Agulhas system from a coupled physical-biological model. Deep Sea Research I, 52, 1300–1318.

Machu, E., Garçon, V., 2001. Phytoplankton seasonal distribution from SeaWiFS data in the Agulhas Current system. Journal of Marine Research, 59, 795-812.

Macko, S.A., Engel, M.H., Qian, Y., 1994. Early diagenesis and organic matter preservation - a molecular stable carbon isotope perspective. Chemical Geology, 114, 365 – 379.

Maksymowska, D., Richard, P., Piekarek-Jankowska, H., Riera, P., 2000. Chemical and isotopic composition of the organic matter sources in the Gulf of Gdansk (southern Baltic Sea). Estuarine, Coastal and Shelf Sciences, 51, 585–598.

Marañón, E, Beherenfeld, M.J., González, N., Mouriño B, Zubkov, M.V., 2003. High variability of primary production in oligotrophic waters of the Atlantic Ocean: uncoupling from phytoplankton biomass and size structure. Marine Ecology Progress Series, 257, 1–11.

Marsay, C.M., Sanders, R.J., Henson, S.A., Pabortsava, K., Achterberg, E.P., Lampitt, R.S., 2015. Attenuation of sinking particulate organic carbon flux through the mesopelagic ocean. Proceedings of the National Academy of Sciences, U.S.A, 112, 1089–1094.

Marshall, J., Radko, T., 2003. Residual-mean solutions for the Antarctic circumpolar current and its associated overturning circulation. Journal of Physical Oceanography, 33, 2341–2354.

Martin, J.H., Fritzwater, S.E., Gordon, R.M., 1990. Iron deficiency limits phytoplankton growth in Antarctic waters. Global Biogeochemical Cycles, 4, 5–12.

Martiny, A.C., Vrugt, J.A., Primeau, F.W., Lomas, M.W., 2013. Regional variation in the particulate organic carbon to nitrogen ratio in the surface waters. Global Biogeochemical Cycles, 27(3), 723-731.

McGillicuddy, D.J. Jr., 2016. Mechanism of physical-Biological –Biochemical Interaction at the Oceanic Mesoscale. Annual Review in Marine Sciences, 8, 125-159.

McGillicuddy, D.J., Anderson, L.A., Bates, N.R., Bibby, T., Buesseler, K.O., Carlson, C.A., Davis, C.S., Ewart ,C., Falkowski, P.G., Goldthwait, S.A., Hansell, D.A., Jenkins, W.J., Johnson, R., Kosnyrev, V.K., Ledwell ,J.R., Li Q.P., Siegel, D.A., Steinberg, D.K., 2007. Eddy/wind interactions stimulate extraordinary mid-ocean plankton blooms. Science, 316, 1021- 1026.

McGillicuddy, D.J., Anderson, L.A., Doney, S.C., Maltrud, M.E., 2003. Eddy-driven sources and sinks of nutrients in the upper ocean: results from a 0.1° resolution model of the North Atlantic. Global Biogeochemical Cycles 17, 1035-1055.

McGillicuddy, D.J., Robinson, A.R., 1997. Eddy-induced nutrient supply and new production in the Sargasso Sea. Deep Sea Research II, 44, 1427-1450.

McGillicuddy, D.J., Robinson, A.R., Siegel, D.A., Jannasch, H.W., Johnson, R., Dickey, T.D., McNeil, J., Michaels, A.F., Knap A.H., 1998. Influence of mesoscale eddies on new production in the Sargasso Sea, Nature, 394, 263– 266.

Menzel, D.W., and Goering, J.J., 1966. The distribution of organic detritus in the ocean. Limnology and Oceanography, 11, https://doi.org/10.4319/lo.1966.11.3.0333.

Menzel, D.W., Ryther, J.H., 1964. The composition of particulate organic matter in the western North Atlantic. Limnology and Oceanography, 9, https://doi.org/10.4319/lo.1964.9.2.0179.

Metzl, N., 2009. Decadal increase of oceanic carbon dioxide in Southern Indian Ocean surface waters (1991–2007). Deep Sea Research II, 56, 607–619.

Metzl, N., Beauverger, C., Brunet, C., Goyet, C., Poisson, A., 1991. Surface water pCO_2 in the Western Indian sector of the Southern Ocean: a highly variable CO_2 source/sink region during the austral summer. Marine Chemistry, 35, 85-–95

Mino, Y., Saino, T., Suzuki, K., Marañón, E., 2002. Isotopic composition of suspended particulate nitrogen (δ15Nsus) in surface waters of the Atlantic Ocean from 50°N to 50°S. Global Biogeochemical Cycles, 16 (4), 7–9.

Mishra, R.K., Jena, B., Anilkumar, N., Sinha, R.K., 2017. Shifting of phytoplankton community in the frontal regions of Indian Ocean sector of the Southern Ocean using in situ and satellite data. Journal of Applied Remote Sensing, 11(1), 016019 doi: 10.1117/1.JRS.11.016019.

Mishra, R.K., Naik, R.K., Venkataramana, V. Jena, B., Anilkumar, N., Soares, M.A., Sarkar, A., Singh, A., 2020. Phytoplankton biomass and community composition in the frontal zones of Southern Ocean. Deep Sea Research II, https://doi.org/10.1016/j.dsr2.2020.104799.

Montoya, J.P., 1994. Nitrogen isotope fractionation in the modem ocean: Implication for the sedimentary record. In: Zahn, R., Pedersen, T.F., Kaminski, M.A., Labeyrie, L. (Eds.1, Carbon cycling in the Glacial Ocean: Constraints on the Ocean's Role in Global Change. Springer, Berlin, pp. 259-280.

Montoya, J.P., Horrigan, S.G., McCarthy, J.J., 1990. Natural abundance of 15N in particulate nitrogen and zooplankton in the Chesapeake Bay. Marine Ecology Progress Series, 65, 35-61.

Moore, C.M., Hickman, A.E., Poulton, A.J., Seeyave, S., Lucas, M.I., 2007. Iron-light interactions during the CROZet natural iron bloom and EXport experiment (CROZEX): II – Taxonomic responses and elemental stoichiometry. Deep-Sea Research II, 54, 2066–2084.

Moore, L.R., Post, A.F., Rocap, G., Chisholm, S.W., 2002. Utilization of different nitrogen sources by marine cyanobacteria *Prochlorococcus* and Synechococcus. Limnology and Oceanography, 47, 989-996.

Naik, R.K., George, J.V., Soares, M.A., Asha Devi, Anilkumar, N., Roy, R., Bhaskar, P.V., Murokesh, N., Achuthankutty, C.T., 2015. Phytoplankton community structure at the juncture of the Agulhas Return Front and Subtropical Front in the Indian Ocean sector of Southern Ocean: Bottom-up and top-down control. Deep Sea Research II, http://dx.doi.org/10.1016/j.dsr2.2015.01.002i

Nielsen, E.S., Hansen, V.K., 1959. Light adaptation in marine phytoplankton populations and its interrelation with temperature. Physiologia Plantarum, 12, 353–370.

O'Leary, T., Trull, T.W., Griffiths, F.B., Tilbrook, B., Revill, A.T., 2001. Euphotic zone variations in bulk and compound-specific 13C of suspended organic matter in the subantarctic ocean, south of Australia. Journal of Geophysical Research, 106, 31669–31684.

Omand, M.M., and Mahadevan, A., 2015. The shape of the oceanic nitracline.Bigeosciences, 12(11), 3273–3287.

Orsi, A.H., Whitworth, T., Nowlin, W.D., 1995. On the meridional extent and fronts of the Antarctic Circumpolar Current. Deep Sea Research, 42 (5), 641–673.

Ostrom, N. E., Macko, S. A., Deibel, D. and. Thompson, R.J., 1997. Seasonal variation in the stable carbon and nitrogen isotope biogeochemistry of a coastal cold ocean. Geochimica et Cosmochimica Acta, 61, 2929–2942.

Owens, N.J.P., Rees, A.P., 1989. Determination of N-15 at sub-microgram levels of nitrogen using automated continuous-flow isotope ratio mass-spectrometry. Analyst. 114, 1655-1657.

Pace, M.L., Knauer, G.A., Karl, D.M., Martin, J.H., 1987. Primary production and vertical flux in the eastern Pacific Ocean. Nature, 325, 803–804.

Parslow, J.S., Moyd, P.W., Rintoul, S.R., Griffits, M.F., 2001. A persistent subsurface chlorophyll maximum in the Interpolar Frontal Zone south of Australia: Seasonal

progression and implications for phytoplankton-light-nutrient interactions. Journal of Geophysical Research, 106, 31,543-31, 557

Pavithran, S., Anilkumar, N., Krishnan, K.P., Noronha, S.B., George, J.V., Nanajkar, M., Chacko, R., Dessai, D.R.G., Achuthankutty, C.T., 2011. Contrasting pattern in chlorophyll a distribution within the Polar Front of the Indian sector of Southern Ocean during austral summer 2010. Current Science, 102(6), 899-903.

Pavithran, S., Anilkumar, N., Krishnan, K.P., Sharon, B.N., Jenson, V.G., 2012. Contrasting pattern in chlorophyll a distribution within the Polar Front of the Indian sector of Southern Ocean during austral summer 2010. Current Science, 102, 6.

Perissinotto, R., Mayzaud, P., Nichols, P.D., Labat, J.P., 2007. Grazing by Pryosoma *atlanticum* (Tunicata, Thaliacea) in the south Indian Ocean. Marine Ecology Progress Series, 330, 1-11.

Pillai, H.U.K., Anilkumar, N., Achuthankutty, C.T., Mendes, C.R., Sabu, P., Jayalakshmi, K.V., Asha Devi, C.R., Dessai, D., George, J., Pavithran, S., Hari Devi, C.K, Tripathy, S.C, Menon, N.R., 2018. Planktonic food web structure at SSTF and PF in the Indian sector of the Southern Ocean during austral summer 2011. Polar Research, 37, 1495545. https://doi.org/10.1080/17518369.2018.1495545

Pollard, R., Lucas, M., Read, J., 2002. Physical controls on biogeochemical zonation in the Southern Ocean. Deep Sea Reasearch II, 49, 3289–3305.

Popp, B.N., Laws, E.A., Bidigare, R.R., Dore, J.E., Hanson, K.L., Wakeham, S.G., 1998. Effect of phytoplankton cell geometry on carbon isotopic fractionation. Geochimica et Cosmochimica Acta, 62(1), 69-77.

Popp, B.N., Takigiku, R., Hayes, J.M., Louda, J.W., Baker, E.W., 1989. The post-Paleozoic chronology and mechanisms of ^{13}C depletion in primary marine organic matter. American Journal of Science, 289, 436-454.

Popp, B.N., Trull, T., Kenig, F., Wakeham, S.G., Rust, T.M., Tilbrook, B., Griffiths, B.F., Wright, S.W., Marchant, H.J., Bidigare, R.R., Laws, E.A., 1999. Controls on the carbon isotopic composition in Southern Ocean phytoplankton. Global Biogeochemical Cycles, 13(4), 827-843.

Prasanna Kumar, S., Narvekar J., 2005. Seasonal variability of the mixed layer in the central Arabian Sea and its implication on nutrients and primary productivity. Deep-Sea Research II, 52, 1848–1861.

Prasanna, K., Ghosh, P., Anilkumar, N., 2015. Stable isotopic signatures of Southern Ocean deep water CO_2 ventilation .Deep Sea Research II, 118, 177-185.

Quay, P. D., Sonnerup, R., Westby, T., Stutsman, J., and McNichol, A., 2003. Changes of the$^{13}C/^{12}C$ of dissolved inorganic carbon in the ocean as atracer of anthropogenic CO_2 uptake. Global Biogeochemical Cycles, 17(1), 1004, doi: 10.1029/2001GB001817

Ramaiah, N., Fernandes, V., Rodregues, V., Paul, J., Gauns, M., 2009. Bacterioplankton abundance and production in Indian Ocean Regions. Indian Ocean Biogeochemical processes and Ecological variability. Geophysical Monograph Series, 185. 10.1029/2008GM000711.

Rau, G.H., Takahashi, T., Marais, D.J.D., Repeta, D.J., Martin, J.H., 1992. The relationship between $\delta^{13}C$ of organic matter and $[CO_2(aq)]$ in ocean surface water:

data from a JGOFS site in the northeast Atlantic Ocean and a model. Geochimica et cosmochimica Acta., 56(3), 1413–1419.

Rau, G.H., Teyssie, J.L., Rassoulzadegan, F., Fowler, S., 1990. C-13/C-12 and N-15/N-14 variations among size-fractionated marine particles: implications for their origin and trophic relationships. Marine Ecology Progress Series, 59, 33–38.

Raymond, P.A., Bauer, J.E., 2001. Use of ^{14}C and ^{13}C natural abundances for evaluating riverine, estuarine and coastal DOC and POC sources and cycling: A review and synthesis. Organic Geochemistry, 32, 469-485.

Redfield, A., 1958. The biological control of chemical factors in the environment. American Scientist, 46(3).

Reynolds, S.E., Mather, R.L., Wolff, G.A., Williams, R.G., Landolfi, A., Sanders, R., Woodward, E.M.S., 2007. How widespread and important is N_2 fixation in the North Atlantic Ocean? Global Biogeochemical Cycles, **21**, GB4015, doi:10.1029/2006GB002886.

Riebesell, U., Schulz, K.G., Bellerby, R.G.J., Botros, M., Fritsche, P., Meyerhöfer, M., Neill, C., Nondal, G., Oschlies, A., Wohlers, J., Zöllner, E., 2007. Enhanced biological carbon consumption in a high CO_2 ocean. Nature, 450, 545–548.

Rintoul, S.R., Naveira Garabato, A.C., 2013. Chapter 18 – dynamics of the Southern Ocean circulation. In: Gerold, Siedler, Stephen, M., Griffies, J.G., Church, J.A. (Eds.), Ocean Circulation and Climate. A 21st Century Perspective. Academic Press, International Geophysics, 103, 471–492.

Robinson, C., Ramaiah, N., 2011. Microbial heterotrophic metabolic rates constrain the microbial carbon pump, Microbial Carbon Pump in the Ocean. The American Association for the Advancement of Science, USA. 52–53.

Rontani, J.F., Zabeti, N and Wakeham, S.G., 2011. Degradation of particulate organic matter in the Equatorial Pacific ocean: Biotic or abiotic? Limnology and Oceanography, 56(1), 333-349.

Sabu, P., Anilkumar, N., George, J.V., Chacko, R., Tripathy, S.C., Achuthankutty, C.T., 2014. The influence of air-sea-ice interactions on an anomalous phytoplankton bloom in the Indian Ocean sector of the Antarctic zone of the Southern Ocean during the austral summer, 2011. Polar Science, 1-15.

Sabu, P., George, J.V., Anilkumar, N., Chacko, R., Valsala, V., Achuthankutty, C.T., 2015. Observations of watermass modification by mesoscale eddies in the southern subtropical Indian Ocean. Deep Sea Research II, 118 (B), 152-161.

Sackett, O., Petrou, K., Reedy, B., De Grazia, A., Hill, R., Doblin, M., Beardall, J., Ralph, P., Heraud, P., 2013. Phenotypic Plasticity of Southern Ocean Diatoms: Key to Success in the Sea Ice Habitat? PLoS ONE, 8(11): e81185. doi:10.1371/journal.pone.0081185

Saino, T., Hattori, A., 1987. Geographic variation of the water column distribution of suspended particulate organic nitrogen and its ^{15}N natural abundance in the Pacific and its marginal seas. Deep-Sea Research I, 34, 807-827

Sakata, S., Hayes, J.M., McTaggart, A.R., Evans, R.A., Leckrone, K.J., Togasaki, R.K., 1997. Carbon isotopic fractionation associated with lipid biosynthesis by a

cyanobacterium: relevance for interpretation of bio-marker records. Geochimica et cosmochimica Acta., 61, 5379-5389.

Sallée, J.B., Morrow, R., Speer, K., 2008. Eddy heat diffusion and Subantarctic mode water formation. Geophysical Research Letters. 35, L05607.http://dx.doi.org/10.1029/2007GL032827.

Sardessai, S., Shetye, S., Maya, M.V., Mangala, K.R., Prasanna Kumar, S., 2010. Nutrient characteristics of water masses and their seasonal variability in the eastern equatorial Indian Ocean. Marine Environmental Research. 70 (3-4), 272-282.

Sarmiento, J.L., Gruber, N., 2006. Ocean Biogeochemical Dynamics. Princeton, Woodstock: Princeton University press, Geological Magazine, 144, 1034, doi:https://doi.org/10.1017/S0016756807003755.

Sarmiento, J.L., Toggweiler, J.R., 1984. A new model for the role of the oceans in determining atmospheric pCO_2. Nature, 308, 621 – 624.

Savoye, N., Aminot, A., Treguer, P., Fontugne, M., Naulet, N., Kerouel, R., 2003. Dynamics of particulate organic matter $\delta^{15}N$ and $\delta^{13}C$ during spring phytoplankton blooms in a macrotidal ecosystem (Bay of Seine, France). Marine Ecology Progress Series, 255, 27-41.

Schneider, B., Schlitzer, R., Fischer, G., Nöthig, E.-M., 2003. Depth-dependent elemental compositions of particulate organic matter (POM) in the ocean. Global Biogeochemical Cycles, 17(2), 1032, doi:10.1029/2002GB001871

Séférian, R., Ludicone, D., Bopp, L., Roy, T., Madec, G., 2012. Water mass analysis of effect of climate change on air-sea CO_2 fluxes: The Southern Ocean. Journal of Climate, 25 (11) 3894-3908.

Segschneider, J., Bendtsen, J., 2013. Temperature-dependent remineralisation in a warming ocean increases surface pCO_2 through changes in marine ecosystem composition. Global Biogeochemical Cycles, 27, 1214–1225, doi:10.1002/ 2013GB004684.

Sen Gupta, A., England, M.H., 2006. Coupled ocean–atmosphere–ice response to variations in the Southern Annular Mode. Journal of Climate, 19, 4457–4486.

Sheridan, C.C., Lee, C., Wakeham, S.G., Bishop, J.K.B., 2002. Suspended particulate organic composition and cycling in surface and midwaters of the Equatorial Pacific Ocean. Deep Sea Research I, 49, 1983-2008.

Sherr, E.B., Sherr, B.F., 2007. Heterotrophic dinoflagellates: a significant component of microzooplankton biomass and major grazers of diatoms in the sea. Marine Ecology Progress Series, 352, 187-197.

Sherr, E.B., Sherr, B.F., 2007. Heterotrophic dinoflagellates: a significant component of microzooplankton biomass and major grazers of diatoms in the sea. Marine Ecology Progress Series, 352, 187-197.

Shetye, S., Rahul Mohan, Patil, S., Jena, B., Chacko, R., George, J.V., Noronha, S., Singh, N., Lakshmi, P., 2015. Oceanic pCO_2 in the Indian sector of the Southern Ocean during the austral summer-winter transition phase. Deep Sea Research II, 118, 250-260.

Shetye, S.S., Sudhakar, M., Ramesh, R., Mohan, R., Patil, S., Laskar, A., 2012. Sea surface pCO2 in the Indian Sector of the Southern Ocean during Austral summer of 2009. Advanced Geosciences, 28, 79-92.

Siegel, D.A., Buesseler, K.O., Behrenfeld, M.J., Benitez-Nelson, C.R., Boss, E., Brzezinski, M.A., Doney, S.C., 2016. Predication of the export and fate of global ocean net primary production: the Exports science plan. Frontiers in Marine Science, 3, 22.

Sinninghe Damst´e, J.S., Rampen, S., Irene, W., Rupstra, C., Abbas, B., Muyzer, G., Schouten, S., 2003. A diatomaceous origin for long-chain diols and mid-chain hydroxy methyl alkanoates widely occurring in Quaternary marine sediments: Indicators for high-nutrient conditions. Geochimica et Cosmochimica Acta, 67, 1339–1348.

Smetacek, V., 1999. Diatoms and the ocean carbon cycle. Protist, 150, 25 – 32.

Smith, Jr. W.O., Comiso, J.C., 2008. Influence of sea ice on primary production in the Southern Ocean: a satellite perspective. Journal of Geophysical Research, 113, C05S93, doi:10.1029/2007JC004251.

Soares, M.A., Bhaskar, P.V., Anilkumar, N., Naik, R.K., George, J.V., Mishra, R.K., Dessai, D.G., 2020a. Characteristics of particulate organic matter within the photic water column: A case study across the fronts in the Indian sector of the Southern Ocean. Deep Sea Research-II (in press).

Soares, M.A., Sabu, P., George, J.V., Naik, R.K., Anilkumar, N. and Dessai, D. G., 2020a. Nutrient dynamics at the juncture of Agulhas Return Front and Subtropical

Front in the Indian sector of the Southern Ocean during the austral summer. Polar science, https://doi.org/10.1016/j.polar.2020.100551.

Sokolov, S., Rintoul, S.R., 2002. Structure of Southern Ocean fronts at 140°E. Journal of Marine Systems, 37, 151-184.

Sommer, U., 1989. Maximal growth rates of Antarctic phytoplankton: only weak dependence on cell size. Limnology and Oceanography, 34, 1109-1112.

Suess, E., 1980. Particle organic carbon flux in the Ocean's surface productivity and oxygen utilization. Nature, 288, 260–263.

Sweeney, E.N., McGillicudy, D.J., jr., Buesseler, K.O., 2003. Biogeochemical impacts due to mesoscale eddy activity in the Sargasso Sea as measures at the Bermuda Atlantic Time-Series (BATS) site. Deep Sea Research II, 50, 3017 – 39.

Takahashi, T., Sutherland, S.C., Wanninkhof, R., Sweeney C., Feely R.A., et al. 2009. limatological mean and decadal change in surface ocean pCO_2, and net sea–air CO_2 flux over the global oceans. Deep Sea Research I, 56:554–77.

Takahashi, T., Sweeney, C., Hales, B., Chipman, D.W., Newberger, T., Goddard, J.G., Iannuzzi, R.A., Sutherland, S.C., 2012. The changing carbon cycle in the Southern Ocean. Oceanography, 25, 26 – 37.

Talmy, D., Martiny, A.C., Hill, C., Hickman, A.E., and Follows, M.J., 2016. Microzooplankton regulation of surface ocean POC:PON ratios. Global Biogeochemical Cycles, 30, 311–332, doi:10.1002/2015GB005273.

Thomas, D.N., Dieckmann, G.S., 2002. Antarctic sea ice-a habitat for extremophiles. Science, 295, 641–644.

Tiwari, M., Nagoji, S., Kartik, T., Drishya, G., Parvathy, R.K., Rajan, S., 2013. Oxygen isotope-salinity relationships of discrete oceanic regions from India to Antarctica vis-à-vis surface hydrology processes. Journal of Marine System, 113-114, 88-93.

Tremblay, L., Caparros, J., Leblanc, K., Obernosterer, I., 2015. Origin and fate of particulate and dissolved organic matter in a naturally iron-fertilized region of the Southern Ocean. Biogeosciences, 12, 607-621.

Tripathy, S.C., Pavithran, S., Sabu, P., Pillai, H.U.K., Dessai, D.R.G., Anilkumar, N., 2015. Deep chlorophyll maximum and primary productivity in Indian Ocean sector of the Southern Ocean: Case study in the Subtropical and Polar Front during austral summer 2011. Deep Sea Research II, 118 (B), 240-249.

Tsukasaki, N., Tanoue, E., 2010. Chemical characterization and dynamics of particulate combined amino acids in Pacific surface waters. Journal of Marine systems, 79, 173–184.

Valkman, J.K., Tanoue, E., 2002. Chemical and biological studies of particulate organic matter in ocean. Journal of Oceanography, 58, 265-279.

van Heukelem, 2002. HPLC phytoplankton pigments: Sampling, laboratory methods and quality assurance procedure. In: Ocean optics protocols for Satellite Ocean Color Sensor (eds) Mueller J, 504 Fragion G, Revision 3, Volume 2, NASA technical memorandum 2002-210004, pp. 258–268.

Van Mooy, B.A., Keil, R.G., Devol A.H., 2002. Impact of suboxia on sinking particulate organic carbon: Enhanced carbon flux and preferential degradation of amino acids via denitrification. Geochimica et Cosmochimica Acta, 66(3), 457–465.

Veldhuis, M.J.W., Timmermans, K.R., Croot, P., van der Wagt, B., 2005. Picophytoplankton; a comparative study of their biochemical composition and photosynthetic properties. Journal of Sea Research. 53, 7-24

Venables, H. J., Meredith, M.P., 2014. Feedbacks between ice cover, ocean stratification, and heat content in Ryder Bay, western Antarctic Peninsula. Journal of Geophysical Research: Oceans, 119, 5323–5336. doi: 10.1002/2013JC009669

Venkatachalam, S., Ansorge, I.J., Mendes, A., Melato, L.I., Matcher, G.F., Dorrington, R.A., 2017. A pivotal role for ocean eddies in the distribution of microbial communities across the Antarctic Circumpolar Current. PLoS ONE 12(8): e0183400. https://doi.org/10.1371/journal.pone.0183400

Venkataramana, V., Anilkumar, N., Swalding, K., Mishra, R.K., Tripathy, S.C., Sarkar, A., Soares, M.A., Sabu, P. and Pillai, H.U.K., 2020. Distribution of zooplankton in the Indian sector of the Southern Ocean. Antarctic Science. https://doi.org/10.1017/S0954102019000579.

Verdeny, E., Masque', P., Maiti, K., Garcia-Orellana, J., Bruach, J.M., Mahaffey,C.,Benitez-Nelson, C.R., 2008. Particle export within cyclonic Hawaiian lee eddies derived from ^{210}Pb–^{210}Po disequilibria. Deep-Sea Research II, 55, 1461-1472.

Volk, T., Hoffert, M.I., Ocean carbon pumps: analysis of relative strengths and efficiencies in ocean-driven atmospheric CO_2 changes. The Carbon Cycle and Atmospheric CO_2: Natural Variations Archean to Present. Washington, DC: American Geophysical Union, 1985, 99-110.

Wada, E., Hattori, A., 1978. Nitrogen isotope effects in the assimilation of inorganic nitrogenous compounds by marine diatoms. Geomicrobiology Journal, 1, 85-101.

Wada, E., Hattori, A., 1991. Nitrogen in the sea: Forms, Abundances, and rate processes. CRC Press, Boca Raton, Fla. pp. 208–212.

Wada, E., Terasaki, M., Kabaya, Y., Nemoto, T., 1987. ^{15}N and ^{13}C abundances in the Antarctic Ocean with emphasis on biogeochemical structure of food web. Deep Sea Research, 34, 829-841.

Waite, A.M., Muhling, B.A., Holl, C.M., Beckley, L.E., Montoya, J.P., Strzelecki, J., Thompson, P.S., Presant, S., 2007. Food web structure in two counter-rotating eddies based on $\delta^{15}N$ and $\delta^{13}C$ isotopic analysis. Deep Sea Research II, 54, 1055-1075.

Wakeham, S.G., Hedges, J.I., Lee, C., Peterson, M.L., Hernes, P.J., 1997. Composition and transport of lipid biomarkers through the water column and surficial sediments of the equatorial Pacific Ocean. Deep Sea Research II, 44, 9-10.

Wang Y, Zhang H-R, Chai F, Yuan Y., 2018. Impact of mesoscale eddies on chlorophyll variability off the coast of Chile. PLoS ONE 13(9): e0203598. https://doi.org/10.1371/journal.pone.0203598

Waser, N. A., Z. Yu, K. Yin, B. Nielsen, P. J. Harrison, D. H. Turpin, Calvert, S.E.,1999. Nitrogen isotopic fractionation during a simulated diatom spring bloom:

Importance of N-starvation in controlling fractionation. Marine Ecology Progress Series, 179, 291– 296.

Waser, N.A.D., Harrison, P.J., Nielson, B., Calvert, S.E., Turpin, D.H., 1998. Nitrogen isotope fractionation during the uptake and assimilation of nitrate, nitrite, ammonium, and urea by a marine diatom. Limnology and Oceanography 43, 215—224.

Weber, T., Cram, J.A., Leung, S.W., DeVries, T., Deutsch, C., 2016. Deep ocean nutrients imply large latitudinal variation in particle transfer efficiency. Proceedings of the National Academy of Sciences, 113(31), 8606–8611, doi:10.1073/pnas.1604414113.

Wells, N.C., Ivchenko, V.O., Best, S.E., 2000. Instabilitiesin the Agulhas Retroflection Current system: A comparative model study. Journal of Geophysical Research. 105, 3233-3241.

Wilson, J.D., Barker, S., Ridgwell A., 2012. Assessment of the spatial variability in particulate organic matter and mineral sinking fluxes in the ocean interior: Implications for the ballast hypothesis. Global Biogeochemical Cycles, 26, GB4011, doi:10.1029/2012GB004398.

Wright, S.W., van den Enden, R.L., Pearce, I., Davidson, A.T., Scott, F.J., and Westwood, K.J., 2010. Phytoplankton community structure and stocks in the Southern Ocean (30–80◦E) determined by CHEMTAX analysis of HPLC pigment signatures. Deep Sea Research II, 57, 758–778.

Yin, X., Li, Y., Qiao, L., Wang, A., XU, Y., Chen, J., 2014. Source and spatial distributions of particulate organic carbon and its isotope in surface waters of Prydz Bay, Antarctica, during summer. Advance in Polar Science, 25, 175 – 182.

Zeitzschel, B., 1970. The quantity, composition and distribution of suspended particulate matter in the Gulf of California. Marine Biology, 7, 305–318.

Zhang, R., Chen, M., Guo, L., Gao, Z., Ma, Q., Cao, J., Qiu, Y., Li, Y., 2011. Variations in the isotopic composition of particulate organic carbon and their relation with carbon dynamics in the western Arctic Ocean. Deep Sea Research II, 81–84, 72–78.

Zhang, R., Zheng, M., Chen, M., Ma, Q., Cao, J., Qiu, Y., 2014. An isotopic perspective on the correlation of surface ocean carbon dynamics and sea ice melting in Prydz Bay (Antarctica) during austral summer. Deep Sea Research I, 83, 24–33.

Zhang, S., Curchitser, E.N., Kang, D., Stock, C.A., Dussin, R., 2018. Impacts of mesoscale eddies on the vertical nitrate flux in the Gulf stream region. Journal of Geophysical Research: Oceans, 123, 497–513.

Zhu, Y., Qiu, B., Lin, X., Wang, F., 2018. Interannual eddy kinetic energy modulations in the Agulhas Return Current. Journal of Geophysical Research: Oceans, 123, 6449–6462.

Zubkov, M.V., Fuchs, B.M., Tarran, G.A., Burkill, P.H., Amann, R., 2003. High rate of uptake of organic nitrogen compounds by Prochlorococcus Cyanobacteria as a key to their dominance in oligotrophic oceanic waters. Applied and Environmental Microbiology, 69(2), 1299-1304.

Research Publications from this thesis

- **Soares, M.A**., Bhaskar, P.V., Anilkumar, N. Naik, R.K., George, J.V., Mishra, R.K., Dessai, D.G., 2020. Characteristics of particulate organic matter within the photic water column: A case study across the fronts in the Indian sector of the Southern Ocean***. Deep Sea Research-II***.

- **Soares, M.A.,** Sabu, P., George, J.V., Naik, R.K., Anilkumar, N., Dessai, D.G., **2020**. Nutrient dynamics at the juncture of Agulhas Return Front and Subtropical Front in the Indian sector of the Southern Ocean during the austral summer. ***Polar Science***. https://doi.org/10.1016/j.polar.2020.100551.

- **Soares, M.A**., Anilkumar, N., **2017**. Indian contributions to Chemical Studies in the Indian sector of Southern Ocean. Proceedings of Indian National Science Academy **(PINSA),** 83 (2), 377-384.

- **Soares, M. A**., Bhaskar, P.V., Naik, R.K., Dessai, D.R.G., George, J.V., Tiwari, M., Anilkumar, N., **2015.** Latitudinal $\delta^{13}C$ and $\delta^{15}N$ variations in Particulate Organic Matter (POM) in surface waters from the Indian Ocean sector of Southern Ocean and the Tropical Indian Ocean in 2012. **Deep sea research II**, 118; 186-196.

Papers Presented at Conferences

- **Soares, M.A**., Sabu, P. Naik, R.K., Anilkumar, N., Mishra, R.K., Bhaskar, P.V., George, J.V., Sarkar, A. Influence of eddies on the characteristics of suspended particulate organic matter in Subtropical Front of the Indian sector of Southern Ocean, has been presented presentation at the National Oceanography Workshop to be held at INCOIS, Hyderabad, November, **2018.**

- **Soares**, **M.A.,** Bhaskar, P. V., Anilkumar, N., Naik, R.K., George J.V., and Dessai, D. Autotrophic and heterotrophic processes across the fronts in the Indian sector of Southern Ocean:Insights from $\delta^{13}C$ characteristics of particulate organic matter. Paper Presentation In. Book of Abstracts OSICON, Thiruvananthapuram, Kerela, **2017**

- **Soares, M.A.,** Anilkumar, N., Bhaskar, P.V., Sabu, P., Mishra, R.K., Naik R.K., Sarkar, A., George, J.V., Characteristics Of Particulate Organic Matter Across The Fronts In The Southern Ocean: A Stable Isotope Approach. Paper Presentation In. Book of Abstracts, National Conference on Polar Sciences, Vasco, Goa, pp 58, **2017**

Other Publications associated with this Thesis

- *Naik, R. K. George, J.V., **Soares, M.A**., Anilkumar, N., Mishra, R.K., Roy,R., Bhaskar, P.V., Sivadas, S., Murukesh, N., Chako, R., Achuthankutty, C.T.,2020. Observations of surface water phytoplankton community in the Indian Ocean: A transect from the tropics to the polar latitudes**. Deep Sea Research-II.***
- *Venkararamana,V., Anilkumar, N., Swadling, K., Mishra, R.K. Tripathy, S.C., Sarkar, A., **Soares, M.A**., Sabu,P., Pillai, H.U.K., 2020. Distribution of zooplankton in the Indian sector of the Southern Ocean. **Antarctic Science.***
- *Mishra, R.K., Naik, R.K., Venkararamana,V., Jena,B., Anilkumar, N., **Soares, M.A**., Sarkar,A., Singh, A.,2020. Phytoplankton biomass and community composition in the frontal zones of Southern Ocean. **Deep Sea Research-II.***
- *Asha Devi, C.R., Sabu, P., Naik, R.K., Bhaskar, P.V., Achuthankutty, C.T., **Soares, M.A**., Anilkumar, N., Sudhakar, M.,2020. Microzooplankton concerning the plankton food web in subtropical frontal region of the Indian Ocean sector of the Southern Ocean during austral summer 2012. **Deep Sea Research-II.***
- *George, J.V., Anilkumar, N., Nuncio, M., **Soares, M.A**., Naik, R.K., Tripathy, S.C., **2018.** Upper layer diapycnal mixing and nutrient flux in the subtropical frontal region of the Indian sector of the Southern Ocean. **Journal of Marine System**, 187, 197-205.*
- *Mishra**,** R.K. Jena, B. Anil Kumar, N. Bhaskar P.V. and **Soares**. **M.A., 2017**. Inter-annual variability of chlorophyll-a and diatoms in the frontal ecosystem of Indian Ocean sector of the Southern Ocean. **Polish Polar Research**, vol. 38, no. 3, pp. 375-390.*
- *Naik., R. K., George, J.V., **Soares, M. A.,** Asha Devi., Anilkumar, N., Rajdeep Roy., Bhaskar, P. V., Nuncio, M., Achuthanakutty, C.T., **2015.** Phytoplankton community structure at Subtropical Front in the Indian Ocean sector of Southern Ocean: Bottom-up and top-down control. **Deep sea research II**, 118; 233-239.*

Deep-Sea Research II 118 (2015) 186–196

Contents lists available at ScienceDirect

Deep-Sea Research II

journal homepage: www.elsevier.com/locate/dsr2

Latitudinal $\delta^{13}C$ and $\delta^{15}N$ variations in particulate organic matter (POM) in surface waters from the Indian ocean sector of Southern Ocean and the Tropical Indian Ocean in 2012

Melena A. Soares, Parli V. Bhaskar*, Ravidas K. Naik, Deepti Dessai, Jenson George, Manish Tiwari, N. Anilkumar

National Centre for Antarctic & Ocean Research, Earth Science System Organization, Vasco-da-Gama, Goa 403804, India

ARTICLE INFO

Available online 17 June 2015

Keywords:
Carbon isotope
Nitrogen isotope
Particulate organic matter
Southern Ocean
Indian Ocean

ABSTRACT

Surface water samples were collected onboard ORV Sagar Nidhi from 11 stations in the Tropical Indian Ocean (TIO) and 9 stations in the Indian Ocean sector of Southern Ocean (IOSO) (between 3°N and 53°S) during the austral summer 2012 to understand $\delta^{13}C$ and $\delta^{15}N$ signatures of particulate organic matter (POM) in the two different oceanic regimes. Organic carbon and nitrogen concentrations (%C and %N) and $\delta^{13}C$ and $\delta^{15}N$ values ($\delta^{13}C_{(POM)}$ and $\delta^{15}N_{(POM)}$) of POM were analysed along with a suite of supporting oceanographic parameters. Overall, large-scale variations in %C, %N, $\delta^{13}C_{(POM)}$ and $\delta^{15}N_{(POM)}$ values were observed in surface waters, which may be influenced by physical and biological processes. The $\delta^{13}C_{(POM)}$ values ranged from −26.82‰ to −21.40‰ and were higher in the subtropical waters (40–43°S), with an increase of approximately 3‰. $\delta^{15}N_{(POM)}$ values varied over a wide range, from −5.09‰ to 4.09‰, with higher $\delta^{15}N_{(POM)}$ in the nitrate-depleted subtropical waters. $\delta^{13}C_{(POM)}$ had a significant relation with temperature and an inverse relation with total CO_2 (tCO_2) beyond 40°S. The elemental C:N ratio ranged from 4.4 to 10.8 in the tropical waters, with higher ratios in equatorial waters (1°N–3°S). The biological community structure and diverse biological processes influence the spatial variations of $\delta^{13}C_{(POM)}$ and $\delta^{15}N_{(POM)}$ values in the study area. The selective enrichment of carbon of POM in tropical surface waters may be due to the dominance of picoplankton and associated biological processes. Beyond 40°S, a combination of physical factors including SST, eddies along with the changing biological community, especially the dominance of dinoflagellates in the subtropical front and diatoms in the polar front appears to control the latitudinal variability of POM characteristics.

1. Introduction

Particulate organic matter (POM) is a key component of the biological pump which links surface productivity to the deep-ocean. POM is comprised of particles of diverse size and derived from various sources including broken phytoplankton cells, bacterioplankton, aggregates, faecal pellets of grazers, etc. (Parsons, 1963; Valkman and Tanoue, 2002 and references within). Organic carbon from POM forms a small fraction of total organic carbon in marine environment; almost 97–99% of POM gets remineralized in the photic layers while a very small fraction gets buried into the bottom sediment (Hedges and Keil, 1995; Honjo et al., 2008). Hence, POM controls the efficiency and quality of 'biological pump' linking the surface productivity to deep carbon export (Gordon and Goñi, 2003; Duforet-Gaurier et al., 2010). Chemical characterisation of POM including isotopic analyses of carbon and nitrogen help us to gain insights into various processes that influence the quality of carbon exported to the deep-ocean. Unlike other biomarkers, the stable isotopic ratios of carbon and nitrogen are not affected by abiotic processes like photochemical degradation or structural modification and hence can be used as a tool to understand the processes/sources (fixation, upwelling, atmospheric inputs, remineralization, etc.) and fate of organic matter in marine systems (Hedges, 1992; Druffel et al., 1996; Raymond and Bauer, 2001).

The natural abundances of stable carbon and nitrogen isotope ratios of POM ($\delta^{13}C_{(POM)}$ and $\delta^{15}N_{(POM)}$) are often used to study the conditions prevailing at the time of carbon fixation, as various factors including pCO_2, availability of nutrients, upwelling processes, temperature and biological community structure determine the isotopic fractionation of carbon in POM (Popp et al.,

* Corresponding author.
E-mail address: bhaskar@ncaor.gov.in (P.V. Bhaskar).

http://dx.doi.org/10.1016/j.dsr2.2015.06.009
0967-0645/

1989; Laws et al., 1995; Bidigare et al., 1997; Gruber et al., 1999; Zhang et al., 2014). $\delta^{13}C_{(POM)}$ is largely influenced by the source of inorganic carbon (air–sea exchange, upwelling, mixing, etc.) and the phytoplankton community (autotrophs and mixotrophs), while heterotrophs prefer assimilation of dissolved organic carbon over inorganic carbon [$CO_{2(aq)}$] (Hayes, 1993; Bentaleb et al., 1998). On the other hand, $\delta^{15}N_{(POM)}$ is used to study processes involved in cycling of organic matter, specially nitrogen related processes like nitrate uptake, nitrification, denitrification, remineralisation, etc. (Mopper and Degens, 1978; Wada et al., 1987).

Isotopic studies on POM have been carried out in the Southern Ocean (Kennedy and Robertson, 1995), the Arctic Ocean (Zhang et al., 2011), the Antarctic-Prydz Bay (Zhang et al., 2014) and the Atlantic Ocean (Rau et al., 1992; Lara et al., 2010) mainly to perceive the variability of $\delta^{13}C_{(POM)}$ and understand the influence of environmental factors (temperature, nutrients, melting ice, $CO_{2(aq)}$), carbon biochemistry and phytoplankton composition. However, limited information exists on the isotopic nature of POM in relation to biological productivity, speciation and oceanography from the Indian Ocean sector of the Southern Ocean (IOSO). Earlier isotopic studies of POM in IOSO were restricted to the Crozet Basin, Indian sector of the Subantarctic Southern Ocean (Kaehler et al., 2000), the Southern Ocean, south of Australia (Lourey et al., 2004) and the Leeuwin Current (LC), off Western Australia (Waite et al., 2007). To the best of our knowledge, there is very little information about the distribution of $\delta^{13}C_{(POM)}$ and $\delta^{15}N_{(POM)}$ in TIO (Francois et al., 1993).

Both IOSO and TIO are two different oceanographic regimes with contrasting hydrodynamic features. The IOSO extends from 40°S up to the Antarctic coastline and is connected to the Atlantic and Pacific sectors of the Southern Ocean. The IOSO is influenced by diverse physical processes (sharp temperature gradients, strong currents, constantly high wind speeds) and experiences strong seasonal changes. Moreover, IOSO shows large scale meridional changes in temperature and salinity, resulting in the formation of various oceanic fronts including the Subtropical Front (STF), the Sub-Antarctic Front (SAF) and the Polar Front (PF). The IOSO is strongly influenced by the Antarctic Circumpolar Current (ACC) and the Agulhas Return Front (ARF) (Orsi et al., 1995; Belkin and Gordon 1996; Holliday and Read, 1998; Anilkumar et al., 2006). The wind and current induced mixing and northward transport of both seawater and solutes from its source in the Antarctic shelf are keys to the supply of nutrient rich and oxygen rich waters to mid-latitudes. Although these waters are relatively nutrient rich and support varied food-webs, the overall productivity is patchy, thereby making biogeochemical processes (carbon sink and source) in these waters very complex and sensitive to short-term sporadic events (including eddies, varying insolation etc.) (Deacon, 1933; Jasmine et al., 2009). The biological response and adaptation across these fronts has thrown light on the existence of different trophic processes, including an active microbial loop (DOM uptake) along with a strong microzooplankton grazing (flagellate and ciliate dominated system) (Jasmine et al., 2009).

TIO gets input from various water masses such as the Arabian Sea high saline waters, Bay of Bengal waters, Indonesian through flow, tropical surface waters, etc. (Prasanna Kumar and Narvekar, 2005; Sardessai et al., 2010; George et al., 2013). These waters are bounded by the Asian landmass on the north and the African landmass on the west, which influence the current patterns, nutrient redistribution, productivity patterns and the biogeochemistry of these waters (Burkill et al., 1993). The equatorial Indian Ocean also experiences Wyrtki jet which makes it less productive than equatorial Pacific and Atlantic (Wyrtki, 1973; George et al., 2013). The TIO also includes the south-western Indian Ocean gyre, which lies between 10°S and 35°S and extends from Madagascar to Australia. These waters are also known for its patchy but low productivity and oligotrophic growth conditions (Jena et al., 2013).

Under the Indian Southern Ocean Studies Program, a multidisciplinary approach is being adopted to address the carbon biogeochemical processes and food-web dynamics in IOSO. Organic carbon inventory, its sources and links to various oceanographic processes are some of the key scientific issues being investigated under this program. As a part of these investigations, chemical characterisation of POM and stable isotopic analyses of carbon and nitrogen were carried out. The present work investigates the spatial variation of $\delta^{13}C_{(POM)}$ and $\delta^{15}N_{(POM)}$ in surface waters of the TIO and IOSO having two contrasting biogeochemical environments, varied food-web dynamics and biological community structure. We also make an attempt to delineate the key factors controlling the signatures of carbon and nitrogen isotopes in these two different oceanic regimes.

2. Material and methods

2.1. Sampling

Surface seawater samples were collected on-board ORV Sagar Nidhi during December 2011–January 2012 at selected locations within the oceanic areas of TIO and IOSO between 3°N and 53°S (Fig. 1). Based on the sea-level anomaly data (Fig. S1, Supplementary data), a cold core eddy was identified at 40°S, 56.5°E which showed distinct anomalies in hydrography and nutrient concentrations.

Seawater samples were collected in precleaned plastic buckets for nutrient analyses, chlorophyll *a*, tCO_2 and %C, %N, $\delta^{13}C$ and $\delta^{15}N$ of POM. Hydrography data was obtained from on board thermosalinograph (Seabird Electronics SeaCat 21) in TIO and CTD in IOSO.

2.2. Nutrient analyses

Seawater sub-samples were collected in 250 ml Nalgene bottles and kept frozen at −20 °C until analyses. Prior to analyses, the samples were thawed and brought to room temperature. The dissolved nutrients (nitrate, nitrite, ammonium, phosphate, and silicate) were measured using an auto-analyser (Model: Skalar Analytical San++ 8505 Interface v3.05, The Netherlands) following standard colorimetric methods (Grasshoff et al., 1983). Standards were used to calibrate the auto-analyser and frequent baseline checks were made. The standard deviation for all nutrients analysed was ±1%.

2.3. Analyses of chlorophyll a by flourometry and phytoplankton marker pigments by HPLC

Three litres of seawater were filtered through GF/F Whatman filters for chlorophyll *a* (Chl *a*) analyses by fluorometry and pigment analyses by HPLC. These samples were kept frozen (−20 °C) prior to analyses. For Chl *a* analyses, frozen samples were placed in 15 ml centrifuge tubes and extracted overnight at 4 °C using 10 ml of 90% acetone. The extracted samples were then transferred to 10 ml cuvettes and measured fluorometrically using Turner's AU 10 Fluorometer (Turner Designs Inc., USA). Calibration was carried out using standard chlorophyll *a* pigment (DHI, Denmark).

For pigment analyses, the frozen samples were placed in 15 ml centrifuge tubes, extracted for 5 min in ultrasonic bath filled with ice-water and overnight at 4 °C using 3 ml 90% acetone. The extracts were stored overnight at −20 °C for HPLC analysis. The entire extraction procedure was carried out in dim light conditions and at low temperature to minimise degradation of pigments. The

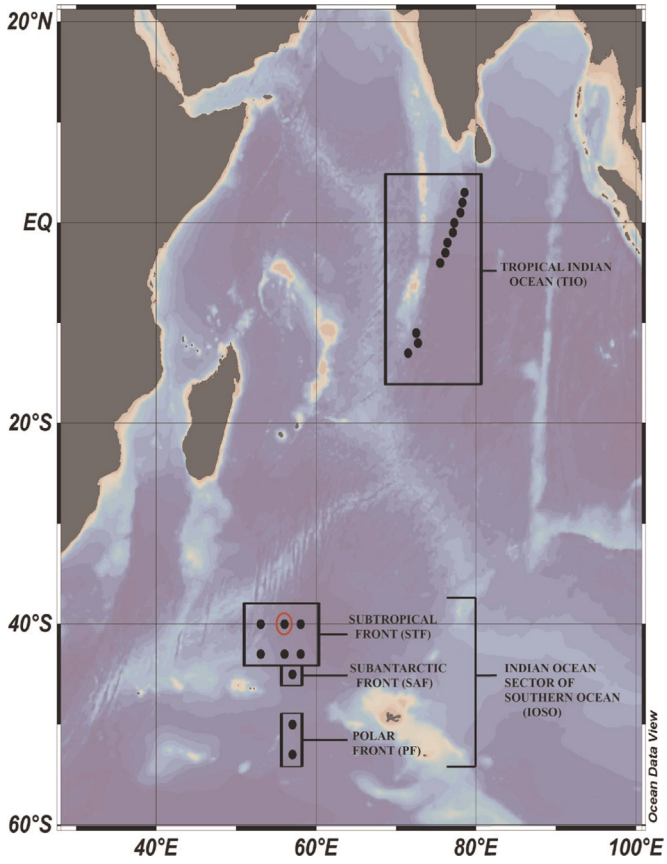

Fig. 1. Map showing the sampling stations during an expedition onboard ORV Sagar Nidhi in austral summer, 2012. Encircled station experienced a cold core eddy.

HPLC analysis was carried out following the method of Bidigare et al. (2002). According to the standard practice, chemotaxonomically similar marker pigments were grouped together and pigment indices were calculated (Bhaskar et al., 2011; Naik et al., 2011) following the method of Barlow et al. (2007).

Diagnostic pigment (DP) index was used to assess the community structure by confirming the significant relationship between DP and Chl *a* by ($r=0.871$, $n=15$, $p<0.0001$). Details of diagnostic pigment index used for this study are described elsewhere in this issue (Naik et al., 2015).

2.4. Total carbon dioxide (tCO_2)

For tCO_2 concentration in seawater, sub-samples were collected in 60 ml glass bottles and poisoned with 0.3 ml of saturated mercuric chloride. Twenty five milliliter of sample was transferred into a sample reaction vessel, acidified with 3 ml of 8.5% orthophosphoric acid and the gas was completely purged by bubbling. Gaseous CO_2 was trapped in a cell containing ethanolamine and photometrically back-titrated using a coulometer (Model 5015, U.I. C. Inc., USA).

Calibrations were carried out using a certified reference material (CRMs, Batch #104) supplied by A. Dickson (SIO, University of California, USA) and using preweighed and dried Na_2CO_3. During the calibration, water blanks were used for instrument baseline check. Similarly, acid blanks were deducted from all the sample analyses. Calibrations with Dickson standard were carried out regularly. The overall precision and accuracy of the analyses were ≤ 2 μM and 4 μM, respectively.

2.5. %C, %N, $\delta^{13}C$ and $\delta^{15}N$ of POM

Sub-samples for POM analyses were immediately transferred to acid-cleaned plastic carboys and filtered through 0.7 μm pore size precombusted (450 °C for 4 h) Whatman GF/F filters and the filters were stored at −20 °C until analysis. The filters were decalcified by exposing to fumes of HCl (35%) for 12 h in a desiccator, dried and packed tightly in tin cups for analysis of %C, %N and stable isotopic ratios ($\delta^{13}C_{(POM)}$ and $\delta^{15}N_{(POM)}$). $\delta^{13}C_{(POM)}$ and $\delta^{15}N_{(POM)}$ were measured using an Isoprime Stable Isotope Ratio Mass Spectrometer in continuous-flow mode coupled with an Elemental Analyzer (Isoprime, Vario Isotope Cube) (Owens and Rees, 1989) at the Marine Stable Isotope laboratory of National Centre for Antarctic and Ocean Research, Goa, India. The isotopic ratios expressed in per mil notation were calculated as follows:

$$\delta^{13}C \text{ or } \delta^{15}N\ (‰) = [(R(\text{sample})/R(\text{standard}) - 1] \times 1000,$$

where $R = {}^{15}N/{}^{14}N$ or ${}^{13}C/{}^{12}C$

$\delta^{13}C$ values are reported with respect to VPDB and $\delta^{15}N$ values are reported with respect to air-N_2. The reference standards used for normalising to VPDB and air-N_2 scale are cellulose (IAEA-CH-3) and ammonium sulphate (IAEA-N1), respectively. The external precisions for $\delta^{13}C$ and $\delta^{15}N$ are $\pm 0.05‰$ and $\pm 0.08‰$ (1σ standard deviation), respectively, and for %C and %N are $\pm 0.29\%$ and $\pm 0.35\%$ (1σ standard deviation), respectively, obtained by repeated measurements of IAEA-CH-3 & IAEA-N1 ($n=27$).

3. Results

3.1. Hydrography

The sea-surface temperature (SST) and salinity (SSS) within TIO exhibited less variability in comparison to IOSO. In TIO, SST ranged between 28.21 and 29.33 °C and SSS varied between 34.13 and 35.21. SSS values declined by 0.99 along the transect, mainly south of the equator. The mean and ranges for hydrographic parameters are presented in Table 1. In contrast, IOSO exhibited large-scale SST variations. The surface temperature within IOSO decreased from 19.25 to 3.79 °C (Fig. 2a) while SSS values decreased from 35.60 to 33.81. Zonally along 40°S, SST varied by 3.7 °C while SSS varied by ~1, with lower SST and SSS at 56.5°E. A similar decline in SST (~4 °C) and SSS (by ~1) was also observed along 43°S transect (Fig. 2b).

3.2. Nutrients, tCO_2 and Chl a

In TIO, surface nitrate concentration was low and ranged from 0.07 to 0.61 μM, whereas in the IOSO waters, nitrate was the lowest in STF (0.61 μM) and maximum in PF (23.35 μM) (Fig. 2c). The surface nitrate concentration increased by an order of magnitude between SAF and PF. Ammonium concentrations ranged from 1.49 to 2.13 μM in TIO and from 1.29 to 2.64 μM in IOSO (Table 1). The average N:P ratios were 2.01, 4.08, 3.19 and 8.97 in TIO, STF, SAF and PF, respectively (Table 1). The N:Si ratio was >1 in the entire study area, despite low nitrate. It was closer to 1 in TIO with an average of 1.34, while in IOSO average N:Si ratios varied from 3.71 to 5.44. Larger variations in N:Si ratios within IOSO were observed in the STF (1.46 to 12.14) compared to PF (3.04 to 6.57) (Table 1). The concentrations of tCO_2 increased from TIO to PF and ranged from 1905.88 μM to 2162.99 μM (Table 1). Within TIO, tCO_2 concentration did not show a specific trend as it first increased towards equator, then declined sharply across the equator followed by a sharp increase (Fig. 2d). In the IOSO waters, the tCO_2 concentrations showed a steady increase from 2026 μM in the STF to 2162.99 μM in the PF (Fig. 2d).

Table 1
Average values of SST (°C), salinity, tCO_2 (μM), NO_3 (μM), NH_3 (μM), N:P, N:Si (where $N = NO_3 + NO_2 + NH_3$), Chl *a*, %C, %N, C:N (w/w), POC:Chl *a* (w/w), $\delta^{13}C_{(POM)}$, $\delta^{15}N_{(POM)}$ and dominating phytoplankton community (% abundance) in surface samples along the cruise transect. Range is in parentheses.

Region	Latitude	SST (°C)	Salinity	tCO_2 (μM)	NO_3 (μM)	NH_3 (μM)	N:P	N:Si	Chl *a* (mg m^{-3})	% C	% N	C:N	POC:Chl *a*	$\delta^{13}C_{(POM)}$ (‰)	$\delta^{15}N_{(POM)}$ (‰)	Dominant phytoplankton community[a] (% abundance)
TIO	3°N–13°S	**28.65** (28.21–29.33)	**34.56** (34.13–35.21)	**1961.70** (1905.88–2045.92)	**0.28** (0.07–0.61)	**1.89** (1.49–2.13)	**2.01** (1.73–2.30)	**1.34** (1.11–1.80)	**0.47** (0.29–0.71)	**0.47** (0.22–0.72)	**0.07** (0.04–0.12)	**7.25** (4.44–10.85)	**79.49** (35.05–168.4)	**−26.28** (−26.82 to -25.52)	**−0.88** (−5.09 to 2.45)	**Prokaryotes (46%)**
STF	40–43°S	**15.44** (11.18–19.25)	**34.72** (33.81–35.60)	**2058.07** (2026–2099)	**5.24** (0.61–10.58)	**1.90** (1.29–2.30)	**4.08** (1.90–7.24)	**5.44** (1.46–12.14)	**0.46** (0.11–1.13)	**0.76** (0.39–1.14)	**0.15** (0.07–0.26)	**5.79** (3.25–12.71)	**156.74** (62.93–324.46)	**−22.81** (−24.55 to −21.40)	**2.05** (0.68 to 4.09)	**Flagellates (93%)**
SAF	45°S	**11.21**	**33.82**	**2069.39**	**2.73**	**1.82**	**3.19**	**3.71**	**0.81**	**0.25**	**0.06**	**4.17**	**38.97**	**−24.81**	**2.89**	**Diatoms (59%)**
PF	50–53°S	**4.26** (3.79–4.73)	**33.82** (33.81–33.84)	**2155.13** (2146.26–2162.99)	**23.18** (23.00–23.35)	**2.25** (1.85–2.64)	**8.97** (7.05–10.89)	**4.80** (3.04–6.57)	**0.48** (0.34–0.62)	**0.73** (0.56–0.86)	**0.14** (0.10–0.18)	**5.27** (4.94–5.60)	**106.34** (88.04–124.65)	**−25.82** (−25.99 to −25.65)	**0.29** (0.26 to 0.32)	

[a] Dominant phytoplankton community is based on diagnostic pigment index.

Chl *a* concentration in the surface water ranged from 0.11 to 1.13 mg m^{-3} in the study area and did not show any specific trend. The Chl *a* concentration remained < 0.75 mg m^{-3} in the TIO with a maximum of 0.71 mg m^{-3} at 4°S. In IOSO, higher concentrations of Chl *a* were observed at STF and SAF (Fig. 2e). The average Chl *a* concentration in TIO, STF and PF were 0.47, 0.46 and 0.48 mg m^{-3}, respectively (Table 1).

3.3. Characteristics of POM

%C of POM ranged from 0.22% to 1.14% in the entire study area. The average %C in the TIO waters was 0.47% and ranged from 0.22% to 0.72% (Table 1). %C was minimum at the equator and was higher on both sides of the equator (Fig. 3a). In IOSO, average %C of POM decreased from 0.76% in STF to 0.25% in SAF and again increased to 0.73% in PF (Table 1). Large scale zonal variation was observed at STF, ranging from 0.39% to 1.14%. The %C at SAF was lowest (0.25%) and increased thereafter to 0.86% in PF (Fig. 3a). The spatial variation of %N in the surface waters was similar to %C (Fig. 3b). In TIO, the values ranged from 0.04% to 0.12%, while in IOSO it ranged from 0.07% to 0.26% (Table 1). The average %N values of POM were maximum in STF (0.15%) and minimum in SAF (0.06%) (Table 1).

$\delta^{13}C_{(POM)}$ was lower in TIO with an average of −26.28‰ while in the IOSO waters, the average $\delta^{13}C_{(POM)}$ values ranged from −22.81‰ in STF to −25.82‰ in PF (Table 1). Within STF, $\delta^{13}C_{(POM)}$ varied from −24.55‰ to −21.40‰ with enrichment of heavier carbon in the eddy influenced station. In PF, the $\delta^{13}C_{(POM)}$ ranged from −25.99‰ to −25.65‰ (Fig. 3c). $\delta^{15}N_{(POM)}$ showed large variations in the study area ranging from −5.09‰ to 4.09‰. $\delta^{15}N_{(POM)}$ in TIO was lower, ranged from −5.09‰ to 2.45‰ and did not show any specific trend (Fig. 3d). In IOSO, $\delta^{15}N_{(POM)}$ was higher in STF (0.68‰ to 4.09‰) which decreased in PF (0.26‰ to 0.32%) (Table 1).

The average C:N ratio in the TIO surface waters was 7.25, which was higher than Redfield ratio of plankton (6.63), and showed a wide variation from 4.44 to 10.85 (Fig. 3e). In IOSO, the C:N ratios ranged from 3.25 to 12.71 while the average ratios ranged from 5.79 in STF to 5.27 in PF (Table 1). The POC:Chl *a* ratio ranged from 35.05 to 168.40 in TIO and from 38.97 to 324.46 in the IOSO with the maximal value in STF. The average POC:Chl *a* ratios varied from 156.74 in STF to 38.97 in SAF and 106.34 in PF.

3.4. Statistical analyses

In order to identify key factors influencing the POM characteristics and isotopic ratios, a simple Spearman's rank correlation was calculated using Excel software. In the absence of pH data, $[CO_2]_{aq}$ could not be calculated and hence all statistical analyses were carried out with tCO_2 as a representative. tCO_2 solubility in surface waters is controlled by SST as thermal fractionation of carbon isotopic signatures of tCO_2 and subsequent carbon fixation is reflected in $\delta^{13}C_{(POM)}$. $\delta^{13}C_{(POM)}$ had a positive correlation with SST ($r = 0.6815$; $p < 0.05$) and an inverse correlation with tCO_2 ($r = -0.7867$; $p < 0.005$) in IOSO (Fig. 4b and d) but insignificant correlations in TIO (Fig. 4a and c). In TIO, $\delta^{13}C_{(POM)}$ and %C showed a significant positive correlation ($r = 0.9199$; $p < 0.0001$) whereas in IOSO it was not significant (Fig. 4e and f). Availability of nutrients influences the carbon fixation process and fractionation of nitrogen isotopic signatures during nutrient uptake. $\delta^{13}C_{(POM)}$ ($r = -0.7504$; $p < 0.05$) (Fig. 4h) and $\delta^{15}N_{(POM)}$ ($r = -0.8687$; $p \leq 0.005$) (Fig. 5b) were inversely correlated with nitrate only in IOSO. tCO_2 showed an inverse correlation with SST ($r = 0.9010$; $p \leq 0.001$) (Fig. 6a) in IOSO, indicating greater solubility in colder waters. Although Chl *a* is used as an indicator of phytoplankton biomass, it is not the dominant representative pigment for all forms of phytoplankton groups including

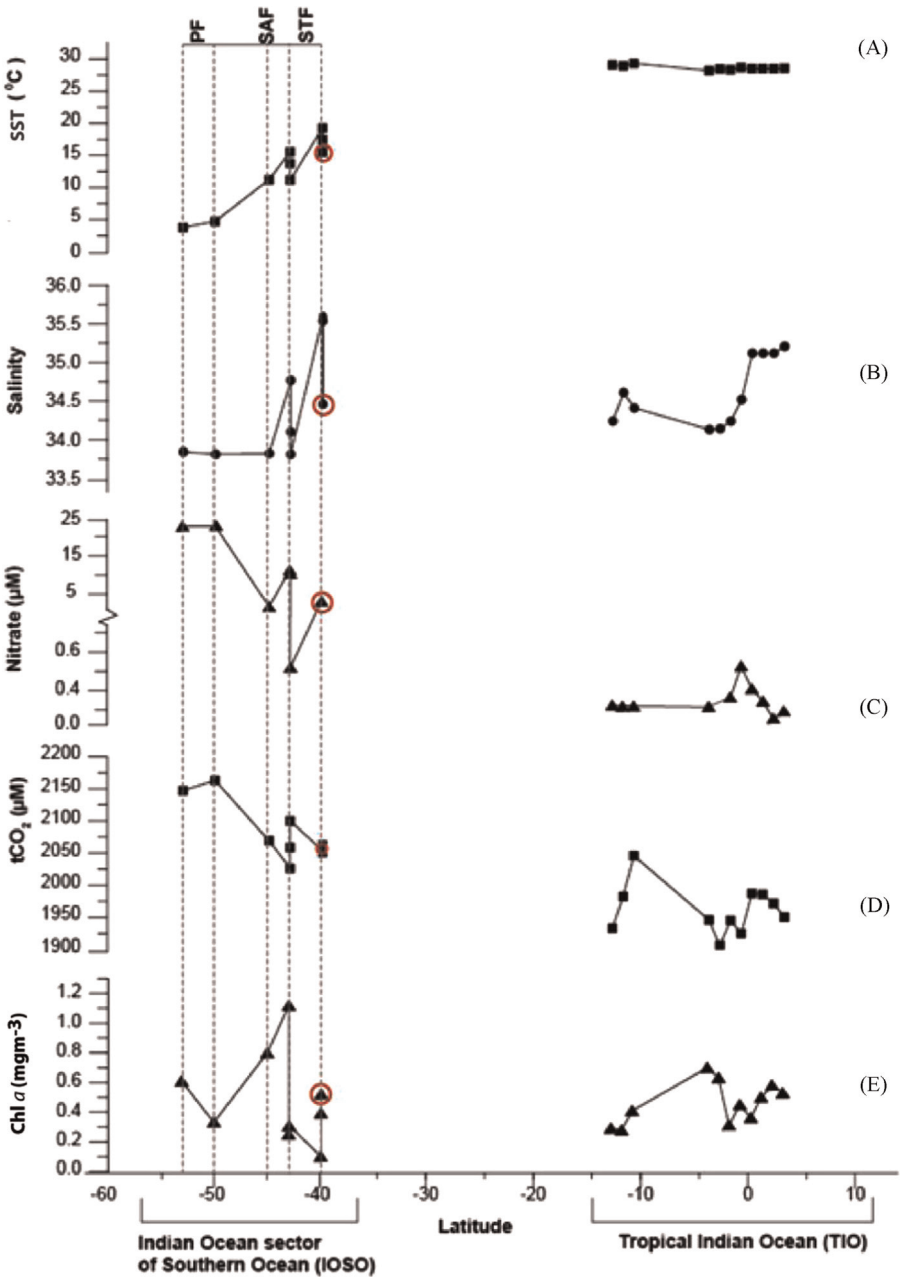

Fig. 2. Latitudinal variations of (a) temperature (°C), (b) salinity, (c) nitrate (μM), (d) tCO_2 (μM) and (e) chlorophyll *a* (mg m^{-3}) in surface waters of TIO and IOSO during 2012. Encircled station experienced a cold core eddy.

flagellates. This is also reflected in statistically insignificant correlations of Chl *a* concentrations with $\delta^{13}C_{(POM)}$ (Fig. 6b) and %C in IOSO. $\delta^{15}N_{(POM)}$ and %N showed a positive correlation only in TIO ($r=0.8357$; $p<0.0005$) (Fig. 7a). Both %C and %N showed a significant linear correlation ($r=0.7701$; $p<0.0001$) in the entire study area (Fig. 7b).

4. Discussion

4.1. TIO

The TIO waters were warm (avg. 28.65 °C) but showed slightly large variations in SSS (~1 psu). The decline in salinity is distinct immediately at the south of the equator, which may be due to increased localised precipitation associated with the presence of the Inter Tropical Convergence Zone (ITCZ) at the south of equator, as reported earlier (Tiwari et al., 2013). These waters were low in nitrate (Fig. 2c) and had moderate Chl *a* values (Fig. 2e). $\delta^{13}C_{(POM)}$ (−26.82‰ to −25.52‰) showed small scale spatial variations (Table 1) and weak correlations with SST and tCO_2 (Fig. 4a and c). Similar relation between $\delta^{13}C$ of marine plankton and SST has been reported in tropical waters (Degens et al., 1968; Fontugne and Duplessy, 1981). The observed weak correlation may be explained by the following reasons: (1) isotopic fractionation of carbon during photosynthesis and biosynthesis of organic molecules like proteins, lipids and carbohydrates are species specific and varies with cell size, cell physiology and growth rate and independent of thermal effect (Goericke and Fry, 1994; Popp et al., 1998); (2) microbial degradation of POM resulting in preferential removal of labile fraction (Eadie and Jeffrey, 1973), and accumulation of lipids in POM (Minagawa et al., 2001). In the sampling sites of TIO, prokaryotic picoplankton was dominant (Table 1). From the literature it is evident that picoplankton biomass is a

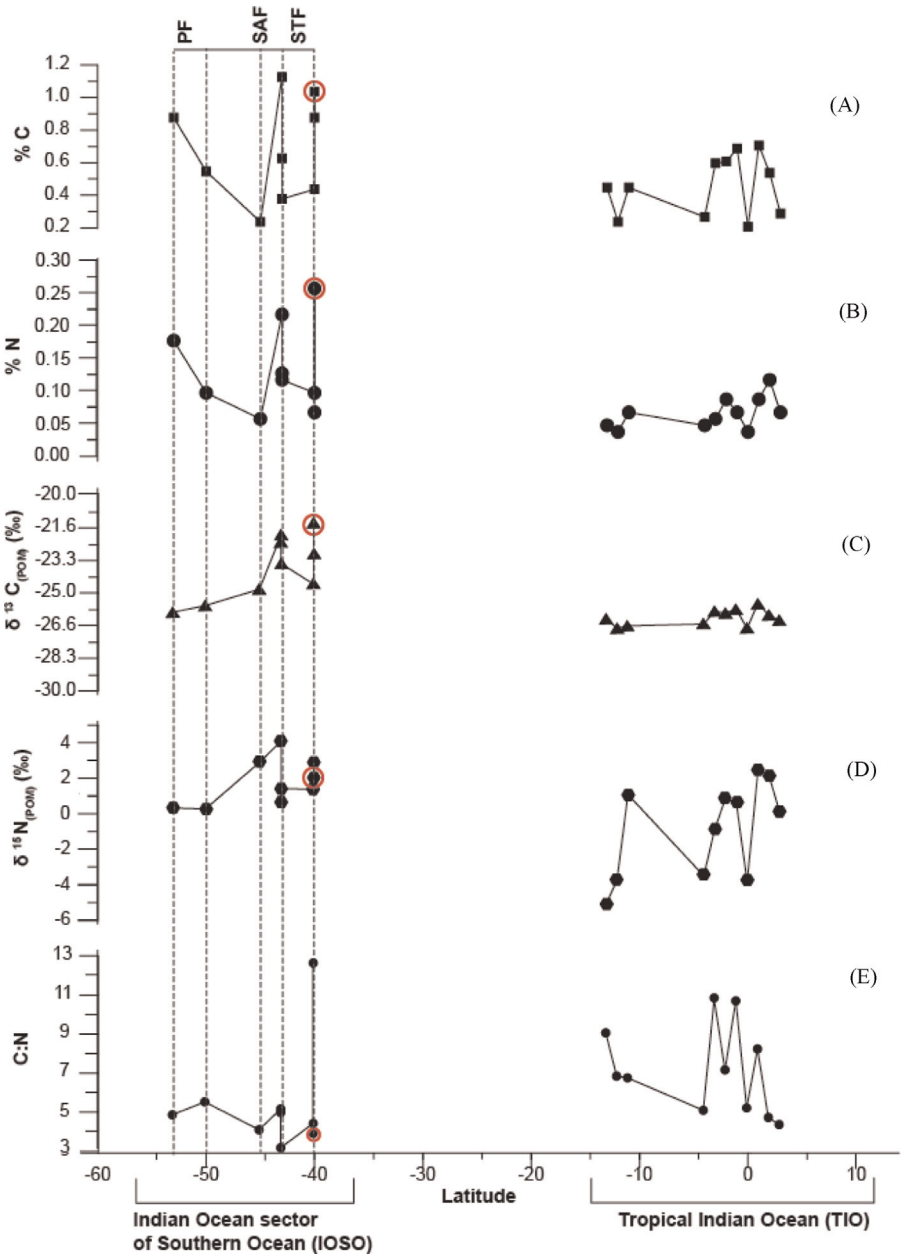

Fig. 3. Latitudinal variations of (a) %C, (b) %N, (c) $\delta^{13}C_{(POM)}$‰ (d) $\delta^{15}N_{(POM)}$‰ and (e) C:N (w/w) ratio of POM in surface waters of TIO and IOSO during 2012. Encircled station experienced a cold core eddy.

major contributor to the total biomass in warm waters with low nutrient concentration (NO_3+NO_2 <1 μM) (Agawin et al., 2000). In general, $\delta^{13}C$ of marine phytoplankton is in a range from -24‰ to -17.5‰ (Bidigare et al., 1999). In the present study, the average $\delta^{13}C_{(POM)}$ values in TIO were lower than those reported by Bidigare et al. (1999) and Fontugne and Duplessy (1981) but closer to the $\delta^{13}C$ values of picoplankton reported by Rau et al. (1990). Prokaryotic picoplankton are reported to have small isotope fractionation during carbon fixation (Popp et al., 1998) but preferentially incorporate lighter carbon molecules during lipid biosynthesis (Sakata et al., 1997). The microbial degradation of such POM may result in enrichment of lighter carbon due to accumulation of less labile residual lipid fraction in POM. Moreover, $\delta^{13}C_{(POM)}$ is an accumulated signal over time while both SST and tCO_2 are instantaneous values prevailing at the time of sampling.

The POC/Chl *a* ratio has been used as an indicator of phytoplankton derived fresh organic carbon and ratio <200 may indicate major contribution from phytoplankton derived organic matter (Bentaleb et al., 1998; Savoye, et al., 2003). The POC/Chl *a* ratios in TIO were generally <200 for the surface waters and showed moderate C:N ratios (<7), except for a few stations. Dominance of picoplankton in oligotrophic waters is an indicator of an active microbial loop as the major carbon pathway and heterotrophic bacteria are important contributors to the organic carbon pool (Azam et al., 1983; Marañón et al., 2003). Previous studies in the oligotrophic equatorial Indian Ocean have indicated greater contribution of heterotrophic bacterial production to the biological production (Fernandes et al., 2008; Ramaiah et al., 2009). Selective mineralisation of POM resulting in preferential removal of nitrogen rich compounds by heterotrophic bacteria is fairly well-known in marine environments (Eadie and Jeffrey, 1973; Harvey et al., 1995; Kolasinski et al., 2012). The greater bacterial productivity in TIO coupled with selective N-removal

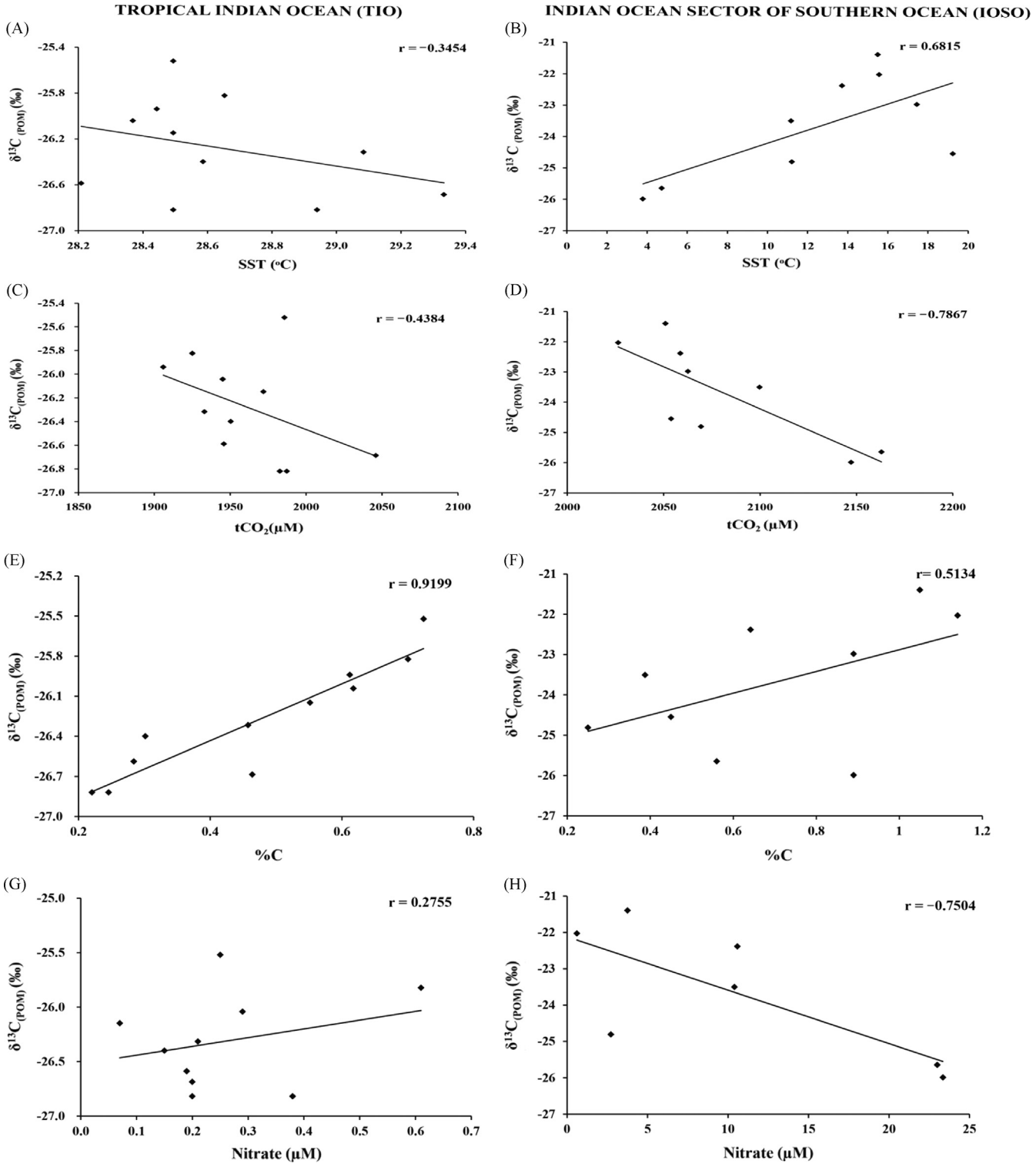

Fig. 4. Spearman's rank correlation analysis of $\delta^{13}C_{(POM)}$ with (a, b) SST (°C) and (c, d) tCO_2 (μM) in surface waters of TIO and IOSO during austral summer, 2012.

may be responsible for the higher C:N ratio (> 7) in the equatorial waters.

$\delta^{15}N_{(POM)}$ in TIO showed large scale variations (−5.09‰ to 2.45‰) (Fig. 3d). $\delta^{15}N_{(POM)}$ did not correlate with nitrate concentrations (Fig. 5a), and had a significant correlation with %N (Fig. 7a). The $\delta^{15}N_{(POM)}$ in TIO was significantly lower than those of marine organic matter (3‰ to 12‰)(Wada and Hattori, 1991; Maksymowska et al., 2000). However, it was apparently in the range (−4‰ to −5‰) observed by Altabet and Francois (2001) and (−3‰ to +7‰) reported by Lourey et al. (2003), in the Southern Ocean region. The extremely low $\delta^{15}N_{(POM)}$ at some stations in TIO could be attributed to the uptake of ^{14}N enriched ammonium (Altabet, 1988; Waser et al., 1999) by picoplankton in low nitrate waters. The $\delta^{15}N_{(POM)}$ values closer to zero was attributed to nitrogen fixation (Saino and Hattori, 1987) and early diagenesis (Chen et al., 2008). On the other hand, the ability of picoplankton to take up varied nitrogen species, from nitrate to dissolved organic nitrogen (Zubkov et al., 2003,Gracía-Fernández

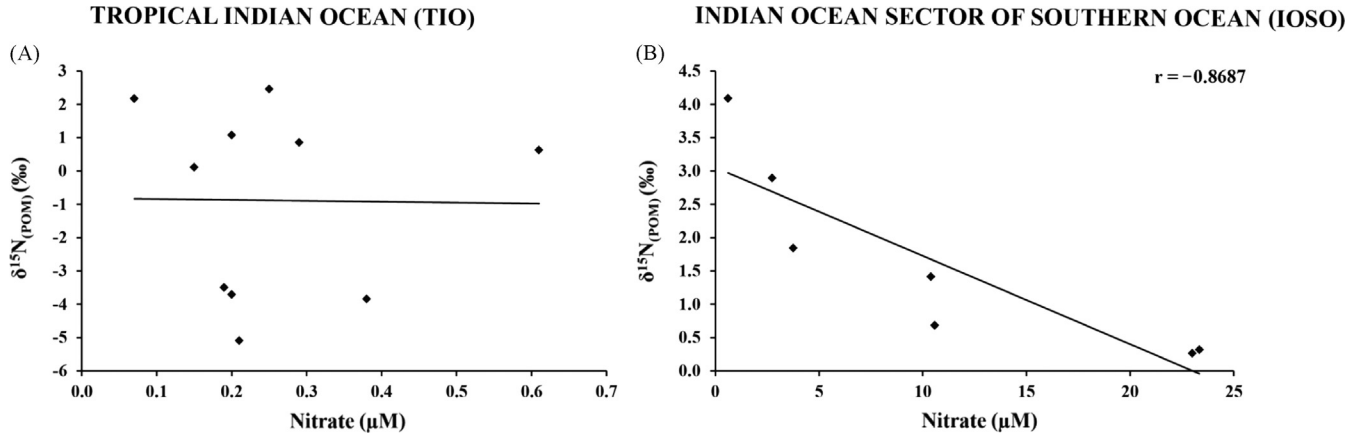

Fig. 5. Spearman's rank correlation of $\delta^{15}N_{(POM)}$ with nitrate in surface waters of (a) TIO and (b) IOSO during austral summer, 2012.

et al., 2004),) may explain higher $\delta^{15}N_{(POM)}$ values in TIO. However, the processes that might be influencing the wide variation of $\delta^{15}N_{(POM)}$ in these waters were not clearly explained.

4.2. IOSO

A general trend with a southward lowering of $\delta^{13}C_{(POM)}$ was observed from 40°S onwards, as observed in most of the high latitude regions. The decrease in temperature along with the prevalence of high wind speed in IOSO favours greater wind driven mixing, thereby increasing the concentration of tCO_2 with low $\delta^{13}C$ in surface waters. The incorporation of isotopically lighter CO_2 by phytoplankton results in low $\delta^{13}C_{(POM)}$ in surface waters (Fontugne and Duplessy, 1981; Rau et al., 1992; Goericke and Fry, 1994; Gruber et al., 1999). This is reflected in the linear positive correlation of $\delta^{13}C_{(POM)}$ with SST (Fig. 4b) and a negative relation with tCO_2 (Fig. 4d). The isotopic values observed in IOSO are comparable to those observed elsewhere in the South Pacific (−27.89‰ to −24.47‰), the Arctic (−28.5‰ to −21.1‰) and the Prydz bay, Antarctica (−27.4‰ to −19.0‰) (Kennedy and Robertson, 1995; Zhang et al., 2011, 2014).

The STF waters experienced high wind speed and eddies during the study period. Previous studies by Kolasinski et al. (2012) in eddy prone Mozambique channel have observed heavier $\delta^{13}C_{(POM)}$ and $\delta^{15}N_{(POM)}$ within the eddy, and have attributed it to uptake of deep water nitrate brought up due to upwelling combined with a shift in phytoplankton community to large diatoms. Although, in the present study the lowest C:N ratio (Fig. 3e) in the subtropical region coincided with high $\delta^{13}C_{(POM)}$ (Fig. 3c) in the eddy influenced station (40°S, 56.3°E) (Fig. S1, supplementary data), the $\delta^{15}N_{(POM)}$ values (Fig. 3d) did not match the typical $\delta^{15}N$ of nitrate from deep waters or new production. This may be because the eddy was a long standing eddy (Fig. S2, supplementary data), and the phytoplankton biomass (Chl *a*) was highly variable in STF and dominated by flagellates (Table 1). Flagellates, especially dinoflagellates, are known to have assimilatory enzymes like phosphoenolpyruvate carboxylase and phosphoenolpyruvate carboxykinase that result in less isotopic discrimination during carbon uptake, thereby making the $\delta^{13}C_{(POM)}$ heavier (Bentaleb et al., 1996, 1998; Gaul et al., 1999; Lara et al., 2010). The lack of statistically significant correlation between $\delta^{13}C_{(POM)}$ and Chl *a* (Fig. 6b) may be due to the dominance of flagellates in these waters. In STF, POM was enriched in ^{13}C, coinciding with low C:N ratio except at one station (40°S, 58.5°E), where mesozooplankton biomass was high and dominated by copepods. The predominance of flagellates in STF coupled with SST appeared to play an important role in influencing $\delta^{13}C_{(POM)}$.

The surface waters in PF were highlighted by typically high nutrient low chlorophyll (HNLC) conditions, wherein increased availability of nitrate did not match observed phytoplankton biomass (Chl *a*). The N:Si ratio <1 generally favours the dominance of diatoms. Although the N:Si ratio was >1, silicate concentration was never limiting and in fact favoured the growth of diatoms in these waters, which was evident from diagnostic pigment study (Table 1). The average C:N ratio of POM was slightly lower than Redfield ratio of plankton. The low POC:Chl *a* ratio also indicate the existence of fresh organic matter and the prevalence of autotrophy (Bentaleb et al., 1998; Savoye et al., 2003).

In IOSO, $\delta^{13}C_{(POM)}$ had a positive correlation with %C (Fig. 4f) which may indicate the role of biology in the isotopic fractionation

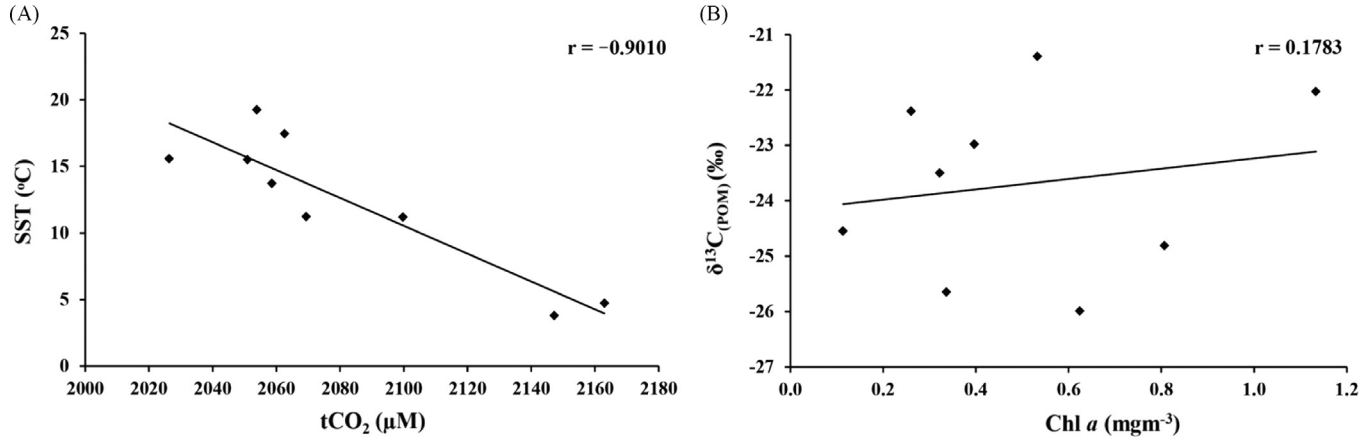

Fig. 6. Spearman's rank correlation of (a) SST (°C) with tCO_2 (μM) and (b) $\delta^{13}C_{(POM)}$ with Chl *a* (mg m^{-3}) in surface waters of IOSO during austral summer, 2012.

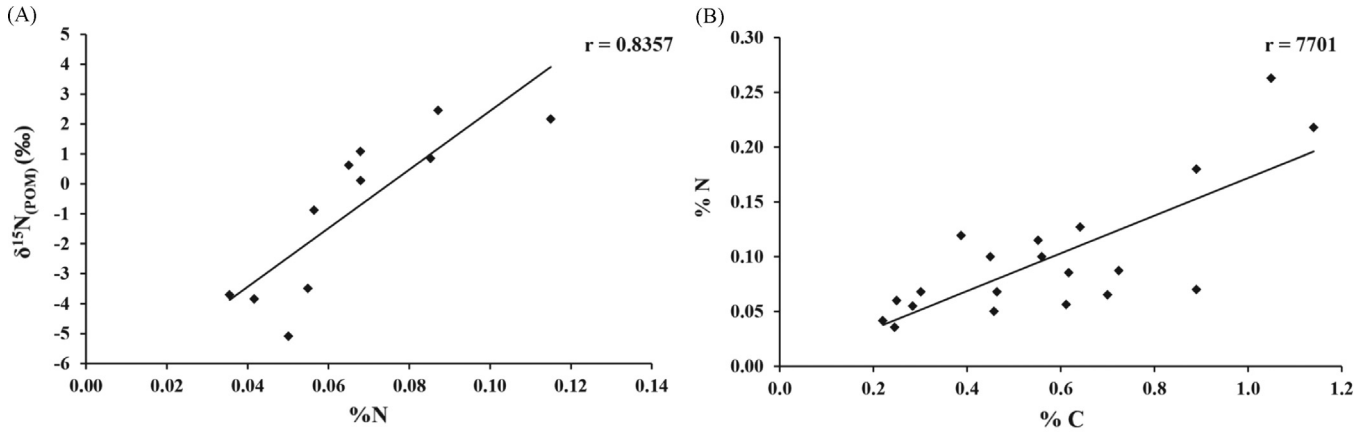

Fig. 7. Spearman's rank correlation of (a) $\delta^{15}N_{(POM)}$ with %N in surface waters of TIO and (b) %C with %N of POM in surface waters at all the sampling sites.

as suggested by Eadie and Jeffrey (1973) and Zhang et al. (2014). The low $\delta^{13}C_{(POM)}$ (Fig. 4d) observed in IOSO may be due to increased availability and uptake of isotopically lighter tCO_2 (Popp et al., 1989; Lourey et al., 2004) by phytoplankton. An inverse relation between nitrate and $\delta^{15}N_{(POM)}$ (Fig. 5b) may be due to a preferential uptake of lighter nitrogen species by phytoplankton in nitrate replete waters (Wada and Hattori, 1978; Wada, 1980; Checkley and Miller, 1989; Mino et al., 2002).

5. Conclusions

In this study, the importance of different phytoplankton community in shaping the isotopic signatures of POM in two different oceanic regimes was evident. In the warm oligotrophic tropical surface waters, small scale depletion in $\delta^{13}C_{(POM)}$ and a wide range of $\delta^{15}N_{(POM)}$ was explained by the dominance of picophytoplankton. The role of heterotrophy in sustaining the picoplankton biomass was however, not clear. Unlike TIO, physical factors including SST and eddies play a major role in determining the isotopic characteristics of POM in IOSO. Higher $\delta^{15}N_{(POM)}$ in waters influenced by a cold core eddy in STF do not indicate new production but the dominance of flagellates in those waters influenced the $\delta^{13}C_{(POM)}$, which may be due to their non-discriminative uptake of C and N. The increasing availability of nutrients favours the growth of diatoms beyond 50°S. As a result, enhanced photosynthetic isotopic fractionation may result in depletion of $\delta^{13}C$ and $\delta^{15}N$ in polar waters. However, the role of grazers and microbial degradation in influencing the isotopic signatures of POM could not be addressed in this study.

Acknowledgments

The authors would like to acknowledge Director, NCAOR for his continued support of the Indian Southern Ocean Program. The authors sincerely acknowledge Dr. C.T. Achuthankutty, expedition leader of ISOE-2012, for his support and leadership during the expedition. We also express our sincere thanks to the Ministry of Earth Sciences for funding this program. The authors also acknowledge Mr. Siddesh Nagoji, for carrying out IRMS analysis in at NCAOR. Manish Tiwari thanks ISRO-GBP for financial support. Our sincere acknowledgement to Capt. S. Williams and his crew onboard ORV Sagar Nidhi for ensuring proper sampling under Southern Ocean conditions. This is NCAOR's contribution number 23/2015.

Appendix A. Supplementary material

Supplementary data associated with this article can be found in the online version at http://dx.doi.org/10.1016/j.dsr2.2015.06.009.

References

Agawin, N.S.R., Duarte, C.M., Agustí, S., 2000. Nutrient and temperature control of the contribution of picoplankton to phytoplankton biomass and production. Limnol. Oceanogr. 45 (3), 591–600.
Altabet, M.A., 1988. Variations in nitrogen isotopic composition between sinking and suspended particles: Implications for nitrogen cycling and particle transformations in the open ocean. Deep-Sea Res. I 35, 535–554.
Altabet, M.A., Francois, R., 2001. Nitrogen isotope biogeochemistry of the Antarctic Polar Frontal Zone at 170W. Deep-Sea Res. II 48, 4247–4273.
Anilkumar, N., Luis Alvarinho, J., Somayaluju, Y.K., Ramesh Babu, V., Dash, M.K., Pednekar, S.M., Babu, K.N., Sudhakar, M., Pandey, P.C., 2006. Fronts, water masses and heat content variability in the Western Indian sector of the Southern Ocean during austral summer 2004. J. Mar. Syst. 63 (1–2), 20–34.
Azam, F., Fenchel, T., Field, J.G., Gray, J.S., Meyer-Reil, L.A., Thingstad, F., 1983. The ecological role of water-column microbes in the sea. Mar. Ecol. Prog. Ser. 10, 257–263.
Barlow, R., Stuart, V., Lutz, V., Sessions, H., Sathyendranath, S., Platt, T., Kyewalyanga, M., Clementson, L., Fukasawa, M., Watanabe, S., Devred, E., 2007. Seasonal pigment patterns of surface phytoplankton in the subtrophical southern hemisphere. Deep-Sea Res. I 54 (10), 1687–1703.
Belkin, I.M., Gordon, A.L., 1996. Southern Ocean fronts from the Greenwich Meridian to Tasmania. J. Geophys. Res. 101, 3675–3696.
Bentaleb, I., Fontugne, M., Descolas-Gros, C., Girardin, C., Mariotti, A., Pierre, C., Brunet, C., Poisson, A., 1996. Organic carbon isotopic composition of phytoplankton and sea-surface pCO_2 reconstructions in the Southern Indian Ocean during the last 50,000 yr. Org. Geochem. 24, 399–410.
Bentaleb, I., Fontugne, M., Descolas-Gros, C., Girardin, C., Mariotti, A., Pierre, C., Brunet, C., Poisson, A., 1998. Carbon isotopic fractionation by plankton in the Southern Indian Ocean: relation between $\delta^{13}C$ of particulate organic carbon and dissolved carbon dioxide. J. Mar. Syst. 17, 39–58.
Bhaskar, P.V., Roy, R., Gauns, M., Shenoy, D.M., Rao, V.D., Mochemadkar, S., 2011. Identification of non-indigenous phytoplankton species dominated bloom off Goa using inverted microscopy and pigment (HPLC) analysis. J. Earth Syst. Sci. 120 (6), 1145–1154.
Bidigare, R.R., van Heukelem, L., Trees, C.C., 2002. HPLC phytoplankton pigments: sampling, laboratory methods and quality assurance procedure. In: Mueller, J., Fragion, G. (Eds.), Ocean Optics Protocols for Satellite Ocean Color Sensor 3, 2002, NASA Technical Memorandum 2002-210004. Greenbelt, Maryland, pp. 258–268.
Bidigare, R.R., Hanson, K.L., Buesseler, K.O., Wakeham, S.G., Freeman, K.H., Pancost, R.D., Millero, F.J., Steinberg, P., Popp, B.N., Latasa, M., Landry, M.R., Laws, E.A., 1999. Iron-stimulated changes in ^{13}C fractionation and export by equatorial Pacific phytoplankton: toward a paleogrowth rate proxy. Paleoceanography 12 (5), 589–595.
Bidigare, R.R., Fluegge, A., Freeman, K.H., Hanson, K.L., Hayes, J.M., Hollander, D., Jasper, J.P., King, L.L., Laws, E.A., Milder, J., Millero, F.J., Pancost, R., Popp, B.N., Steinberg, P.A., Wakeham, S.G., 1997. Consistent fractionation of ^{13}C in nature and in the laboratory: growth-rate effects in some haptophyte algae. Glob. Biogeochem. Cycle 11, 279–292.
Burkill, P.H., Mantoura, R.C.F., Owens, N.J.P., 1993. Biogeochemical cycling in the northwestern Indian Ocean: a brief overview. Deep-Sea Res. II 40 (3), 643–649.
Checkley, D.M., Miller, C.A., 1989. Nitrogen isotope fractionation by oceanic Zooplankton. Deep-Sea Res. A36, 1449–1456.

Chen, F., Zhang, L., Yang, Y., Zhang, D., 2008. Chemical and isotopic alteration of organic matter during early diagenesis: evidence from the coastal area offshore the Pearl River estuary, South China. J. Mar. Syst. 74, 372–380.
Deacon, G.E.R., 1933. A general account of the hydrology of the Southern Atlantic Ocean. Discov. Rep. 7, 171–238.
Degens, E.T., Behrendt, M., Gotthart, B., Reppmann, E., 1968. Metabolic fractionation of carbon isotopes in marine plankton II. Data on samples collected off the coasts off Peru and Ecuador. Deep-Sea Res. 15, 11–20.
Druffel, E.R.M., Griffin, S., Bauer, J.E., Wolgast, D., Wang, X., 1996. Distribution of particulate organic carbon and radiocarbon in the water column from the upper slope of the abyssal NE Pacific Ocean. Deep-Sea Res. II 45, 667–687.
Duforet-Gaurier, L., Loisel, L., Dessailly, D., Nordkvist, K., Alvain, S., 2010. Estimates of particulate organic carbon over the euphotic depth from in situ measurements application to satellite data over the Global Ocean. Deep-Sea Res. I 57, 351–367.
Eadie, B.J., Jeffrey, L.M., 1973. ^{13}C analyses of ocean particulate organic matter. Mar. Chem. 1, 199–209.
Fernandes, V., Rodrigues, N., Ramaiah, N., Paul, J.T., 2008. Relevence of Bacterioplankton abundance and production in the oligotrophic equatorial Indian Ocean. Aquat. Ecol. 42, 511–519.
Fontugne, M.R., Duplessy, J.C., 1981. Organic carbon isotopic fractionation by marine plankton in the temperature range −1 to 31 °C. Oceanol. Acta 4 (1), 85–90.
Francois, R., Altabet, M.A., Goericke, R., McCorkle, D.C., Brunet, C., Poisson, A., 1993. Changes in the $\delta^{13}C$ of surface water particulate organic matter across the subtropical convergence in the SW Indian Ocean. Glob. Biogeochem. Cycle 7 (3), 627–644.
Gaul, W., Anita, N.A., Koeve, W., 1999. Microzooplankton grazing and nitrogen supply of phytoplankton growth in the temperate and subtropical North east Atlantic. Mar. Ecol. Prog. Ser. 189, 93–104.
George, J.V., Nuncio, M., Chacko, R., Anilkumar, N., Noronha, S.B., Patil, S.M., Pavithran, S., Alappattu, D.P., Krishnan, K.P., Achuthankutty, C.T., 2013. Role of physical processes in chlorophyll distribution in the western tropical Indian Ocean. J. Mar. Syst. 113–114, 1–12.
Goericke, R., Fry, B., 1994. Variations of marine plankton $\delta^{13}C$ with latitude, temperature, and dissolved CO_2 in the world Ocean. Glob. Biogeochem. Cycle 8, 85–90.
Gordon, E.S., Goñi, M.A., 2003. Source and distribution of terrigenous organic matter delivered by the Atchafalaya River to sediments in the northern Gulf of Mexico. Geochim. Cosmochim. Acta 67, 2359–2375.
Gracía-Fernández, J.M., de Marsa, N.T., Diez, J., 2004. Streamlined regulation and gene loss as adaptive mechanisms in Prochlorococcus for optimised nitrogen utilization in oligotrophic environments. Microbiol. Mol. Biol. Rev. 68 (4), 630–638.
Grasshoff, K., Ehrhardt, M., Kremling, K., 1983. Methods of Seawater Analysis, 2nd eds. Verlag Chemie, Weinheim, Germany.
Gruber, N., Keeling, C.D., Bacastow, R.B., Guenther, P.R., Lueker, T.J., Wahlen, M., Meijer, H.A.J., Mook, W.G., Stocker, F.T., 1999. Spatiotemporal patterns of carbon-13 in the global surface oceans and the oceanic Suess effect. Glob. Biogeochem. Cycle 13 (2), 307–335.
Harvey, H.R., Tuttle, J.H., Bell, J.T., 1995. Kinetics of phytoplankton decay during simulated sedimentation-changes in biochemical composition and microbial activity under oxic and anoxic conditions. Geochim. Cosmochim. Acta 59, 3367–3377.
Hayes, J.M., 1993. Factors controlling ^{13}C contents of sedimentary organic compounds: principles and evidence. Mar. Geol. 113, 111–125.
Hedges, J.I., 1992. Global Biogeochemical Cycles: progress and problems. Mar. Chem. 39, 67–93.
Hedges, J.I., Keil, R.G., 1995. Sedimentary organic matter preservation: an assessment and speculative synthesis. Mar. Chem. 49, 81–115.
Holliday, N.P., Read, J.F., 1998. Surface oceanic fronts between Africa and Antarctica. Deep-Sea Res. I 45, 217–238.
Honjo, S., Manganini, S.L., Krishfield, R.A., Francois, R., 2008. Particulate organic carbon fluxes to the ocean interior and factors controlling the biological pump: a synthesis of global sediment trap programs since 1983. Prog. Oceanogr. 76, 217–285.
Jasmine, P., Muraleedharan, K.R., Madhu, N.V., Asha Devi, C.R., Alagarsamy, R., Achuthankutty, C.T., Jayan, Z., Sanjeevan, V.N., Sahayak, S., 2009. Hydrographic and production characteristics along 45°E longitude in the southwestern Indian Ocean and Southern Ocean during austral summer 2004. Mar. Ecol. Prog. Ser. 389, 97–116.
Jena, B., Sahu, S., Avinash, K., Swain, D., 2013. Observation of oligotrophic gyre variability in the south Indian Ocean: environmental forcing and biological response. Deep-Sea Res. I 80, 1–10.
Kaehler, S., Pakhomov, E.A., Mcquaid, C.D., 2000. Tropical structure of the marine food web at the Prince Edward Islands (Southern Ocean) determined by $\delta^{13}C$ and $\delta^{15}N$ analysis. Mar. Ecol. Prog. Ser. 208, 13–20.
Kennedy, H., Robertson, J., 1995. Variations in the isotopic composition of particulate organic carbon in surface waters along an 88W transect from 67°S to 54°S. Deep-Sea Res. II 42, 1109–1122.
Kolasinski, J., Kaehler, S., Jaquemet, S., 2012. Distribution and sources of particulate organic matter in a mesoscale eddy dipole in the Mozambique Channel (Southwestern Indian Ocean): insites of C and N stable isotopes. J. Mar. Syst. 96–97, 122–131.
Lara, R.J., Alder, V., Franzosi, C.A., Kattner, G., 2010. Characteristics of suspended particulate organic matter in the southwestern Atlantic: influence of temperature, nutrient and phytoplankton features on the stable isotope signature. J. Mar. Syst. 79, 199–209.
Laws, E.A., Popp, B.N., Bidigare, R.R., Kennicutt, M.C., Macko, S.A., 1995. Dependence of phytoplankton carbon isotopic composition on growth rate and [CO2]aq: theoretical considerations and experimental results. Geochim. Cosmochim. Acta 59 (6), 1131–1138.
Lourey, M.J., Trull, T.W., Sigman, D.M., 2003. Sensitivity of $\delta^{15}N$ of nitrate, surface suspended and deep sinking particulate nitrogen to seasonal nitrate depletion in the Southern Ocean. Glob. Biogeochem. Cycle 17 (3), 1081. http://dx.doi.org/10.1029/2002GB001973.
Lourey, M.J., Trull, T.W., Tilbrook, B., 2004. Sensitivity of $\delta^{13}C$ of Southern Ocean suspended and sinking organic matter to temperature, nutrient utilization, and atmospheric CO_2. Deep-Sea Res. I 51 (2), 281–305.
Maksymowska, D., Richard, P., Piekarek-Jankowska, H., Riera, P., 2000. Chemical and isotopic composition of the organic matter sources in the Gulf of Gdansk (southern Baltic Sea). Estuar. Coast. Shelf Sci. 51, 585–598.
Marañón, E., Beherenfeld, M.J., González, N., Mouriño, B., Zubkov, M.V., 2003. High variability of primary production in oligotrophic waters of the Atlantic Ocean: uncoupling from phytoplankton biomass and size structure. Mar. Ecol. Prog. Ser. 257, 1–11.
Minagawa, M., Ohashi, M., Kuramoto, T., 2001. $\delta^{15}N$ of PON and nitrate as a clue to the origin and transformation of nitrogen in the subarctic North Pacific and its marginal sea. J. Oceanogr. 57, 285–300.
Mino, Y., Saino, T., Suzuki, K., Marañón, E., 2002. Isotopic composition of suspended particulate nitrogen ($\delta^{15}N$sus) in surface waters of the Atlantic Ocean from 50°N to 50°S. Glob. Biogeochem. Cycle 16 (4), 7–9.
Mopper, K., Degens, E.T., 1978. Organic carbon in the ocean: nature and cycling In: Bolin, B., Degens, E.T., Kempe, S., Ketner, P. (Eds.), The Global Carbon Cycle. SCOPE XIII. John Wiley & Sons, New York, pp. 293–316.
Naik, R.K., Anil, A.C., Narale, D.D., Chitari, R.R., Kulkarni, V.V., 2011. Primary description of surface water phytoplankton pigment patterns in the Bay of Bengal. J. Sea Res. 65 (4), 435–441.
Naik, R.K., George, J.V., Soares, M.A., Devi, Asha, Anilkumar, N., Roy, R., Bhaskar, P.V., Murukkesh, N., Achuthankutty, C.T., 2015. Phytoplankton community structure at the juncture of the Agulhas Return Front and Subtropical Front in the Indian Ocean sector of Southern Ocean: bottom-up and top-down control. Deep-Sea Res. II . http://dx.doi.org/10.1016/j.dsr2.2015.01.002i.
Orsi, A.H., Whitworth, T., Nowlin, W.D., 1995. On the meridional extent and fronts of the Antarctic Circumpolar Current. Deep-Sea Res. 42 (5), 641–673.
Owens, N.J.P., Rees, A.P., 1989. Determination of N-15 at sub-microgram levels of nitrogen using automated continuous-flow isotope ratio mass-spectrometry. Analyst 114, 1655–1657.
Parsons, T.R., 1963. Suspended organic matter in sea water. Prog. Oceanogr. 1, 205–239.
Popp, B.N., Takigiku, R., Hayes, J.M., Louda, J.W., Baker, E.W., 1989. The post-Paleozoic chronology and mechanism of ^{13}C depletion in primary marine organic matter. Am. J. Sci. 289 (4), 436–454.
Popp, B.N., Laws, E.A., Bidigare, R.R., Dore, J.E., Hanson, K.L., Wakeham, S.G., 1998. Effect of phytoplankton cell geometry on carbon isotopic fractionation. Geochim. Cosmochim. Acta 62 (1), 69–77.
Prasanna Kumar, S., Narvekar, J., 2005. Seasonal variability of the mixed layer in the central Arabian Sea and its implication on nutrients and primary productivity. Deep-Sea Res. II 52, 1848–1861.
Ramaiah, N., Fernandes, V., Rodrigues, V.V., Paul, J.T., Gauns, M., 2009. Bacterioplankton abundance and production in Indian Ocean Regions. Indian Ocean biogeochemical processes and ecological variability, AGU Geophys. Monogr. Ser. 185, 119–132. http://dx.doi.org/10.1029/2008GM000711.
Rau, G.H., Teyssie, J.L., Rassoulzadegan, F., Fowler, S., 1990. $^{13}C/^{12}C$ and $^{15}N/^{14}N$ variations among size-fractionated marine particles: implications for their origin and trophic relationships. Mar. Ecol. Prog. Ser. 59, 33–38.
Rau, G.H., Takahashi, T., Marais, D.J.D., Repeta, D.J., Martin, J.H., 1992. The relationship between $\delta^{13}C$ of organic matter and $[CO_2(aq)]$ in ocean surface water: data from a JGOFS site in the northeast Atlantic Ocean and a model. Geochim. Cosmochim. Acta 56 (3), 1413–1419.
Raymond, P.A., Bauer, J.E., 2001. Use of ^{14}C and ^{13}C natural abundances for evaluating riverine, estuarine and coastal DOC and POC sources and cycling: a review and synthesis. Org. Geochem. 32, 469–485.
Saino, T., Hattori, A., 1987. Geographical variation of the water column distribution of suspended particulate organic nitrogen and its ^{15}N natural abundance in the Pacific and its marginal seas. Deep-Sea Res. A34, 807–827.
Sakata, S., Hayes, J.M., McTaggart, A.R., Evans, R.A., Leckrone, K.J., Togasaki, R.K., 1997. Carbon isotopic fractionation associated with lipid biosynthesis by a cyanobacterium: relevance for interpretation of bio-marker records. Geochim. Cosmochim. Acta 61, 5379–5389.
Sardessai, S., Shetye, S., Maya, M.V., Mangala, K.R., Prasanna Kumar, S., 2010. Nutrient characteristics of water masses and their seasonal variability in the eastern equatorial Indian Ocean. Mar. Environ. Res. 70 (3–4), 272–282.
Savoye, N., Aminot, A., Treguer, P., Fontugne, M., Naulet, N., Kerouel, R., 2003. Dynamics of particulate organic matter $\delta^{15}N$ and $\delta^{13}C$ during spring phytoplankton blooms in a macrotidal ecosystem (Bay of Seine, France). Mar. Ecol. Prog. Ser 255, 27–41.
Tiwari, M., Nagoji, S., Kartik, T., Drishya, G., Parvathy, R.K., Rajan, S., 2013. Oxygen isotope-salinity relationships of discrete oceanic regions from India to Antarctica vis-à-vis surface hydrology processes. J. Mar. Syst. 113–114, 88–93.
Valkman, J.K., Tanoue, E., 2002. Chemical and biological studies of particulate organic matter in ocean. J. Oceanogr. 58, 265–279.

Wada, E., 1980. Nitrogen isotope fractionation and its significance in biogeochemical processes occurring in marine environments In: Goldberg, E.D., Horibe, Y., Saruhashi, K. (Eds.), Isotope Marine Chemistry. Uchida Rokahuko Publishing Company, Tokyo, pp. 375–398.
Wada, E., Hattori, A., 1978. Nitrogen isotope effects in the assimilation of inorganic nitrogenous compounds by marine diatoms. Geomicrobiol. J. 1, 85–101.
Wada, E., Hattori, A., 1991. Nitrogen in the Sea: Forms, Abundances, and Rate Processes. CRC Press, Boca Raton, FL, pp. 208–212.
Wada, E., Terasaki, M., Kabaya, Y., Nemoto, T., 1987. ^{15}N and ^{13}C abundances in the Antarctic Ocean with emphasis on biogeochemical structure of food web. Deep-Sea Res. I 34, 829–841.
Waite, A.M., Muhling, B.A., Holl, C.M., Beckley, L.E., Montoya, J.P., Strzelecki, J., Thompson, P.S., Presant, S., 2007. Food web structure in two counter-rotating eddies based on $\delta^{15}N$ and $\delta^{13}C$ isotopic analysis. Deep-Sea Res. II 54, 1055–1075.
Waser, N.A., Yu, Z., Yin, K., Nielsen, B., Harrison, P.J., Turpin, D.H., Calvert, S.E., 1999. Nitrogen isotopic fractionation during a simulated diatom spring bloom: importance of N-starvation in controlling fractionation. Mar. Ecol. Prog. Ser. 179, 291–296.
Wyrtki, K., 1973. An equatorial jet in the Indian Ocean. Science 181, 262–264.
Zhang, R., Zheng, M., Chen, M., Ma, Q., Cao, J., Qiu, Y., 2014. An isotopic perspective on the correlation of surface ocean carbon dynamics and sea ice melting in Prydz Bay (Antarctica) during austral summer. Deep-Sea Res. I 83, 24–33.
Zhang, R., Chen, M., Guo, L., Gao, Z., Ma, Q., Cao, J., Qiu, Y., Li, Y., 2011. Variations in the isotopic composition of particulate organic carbon and their relation with carbon dynamics in the western Arctic Ocean. Deep-Sea Res. II 81–84, 72–78.
Zubkov, M.V., Fuchs, B.M., Tarran, G.A., Burkill, P.H., Amann, R., 2003. High rate of uptake of organic nitrogen compounds by Prochlorococcus Cyanobacteria as a key to their dominance in oligotrophic oceanic waters. Appl. Environ. Microbiol. 69 (2), 1299–1304.

Deep–Sea Research II 178 (2020) 104851

Contents lists available at ScienceDirect

Deep-Sea Research Part II

journal homepage: http://www.elsevier.com/locate/dsr2

Characteristics of particulate organic matter within the photic water column: A case study across the fronts in the indian sector of the Southern Ocean

Melena A. Soares *, Parli V. Bhaskar, N. Anilkumar, Ravidas K. Naik, Jenson V. George, Rajani Kanta Mishra, Deepti G. Dessai

National Centre for Polar and Ocean Research, Ministry of Earth Sciences, Headland Sada, Vasco Da Gama, Goa, India

ARTICLE INFO

Keywords:
Particulate organic matter
Autotrophy
Heterotrophy
Subtropical front
Polar front
Southern ocean

ABSTRACT

During austral summer 2012, seawater samples were collected from the upper 120 m of the water column, across the frontal zones in the Indian Ocean sector of the Southern Ocean. Suspended particulate organic matter from seawater was characterised, from its organic carbon and nitrogen content, and $\delta^{13}C_{(POM)}$. There was a marked difference in $\delta^{13}C_{(POM)}$ across the three frontal zones. It was depleted from the Subtropical frontal zone (−24.48 ± 1.94‰) to the Subantarctic frontal zone (−25.53 ± 0.62‰) and the Polar frontal zone (−26.69 ± 1.22‰). Within the water column, Particulate Organic Carbon (POC) and Particulate Nitrogen (PN) decreased with depth, especially below the deep chlorophyll maxima. Principal Component Analysis of $\delta^{13}C_{(POM)}$ and the environmental variables showed two clusters, one cluster, within the Subtropical and Subantarctic frontal zones, whereas the other cluster was in the Polar frontal zone. Statistical analysis of $\delta^{13}C$ with particulate organic carbon, nitrogen, apparent oxygen utilization, chlorophyll *a* and phytoplankton community, indicated that biological community structure strongly influenced the particulate organic matter characteristics in the upper water column. The study also revealed that both autotrophic and heterotrophic processes play a significant role in the waters of the Subtropical and Subantarctic frontal zones. Furthermore, physical factors like eddies and advection influence the community structure and food web dynamics of the region. However, in the Polar frontal zone, autotrophic processes were dominant, supported by the abundance of nutrients and prevalence of larger phytoplankton community (diatoms).

1. Introduction

Southern Ocean (SO) has a significant role in the global ocean circulation and climate change. One of the characteristic features of the SO is the presence of the Antarctic Circumpolar Current (ACC) and associated fronts. The ACC plays a prominent role in the transport of heat, salts, and organic components across the world oceans (Deacon, 1933; Pollard et al., 2002). There are three major fronts associated with the ACC, namely the Subtropical Front (STF), Subantarctic front (SAF) and Polar Front (PF). All these fronts were characterised by strong seasonal variability in the environmental conditions with strong winds, ocean currents, ice cover, etc., which makes it a unique system (Tynan, 1998; Boyd and Ellwood, 2010; Rintoul and Naveira Garabato, 2013). These fronts have distinct and homogenous physical and biochemical properties (Belkin and Gordon, 1996; Sokolov and Rintoul, 2002; Anilkumar et al., 2006). The extent of these fronts reported in some of the earlier studies in the Indian Ocean sector of the Southern Ocean (IOSO) is given in Table 1.

The Subtropical Front Zone (STFZ), is the region bounded between the STF in the north and SAF in the south. It is a region of mixing of warmer, nutrient-poor subtropical waters with, cooler, nutrient-rich subantarctic waters. This region is influenced by eddies, which alter the nutrients and organic matter composition (Boyd et al., 1999; Jullion et al., 2010; Sabu et al., 2015; George et al., 2018). Another feature of the STFZ is the high, but patchy, primary productivity, and the abundance of micro and mesozooplankton (Llido et al., 2005). The frontal zone south of the STFZ is the Subantarctic Front Zone (SAFZ), which extends from the SAF to the PF. The decline of nutrients due to stratification in this region is responsible for a succession in phytoplankton community (Deppeler and Davidson, 2017). The physico-chemical

* Corresponding author. Tel.: +91 832 2525636.
E-mail address: melena@ncpor.res.in (M.A. Soares).

https://doi.org/10.1016/j.dsr2.2020.104851
Received 22 February 2019; Received in revised form 12 June 2020; Accepted 15 August 2020
Available online 26 August 2020

Table 1
Summary of Fronts identified in some of the earlier studies in the ISSO and the zonation assigned in the present study.

Author	Year of Sampling	Front	Latitude
Anilkumar et al., 2006	Austral summer, 2004	STFZ (SSTF + ARF + SAF1)	40°S-43°S
		SAF	45–48
		PF1	49–50
		PF2	52–54
Tiwari et al., 2013	Austral summer 2010	STF	40–43
		SAF	44–49
		PF	50–54
Shetye et al., 2015	Austral summer 2009, 2010	SSTF	39–41
		SAF	44–48
		PF	49–59
Soares et al., 2015 & Present study	Austral summer 2012	STF	40–43
		SAF	44–48
		PF	50–53

conditions in this zone favour the growth of smaller phytoplankton and microzooplankton (Jasmine et al., 2009; Boyd et al., 2016). The Polar Fontal zone (PFZ) extends beyond 50°S to the Southern boundary. Of all these three frontal zones, the PFZ is known to be more productive during the austral summer, due to the availability of sunlight and the influx of micro and macro nutrients, contributed by ice melt (Jasmine et al., 2009; Sabu et al., 2014).

Frontal zones in the IOSO are known to exhibit a High Nutrient Low Chlorophyll (HNLC) property. Several attempts have been made to explain the patchy primary productivity and the HNLC phenomenon in this region based on lower amounts of solar energy and limiting micronutrients for optimum phytoplankton growth (Martin et al., 1990; Sakshaug and Slagstad, 1991). Deepening of the mixed layer and zooplankton grazing has also been suggested as influencing factors (Nelson and Smith, 1991; Dubischar and Bathmann, 1997). Primary productivity (PP) in the ocean plays a major role in drawing down atmospheric CO_2 by producing organic matter, part of which, over time is transported to deeper waters as particulate organic matter (POM) (Volk and Hoffert, 1985). A major portion of the POM produced in the surface waters undergoes biochemical modifications within the food-web and is recycled in the upper water-column (Alldredge et al., 1993; Prahl et al., 2000; Verity et al., 2000; Martineau et al., 2004). The quality of POM in-terms of its biochemical composition, determines the lability of POM in the marine system, and thus plays a significant role in determining the fate of POM, especially, regarding its downward flux or remineralisation in the water column (Tremblay et al., 2015; Aumont et al., 2017).

Earlier studies in the IOSO, focussed on CO_2 (Shetye et al., 2015; Prasanna et al., 2015), primary productivity (Tripathy et al., 2015, 2018) and zooplankton (Jasmine et al., 2009; Pillai et al., 2018). They indicated that, the biogeochemistry of different frontal zones exhibit different controlling factors and dominant biochemical processes. However, this region is understudied in-terms of POM characterisation, its transformation and influential processes on POM changes within the water column.

The isotopic ratio of carbon in POM ($\delta^{13}C_{(POM)}$) is influenced by various environmental factors in the ocean, and the cell physiology of phytoplankton, therefore $\delta^{13}C_{(POM)}$ is often used as a proxy to understand the factors influencing the composition of POM. Also, earlier studies of POM in the SO, and other oceanic regions supported that the isotopic ratios of carbon in POM ($\delta^{13}C_{(POM)}$) are sensitive to different environmental variables like temperature, CO_2, nutrients availability, as well as phytoplankton variables like cell size, shape, and growth rate (Rau et al., 1992; Popp et al., 1998, 1999). In Antarctic waters, $\delta^{13}C_{(POM)}$ has been used as a tool to understand the factors influencing the composition of suspended POM in the surface waters and to study sinking particles in the water-column using sediment traps (Henley et al., 2012). Stable isotopic composition of POM helped shed light on the food-web structure off Western Australia waters (Waite et al., 2007), trophic interactions (Kling et al., 1992), and the pathway of organic matter through various biological communities (Kaehler et al., 2000). Similar studies of POM carried out in the other sectors of the SO, using $\delta^{13}C_{(POM)}$ as a tool, include studies in the SO region south of Australia to understand the sensitivity of $\delta^{13}C_{(POM)}$ to the environmental variables in the upper water column (O'Leary et al., 2001; Lourey et al., 2004) and POM studies using sediment traps (Wada et al., 1987). Likewise, the factors influencing the characteristics of POM, based on $\delta^{13}C_{(POM)}$ variability, have been addressed in the surface waters of the Atlantic sector of the SO (Lara et al., 2010) and in an iron fertilized eddy region (Berg et al., 2011) of the Atlantic sector of the SO. A similar study was carried out in the surface waters of the Pacific sector of the SO by Kennedy and Robertson (1995). Even though there have been some studies in the IOSO, most of the previous studies in IOSO, were restricted to the surface waters or involved sediment traps, and include only a few water-column studies of POM. Although, the latitudinal variability of $\delta^{13}C_{(POM)}$ has been assessed in the IOSO (Soares et al., 2015), we further this work by explaining the contributing factors to the $\delta^{13}C_{(POM)}$ variability and dominant processes in the upper water column (120 m) in this region of the IOSO.

The complexity in the environmental setting of the study area, suggests that physical factors have a significant role in a change of the biological community structure and subsequently the POM characterisation. The processes in the water column alter the biochemical composition of POM, and the quality of POM determines the extent of POM transferred to the deeper waters. Using stable isotopic ratios of carbon and other attributes of POM (like C:N, POC:Chl-*a*), we attempt to delineate the possible processes influencing the composition of the POM transferred to a deeper depth. This study attempts to understand the biological processes and change in major trophic process (autotrophic and heterotrophic) within the 120-m water column across the three frontal zones in the IOSO, as reflected in the $\delta^{13}C_{(POM)}$ and other POM characteristics.

2. Material and methods

2.1. Sampling

Seawater samples were collected on-board *RV Sagar Nidhi* during an expedition in December 2011–January 2012 at five locations between 40°S and 53°S within the IOSO (Fig. 1). Samples were collected from 7 different depths from the sea surface to 120 m (0, 10, 30, 50, 75, 100, 120 m) using Niskin bottles mounted on a CTD rosette, and sub-sampled for the analysis of nutrients, Dissolved Oxygen (DO), tCO_2, chlorophyll *a* (Chl-*a*), particulate organic carbon (POC) and nitrogen (PN) and stable isotopic ratio of carbon in POM ($\delta^{13}C_{(POM)}$). Hydrography data (temperature and salinity) were obtained from CTD (Seabird Electronics, SBE911+, USA). Based on hydrographic features noted in the current study and in comparison with the earlier studies (Table 1) in the IOSO, the sampling stations in the present study were grouped into different zones, 2 stations (40°S and 43°S) belonged to STFZ, 1 station (45°S) in the SAFZ and 2 stations (50°S and 53°S) in the PFZ (Tables 1 and 2). The demarcation of mixed layer depth (MLD) was based on the density criterion as described in Kara et al. (2003) and was calculated following a 0.03 kg m^{-3} density difference criteria from below 10-m. This study addresses the upper 120 m, however the euphotic depth (PAR > 1% of the surface value) was always above 100 m (Table 2).

2.2. Dissolved Oxygen (DO)

Sub-samples for DO were collected directly from Niskin samplers, into 125 ml glass bottles before any other samples being collected. These samples were fixed with Winkler's A and Winkler's B and titrated against sodium thiosulphate following Winkler's method (Grasshoff et al., 1983) using an auto-titrator.

The apparent oxygen utilization (AOU) is often used as an indicator

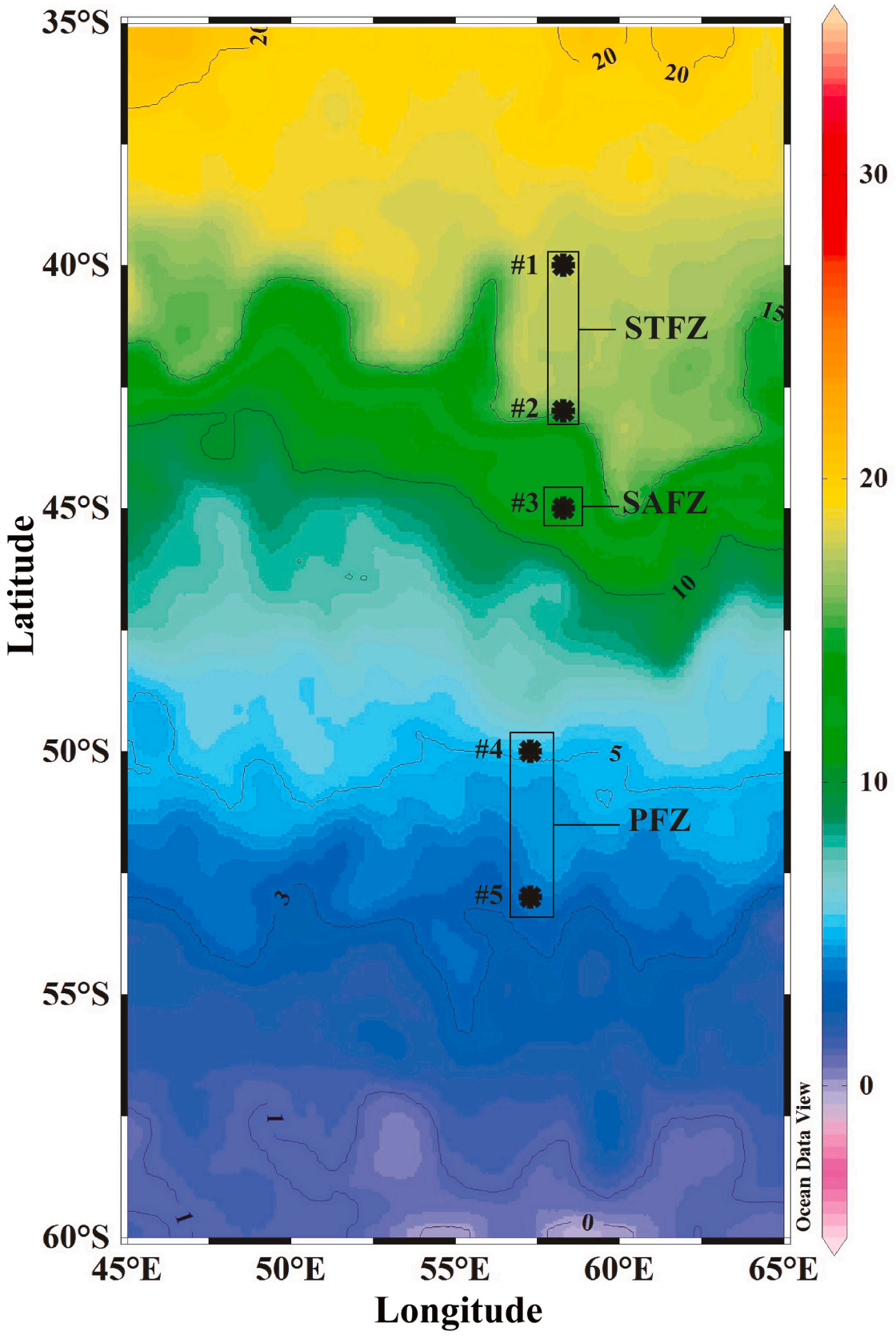

Fig. 1. Sea surface temperature overlayed with the sampling locations and the zones in the ISSO during the austral summer 2012.

Table 2
Range of salinity, tCO_2 (μM), phosphate (PO_4), N:P, N:Si, POC (μg/L), PN (μg/L), C:N (M/M), $\delta^{13}C_{(POM)}$, AOU (μM) and dominant phytoplankton community based on DPI (Diagnostic pigment index) across the fronts in the cruise transect.

Region	Station	Latitude	Euphotic depth(m)	Salinity	tCO_2 (μM)	PO_4 (μM)	N:P	N:Si	POC (μg/L)	PN (μg/L)	C:N (M/M)	$\delta^{13}C_{(POM)}$ (‰)	AOU (μM)	Dominant phytoplankton community
Sub-Tropical Frontal Zone (STFZ)	#1	40°S	74	35.37–35.53	2045–2091	1.34–1.61	1.89–4.94	1.44–2.22	15.10–58.94	1.47–7.83	4.28–21.88	-26.36 to -22.98	-4.68 to 24.69	Flagellates 83.3%
	#2	43°S	34	34.80–35.29	2002–2126	1.18–1.64	2.33–6.01	2.18–3.42	17.82–74.66	2.65–16.63	3.14–8.50	-27.04 to -21.59	-10.66 to 21.28	
Sub Antarctic Frontal Zone (SAFZ)	#3	45°S	56	34.66–34.96	2049–2252	1.18–1.75	3.19–8.10	2.75–3.85	21.28–36.78	4.02–7.55	4.86–6.53	-26.21 to -24.81	-0.13 to 31.21	Flagellates 65.8%
Polar Frontal Zone (PFZ)	#4	50°S	85	33.81–33.83	2158–2203	2.44–3.65	7.05–9.04	3.52–7.18	31.16–41.97	5.86–8.32	4.67–6.76	-28.30 to -24.00	-3.19 to 20.36	Diatoms 63.1%
	#5	53°S	62	33.78–33.92	2079–2205	1.79–2.83	9.44–1.89	1.19–3.04	42.34–54.94	8.07–16.74	3.28–6.32	-26.88 to -25.99	-0.51 to 24.09	

of biological activity like respiration and remineralisation in the ocean, as biological activity results in a change in the concentration of oxygen in the ambient waters. AOU was calculated as the difference of oxygen gas solubility ($O_{2(sat)}$) and the measured oxygen concentration (O_2). Oxygen gas solubility was calculated as a function of *in-situ* temperature and salinity at one atmosphere of total pressure (Benson and Krause, 1984), assuming the surface waters are near saturation.

$$Apparent\ Oxygen\ Utilization\ (AOU) = O_{2(sat)} - O_{2.} \quad (1)$$

2.3. Total carbon dioxide (tCO_2)

Sub-samples were collected in 60 ml glass bottles and fixed by adding 0.3 ml of saturated mercuric chloride and analysed using a coulometer (Model 5015, U.I.C. Inc., USA), as described in Soares et al. (2015). The overall precision and accuracy of the analyses were ≤2 μM.

2.4. Nutrient analyses

Seawater sub-samples were collected in 250 ml Nalgene bottles and kept frozen at −20 °C until analyses. Prior to analysis the samples were thawed and brought to room temperature for the analysis of nitrate, nitrite, ammonium, phosphate and silicate, by auto-analyzer (Model: Skalar Analytical San++ 8505 Interface v3.05, the Netherlands) following standard colorimetric methods (Grasshoff et al., 1983). Standards were used to calibrate the auto-analyzer and frequent baseline checks were made. The standard deviation for all nutrients analysed was ±1%.

2.5. Chlorophyll *a* and phytoplankton marker pigments

Three liters of seawater was filtered through GF/F Whatman filters, for Chlorophyll *a* (Chl-*a*) analyses by fluorometry using Turner's AU 10 Fluorometer (Turner Designs Inc., USA). Pigment analyses were carried out following the method of van Heukelem (2002) using High Performance Liquid Chromatography (HPLC), and Diagnostic pigment index (DPI) was used to assess the community structure by confirming the significant relationship between DPI and total Chl-*a* ($r = 0.871$, $n = 15$, $p < 0.0001$). Details of analysis and calculation for DPI used for this study have been adopted from Naik et al. (2015).

2.6. POC, PN and $\delta^{13}C$ of POM

Sub-samples for the POM analyses collected in acid-cleaned plastic carboys and five litres of seawater was filtered through 0.7 μm pore size precombusted (450 °C for 4 h) Whatman GF/F filters and stored at −20 °C until analysis. The sample filters were decarbonated to ensure the sample was free from the contribution of inorganic carbon and analysed for POC, PN and stable isotopic ratios ($\delta^{13}C$) of POM (as described in Maya et al., 2011; Soares et al., 2015) using an Isoprime Stable Isotope Ratio Mass Spectrometer in continuous-flow mode coupled with an Elemental Analyzer (Isoprime, Vario Isotope Cube) (Owens and Rees, 1989), at the Marine Stable Isotope laboratory of National Centre for Polar and Ocean Research, Goa, India. The external precision for $\delta^{13}C$ is ±0.05‰ (1σ standard deviation) and for %C and %N are ±0.29% and ±0.35% (1σ standard deviation), respectively, obtained by repeated measurements of IAEA–CH–3 and Ammonium sulphate IAEA-N1 ($n = 27$). The %C and %N are converted to (μg/L) of POC and PN.

2.7. Statistical analysis

To understand the major processes governing the variability of POM properties across the fronts, and the factors influencing the POM

characteristics, principle component analysis (PCA) was carried out using XLSTAT. Also, Spearman's correlation analysis using EXCEL was undertaken to understand the relation of various environmental parameters with $\delta^{13}C_{(POM)}$ and the POM characteristics.

3. Results

3.1. Hydrography and dissolved gases

The sea surface temperature dropped by ~11 °C, from an average of 15.32 ± 1.41 °C in the STFZ to 3.97 ± 0.77 °C in the PFZ (Fig. 1). The range of temperature in the upper water column of the STFZ, SAFZ and PFZ was 13.46 to 17.58 °C, 11.63 to 14.55 °C and 2.20 to 4.73 °C, respectively (Fig. 2a; Table 2). Similarly, the salinity dropped by ~1.5 across the fronts from the STFZ (35.26 ± 0.26) to the PFZ (33.83 ± 0.03) and ranged from 34.80 to 35.53 in the STFZ, 34.66 to 34.96 in the SAFZ and 33.78 to 33.92 in the PFZ (Table 2). It was also observed that the MLD increased from 37 m in the STF to 106 m towards the PFZ (Fig. 2a). It is evident from sea level anomaly (SLA) that the STFZ is an eddy prone region (Fig. 2b), with numerous cyclonic and anticyclonic eddies indicated from the positive and negative in SLA, and geostrophic current vectors suggest STFZ and SAFZ are dynamic zones (Fig. 2b).

The colder PFZ waters were richer in oxygen as compared to the STFZ and SAFZ. DO increased from the STFZ (243 μM) to PFZ (329 μM) in the surface waters. Within the upper water column, DO displayed a range from 234 to 262 μM in the STFZ and 241 to 257 μM in SAFZ, and 312 to 329 μM in PFZ (Fig. 3a). PFZ water column was well oxygenated and did not show much variability with depth. However, it decreased beyond the deep chlorophyll maximum (DCM) in the STFZ and SAFZ. In the surface, tCO_2 varied from 2063 μM (STFZ) to 2163 μM (PFZ), while within the water column it varied from 2002 to 2126 μM in the STFZ, to 2049 to 2252 μM in the SAFZ and 2079 to 2205 μM in the PFZ (Table 2). Also, an increase of tCO_2 with depth was observed at all locations in the study area.

3.2. Nutrients

The nitrate concentration was low (<3 μM) in the upper 50 m of the STFZ and SAFZ. Moreover, nitrate in the surface waters increased by ~20 fold, southward from 0.61 μM (STFZ) to 23.35 μM (PFZ). Within the upper water column, nitrate ranged from 0.25 to 7.20 μM (STFZ), 2.03 to 11.37 μM (SAFZ), followed by 15.01 to 28.46 μM (PFZ), with more than 2-fold increase with depth (Fig. 3b). There existed an evident nitracline at approximately 50 m in the STFZ and SAFZ. Likewise, silicate increased from 1.12 μM to 8.78 μM in the surface waters, from STFZ to PFZ, and increased with depth, especially, in the STFZ and SAFZ. Within the water column, silicate ranged from 1.04 to 4.42 μM in the STFZ, 1.19 to 4.92 μM in the SAFZ and 2.80 to 25.81 μM in the PFZ (Fig. 3c). Likewise, the phosphates also increased towards the PFZ, even though the column variability was low (Fig. 3d). Phosphates ranged from 1.18 μM to 1.64 μM at the STFZ, which was similar to the SAFZ, but comparatively lower than the PFZ, where phosphates ranging from 1.79 μM to 3.65 μM (Table 2).

3.3. Chl-a and diagnostic pigment index (DPI)

The highest variability in Chl-*a* was observed in the STFZ. Also, the overall highest and the lowest values were also observed within this zone (Fig. 4a). This is also evident from the satellite Chl, which suggest high but patchy productivity within the STFZ (Fig. 4b). Chl-*a* varied from 0.05 to 1.19 μg/L in the STFZ, followed by SAFZ (0.07 to 0.81 μg/L) and PFZ (0.07 to 0.67 μg/L), with a sharp decrease below the DCM depth (Fig. 4a). The depth of DCM increased from the STFZ to the PFZ.

The DPI derived from the pigment data indicated the percentage contribution of phytoplankton functional groups. Distinct variation in phytoplankton community dominance was observed between STFZ and PFZ; also, a variation in the contribution from each phytoplankton community towards the total phytoplankton production was observed in the 3 zones. The STFZ and SAFZ was dominated by the flagellate community (nanoflagellates), followed by the prokaryotic picophytoplankton community and a contribution from diatoms at 40°S (Fig. 5a). Although the dominance of flagellates was consistent in the upper water column (120 m) at the STFZ and SAFZ, the contribution of prokaryotes decreased and diatoms increased from 43°S to 45°S (Fig. 5b and c). The contribution from prokaryotic phytoplankton was highest in the STFZ and decreased from 40°S (STFZ) to 53°S (PFZ). The PFZ waters were dominated by diatoms (Table 2) followed by the flagellates, and the contribution from the prokaryotic phytoplankton was very low and almost negligible in these waters (Fig. 5d and e).

3.4. Characteristics of POM

POC and PN of POM at STFZ varied over a wide range. POC ranged from 15.10 to 74.66 μg/L and PN from 1.47 to 16.63 μg/L, respectively (Table 2). The concentration of POC and PN decreased towards the SAFZ (Fig. 6a and b) and varied from 21.09 to 36.78 μg/L and 4.02 to 7.55 μg/L, respectively. However, further in the PFZ the POC increased, ranging from 31.16 to 54.94 μg/L and was similar to the PN, which increased in the PFZ and ranged from 5.86 to 16.74 μg/L.

The molar ratio of C:N showed wide variability in the STFZ ranging from 3.14 to 21.88 (avg. 9.44 ± 5.93) with the highest values at 40°S; 4.86 to 6.53 in the SAFZ (avg. 5.39 ± 0.88); and from 4.67 to 6.76 in the PFZ (avg. 5.61 ± 1.15) with lower variability within the water column (Table 2). The POC:Chl-*a* was calculated to understand the freshness of

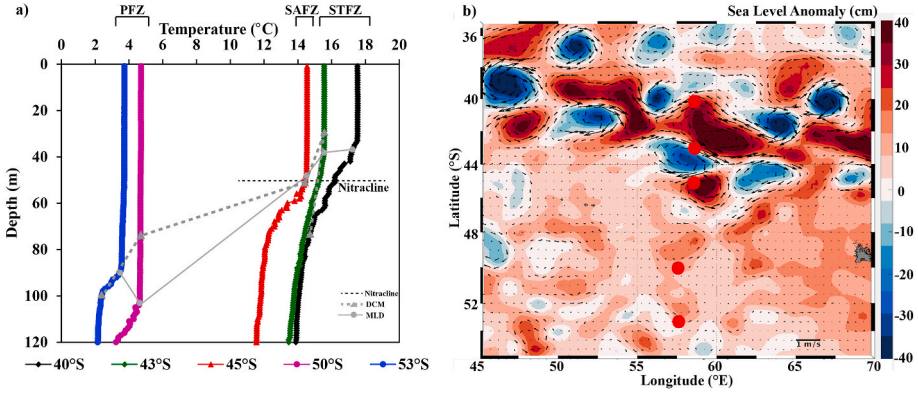

Fig. 2. a)Vertical profile of temperature at the sampling locations with the MLD and DCM marked at each sampling location; b) Sea level anomaly and current vectors overlaid with the sampling locations marked (Red circle). (For interpretation of the references to colour in this figure legend, the reader is referred to the Web version of this article.)

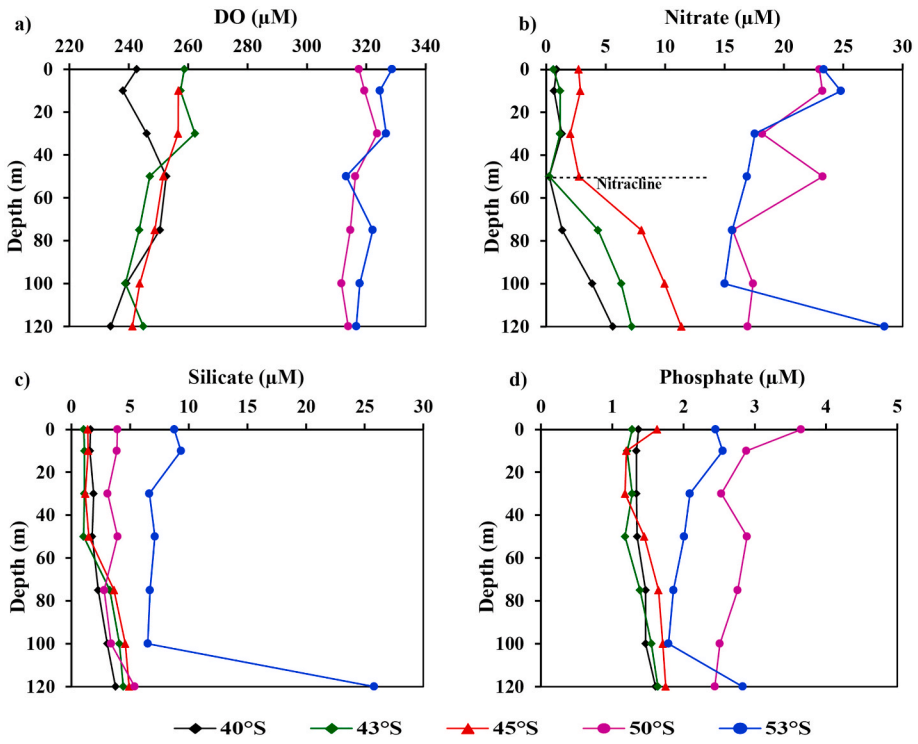

Fig. 3. Vertical variation of a) Dissolved Oxygen (DO μM); b) nitrate (μM); c) silicate (μM); and d) phosphate (μM).

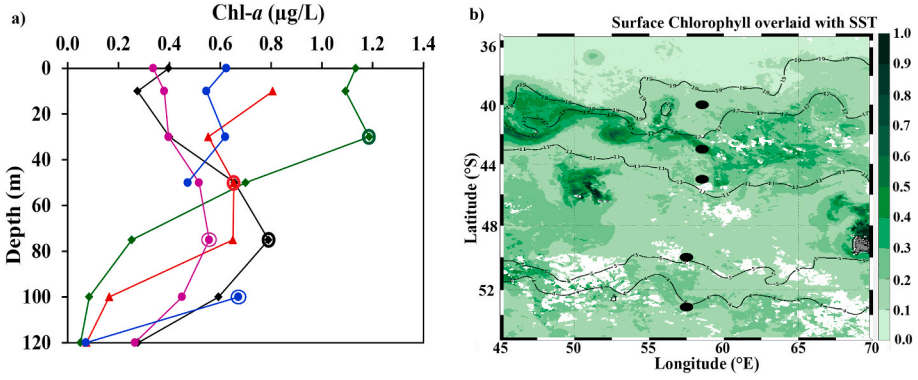

Fig. 4. a) Vertical variation of chlorophyll *a* (Chl-*a*, μg/L), encirled values indicate DCM; b)satellite image of chlorophyll overlaid with averaged SST during the study period.

the POM samples. This ratio can further be used to identify the dominant trophic process contributing towards the observed POM characteristics. POC:Chl-*a* ratio ranged from 23 to 366 in the STFZ, wherein the POC:Chl-*a* was comparatively higher in the surface waters compared to the subsurface (Fig. 6c). In the SAFZ and PFZ, it ranged from 26 to 444 and 39 to 125 respectively. The POC:Chl-*a* values generally increased with depth, except at 40°S.

$\delta^{13}C_{(POM)}$ also showed large variation in the STFZ, ranging from −27.04‰ to −21.59‰, and from −26.21‰ to −24.81‰ in the SAFZ waters. $\delta^{13}C_{(POM)}$ was most depleted in the PFZ (Fig. 6d), and ranged from −28.30‰ to −25.65‰ except for a higher value of −24.00‰ at 50°S.

3.5. Statistical analysis

The study site is a highly dynamic region. In a region with such complex environmental setting, varied physical and biochemical factors interact. Statistical analysis of environmental variables was used to deduce the major influencing factors in the IOSO. In the entire study area, $\delta^{13}C_{(POM)}$ had an inverse correlation with tCO_2 ($r = -0.655$; $p < 0.0001$), and positive correlation with POC ($r = 0.639$, $p < 0.0001$). Also, overall POC had a positive linear correlation with PN ($r = 0.791$, $p < 0.0001$). However, in the STFZ and SAFZ, $\delta^{13}C_{(POM)}$ had a significant correlation with nitrate, silicate, POC, and AOU (Table 3), in contrast to the PFZ, where $\delta^{13}C_{(POM)}$ did not show any significant correlation with any environmental variables.

PCA was carried out using environmental variables to identify the controlling factors in different zones. The study area displayed two distinct clusters, one cluster comprising the STFZ and the SAFZ, while the other cluster comprised only the PFZ. The cumulative percentage contribution was 80.40%, with a contribution of 63.03% from Factor-1 and 17.37% contribution from Factor-2 (Fig. 7). This analysis indicated that the STFZ and SAFZ have similar controlling factors, whereas the PFZ is governed by a different process. Therefore, in further discussion the STFZ and SAFZ are discussed together.

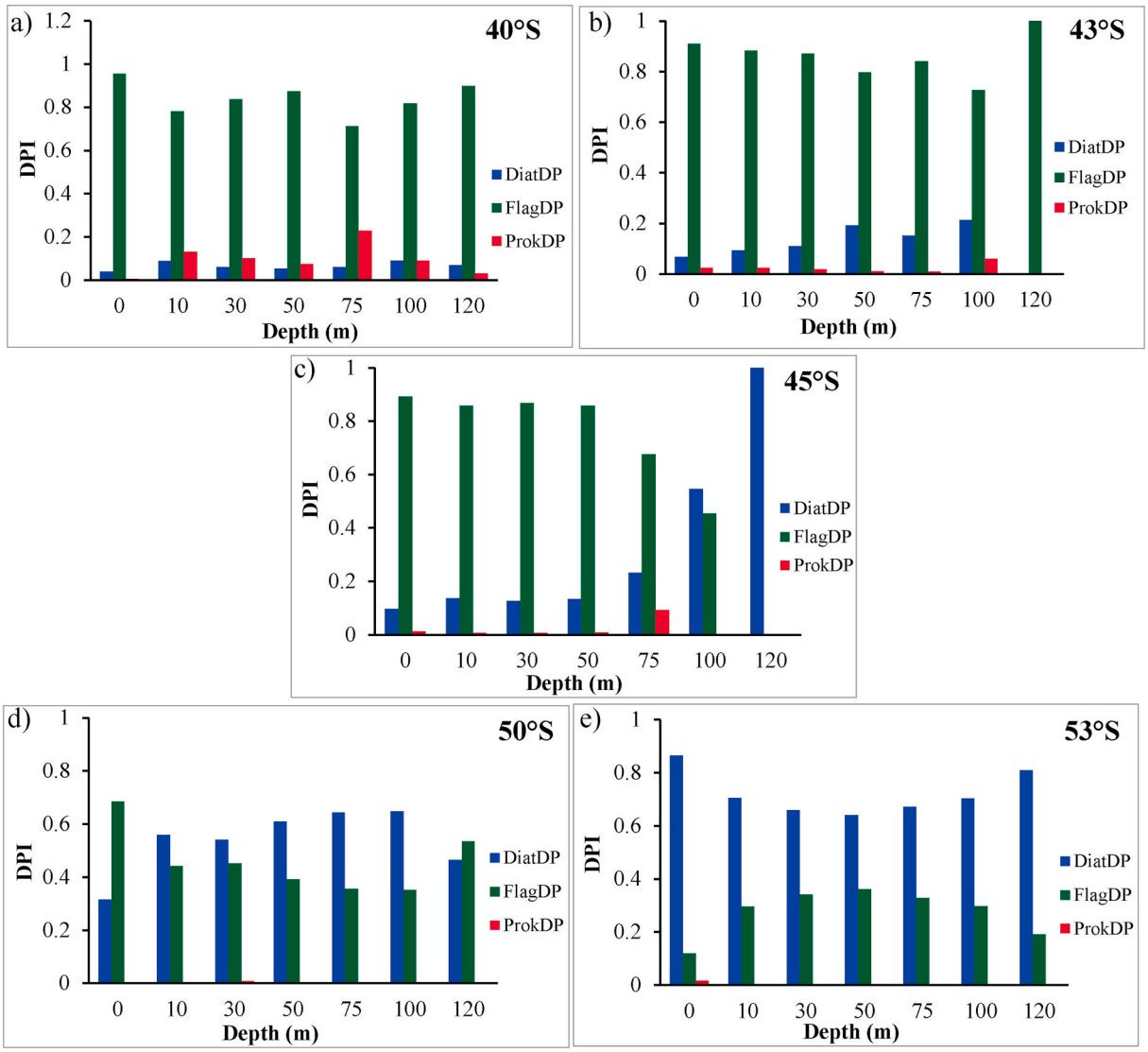

Fig. 5. Variation of dominant phytoplankton community based on DPI (Diagnostic pigment index) at different sampling locations in the 3 zones: a) and b) in the STFZ, c) in SAFZ, and d) and e) in the PFZ.

4. Discussion

In the present study, the spatial and depth-wise variations observed in temperature, dissolved gases and nutrients were similar to previous studies in this area (Jasmine et al., 2009; Gandhi et al., 2012; Soares et al., 2015). Also, the POC, PN and $\delta^{13}C_{(POM)}$ values matched earlier reports from the SO (Francois et al., 1993; O'Leary et al., 2001).

A recent study in the IOSO, indicated that, the variability in phytoplankton biomass at the frontal zones of IOSO was linked to the presence of a well-defined DCM which corresponded to the upper boundary of the thermal mixed layer (Tripathy et al., 2015). The deeper MLD in the PFZ is accompanied with higher availability of nutrients in the water column, especially nitrates and silicates (Fig. 3b and c) and the dominance of larger phytoplankton (Diatoms, Table 2). Clarke et al. (2008) postulated that stratification and stability of the water column governs the type of phytoplankton community that would dominate. For instance, a stable water column with nutrient availability favours the proliferation of diatoms, which was also noted during this study in the PFZ. Furthermore, in the present study the DCM was noted at the base of the euphotic zone (Table 2) at most locations, ascertaining the role of light intensity on the phytoplankton adaptation and the depth of DCM (Nielson and Hansen, 1959). Also, the DCM was at the base of the mixed layer, suggesting the role of nutrient concentration. The observed increase of POC and PN at the DCM depth suggest the POM samples may have been dominated by phytoplankton (Liu et al., 2018), also supported by the POC:Chl-*a* ratio (≤100) at this depth, suggesting fresh organic matter. The deepening of the DCM from STFZ to the PFZ of IOSO during the study was a collective response of stratification, euphotic depth, the increase in nutrient concentration towards the PFZ, and the dominance of diatoms towards the PFZ, as suggested in earlier studies (Cullen, 1982; Parslow et al., 2001). It was also noted that the deeper the DCM, the higher is the contribution to the POM in the photic water column implied from the column integrated Chl-*a* and POC in the water column down to the DCM depth.

Moreover, the DCM is known to act as a major source of POM for export beyond the photic zone (Pollehne et al., 1993). However, the accumulation of POM at the DCM, due to stratification, can cause an increase in the residence time of POM within the water column making it liable to microbial remineralisation or grazing (Abdel-Moati, 1990; Gomi et al., 2010). This explains the observed decrease in POC and PN below the DCM depth at most locations. This also suggests an alteration of the POM composition in the upper water column due to varied processes like heterotrophic activities including grazing and remineralisation, prior to its escape beyond the MLD. This phenomenon is well

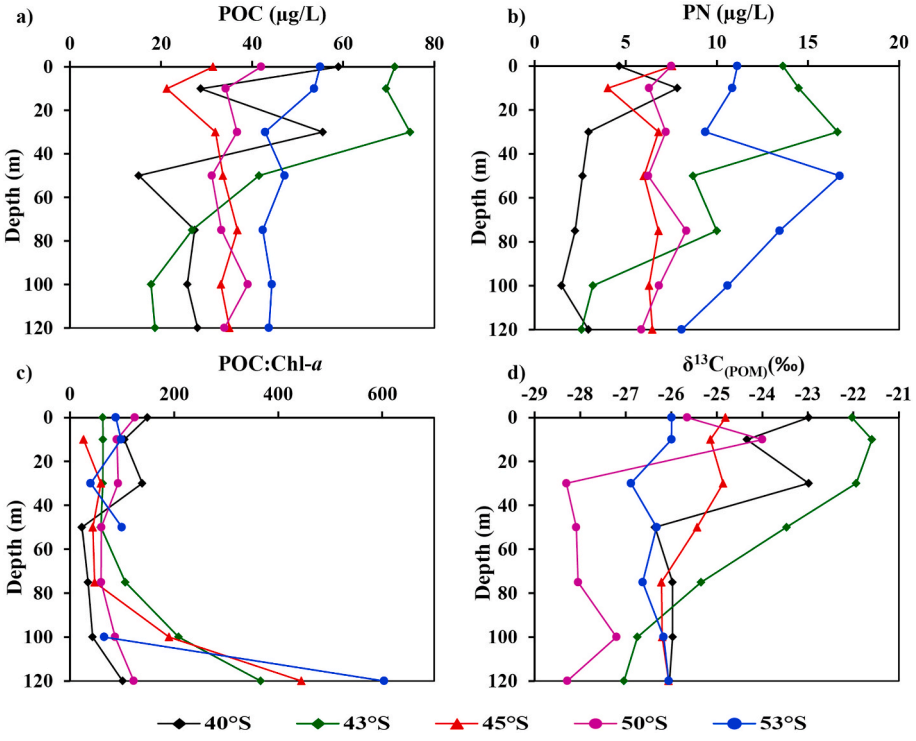

Fig. 6. Vertical variation of a) POC (µg/L), b) PN (µg/L), c) POC:Chl-*a*, and d) $\delta^{13}C_{(POM)}$ (‰).

Table 3
Correlation coefficients from simple regressions of $\delta^{13}C_{(POM)}$ with NO_3, SiO_4, % C, AOU in the STFZ and SAFZ.

Chemical Variables	r, *p*, in STFZ	r, *p*, in SAFZ
$\delta^{13}C_{(POM)}$, NO_3	−0.677, ≤0.005	−0.905, <0.001
$\delta^{13}C_{(POM)}$, SiO_4	−0.830, <0.0001	−0.913, <0.001
$\delta^{13}C_{(POM)}$, POC	0.961, <0.0001	−0.550, <0.05
$\delta^{13}C_{(POM)}$, AOU	−0.916, <0.0005	−0.918, ≤0.0005
POC, AOU	−0.893,<0.0001	0.602, <0.05

supported by some studies in this region, which postulate, that the transfer of biogenic carbon to deeper waters is low as a result of efficient breakdown and remineralisation of organic matter within the upper water column (Blain et al., 2002; Coppola et al., 2005; Robinson and Ramaiah, 2011).

4.1. STFZ and SAFZ

The STFZ waters were warmer (Fig. 2a) with low nutrient concentrations (Fig. 3b and c). This zone is influenced by the subtropical gyre in the north (Jena et al., 2013), which brings in oligotrophic warm waters that merge with nutrient rich cooler waters from the south (Boyd et al., 1999). This is a distinct feature of the region.

STFZ is also known to be an eddy prone region (Marshall and Radko, 2003; Sabu et al., 2015) which influences its thermodynamics and biogeochemical processes. STFZ have numerous cyclonic and anticyclonic eddies (Fig. 2b), responsible for upwelling and downwelling phenomenon (George et al., 2018). Eddies are often responsible for vertical and horizontal advection of waters (Sabu et al., 2015; George et al., 2018) and have proven to be significant contributors towards lateral particle transport and alteration of POM characteristic via allocthonous and autochthonous production (Freudenthal et al., 2001; Kolasinki et al., 2012). In the current study, the presence of a cyclonic eddy in the vicinity, and advection of these upwelled waters, was evident from the sea level anomaly and surface currents (Fig. 2b). Additionally, the sampling location 40°S was noted to be at the

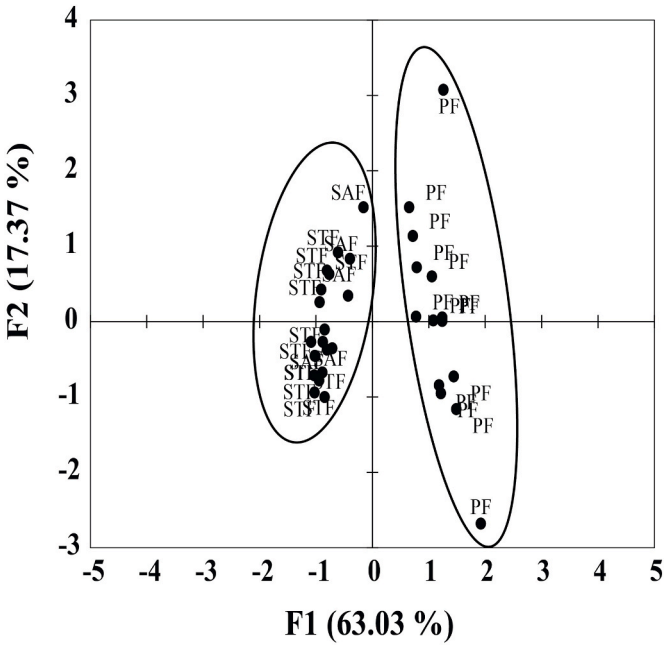

Fig. 7. PCA showing distribution of different station depth samples in the 3 zones: indicating the STFZ and SAFZ are grouped together, while the PFZ is separate and.

periphery of an anticyclonic eddy. This eddy driven transport (upwelling and advection), mostly cause a redistribution of nutrients in the upper waters, contributed to the large variability in Chl-*a* observed within the STFZ. The variability in Chl-*a,* is evident from the *in-situ* Chl-*a* (Fig. 4a) and visible in the satellite image (Fig. 4b). Previous studies (McGillicuddy et al., 1998; Kahru et al., 2007) explained the enhanced Chl-*a* at the core and periphery of cyclonic and anticyclonic eddies respectively. This corroborates the higher Chl-*a* at 43°S (the periphery of an

anticylonic eddy) in our study. The variability in the phytoplankton productivity and trophic processes is reflected in the POM characteristics (Lara et al., 2010; Henley et al., 2012) and the large variability in the C:N ratio and the $\delta^{13}C_{(POM)}$ in the study region.

During the study, a change in phytoplankton community was evident from the DPI data, with a shift from nanoflagellates in the STFZ, to a mixed community with diatoms (Fig. 5c), which was possibly responsible for a higher utilization of silicates at the SAFZ. This is ascertained from the switch in percentage abundance of the dominant phytoplankton community with depth in the water column at the SAFZ (Fig. 5c).

Flagellates, especially some dinoflagellates, have a mixotrophic (autotrophic and heterotrophic) behaviour. The dominance of flagellates in the STFZ (Fig. 5a and b; Table 2), also suggests, the prevalence of heterotrophic activity (Archer et al., 1996; Sherr and Sherr, 2007) in the STFZ waters, and a trivial contribution at the SAFZ. In regions low in nitrates, and other forms of nitrogen (ammonium) are available, the role of enzymes namely phosphoenolpyruvate carboxylase (PEPC) and phosphoenolpyruvate carboxykinase (PEPCK) present in the flagellates are stimulated. The activity of PEPC and PEPCK is reported to make the dinoflagellates less isotopically discriminative during the uptake of carbon (^{12}C or ^{13}C) in the available chemical form (Bentaleb et al., 1998; Gaul et al., 1999; Lara et al., 2010). This non-selective uptake of ^{13}C rich carbon species could result in more enriched $\delta^{13}C$ values. Thus, the dominance of dinoflagellates in low nutrient waters (nitrates and silicates) at the STFZ possibly favoured the production of isotopically heavier $\delta^{13}C$ of POC, as observed in these waters.

The molar ratios of C:N observed at 40°S in the STFZ, displayed the maximum variability (~4 to 21) and the highest values of C:N ratios (Table 2). These values were much higher than the Redfield's ratio of plankton/fresh organic matter (6.63). A study by Caron et al. (1989) reported that the C:N ratio of salp faecal material can vary from 7.3 to 24.1, irrespective of the species or size of the salp. During the present study, an abundance of salps and pyrosoma was observed at this location (Minu et al., 2015). This suggests the role of these voracious grazers, whose significance in the food web dynamics and recycling of organic matter has been well established (Perissinotto et al., 2007) in influencing the POM composition in these waters. Therefore, the presence of high C:N ratios at 40°S was attributed to the faecal material of salps, which was likely a result of higher grazing. This could act as another contributing factor towards heterotrophic activity and the alteration of POM characteristics within the photic waters at this location.

Furthermore, the POC:Chl-*a* ratio at 40°S, was comparatively higher (>100 but <200) than the other locations especially in the upper 30 m (Fig. 5c). This indicates, that the POM observed in the upper 30 m, included significant input from detrital matter/partially degraded matter (Zeitzchel, 1970; Maksymowska et al., 2000; Coppola et al., 2005). This implies heterotrophic activity, or a contribution from the heterotrophic biological community (Leblanc et al., 2002; Savoye et al., 2003), at this location. However, below 30 m, the POC:Chl-*a* ratio indicates the predominance of fresher organic matter, and significant contribution from autotrophic activity (Bentaleb et al., 1998). Conversely, at the other stations within the STFZ and SAFZ, the POC:Chl-*a* ratios remained <100 in the upper 50 m indicating that the POM was relatively fresh and consisting of living cells and the predominance of autotrophic activity. Nonetheless, below 75 m, POC:Chl-*a* increased suggesting the dominance of heterotrophic activity, and was >200 in the upper 120 m water column (Fig. 6c). This can be attributed to the dominance of smaller size phytoplankton mainly the dinoflagellates and prokaryotic picoplankton, which favours the proliferation of microzooplankton in these waters. Minu et al. (2015) confirmed the abundance of microzooplankton, along with the dominance of heterotrophic dinoflagellates and ciliates in these waters during the study period, which supports the observed heterotrophic activity.

In the STFZ and SAFZ, the $\delta^{13}C_{(POM)}$ decreased with depth within the euphotic water column. Correspondingly, as POC decreased with depth, the apparent oxygen utilization (AOU) became positive, thus indicating that the higher POC in surface waters is mainly a result of photosynthesis, but deeper, respiration alters the POM (Omand et al., 2015). The process of respiration also explains the drop in POC and PN below the DCM. Based on the above observations, the significant inverse correlation of $\delta^{13}C_{(POM)}$ and AOU (Fig. 8a and b) observed in these waters can be interpreted as an outcome of biological respiration/mineralization of POM. Hence, altering the POM and the removal of ^{13}C rich compounds causes the depletion of the resultant $\delta^{13}C_{(POM)}$ below the DCM within the euphotic water column (Eadie and Jeffrey, 1973; Harvey et al., 1995; Kolasinski et al., 2012). Jasmine et al. (2009) highlighted that the microbial loop is highly active, alongside the classic food web in the STFZ, reflected by the abundance of micro zooplankton biomass (Hall et al., 1999). Also, during our study, the contribution of prokaryotic picoplankton was higher in the STFZ followed by the SAFZ (Fig. 5). Prokaryotic picoplankton, mostly flourish in low nutrient, warmer waters, that also supported the proliferation of smaller zooplankton and have often been considered as an indicator of an active microbial loop supported via secondary production (Marañón et al., 2003; Venkataramana et al., 2020) and contribute significantly to the recycling of carbon within the water column (Azam et al., 1983; Fenchel, 2008). Although the bacterial contribution as bacterial C was not clear during the study period, its contribution towards heterotrophy was evident from the AOU and POC correlation (Fig. 9a; Table 3). Moreover, the abundance of micro zooplankton, and the predominance of flagellates and prokaryotic picoplankton contributed significantly towards the observed heterotrophy in these waters.

A significant linear positive correlation was observed between $\delta^{13}C_{(POM)}$ and POC (Fig. 9b). This suggests that the biomass effect is the governing factor (Zhang et al., 2014) in shaping $\delta^{13}C_{(POM)}$. It also implies that the POM characteristics are predominantly a reflection of a combined effect of varied biological processes (primary, secondary, microbial), dominated by heterotrophic activities at 40°S, while at 43°S a combination of autotrophy above the euphotic depth and heterotrophy beyond the euphotic depth was evident. This is also implied from the negative correlation of AOU and POC (Fig. 9a), especially within the STFZ.

4.2. PFZ

It is well established that, at higher latitudes with colder waters, and a region like the SO that is influenced by high winds that favours strong wind driven mixing. This is evident from deepening of MLD southwards, from the STFZ to the PFZ (Fig. 2a). The higher air-sea interactions and low temperature along with wind driven mixing supports higher dissolution of gases (DO, tCO_2) in these waters. However, another major factor responsible for the higher concentration of dissolved gases to the PFZ waters is the existence of a different water mass at the PFZ in the upper water column. Based on the watermass characteristics given by Anilkumar et al. (2006), it is evident from the T-S diagram of the sampling locations during the study (Fig. 10), that the PFZ waters were having characteristics of Antarctic surface waters (AASW). These are low temperature waters and reported to be rich in dissolved gases (Park et al., 1998) and nutrients, as noted at these sampling locations, unlike the STFZ which displayed characteristics of the Subtropical surface waters (STSW). This is reflected in the higher concentration of DO and tCO_2 in the PFZ, having an average of 319 ± 5 μM and 2166 ± 69 μM, respectively. There was a ~5 to 10-fold rise in nutrients, especially nitrate (avg. 23.18 μM) and silicate (avg. 6.35 μM), respectively, in the surface waters (compared to STFZ & SAFZ). The low temperatures with abundant availability of inorganic carbon and nitrogen facilitates the uptake of the lighter carbon isotope (^{12}C) by phytoplankton as a result of isotopic fractionation at the time of photosynthesis, resulting in depleted signatures of $\delta^{13}C_{(POM)}$ (Checkley and Miller, 1989; Goericke and Fry, 1994; Gruber et al., 1999; Mino et al., 2002). Hayes, 1993 reported that the phytoplankton $\delta^{13}C$, is always depleted/lower than the $\delta^{13}C$ of the

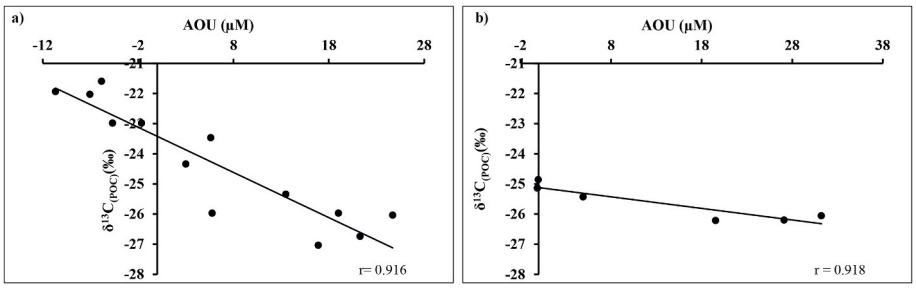

Fig. 8. Spearman's correlation of $\delta^{13}C_{(POM)}$ (‰) with Apparent Oxygen Utilization (AOU) in the euphotic waters of a) STFZ and b) SAFZ.

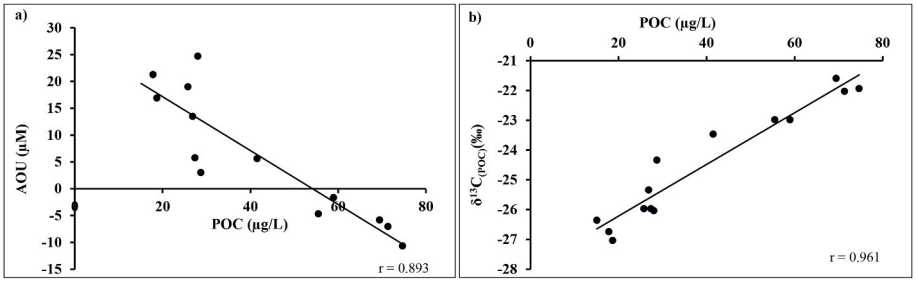

Fig. 9. Spearman's correlation of a) POC (µg/L) with AOU (µM); b) POC with $\delta^{13}C_{(POM)}$ (‰) in the euphotic waters of STFZ.

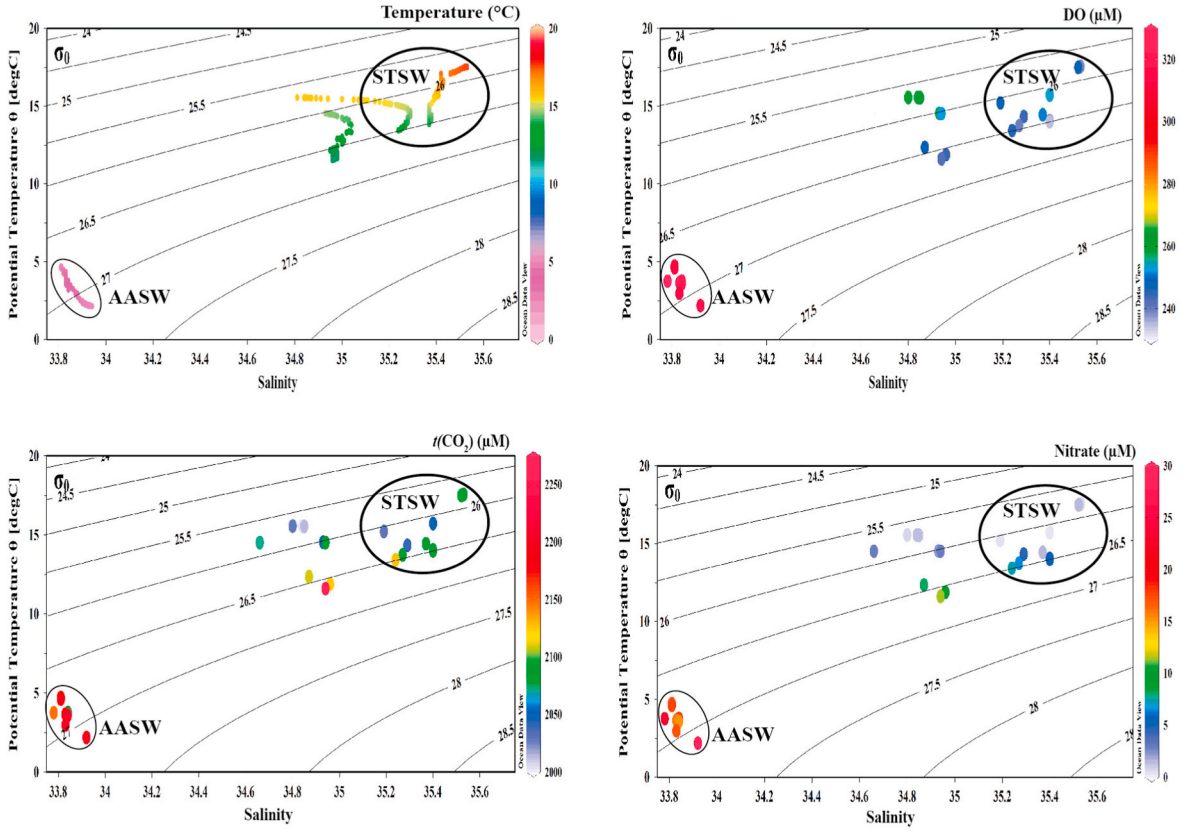

Fig. 10. T-S diagram for all sampling locations in the study area with colours mapped to display (a) temperature (°C); b) DO (µM); c) tCO_2 (µM) and d) nitrate (µM). (For interpretation of the references to colour in this figure legend, the reader is referred to the Web version of this article.)

inorganic source of carbon assimilated by the phytoplankton. An earlier report on the $\delta^{13}C$ of DIC in the surface waters in this region, was estimated to have an average of −1.48 ± 0.12‰, and the $\delta^{13}C$ of the end member of the source CO_2 was proposed to be 9.22 ± 0.26‰ (Prasanna et al., 2015). During the current study, the observed $\delta^{13}C_{(POM)}$ values in the PFZ waters ranged from −28.30‰ to −24.00‰ and matches well with those reported earlier for POC in higher latitudes, ranging from −24.47‰ to −27.89‰ in surface waters of South Pacific (Kennedy and Robertson, 1995), −20.37‰ to −27.00‰ in the Subantarctic ocean south of Australia (O'Leary et al., 2001), and −23.87‰ to −30.62‰ in

surface waters between PF and Antarctic peninsula in the Atlantic (Lara et al., 2010).

Studies have reported that dominant species of phytoplankton and the cell size also have a major role in the POM characterisation and the $\delta^{13}C_{(POM)}$ signatures (Popp et al., 1998, 1999; Henley et al., 2012). The diagnostic pigment data affirmed the dominance of diatoms in these waters (Fig. 5d and e). Previous studies have revealed that diatom dominance can cause a shift in $\delta^{13}C_{(POM)}$ towards the more negative scale of isotopic ratio and can be as depleted as −26‰ to −29‰ and even −32‰ in the colder Antarctic waters, depending on the species abundance (Wada et al., 1987; Henley et al., 2012). The depletion of $\delta^{13}C$ in diatom-dominated waters was attributed to the low growth rates of diatoms and higher fractionation during photosynthetic carbon uptake (Sommer, 1989) in colder, nutrient replete polar waters. The diatom community in the colder polar frontal and Antarctic waters are reported to have a high-level accumulation of lipids, which are used as storage material and for repair and maintenance, especially in polar environments (Fahl and Kattner, 1993; Thomas and Dieckmann, 2002; Sackett et al., 2013). Many diatom species synthesise lipids depleted in ^{13}C, also fucoxanthin, that is one of the main diatom pigments that can contribute to the $\delta^{13}C$ depletion of diatoms and is subsequently reflected in $\delta^{13}C_{(POM)}$ (Sackett et al., 1965; Sinninghe Damsté et al., 2003; Henley et al., 2012). Phytoplankton microscopic analysis during this study revealed the dominance of *Fragilariopsis* spp., followed by *Thalassiosira* spp. *Cheatoceros* spp. (unpublished data), which had been reported to be the dominant species in the PFZ waters in earlier studies. Thus, they possibly contribute to the depleted $\delta^{13}C_{(POM)}$ values due to their lipid storage mechanism in colder waters.

The overall POM content of the PFZ euphotic water column had higher contribution of POC and PN compared to the STFZ and SAFZ, even though the Chl-*a* observed was highly variable within the PFZ water column. Chl-*a* contributed significantly in the photic waters, with a deeper DCM and comparatively higher column integrated Chl-*a* (33.9 mg/m^2 and 42.7 mg/m^2, at 50°S and 53°S, respectively) in the PFZ. Also, the $\delta^{13}C_{(POM)}$ was more depleted and the overall POC:Chl-*a* ratios were observed to be < 100 in this region (Fig. 5c) implying the dominance of autotrophy (Zeitzchel, 1970; Maksymowska et al., 2000; Savoye et al., 2003). It also revealed that the POM comprised primarily living matter and/or freshly produced organic matter. The C:N ratios were low (Table 2) in these waters due to the prevalence of diatoms. It is known that in nutrient replete condition, dominated by diatoms the C:N ratio is comparatively lower than the Redfield's ratio (6.63) as a result of a higher tendency towards uptake and storage of nutrients, mainly nitrates (Lomas and Glibert, 2000; Martiny et al., 2013). This implies, the POM in the PFZ was relatively fresh and includes a major contribution from phytoplankton. This also suggests that the POM characteristics and $\delta^{13}C_{(POM)}$ signatures in this region are mainly controlled by autotrophic processes and the dominant phytoplankton community.

5. Conclusions

From our study, it is evident that biological processes have a major role in determining the POM characteristics and $\delta^{13}C_{(POM)}$ signatures across the fronts in IOSO, although there is a high variability in the hydrographic features (temperature, salinity, wind, influence of eddy) in this region.

Within the euphotic waters of the STFZ and SAFZ, heterotrophy was the dominating process mainly resulting from the coupled activity of heterotrophic nanoflagellates and the abundance of micro and mesozooplankton in this region. Nonetheless, autotrophic processes, contributed considerably in defining the $\delta^{13}C_{(POM)}$. Also, the prevalence of eddy upwelling and eddy driven advection, are contributing physical factors towards the processes responsible for the POM characteristics observed within the euphotic zone in the current study. The PFZ is contrastingly different with the abundant availability of dissolved gases and nutrients for photosynthetic fixation of CO_2 into organic components, makes isotopic fractionation both during air-sea exchange (at the surface), and biological productivity (within column) a strong factor, along with the dominant phytoplankton community towards the characterisation of POM.

Authors contribution

Melena A. Soares: Conceptualization, data curation, writing, revising.
Parli V. Bhaskar: Resources, help in discussion.
N. Anilkumar: Resources, Hydrography data curation.
Ravidas K. Naik: Biological data curation.
Jenson V. George: Hydrography data curation.
Rajani Kanta Mishra: help in revision.
Deepti G Dessai: Chemistry data curation (nutrients).

Declaration of competing interest

The authors declare that they have no known competing financial interests or personal relationships that could have appeared to influence the work reported in this paper.

Acknowledgements

The authors would like to acknowledge the Director of NCPOR for the continued support of the Indian Southern Ocean Program. Our sincere thanks to the Ministry of Earth Sciences, India for funding this program. The authors also acknowledge Dr. Manish Tiwari and Mr. Siddesh Nagoji, for facilitating and carrying out IRMS analysis at MASTIL lab in NCPOR. The authors would like to thank Dr. C.T. Achuthankutty, expedition leader of ISOE-2012, for the support and leadership during the expedition. M. Soares, thanks Dr. Rajdeep Roy (NRSC) for his help. This is NCPOR's contribution number J- 46/2020-21.

Appendix A. Supplementary data

Supplementary data to this article can be found online at https://doi.org/10.1016/j.dsr2.2020.104851.

References

Abdel-Moati, Alaa R., 1990. Particulate organic matter in the subsurface chlorophyll maximum layer of the Southeastern Mediterranean. Oceanol. Acta 13, 307–315.
Alldredge, A.L., Passow, U., Logan, B.E., 1993. The abundance and significance of a class of large, transparent organic particles in the ocean. Deep-Sea Res. I 40, 1131–1140.
Anilkumar, N., Alvarinho, L., Somayaluju, Y.K., Ramesh Babu, V., Dash, M.K., Pednekar, S.M., Babu, K.N., Sudhakar, M., Pandey, P.C., 2006. Fronts, water masses and heat content variability in the Western Indian sector of the Southern Ocean during austral summer 2004. J. Mar. Syst. 63 (1–2), 20–34.
Archer, S.D., Leakey, R.J.G., Burkill, P.H., Sleigh, M.A., 1996. Microbial dynamics in coastal waters of East Antarctica: herbivory by heterotrophic dinoflagellates. Mar. Ecol. Prog. Ser. 139, 239–255.
Azam, F., Fenchel, T., Field, J.G., Gray, J.S., Meyer-Reil, L.A., Thingstad, F., 1983. The ecological role of water-column microbes in the sea. Mar. Ecol. Prog. Ser. 10, 257–263.
Belkin, I.M., Gordon, A.L., 1996. Southern Ocean fronts from the greenwich meridian to tasmania. J. Geophys. Res. 101, 3675–3696.
Benson, B., Krause, D., 1984. The concentration and isotopic fractionation of oxygen dissolved in freshwater and seawater in equilibrium with the atmosphere. Limnol. Oceanogr. 29 (3), 620–632.
Bentaleb, I., Fontugne, M., Descolas-Gros, C., Girardin, C., Mariotti, A., Pierre, C., Brunet, C., Poisson, A., 1998. Carbon isotopic fractionation by plankton in the Southern Indian Ocean: relation between $\delta^{13}C$ of particulate organic carbon and dissolved carbon dioxide. J. Mar. Syst. 17, 39–58.
Berg, G.M., Mills, M.M., Long, M.C., Bellerby, R., Strass, V., Savoye, N., Rottgers, R., Croot, P.L., Webb, A., Arrigo, K.R., 2011. Variation in particulate C and N isotope compostion following iron fertilization in two successive phytoplankton communities in the Southern Ocean. Global Biogochemical. Cy. 25, GB3013. https://doi.org/10.1029/2010GB003824.
Blain, S., Sedwick, P.N., Griffiths, F.B., Quequiner, B., Bucciarelli, E., Fiala, M., Pondaven, P., Treguer, P., 2002. Quantification of algal iron requirements in the Subantarctic Southern Ocean (Indian sector). Deep-Sea Res. II 49, 3255–3273.

Boyd, P.W., Ellwood, M.J., 2010. The biogeochemical cycle of iron in the ocean. Nat. Geosci. 3, 675–682.
Boyd, P., La Roche, J., Gall, M., Frew, R., McKay, R.M.L., 1999. Role of iron, light, and silicate in controlling algal biomass in subantarctic waters SE of New Zealand. J. Geophys. Res. 104, 13391–13404.
Boyd, P.W., Dillingham, P.W., McGraw, C.M., Armstrong, E.A., Cornwall, C.E., Feng, Y. Y., Hurd, C.L., Gault-Ringold, M., Roleda, M.Y., Timmins-Schiffman, E., Nunn, B.L., 2016. Physiological responses of a Southern Ocean diatom to complex future ocean conditions. Nat. Clim. Change 6, 207–213. https://doi.org/10.1038/nclimate2811.
Caron, D.A., Madin, P.L., Cole, J.J., 1989. Composition and degradation of salp fecal pellets: implications for vertical flux in oceanic environments. J. Mar. Res. 47, 829–850.
Checkley, D.M., Miller, C.A., 1989. Nitrogen isotope fractionation by oceanic zooplankton. Deep-Sea Res. A 36, 1449–1456.
Clarke, A., Meredith, M.P., Wallace, M.I., Brandon, M.A., Thomas, D.N., 2008. Seasonal and interannual variability in temperature, chlorophyll and macronutrients in northern Marguerite Bay, Antarctica. Deep-Sea Res. II 55, 1988–2006.
Coppola, L., Roy-Barman, M., Mulsow, S., Poninec, P., Jeandel, C., 2005. Low particulate organic carbon export in the frontal zone of the Southern Ocean (Indian sector) revealed by 234 Th. Deep-Sea Res. I 52, 51–68.
Cullen, J.J., 1982. The deep chlorophyll maximum: comparing vertical profiles of chlorophyll a. Can. J. Fish. Aquat. Sci. 39, 791–803.
Deacon, G.E.R., 1933. A general account of the hydrology of the Southern Atlantic Ocean. Discov. Rep. 7, 171–238.
Deppeler, S.L., Davidson, A.T., 2017. Southern Ocean phytoplankton in a changing climate. Front. Mar. Sci. 4 (40), 1–28. https://doi.org/10.3389/fmars.2017.00040.
Dubischar, C.D., Bathmann, U.V., 1997. Grazing impact of copepods and salps on phytoplankton in the Atlantic sector of the Southern Ocean. Deep-Sea Res. II 44, 415–433.
Eadie, B.J., Jeffrey, L.M., 1973. ^{13}C analyses of ocean particulate organic matter. Mar. Chem. 1, 199–209.
Fahl, K., Kattner, G., 1993. Lipid content and fatty acid composition of algal communities in sea-ice and water from the Weddell Sea (Antarctica). Polar Biol. 13, 405–409.
Fenchel, T., 2008. The microbial loop – 25-years later. J. Exp. Mar. Biol. Ecol. 366, 99–103. https://doi.org/10.1016/j.jembe.2008.07.013.
Francois, R., Altabet, M.A., Goericke, R., McCorkle, D.C., Brunet, C., Poisson, A., 1993. Changes in the $\delta^{13}C$ of surface water particulate organic matter across the subtropical convergence in the SW Indian Ocean. Global Biogeochem. Cycles 7 (3), 627–644.
Freudenthal, T., Neuer, S., Meggers, H., Davenport, G., Wefer, G., 2011. Influence of lateral particle advection and organic matter degradation on sediment accumulation and stable nitrogen isotope ratios along a productivity gradient in the Canary Islands region. Mar. Geol. 177, 93–109.
Gandhi, N., Ramesh, R., Laskar, A.H., Sheshshayee, M.S., Shetye, S., Anilkumar, N., Patil, S.M., Mohan, R., 2012. Variability in primary production and nitrogen uptake rates in the southwestern Indian Ocean and the Southern Ocean. Deep-Sea Res. I 67, 32–43.
Gaul, W., Anita, N.A., Koeve, W., 1999. Microzooplankton grazing and nitrogen supply of phytoplankton growth in the temperate and subtropical North east Atlantic. Mar. Ecol. Prog. Ser. 189, 93–104.
George, J.V., Anilkumar, N., Nuncio, M., Soares, M.A., Naik, R.K., Tripathy, S.C., 2018. Upper layer diapycnal mixing and nutrient flux in the subtropical frontal region of the Indian sector of the Southern Ocean. J. Mar. Syst. 187, 197–205.
Goericke, R., Fry, B., 1994. Variations of marine plankton $\delta^{13}C$ with latitude, temperature, and dissolved CO_2 in the world Ocean. Global Biogeochem. Cycles 8, 85–90.
Gomi, Y., Fukuchi, M., Taniguchi, A., 2010. Diatom assemblages at subsurface chlorophyll maximum layer in the eastern Indian sector of the Southern Ocean in summer. J. Plankton Res. 32 (7), 1039–1050.
Grasshoff, K., Ehrhardt, M., Kremling, K., 1983. Methods of Seawater Analysis, second ed.s. Verlag Chemie, Weinheim, Germany.
Gruber, N., Keeling, C.D., Bacastow, R.B., Guenther, P.R., Lueker, T.J., Wahlen, M., Meijer, H.A.J., Mook, W.G., Stocker, F.T., 1999. Spatiotemporal patterns of carbon-13 in the global surface oceans and the oceanic Suess effect. Global Biogeochem. Cycles 13 (2), 307–335.
Hall, J.A., James, M.R., Bradford-Grieve, J.M., 1999. Structure and dynamics of the pelagic microbial food web of the Subtropical convergence region east of New Zealand. Aquat. Microb. Ecol. 20, 95–105.
Harvey, H.R., Tuttle, J.H., Bell, J.T., 1995. Kinetics of phytoplankton decay during simulated sedimentation-changes in biochemical composition and microbial activity under oxic and anoxic conditions. Geochem. Cosmochim. Acta 59, 3367–3377.
Hayes, J. M, 1993. Factors controlling ^{13}C contents of sedimentary organic compounds: principles and evidence. Marine Geology 113, 111–125.
Henley, S.F., Annett, A.L., Ganeshram, R.S., Carson, D.S., Weston, K., Crosta, X., Tait, A., Dougans, J., Fallick, A.E., Clarke, A., 2012. Factors influencing the stable carbon isotopic composition of suspended and sinking organic matter in the coastal Antarctic sea ice environment. Biogeosciences 9, 1137–1157.
Jasmine, P., Muraleedharan, K.R., Madhu, N.V., Asha Devi, C.R., Alagarsamy, R., Achuthankutty, C.T., Jayan, Z., Sanjeevan, V.N., Sahayak, S., 2009. Hydrographic and production characteristics along 45°E longitude in the southwestern Indian Ocean and Southern Ocean during austral summer 2004. Mar. Ecol. Prog. Ser. 389, 97–116.
Jena, B., Sahu, S., Avinash, K., Swain, D., 2013. Observation of oligotrophic gyre variability in the south Indian Ocean: environmental forcing and biological response. Deep-Sea Res. I 80, 1–10.
Jullion, L., Heywood, K.J., Naveira Garabato, A.C., Stevens, D.P., 2010. Circulation and water mass modification in the Brazil–Malvinas Confluence. J. Phys. Oceanogr. 40, 845–864.
Kaehler, S, Pakhomov, E.A., Mcquaid, C.D., 2000. Tropical structure of the marine food web at the Prince Edward Islands (Southern Ocean) determined by $\delta^{13}C$ and $\delta^{15}N$ analysis. Mar. Ecol. Prog. Ser. 208, 13–20.
Kahru, M., Mitchell, B.G., Gille, S.T., Hewes, C.D., Holm-Hansen, O., 2007. Eddies enhance biological production in the weddell-scotia confluence of the Southern Ocean. Geophys. Res. Lett. 34, L14603. https://doi.org/10.1029/2007GL030430.
Kara, A.B., Rochford, P.A., Hurlburt, H.E., 2003. Mixed layer depth variability over the global ocean. J. Geophys. Res. 108 (C3), 3079. https://doi.org/10.1029/2000jc000736.
Kennedy, H., Robertson, J., 1995. Variations in the isotopic composition of particulate organic carbon in surface waters along an 88°W transect from 67°S to 54°S. Deep-Sea Res. II 42, 1109–1122.
Kling, G.W., Fry, B., Brien, W.J.O., 1992. Stable isotopes and planktonic trophic structure in Arctic lakes. Ecology 73, 561–566.
Kolasinski, J., Kaehler, S., Jaquemet, S., 2012. Distribution and sources of particulate organic matter in a mesoscale eddy dipole in the Mozambique Channel (Southwestern Indian Ocean): insites of C and N stable isotopes. J. Mar. Syst. 96–97, 122–131.
Lara, R.J., Alder, V., Franzosi, C.A., Kattner, G., 2010. Characteristics of suspended particulate organic matter in the southwestern Atlantic: influence of temperature, nutrient and phytoplankton features on the stable isotope signature. J. Mar. Syst. 79, 199–209.
Leblanc, K., Queguiner, B., Fiala, M., Blain, S., Morvan, J., Corvaisier, R., 2002. Particulate biogenic silica and carbon production rates and particulate matter distribution in the Indian sector of the Subantarctic Ocean. Deep-Sea Res. II 49, 3189–3206.
Liu, F., Yin, K., He, L., Tang, S, Yao, J., 2018. Influence on phytoplankton of different developmental stages of mesoscale eddies off eastern Australia. Journal of Sea Research 137, 1–8.
Llido, J., Garçon, V., Lutjeharms, J.R.E., Sudre, J., 2005. Event-scale blooms drive enhanced primary productivity at the subtropical convergence. Geophys. Res. Lett. 32, L15611. https://doi.org/10.1029/2005GL022880.
Lomas, M.W., Glibert, P.M., 2000. Comparisons of nitrate uptake, storage, and reduction in marine diatoms and flagellates. J. Phycol. 36, 903–913.
Lourey, M.J., Trull, T.W., Tilbrook, B., 2004. Sensitivity of $\delta^{13}C$ of Southern Ocean suspended and sinking organic matter to temperature, nutrient utilization, and atmospheric CO_2. Deep-Sea Res. I 51 (2), 281–305.
Maksymowska, D., Richard, P., Piekarek-Jankowska, H., Riera, P., 2000. Chemical and isotopic composition of the organic matter sources in the Gulf of Gdansk (southern Baltic Sea). Estuar. Coast Shelf Sci. 51, 585–598.
Marañón, E., Beherenfeld, M.J., González, N., Mouriño, B., Zubkov, M.V., 2003. High variability of primary production in oligotrophic waters of the Atlantic Ocean: uncoupling from phytoplankton biomass and size structure. Mar. Ecol. Prog. Ser. 257, 1–11.
Marshall, J.T., Radko, T., 2003. Residual-mean solutions for the Antarctic circumpolar current and its associated overturning circulation. J. Phys. Oceanogr. 33, 2341–2354.
Martin, J.H., Fritzwater, S.E., Gordon, R.M., 1990. Iron deficiency limits phytoplankton growth in Antarctic waters. Global Biogeochem. Cycles 4, 5–12.
Martineau, C., Vincent, Q.F., Frenette, J.J., Dodson, J., 2004. Primary consumers and particulate organic matter: isotopic evidence of strong selectivity in the estuarine transition zone. Limnol. Oceanogr. 49, 1679–1686.
Martiny, A.C., Vrugt, J.A., Primeau, F.W., Lomas, M.W., 2013. Regional variation in the particulate organic carbon to nitrogen ratio in the surface waters. Global Biogeochem. Cycles 27 (3), 723–731.
Maya, M.V., Soares, M.A., Agnihotri, R., Prathihary, A.K., Karapurkar, S., Hema, N., Naqvi, S.W.A., 2011. Variations in some environmental characteristics including C and N stable isotopic composition of suspended organic matter in the Mandovi estuary. Environ. Monit. Assess. 175 (1–3), 501–517.
McGillicuddy, D.J., Robinson, A.R., Siegel, D.A., Jannasch, H.W., Johnson, R., Dickey, T. D., McNeil, J., Michaels, A.F., Knap, A.H., 1998. Influence of mesoscale eddies on new production in the Sargasso Sea. Nature 394, 263–266.
Mino, Y., Saino, T., Suzuki, K., Marañón, E., 2002. Isotopic composition of suspended particulate nitrogen (δ15Nsus) in surface waters of the Atlantic Ocean from 50°N to 50°S. Global Biogeochem. Cycles 16 (4), 7–9.
Minu, R.L., Gopalakrishnan, T., Asha Devi, C.R., Pillai, H.U.K., Sanjeevan, V.N., Achutankutty, C.T., 2015. Micro and Mesozooplankton community structure at the Subtropical and Polar fronts during austral summer. In: Southern Ocean Expedition, pp. 25–29, 2012 Technical report 2012.
Naik, R.K., George, J.V., Soares, M.A., Asha Devi, C.R., Anilkumar, N., Roy, R., Bhaskar, P.V., Murukkesh, N., Achuthankutty, C.T., 2015. Phytoplankton community structure at the juncture of the agulhas return front and subtropical front in the Indian Ocean sector of Southern Ocean: bottom-up and top-down control. Deep-Sea Res. II 118, 233–239.
Nelson, D.M., Smith, W.O., 1991. Sverdrup visited: critical depths, maximum chlorophyll levels, and the control of Southern Ocean productivity by the irradiance-mixing. Limnol. Oceanogr. 36, 1650–1661.
Nielsen, E.S., Hansen, V.K., 1959. Light adaptation in marine phytoplankton populations and its interrelation with temperature. Physiol. Plantarum 12, 353–370.
Aumont, Olivier, Hulten Marco van, Matthieu, Roy-Barman, Jean-Claude, Dutay, Christian, Éthé, Marion, Gehlen, 2017. Variable reactivity of particulate organic matter in a global ocean biogeochemical model. Biogeosciences 14, 2321–2341.

Omand, M.M., Perry, M.J., D'Asaro, E., Lee, C., Briggs, N.A., Cetinic, I., Mahadevan, A., 2015. Eddy-driven subduction exports particulate organic carbon from the spring bloom. Science 348 (6231), 222–225.
Owens, N.J.P., Rees, A.P., 1989. Determination of N-15 at sub-microgram levels of nitrogen using automated continuous-flow isotope ratio mass-spectrometry. Analyst 114, 1655–1657.
O'Leary, T., Trull, T.W., Griffiths, F.B., Tilbrook, B., Revill, A.T., 2001. Euphotic zone variations in bulk and compound-specific 13C of suspended organic matter in the subantarctic ocean, south of Australia. J. Geophys. Res. Oceans 106, 31669–31684.
Park, Y.H., Charriaud, E., Fieux, M., 1998. Thermohaline structure of the Antarctic surface waters/winter water in the Indian sector of the Southern Ocean. J. Mar. Syst. 17, 5–23.
Parslow, J.S., Moyd, P.W., Rintoul, S.R., Griffits, M.F., 2001. A persistent subsurface chlorophyll maximum in the Interpolar Frontal Zone south of Australia: seasonal progression and implications for phytoplankton-light-nutrient interactions. J. Geophys. Res. 106 (31), 557, 543-31.
Perissinotto, R., Mayzaud, P., Nichols, P.D., Labat, J.P., 2007. Grazing by pryosoma *atlanticum* (tunicata, thaliacea) in the South Indian ocean. Mar. Ecol. Prog. Ser. 330, 1–11.
Pillai, H.U.K., Anilkumar, N., Achuthankutty, C.T., Mendes, C.R., Sabu, P., Jayalakshmi, K.V., Asha Devi, C.R., Dessai, D., George, J., Pavithran, S., Hari Devi, C. K., Tripathy, S.C., Menon, N.R., 2018. Planktonic food web structure at SSTF and PF in the Indian sector of the Southern Ocean during austral summer 2011. Polar Res. 37, 1495545. https://doi.org/10.1080/17518369.2018.1495545.
Pollard, R., Lucas, M., Read, J., 2002. Physical controls on biogeochemical zonation in the Southern Ocean. Deep-Sea Res. Part II 49, 3289–3305. https://doi.org/10.1016/S0967-0645(02)00084-X.
Pollehne, F., Klein, B., Zeitzschel, B., 1993. Low light adaptation and export production in the deep chlorophyll maximum layer in the northern Indian Ocean. Deep-Sea Res. II 40, 737–752.
Popp, B.N., Laws, E.A., Bidigare, R.R., Dore, J.E., Hanson, K.L., Wakeham, S.G., 1998. Effect of phytoplankton cell geometry on carbon isotopic fractionation. Geochim Cosmochim. Ac. 62 (1), 69–77.
Popp, B.N., Trull, T., Kenig, F., Wakeham, S.G., Rust, T.M., Tilbrook, B., Griffiths, B.F., Wright, S.W., Marchant, H.J., Bidigare, R.R., Laws, E.A., 1999. Controls on the carbon isotopic composition in Southern Ocean phytoplankton. Global Biogeochem. Cycles 13 (4), 827–843.
Prahl, F.G., Dymond, J., Sprarrow, M.A., 2000. Annual biomarker record for export production in the central Arabian Sea. Deep-Sea Res. II 47, 1581–1604.
Prasanna, K., Ghosh, P., Anilkumar, N., 2015. Stable isotopic signatures of Southern Ocean deep water CO_2 ventilation. Deep-Sea Res. II 118, 177–185.
Rau, G.H., Takahashi, T., Marais, D.J.D., Repeta, D.J., Martin, J.H., 1992. The relationship between $\delta^{13}C$ of organic matter and $[CO_2(aq)]$ in ocean surface water: data from a JGOFS site in the northeast Atlantic Ocean and a model. Geochim Cosmochim Ac. 56 (3), 1413–1419.
Rintoul, S.R., Naveira Garabato, A.C., 2013. Chapter 18 – dynamics of the Southern Ocean circulation. In: Gerold, Siedler, Stephen, M., Griffies, J.G., Church, J.A. (Eds.), Ocean Circulation and Climate A 21st Century Perspective, 103. Academic Press, Int. Geophys., pp. 471–492
Robinson, C., Ramaiah, N., 2011. Microbial heterotrophic metabolic rates constrain the microbial carbon pump, Microbial Carbon Pump in the Ocean. The American Association for the Advancement of Science 52–53. USA.
Sabu, P., Anilkumar, N., George, J.V., Chacko, R., Tripathy, S.C., Achuthankutty, C.T., 2014. The influence of air-sea-ice interactions on an anomalous phytoplankton bloom in the Indian Ocean sector of the Antarctic zone of the Southern Ocean during the austral summer. Pol. Sci. 8 (4), 370–384, 2011.
Sabu, P., George, J.V., Anilkumar, N., Chacko, R., Valsala, V., Achuthankutty, C.T., 2015. Observations of watermass modification by mesoscale eddies in the southern subtropical Indian Ocean. Deep-Sea Res. II 118 (B), 152–161.
Sackett, W.M., Eckelmann, W.R., Bender, M.L., Be, A.W.H., 1965. Temperature dependence of carbon isotopic composition in marine plankton and sediments. Science 148, 235–237.
Sackett, O., Petrou, K., Reedy, B., De Grazia, A., Hill, R., Doblin, M., Beardall, J., Ralph, P., Heraud, P., 2013. Phenotypic plasticity of Southern Ocean diatoms: key to success in the sea ice habitat? PloS One 8 (11), e81185. https://doi.org/10.1371/journal.pone.0081185.
Sakshaug, E., Slagstad, D., 1991. Light and productivity of phytoplankton in polar marine ecosystems. Polar Res. 10, 69–85.
Savoye, N., Aminot, A., Treguer, P., Fontugne, M., Naulet, N., Kerouel, R., 2003. Dynamics of particulate organic matter $\delta^{15}N$ and $\delta^{13}C$ during spring phytoplankton blooms in a macrotidal ecosystem (Bay of Seine, France). Mar. Ecol. Prog. Ser. 255, 27–41.
Sherr, E.B., Sherr, B.F., 2007. Heterotrophic dinoflagellates: a significant component of microzooplankton biomass and major grazers of diatoms in the sea. Mar. Ecol. Prog. Ser. 352, 187–197.
Shetye, S., Mohan, Rahul, Patil, S., Jena, B., Chacko, R., George, J.V., Noronha, S., Singh, N., Lakshmi, P., 2015. Oceanic pCO_2 in the Indian sector of the Southern Ocean during the austral summer-winter transition phase. Deep-Sea Res. II 118, 250–260.
Sinninghe Damsté, J.S., Rampen, S., Irene, W., Rupstra, C., Abbas, B., Muyzer, G., Schouten, S., 2003. A diatomaceous origin for long-chain diols and mid-chain hydroxy methyl alkanoates widely occurring in Quaternary marine sediments: indicators for high-nutrient conditions. Geochem. Cosmochim. Acta 67, 1339–1348.
Soares, M.A., Bhaskar, P.V., Naik, R.K., Dessai, D.R.G., George, J.V., Tiwari, M., Anilkumar, N., 2015. Latitudinal $\delta^{13}C$ and $\delta^{15}N$ variations in particulate organic matter (POM) in surface waters from the Indian Ocean sector of Southern Ocean and the tropical Indian ocean in 2012. Deep-Sea Res. 2 (118), 186–196. B.
Sokolov, S., Rintoul, S.R., 2002. Structure of Southern Ocean fronts at 140°E. J. Mar. Syst. 37, 151–184.
Sommer, U., 1989. Maximal growth rates of Antarctic phytoplankton: only weak dependence on cell size. Limnol. Oceanogr. 34, 1109–1112.
Thomas, D.N., Dieckmann, G.S., 2002. Antarctic sea ice-a habitat for extremophiles. Science 295, 641–644.
Tremblay, L., Caparros, J., Leblanc, K., Obernosterer, I., 2015. Origin and fate of particulate and dissolved organic matter in a naturally iron-fertilized region of the Southern Ocean. Biogeosciences 12, 607–621.
Tripathy, S.C., Pavithran, S., Sabu, P., Pillai, H.U.K., Dessai, D.R.G., Anilkumar, N., 2015. Deep chlorophyll maximum and primary productivity in Indian Ocean sector of the Southern Ocean: case study in the Subtropical and Polar Front during austral summer 2011. Deep-Sea Res. II 118 (B), 240–249.
Tripathy, S.C., Patra, Sivaji, Vishnu Vardhan, K., Sarkar, A., Mishra, R.K., Anilkumar, N., 2018. Nitrogen uptake in the surface waters of the Indian sector of Southern Ocean during austral summer. Front. Earth Sci. 12 (1), 52–62.
Tynan, C.T., 1998. Ecological importance of the southern boundary of the antarctic circumpolar current. Nature 392, 708–710.
van Heukelem, 2002. HPLC phytoplankton pigments: sampling, laboratory methods and quality assurance procedure. In: Mueller, J., Fragion, G. (Eds.), Ocean Optics Protocols for Satellite Ocean Color Sensor, 2. NASA technical memorandum 2002-210004, pp. 258–268. Revision 3.
Venkataramana, V., Anilkumar, N., Swalding, K., Mishra, R.K., Tripathy, S.C., Sarkar, A., Soares, M.A., Sabu, P., Pillai, H.U.K., 2020. Distribution of zooplankton in the Indian sector of the Southern Ocean. Antarct. Sci. https://doi.org/10.1017/S0954102019000579.
Verity, P.G., 2000. Grazing experiments and model simulations of the role of zooplankton in phaeocystis food webs. J. Sea Res. 43, 317–343.
Volk, T., Hoffert, M.I., 1985. Ocean Carbon Pumps: analysis of relative strengths and efficiencies in ocean driven atmospheric CO_2 changes. In: Sundquist, E.T., Broecker, W.S. (Eds.), The Carbon Cycle and Atmospheric CO_2: Natural Variations Archean to Present. American Geophysical Union, Washington, D.C, pp. 99–110, 99-110.
Wada, E., Terasaki, M., Kabaya, Y., Nemoto, T., 1987. ^{15}N and ^{13}C abundances in the Antarctic Ocean with emphasis on biogeochemical structure of food web. Deep-Sea Res. 34, 829–841.
Waite, A.M., Muhling, B.A., Holl, C.M., Beckley, L.E., Montoya, J.P., Strzelecki, J., Thompson, P.S., Presant, S., 2007. Food web structure in two counter-rotating eddies based on $\delta^{15}N$ and $\delta^{13}C$ isotopic analysis. Deep Sea Res II 54, 1055–1075.
Zeitzschel, B., 1970. The quantity, composition and distribution of suspended particulate matter in the Gulf of California. Mar. Biol. 7, 305–318.
Zhang, R., Zheng, M., Chen, M., Ma, Q., Cao, J., Qiu, Y., 2014. An isotopic perspective on the correlation of surface ocean carbon dynamics and sea ice melting in Prydz Bay (Antarctica) during austral summer. Deep-Sea Res. I 83, 24–33.

Polar Science 25 (2020) 100551

Contents lists available at ScienceDirect

Polar Science

journal homepage: http://www.elsevier.com/locate/polar

Nutrient dynamics at the juncture of Agulhas Return Front and subtropical front in the Indian sector of the Southern Ocean during the austral summer

Melena A. Soares *, P. Sabu, J.V. George, R.K. Naik, N. Anilkumar, Deepti G. Dessai

National Centre for Polar and Ocean Research, Ministry of Earth Sciences, Goa, India

ARTICLE INFO

Keywords:
Degree of nutrient consumption
Nutrient utilization
Agulhas return front
Subtropical front

ABSTRACT

The northern boundary of the Indian sector of Southern Ocean is marked by the juncture of the Agulhas Return Front and the southern Subtropical Front and is a hydrographically dynamic region. During austral summer, a time series study (13th to 15th January 2012) was conducted in this region (40°S, 58°30′E) to discuss the episodic biochemical changes with respect to nutrient dynamics within the upper (120 m) water column. The observed nitrate was depleted in the upper 50 m. However, there was an influx of nitrate at 6 and 18 h of Day-1. Even though the nitrate was exceptionally low, the system was moderately productive, suggesting the rapid utilization of nitrate at this location. Also, the Degree of Nutrient Consumption, was high at 50 m (~0.4), compared to the rest of the water column indicating the presence of aged/old upwelled waters at 50 m. The observed influx of nutrients could be attributed to the wind induced mixing as well as the wind stress curl driven pumping at the periphery of the anticyclonic eddy at the location. Although the influx of nutrients was low, there was the rapid utilization of nutrients, which triggered a switch in the phytoplankton community structure and subsequently influencing the biogeochemical cycle.

1. Introduction

The Southern Ocean (SO) acts as a link between the Indian, Atlantic, and Pacific Oceans. It is associated with many oceanic currents that help in the transport of heat, salts, and other components across the world oceans (Caldeira and Duffy, 2000). The SO is characterized by a confluence of different water masses and include oceanic fronts, which possess distinct hydrographic properties and biogeochemical features (Deacon, 1933). The Indian Sector of the SO (ISSO) includes a special feature, that is, the Aghulas Return Front (ARF) and marks the northern boundary of the SO (Anilkmuar et al., 2006). The ARF is associated with the Agulhas Return Current (ARC) that flows eastwards up to ~50°S, resulting in surface currents and meanders (Pollard and Read, 2017). The ARC flows parallel to the Subtropical Front (STF) and is influenced by mesoscale eddies (Lutjeharms and Ansorge, 2001; Ansorge and Lutjeharms, 2005). A study by Anilkumar et al. (2006) has revealed that the ARF and STF merge in some regions of the ISSO. The region of the merger is a highly dynamic region, both in terms of hydrography due to eddy shedding and its meandering as well as biogeochemical processes (Machu and Garçon, 2001; Machu et al., 2005; Anilkumar et al., 2006). Also, the STF-ARF merger exhibits higher degree of horizontal variability due to eddies which promotes the faster meridional transport of various biochemical components like nutrients, salts, etc. from subtropics to the polar region (Sabu et al., 2015; George et al., 2018).

The STF-ARF convergence zone is oligotrophic with specifically low nitrate (Read et al., 2000) compared to other southern fronts in the SO. The biological productivity in this region is also low and is often supported by an influx of nutrients from subsurface (Machu et al., 2005; Jena et al., 2013). This region is reported to be dominated by the phytoplankton group haptophyes, mostly flagellates (Schlüter et al., 2011; Naik et al., 2015). However, the micro and meso zooplankton abundance was reported to be lower at the ARF, compared to the STF of the ISSO (Jasmine et al., 2009). Being a hydrographically and biogeochemically dynamic region, a detailed study of the region is warranted.

In recent decades, studies were undertaken to quantify the nutrients supplied (Pollard et al., 2002), nutrient cycling (DeMaster, 2002; Crosta et al., 2005), planktonic utilization of nutrients (Goeyens et al., 1998), and the export of nutrients out of the SO (Hauck et al., 2018) and many others using *in-situ* nutrients data, satellite, model based data and also sediment core, or a combination of more than one data sources.

Even though the studies in the ISSO have increased over time, this

* Corresponding author.
E-mail address: melena@ncpor.res.in (M.A. Soares).

https://doi.org/10.1016/j.polar.2020.100551
Received 9 October 2019; Received in revised form 26 May 2020; Accepted 11 June 2020
Available online 17 June 2020

region is yet understudied as compared to the other sectors of the SO. Earlier studies in the ISSO were addressed to comprehend the nutrient distribution (Rajkumar et al., 2008) and nitrogen uptake (Gandhi et al., 2012; Prakash et al., 2015) across the fronts in this area. These studies have revealed the limitation of nitrogen north of the subtropical front. Although the region is nitrogen depleted, the system is moderately productive, which leads to the need for a better understanding of the nutrient dynamics at this juncture region of the ARF and STF.

The ARF-STF juncture is an eddy prone region accompanied with upwelling and downwelling processes. Earlier studies have revealed that eddies and associated submesoscale physical processes influence the nutrient supply to the photic waters (McGillicuddy and Robinson, 1997; Mahadevan et al., 2008), altering the biological productivity of the region (Mahadevan, 2016). In order to determine the status/age of the upwelled waters, Chen et al. (2004) introduced a parameter called Degree of nutrient consumption (DNC) and was based on nitrates and chlorophyll content of the waters. DNC was based on the assumption that the subsurface waters have higher inorganic nutrient content and lower chlorophyll. Thus, suggesting lower DNC as an indicator of higher utilization of inorganic nutrients supplied from upwelling of subsurface waters during photosynthetic fixation to organic compounds in the photic waters. The present study, attempts to address the nutrient dynamics in terms of its temporal variability over a period of 48 h at the merger of ARF and STF. In this study, DNC is applied as an index to understand the consumption of nitrates supplied to the nutrient depleted photic waters, as the location is associated with episodic supply of nutrients to the photic waters by a combination of submesoscale processes.

2. Material and methods

2.1. Study site and sample collection

Seawater samples were collected on-board *ORV Sagar Nidhi* during an expedition in December 2011–January 2012. For the current study, a two day time series from 13th to 15th January 2012 (48 h) was carried out at a 6 hourly interval at 40°S, 58.30°E (Fig. 1), however, the CTD operations for hydrography studies were carried out at a 3 hourly interval. This location is at the juncture of the ARF and STF, a cross frontal region where the ARF and the STF merge. During the 48 h sampling, utmost care was taken that the ship was at the same location and maintained position using the Dynamic Positioning (DP) system of the vessel during the entire period except during the operation of vertical microstructure profiler. The vessel was brought back to the initial location after each profiler operation to avoid any change in the properties of the water column due to drifting of the vessel. The wind data from the onboard Automatic Weather Station was used. Also, the daily winds data from Advanced Scatterometer (ASCAT) of APDRC (http://apdrc.soest.hawaii.edu) and Sea Surface Height Anomaly (SSHA) data from the Copernicus Marine Environment Monitoring Service (http://marine.copernicus.eu/) for the study period was also used. From SSHA, residual components (u′ and v′) were computed. The daily wind vectors (wind speed with corresponding u and v components) from the ASCAT was used to compute the curl of the wind. The average wind stress curl was calculated for the region from 58°E to 59°E and 39°S to 40°S. The wind stress (τ) was calculated using a constant drag coefficient (1.2×10^{-3}) and air density (1.3 kgm^{-3}). Ekman pumping velocity was also calculated using the equation,

$$w = curl\ \frac{(\tau)}{\rho f} \tag{1}$$

Where ρ *is the density of sea water and f is the coriolis parameter.*

Samples were collected from 7 different depths (0, 10, 30, 50, 75, 100, 120) using Niskin bottles mounted on a CTD rosette. Hydrography data (temperature & salinity) was obtained from CTD (Seabird Electronics, SeaCAT21). MSS90L Microstructure profiler (Sea & Sun Technology, Germany) was used to infer the turbulent kinetic energy (TKE) dissipation rate in the study region. The steps followed for processing of the microstructure profiler data is described in George (2015). Based on the position of the nitricline, we have divided the water column into two sections, 0–60 and 60–120 m for which the average TKE dissipation rate was represented. Sub-sampled for the analysis of dissolved oxygen (DO), dissolved inorganic Carbon (DIC), nutrients (stored at −20 °C, until analysis), Chlorophyll *a* (filtered through GF/F Whatman filters and stored at −20 °C, until analysis). Monthly mean Chlorophyll data from the satellite MODIS aqua (https://coastwatch.pfeg.noaa.gov/) was also used to understand the chlorophyll variability in the study region during the observation period.

2.2. Sample analysis

Sub-samples for DO were fixed with Winkler's A and Winkler's B, and analysed following Winkler's method (Grasshoff et al., 1983) using an auto-titrator. The apparent oxygen utilization (AOU) was calculated as the difference of oxygen gas solubility ($O_{2(sat)}$) and the measured oxygen concentration (O_2). Oxygen gas solubility was calculated as a function of *in situ* temperature and salinity and one atmosphere of total pressure (Benson and Krause, 1984) assuming that the surface waters are near saturation.

$$\text{Apparent Oxygen Utilization (AOU)} = O_{2\ (sat)} - O_2 \tag{2}$$

Seawater samples were analysed for nitrate, nitrite, ammonium, phosphate and silicate, by auto-analyser (Model: Skalar Analytical San++ 8505 Interface v3.05, the Netherlands) following standard colorimetric methods (Grasshoff et al., 1983). The standard deviation for all nutrients analysed was ±1%. The Geochemical tracers, *N** & *Si**

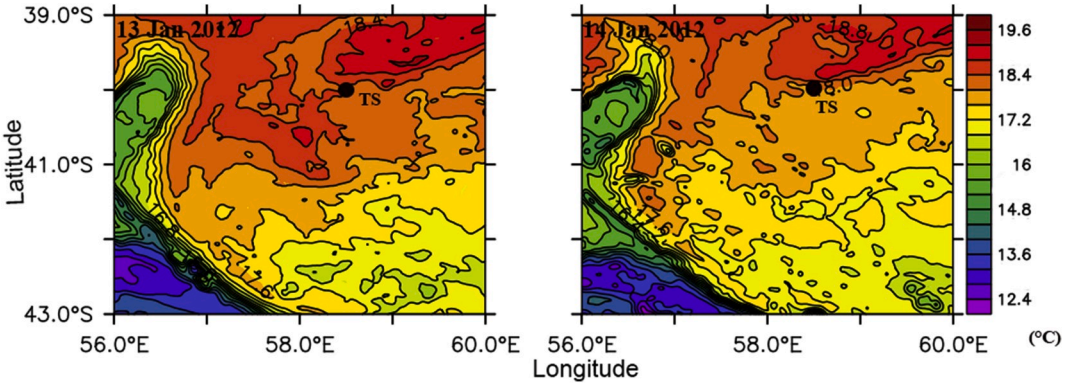

Fig. 1. Time series sampling location (40° S, 58°30′ E) overlaid on AVHRR Sea Surface Temperature (SST) for 13th and 14th January 2012 (station location is marked as black dot).

were used to understand the utilization of nitrates and silicates and its influence on the phytoplankton community (Sarmeinto et al., 2004), in the study area. *N** and *Si** was calculated as follows:

$$N^* = NO_3 - 16PO_4 \quad (3)$$

$$Si^* = Si(OH)_4 - NO_3 \quad (4)$$

Chlorophyll *a* (Chl-*a*) and photosynthetic pigment analysis were carried out by fluorometry and HPLC, as mentioned in Naik et al. (2015).

The Degree of Nutrient Consumption (DNC_c), was calculated based on chlorophyll (Chen et al., 2004). The index was calculated to measure the response of phytoplankton to nitrate and nitrite as expressed below:

$$DNC_c = 0.7xChl/(NO_3^- + NO_2^-) + (0.7xChl) \quad (5)$$

3. Results

3.1. Hydrography and wind

During the observation period, large variability was noticed in the distribution of winds. The wind speed was high (~5 m/s) at the 0:00 h observation, decreased to ~1 m/s at 03:00 h and remained low with minor fluctuations for the remaining period of Day-1. However, there was an increase in wind speed from 24:00 h, and continued to increase in the entire Day-2 of observation to a maximum of >10 m/s at 48:00 h (Fig. 2a). A similar wind pattern was also observed in the satellite data, with a cyclonic circulation of the winds at the location on Day-1 (Fig. 6). It was also noted in the upper column (~18 m), the temperature was ~17.5 °C at 00:00 h of Day-1. An upward sloping of 17.5 °C isotherm from around 30 m was noticed at 03:00 h, and it decreased the surface temperature by 0.1 °C (Fig. 2b). The Mixed Layer Depth (MLD) was at <20 m within which the temperature was almost uniform through the study period, except between 0:00 to 06:00 h of Day-1 and 24:00 to 27:00 h of Day-2 during which the MLD was comparatively deeper (~40 m). Below the MLD, the temperature decreased with strong thermal gradients especially between 40 m and 80 m. The upper column salinity was almost uniform (~35.54) throughout the study period, except at 00:00 h, 03:00 h, 24:00 h and 42:00 h. The salinity was less (<35.54) at 00:00 h where as higher salinity (>35.54) was noticed at 03:00 h, 24:00 h and 42:00 h. During the present study the upper water column was identified as the subtropical surface water [T > 12; S > 35.1 (Anilkumar et al., 2014)]. However, the distribution of isohalines showed oscillations during Day-1, the maximum shift in the isohaline was noticed at 00:00 h of Day-1 (Fig. 2c), and it was observed that the 35.4 contour was shifted from deeper depths about 120 m–60 m indicating the signatures of a short-term upwelling event. The potential density showed a similar variability as that of temperature and salinity (Fig. 2d). Fig. 2e shows the average of the turbulent kinetic energy (TKE) dissipation rate of the upper 60 m and the average of below 60 m (60–120 m) of the study region. The TKE dissipation rate was moderately high (10^{-7} to 10^{-8} W/kg) in the upper 60 m till 18:00 h. Between 18:00 and 30:00 h the TKE dissipation was low ($<10^{-8}$ W/kg) in the upper 60 m compared to the bottom region (60–120 m). After 30:00 h, the TKE dissipation in the upper layer was considerably high ($>10^{-7}$ W/kg) than the lower layer (Fig. 2e).

Since the study region is an eddy prominent area, we have analysed the daily SSHA to understand the role of eddies on this thermohaline structure variability. The AVHRR and SSHA images suggest that the study location was at the periphery of a strong anticyclonic eddy (Figs. 1 and 5). The observed anticyclonic eddy was almost circular in shape with a radius of approximately 110 km. The geostrophic currents show a strong antic-clock wise rotation at the study location with a magnitude of 55 cm/s.

3.2. Chlorophyll, dissolved oxygen and nutrients variability

The observed Chl-*a* was lower in the MLD, throughout the study, with a well defined Deep Chlorophyll Maxima (DCM) at ~50–60 m (except at 24:00 and 36:00 h, where DCM was weak). Although, the surface Chl-*a* low it was more than doubled with an average of 0.68 ± 0.22 mg/m^3 at the DCM (Fig. 3a), and was comparable with earlier studies in this region. Also, DO had an average of 236.16 ± 8.74 μM (Table 1), with maximum oxygen being observed at ~50 m coinciding with the depth of the DCM (Fig. 3b). In general, the observed nitrate was low (below detection level) in the upper water column (up to ~60 m) (Fig. 3c). However, elevated nitrate were observed much below the MLD, and was mostly below 80 m, except at 18:00 h, 30:00 h and 48:00

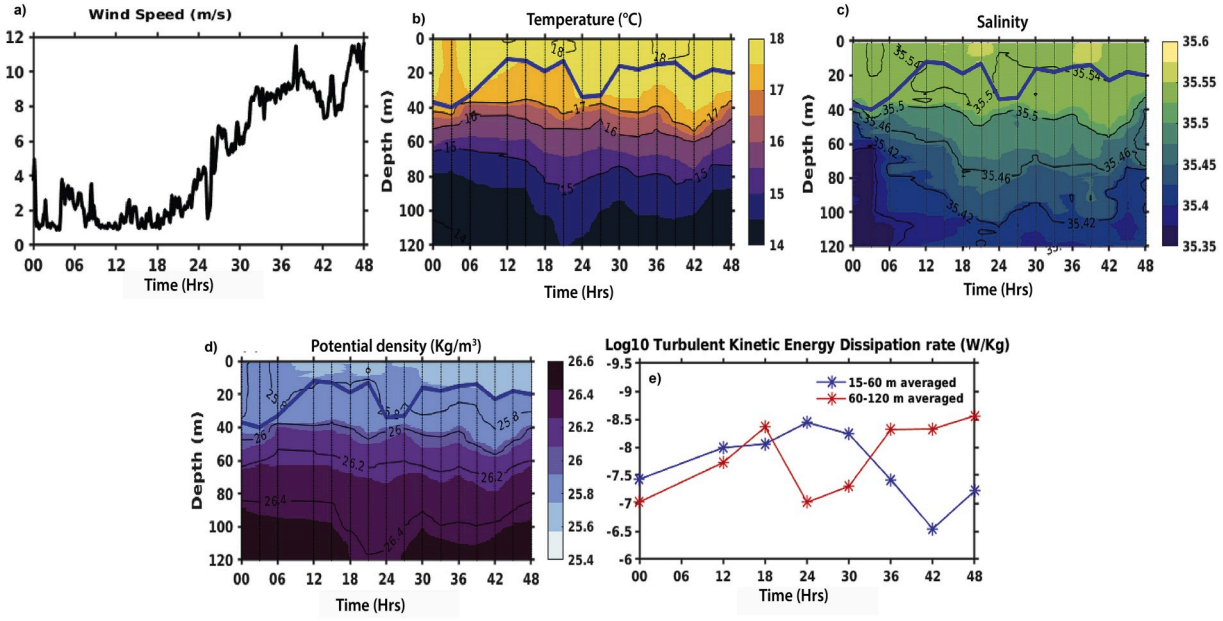

Fig. 2. Time evolution of a) Wind speed, Time-depth evolution of b) Temperature, c) Salinity d) potential density, e) Turbulence kinetic Energy (TKE) dissipation rate.

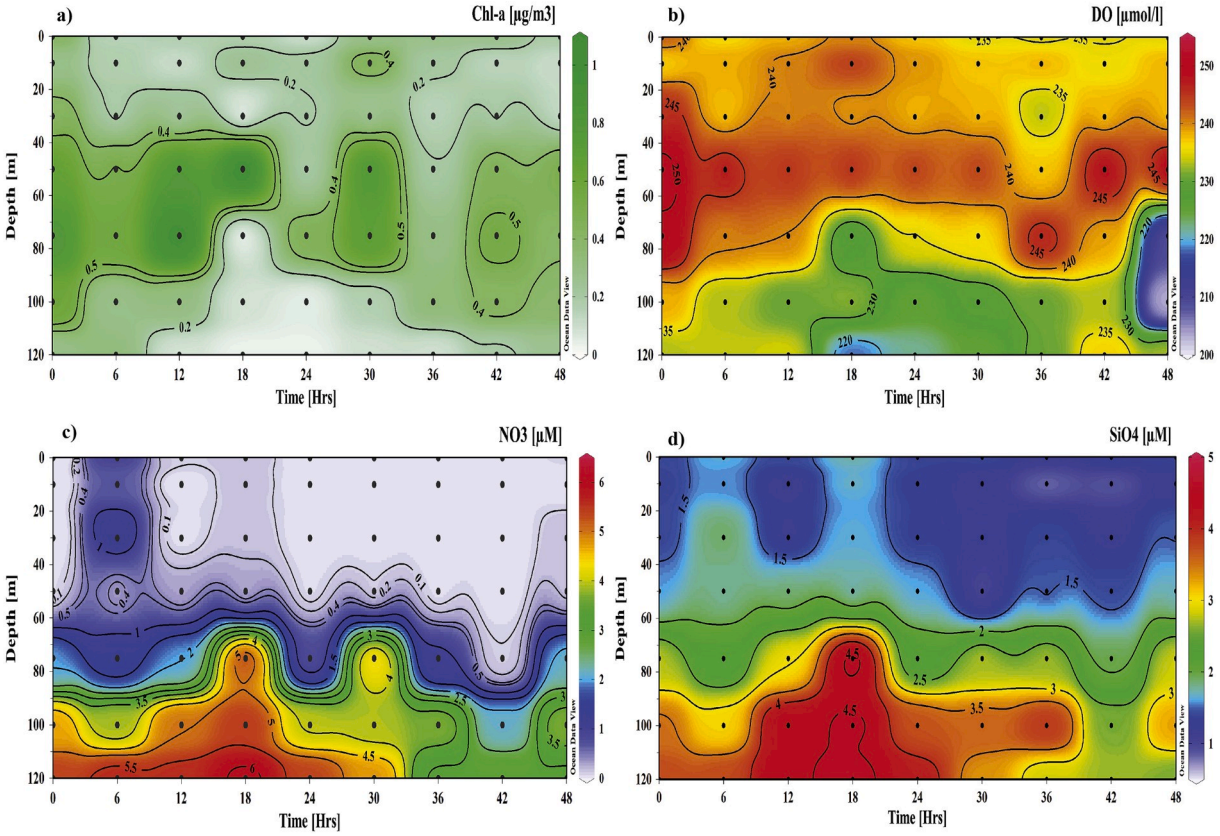

Fig. 3. Time-depth evolution of a) Chlorophyll-a, b) Dissolved oxygen (DO), c) Nitrate, d) Silicate, over the 48 h sampling period.

Table 1
The average values with the standard deviation (SD) of temperature, salinity, dissolved Oxygen (DO), Nitrate (NO_3), Chlorophyll-*a*, Total organic carbon (TOC), Apparent oxygen utilization (AOU), Degree of nutrient consumption (DNC_c), Nitrate utilization (*N), silicate utilization (*Si), N/P and N/Si.

Variables	Average ± SD
Temperature (°C)	16.12 ± 1.52
Salinity	35.48 ± 0.06
DO (µM)	236.16 ± 8.74
NO_3 (µM)	2.54 ± 2.09
SiO_4(µM)	2.24 ± 1.11
Chl-*a* (mg/m^3)	0.32 ± 0.24
AOU (µM)	12.01 ± 13.52
DNC_c	0.17 ± 0.13
*N	−21.08 ± 1.44
*Si	0.63 ± 1.06
N/P	1.65 ± 1.32
N/Si	0.76 ± 0.51

h where the isopleths observed a small upward push. Similarly, the observed silicates and phosphates ranged from 0.84 µM to 4.78 µM and 1.14 µM–1.69 µM, respectively, and were low in the MLD, precisely down to the depth of the DCM. In accordance with the isothermal variability, the nitrate and silicate also showed uplift from 60 m towards the surface (Fig. 3c & d). A small increase in nitrate and silicate was noted at 6:00 h and 18:00 h of Day-1. An increase in the concentration of nitrate and silicates was also observed at 48:00 h on Day-2.

3.3. Attributes of nutrient utilization

The Si* is an indicator of silicate utilization and had an average of 0.63 ± 1.06 µM (Table 1). The Si* was a notch lower at 6:00 h in the upper 30 m; however, at 18 h and 30 h Si* was depleted, below 80 m (Fig. 4a). Contrastingly, N* was much depleted and, with an average of −21.08 ± 1.44 (Table 1). N* matched well with Chl-*a*, suggesting higher utilization (more negative) support higher production, except at 18:00 h and 30:00 h where the average was −20.48 ± 0.39 and −19.47 ± 2.02, respectively (Fig. 4b). The ratios of N/P and N/Si have often been used as indicators to understand the nutrient limitation, utilization and regeneration in an oceanic regime. The ratio N/P was very low (1.65 ± 1.32). It ranged from 0.05 to 3.71, below 50 m of the water column. Likewise, the N/Si ratio was also low in the current study, however it was close to Redfield's ratio (>1), with an average of 0.76 ± 0.51. The DNC_c was based on the chlorophyll and nutrients observed, which suggests the uptake by phytoplankton and in-turn, represents the utilization of nutrients in the upwelled waters. Lower DNC_c values suggest freshly supplied nutrients are spontaneously consumed by the phytoplankton (Chen et al., 2004). The DNC_c varied from 0.01 to 0.52, and was evidently higher (0.42) at approximately 50 m, and decreased significantly (<0.1) below 80 m (Fig. 4c).

4. Discussion

The observed temperature and salinity characteristics ascertained the sampling location was at the ARF-STF juncture region which is normally considered as the northern boundary of the Antarctic Circumpolar Current (Anilkumar et al., 2006). During the study, thermohaline structure witnessed undulations which may be due to the presence of eddy and the prevailing wind over the region. Several previous studies have reported that the STF-ARF juncture is a region of high mesoscale activity and hence cyclonic and anticyclonic eddies are common in this area (Machu and Garcon, 2001; Llido et al., 2005). The AVHRR SST and SSHA analysis (Figs. 1 and 5) ascertained that the study location was at the periphery of an anticyclonic eddy. Furthermore, the

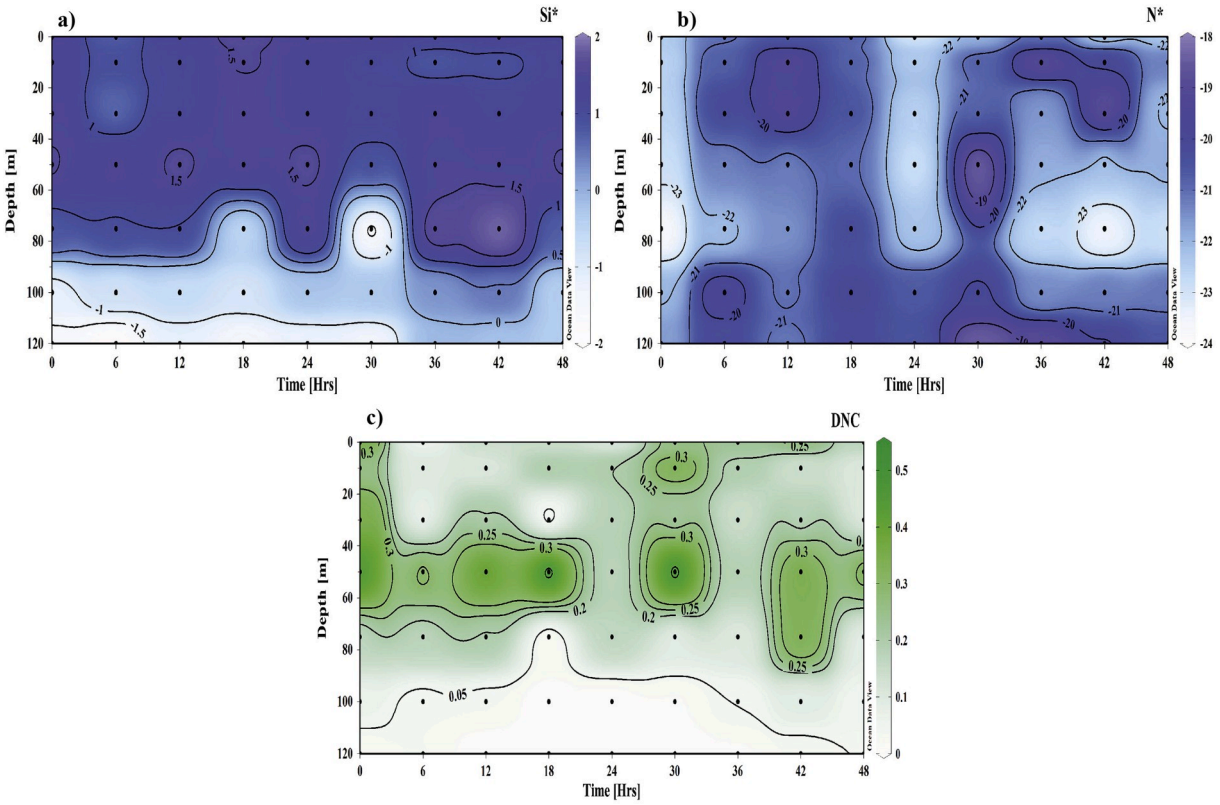

Fig. 4. Time-depth evolution of a) Silicate utilization (Si*), b) Nitrate utilization (N*), c) Degree of Nutrient Consumption (DNCc).

tracking of the eddy using daily SSHA maps found that the anticyclonic eddy was formed in the STF during the first week of November 2011 (figure not shown) and it was 3 months old at time of our observation. It was also observed that the anticyclonic eddy increased the sea level about 40 cm and rotating with a speed of about 55 cm/s.

In general, cyclonic eddies that bring nutrient rich cold deep water from subsurface to surface cause upwelling, and anticyclonic eddies that push the warm surface water to deeper depths creates downwelling. In contrast, during the present study, we have noticed an influx of nutrients supported by low temperature waters, suggesting an upwelling like feature at our observation site which was at the periphery/edge of the anticyclonic eddy. A recent study by Brannigan, 2016 has reported intense sub-mesoscale upwelling from the thermocline to the mixed layer in wind forced anticyclonic eddies. Further, the wind analysis suggests that the magnitude of the wind was weak in the study area on 13th January 2012 (Day-1), except at 00:00 h, which was due to the comparatively high cyclonic wind activity noted just before (12th January 2012) the observation (Fig. 6). However, after 00:00 h of Day-1 the observation location was at the centre of this cyclonic wind circulation where the wind magnitude was low (~1 m/s). However, on 14th (Day-2), the wind system moved towards the east and the study location was observed to be at the periphery of this large wind activity. To understand the wind impact on the upwelling at the periphery of the anticyclonic eddy, we examined the wind stress curl and Ekman pumping during the above period. Previous studies have showed that the positive wind stress curl can generate a favorable impact on the vertical velocity via Ekman pumping (McPhaden et al., 2008; Carranza and Gilli, 2014), thus causing upwelling events. The positive wind stress curl (Fig. 7a) at the location, suggests that the curl was favorable for upwelling. The computed Ekman pumping also showed a favorable upward movement of subsurface water during this time. Hence, the upwelling favorable wind stress curl at the outer periphery of anticyclonic eddy creates

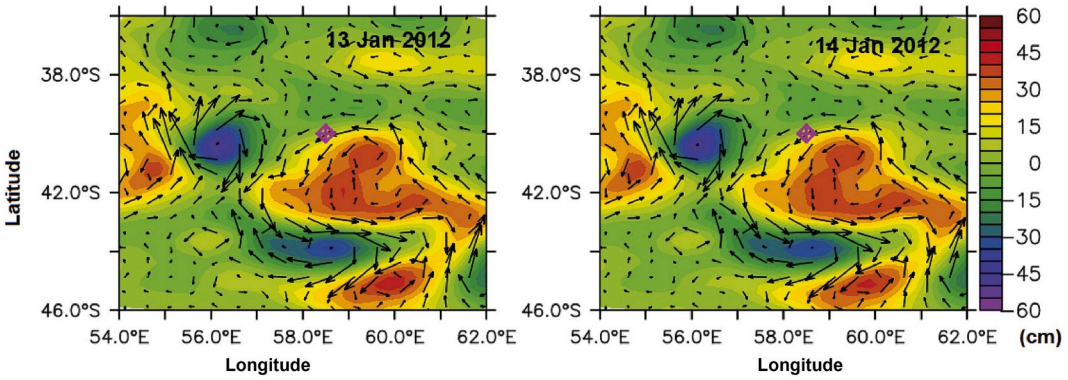

Fig. 5. Sea surface height anomaly (SSHA) overlaid with geostrophic velocity components (u′ and v′) for 13th and 14th January 2012. The sampling location is marked with magenta diamond.

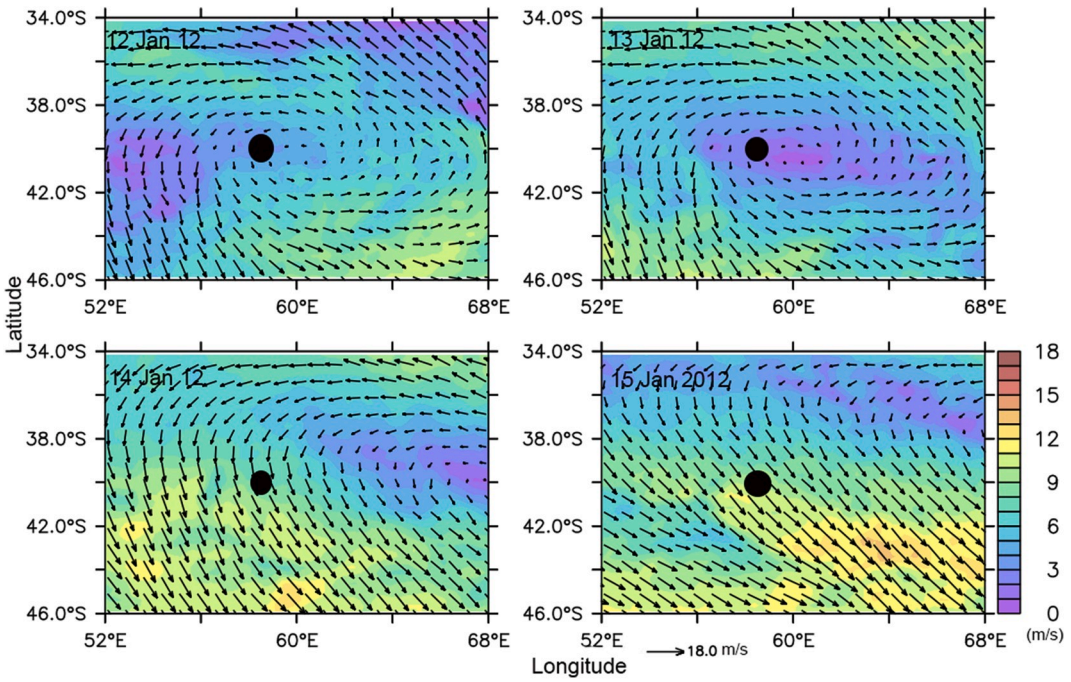

Fig. 6. Wind vectors (wind speed overlaid with wind vectors) from ASCAT over the study area from 12th to 15th January 2012 [station location is marked with black dot].

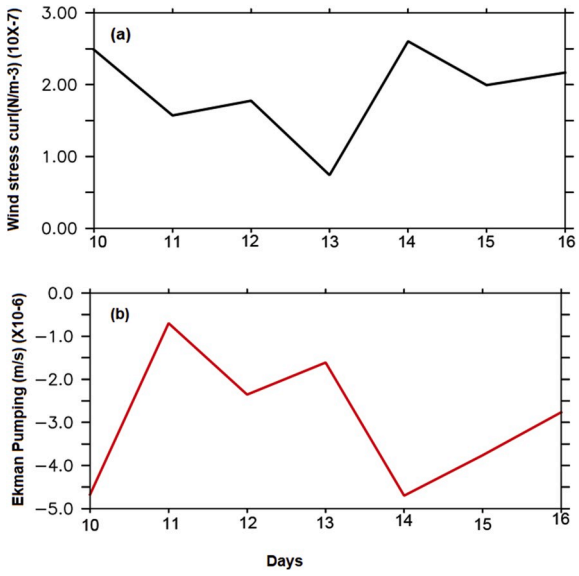

Fig. 7. Time-series of (a) wind stress curl (computed from ASCAT winds) and (b) Ekman pumping variability in the study region [58°E–59°E, 39°S-40°S] from 10th to 16th January 2012.

divergence in the near surface layers which can lead to the uplifting of water column in the thermocline layer which was reflected in the distribution of thermohaline structure. In addition, the high TKE dissipation rate due to the irregular and high wind activity supports short-term mixing events in the upper 60 m till 18:00 h of Day-1 and after 42:00 h of Day-2. Also, the TKE dissipation below 60 m during this period was comparable suggesting the possibility of a contribution of nutrients from the subsurface.

The short lived, episodic influx of nutrients (nitrates and silicates) was observed from ~60 m to the surface, at the outer periphery of the anticyclonic eddy. It is proposed that the influx of nutrients is attributed to the combined effect of the eddy-wind interaction as well as the short term mixing associated with varying winds. Several previous studies (Martin and Richards, 2001; Gaube et al., 2015) have reported that eddy-wind interactions is one of the mechanisms behind the sporadic perturbations in eddy associated regions, especially at the periphery of anticyclonic eddies. Such hydrodynamic processes play a major role in the redistribution and transport of nutrients (Huang and Xu, 2018; Zhang et al., 2018) in eddy dominated fronts of the SO and contribute to the sustenance of the biological productivity in the upper water column. In the present study, the combined effect of small scale wind driven surface mixing in the upper 60 m and a contribution from subsurface upwelling together had a role in the small influx of nutrients in the upper water column, especially, at 6:00 h and 18:00 h of Day-1. This is also indicated from the higher average TKE dissipation rate (Fig. 2e) of the upper 60 m and the rate of Ekman pumping (Fig. 7b) which was comparatively higher on day-1. The role of subsurface mixing was significant between 18:00 h to 30:00 h, and was evident from the TKE dissipation rate below 60 m. This is also supported by the deepening of the MLD, and a downward shift in the isolines of temperature, salinity and density at these time intervals during the study. Furthermore, these factors also explain the undulations noted in the nutricline (Fig. 3c & d) during the study.

The warmer, high saline and low in nutrients (non-detectable) waters were observed mostly overlying the DCM exhibiting an oligotrophic system except the time coinciding with the upwelling event, suggesting the colder waters to bring nutrients to the system. Such processes have been associated with energy transfer, which can be accompanied with the biological utilization of nutrients in warmer surface waters (Zentara and Kamykowski, 1977). Balkanski et al. (1999) also reported that the shoaling or deepening of MLD has a significant role to play in the primary productivity via supply of nutrients through processes like remineralization.

Additionally, we have used DNC_c, an attribute used by Chen et al. (2004, 2005) as an index to express the rapid utilization of upwelled nutrients. The low DNC_c in the upper waters at 6 h and 18 h (Fig. 4c) corroborated with the above explained upwelling at these time intervals, suggesting that DNC_c can also be used as an indicator of nutrient upwelling in the open ocean waters, especially in eddy influenced locations

and cross-frontal regions of the SO. Furthermore, the higher DNC_c at ~50 m coinciding with the DCM depth, throughout the 48 h study, suggests the presence of available unutilized nutrients at the depth of DCM, even though the Chl-*a* was maximum. Moreover, a shift in community with the dominance of diatoms was observed at the surface and 120 m at 18:00 h and 30:00 h (120 m) (Naik et al., 2015). The dominance of the diatoms was highly responsible for the observed over-consumption of silicates as evident from the *Si (Giddy et al., 2012) during this time period.

In general, during the study period, the DNC_c was low below 80 m, which indicates the faster utilization of nutrients supplied. This is reflected in the higher phytoplankton growth and a significant shift in the phytoplankton community especially at ~100–120 m, from a flagellate dominated system to diatoms to prokaryotes followed by diatoms and back to flagellates, as explained in detail by Naik et al. (2015). Additionally, the column integrated Chl-*a* suggests that a major contribution 60–70% of total Chl-*a* in the upper 120 m water column is from the below the DCM (beyond 50 m), and only 30% contribution is from the surface to 30 m. Studies have revealed the presence of DCM in oligotrophic or nutrient depleted oceanic regions is mainly a result of photo-acclimatization and nutrient availability (Kim et al., 2012; Mignot et al., 2014). N/Si ratio <2 (NO_3/Si $\leq$ 1) and the low N:P ratio (<5), observed in the present study also confirm that the region was nitrate limited. Also, a prominent nitricline was evident between ~50 and 75 m (Fig. 3c), above which was the nitrate depleted layer (below detection) and below lay the nitrate replete layer during the study. The nitricline was noted above the DCM at almost all the sampling intervals (Fig. 3a & c), suggesting that the nitricline and the photic depth are significantly responsible for the formation and maintenance of the DCM between 50 and 60 m as reported by Cullen (1982). Hence, upwelling driven eddy-wind interactions occurring at the periphery of an anticyclonic eddy may also be responsible for the shoaling of the nitricline and consequently the DCM. Such processes in the SO play a significant role in triggering a shift of phytoplankton community structure not only at the surface, but also within the upper water column, in response to adapting to the change in environmental factors like light intensity, nutrient availability, due to eddy upwelling (Mishra et al., 2015).

The present study demonstrated the influence of short term episodic eddy-wind interaction on the nutrient dynamics and the biogeochemical processes in the STF which is highly biologically productive compared to other fronts in the SO. Also, the eddies in the subtropical region of ISSO transport warm subtropical water masses to the south and cold sub-antarctic surface waters to the north (Chacko et al., 2014; Sabu et al., 2015). As a result, large amount of heat, nutrients and other components are exchanged across the regions (Lee et al., 2007; Hogg et al., 2008) influencing the biogeochemistry of the polar as well as the subtropical region. Furthermore, a change in the environmental conditions due to the north and south movement of eddies may cause a shift in the phytoplankton community. Mishra et al. (2017) have reported the change in the phytoplankton community in the ISSO due to the change in the environmental conditions. In this point of view, the present study may have wider implications on the various biogeochemical processes across the fronts in the ISSO by altering the nutrient dynamics and hence the various biological communities predominantly existing in this area.

5. Conclusion

The study described the nutrient dynamics and their influence on phytoplankton using the 2-day time-series (6 hrs interval) multi-disciplinary observations conducted at the juncture of ARF-STF, the northern boundary of SO, during austral summer 2012. The study implies that the region was nutrient depleted in the upper 50 m. However, the nutrient utilization attributes suggest an episodic influx of nutrients in the study area and its instantaneous consumption by phytoplankton on Day-1. The study location was identified to be at the periphery of an anticyclonic eddy supported by an upwelling favorable wind. Also, the region was prone to short-term mixing events. Hence, the episodic influx of nutrients observed on Day-1 was due to the eddy-wind as well as the short term mixing at different time intervals during the study. These events influence the nutrient dynamics which triggers a shift in the phytoplankton community of this region. Moreover, such episodic events can have implications on the biogeochemical processes of the polar region via re-distribution of nutrients and other physico-chemical properties.

Acknowledgements

The authors would like to acknowledge Director, NCPOR for the continued support of the Indian Southern Ocean Program. Our sincere thanks to the Ministry of Earth Sciences, India, for funding this program. The authors would like to thank Dr. C.T. Achuthankutty, expedition leader of ISOE-2012, for the support and leadership and the participants for their help during the expedition. Our sincere acknowledgement to Capt. S. Williams and the crew onboard ORV *Sagar Nidhi* for their co-operation and support in ensuring proper sampling under Southern Ocean conditions. This is NCPOR's contribution number J-17/2020-21.

References

Anilkumar, N., Alvarinho, L., Somayaluju, Y.K., Ramesh Babu, V., Dash, M.K., Pednekar, S.M., Babu, K.N., Sudhakar, M., Pandey, P.C., 2006. Fronts, water masses and heat content variability in the Western Indian sector of the Southern Ocean during austral summer 2004. J. Mar. Syst. 63 (1–2), 20–34.

Anilkumar, N., George, J.V., Chacko, R., Nuncio, M., Sabu, P., 2014. Variability of fronts, fresh water input and chlorophyll in the Indian Ocean sector of the Southern Ocean. N. Z. J. Mar. Freshw. Res. 49, 20–40.

Ansorge, I.J., Lutjeharms, J.R., 2005. Direct observations of eddy turbulence at a ridge in the Southern Ocean. Geophys. Res. Lett. 32, 14.

Balkanski, Y., Monfray, P., Battle, M., Heimann, M., 1999. Ocean primary production derived from satellite data: an evaluation with atmospheric oxygen measurement. Global Biogeochem. Cycles 13 (2), 257–271.

Benson, B.B., Krause, D., 1984. The concentration and isotopic fractionation of oxygen dissolved in freshwater and seawater in equilibrium with the atmosphere. Limnol. Oceanograp. 29 (3), 620–632.

Brannigan, L., 2016. Intense submesoscale upwelling in anticyclonic eddies. Geophys. Res. Lett. 43, 3360–3369.

Chen, Chentung Arthur, Hsing, Liyu, 2005. Degree of nutrient consumption as an aging index of upwelling or vertically mixed water in the northern Taiwan Strait. Acta Oceanol. Sin. 24 (1), 115–124.

Chen, Chentung Arthur, Wang, Bingjye, Hsing, Liyu, 2004. Upwelling and degree of nutrient consumption in the Nanwan Bay, southern Taiwan. J. Mar. Sci. Technol. 12 (5), 442–447.

Caldeira, K., Duffy, P.B., 2000. The role of the Southern Ocean in uptake and storage of anthropogenic carbon dioxide. Science 287, 620–622.

Carranza, M.M., Gille, S.T., 2014. Southern ocean wind driven entrainment enhances satellite chlorophyll-a through the summer. J. Geophys. Res.: Oceans 120 (1), 304–323.

Chacko, R., Murukesh, N., George, J.V., Anilkumar, N., 2014. Observational evidence of the southward transport of water masses in the Indian sector of the Southern Ocean. Curr. Sci. 107 (9), 1573–1581.

Crosta, X., Shemesh, A., Etourneau, J., Yam, R., Billy, I., Pichon, J.J., 2005. Nutrient cycling in the Indian sector of the Southern Ocean over the last 50,000 years. Global Biogeochem. Cycles 19, GB3007. https://doi.org/10.1029/2004GB002344.

Cullen, J.J., 1982. The deep chlorophyll maximum: comparing vertical profiles of chlorophyll a. Can. J. Fish. Aquat. Sci. 39, 791–803.

Deacon, G.E.R., 1933. A general account of the hydrology of the Southern Atlantic Ocean. Discov. Rep. 7, 171–238.

DeMaster, D.J., 2002. The accumulation and cycling of biogenic silica in the Southern Ocean: revisiting the marine silica budget. Deep Sea Res., Part II 49, 3155–3167.

Gandhi, N., Ramesh, R., Laskar, A.H., Sheshshayee, M.S., Shetye, S., Anilkumar, N., Patil, S., Mohan, Rahul, 2012. Zonal variability in primary production and nitrogen uptake rates in the southwestern Indian Ocean and the Southern Ocean. Deep Sea Res. I 67, 32–43.

Gaube, P., Chelton, D.B., Samelson, R.M., Schlax, M.G., O'Neill, L.W., 2015. Satellite observations of mesoscale eddy-induced Ekman pumping. J. Phys. Oceanogr. 45, 104–132.

George, J.V., 2015. Role of Physical Processes on the Chlorophyll a Distribution in the Western Tropical Indian Ocean and the Indian Ocean Sector of the Southern Ocean. PhD Thesis. Goa University, India.

George, J.V., Anilkumar, N., Nuncio, M., Soares, M.A., Naik, R.K., Tripathy, S.C., 2018. Upper layer diapycnal mixing and nutrient flux in the subtropical frontal region of the Indian sector of the Southern Ocean. J. Mar. Syst. 187, 197–205.

Giddy, I.S., Swart, S., Tagliabue, A., 2012. Drivers of non-Redfield nutrient utilization in the Atlantic sector of the Southern Ocean. Geophys. Res. Lett. 39, L17604. https://doi.org/10.1029/2012GL052454.

Goeyens, L., Semeneh, M., Baumann, M.E.M., Elsken, M., Shopova, D., Dehairs, F., 1998. Planktonic nutrients utilization and nutrient signatures in the Southern Ocean. J. Mar. Syst. 17 (1–4), 143–157.
Grasshoff, K., Ehrhardt, M., Kremling, K., 1983. Methods of Seawater Analysis. Verlag Chem., Weinheim, p. 600.
Hauck, J., Lenton, A.A., Langlais, C., Matear, R.J., 2018. The fate of carbon and nutrients exported out of the Southern Ocean. Global Biogeochem. Cycles 32, 1556–1573.
Hogg, A., Meredith, M.P., Blundell, J.R., Wilson, C., 2008. Eddy heat flux in the Southern Ocean: response to variable wind forcing. J. Clim. 21, 608–620.
Huang, J., Xu, F., 2018. Observational evidence of subsurface chlorophyll response to mesoscale eddies in the North Pacific. Geophys. Res. Lett. 45, 8462–8470.
Jasmine, P., Muraleedharan, K.R., Madhu, N.V., Asha Devi, C.R., Alagarsamy, R., Achuthankutty, C.T., Jayan, Z., Sanjeevan, V.N., Sahayak, S., 2009. Hydrographic and production characteristics along 45°E longitude in the southwestern Indian Ocean and Southern Ocean during austral summer 2004. Mar. Ecol. Prog. Ser. 389, 97–116.
Jena, B., Sahu, S., Avinash, K., Swain, D., 2013. Observation of oligotrophic gyre variability in the south Indian Ocean: environmental forcing and biological response. Deep-Sea Res. I 80, 1–10.
Kim, D., Yang, E.J., Kim, K.H., Shin, C.-W., Park, J., Yoo, S., Hyun, J.-H., 2012. Impact of an anticyclonic eddy on the summer nutrient and chlorophyll a distributions in the Ulleung Basin, East Sea (Japan Sea). ICES J. Mar. Sci. 69, 23–29.
Lee, M.M., George Nurser, A.J., Coward, A.C., de Cuevas, B.A., 2007. Eddy advective and diffusive transports of heat and salt in the Southern Ocean. J. Phys. Oceanogr. 37, 1376–1393.
Llido, J., Garçon, V., Lutjeharms, J.R.E., Sudre, J., 2005. Event-scale blooms drive enhanced primary productivity at the subtropical convergence. Geophys. Res. Lett. 32, L15611. https://doi.org/10.1029/2005GL022880.
Lutjeharms, J.R.E., Ansorge, I.J., 2001. The Agulhas return current. J. Mar. Syst. 30 (1), 115–138.
Machu, E., Garçon, V., 2001. Phytoplankton seasonal distribution from SeaWiFS data in the Agulhas Current system. J. Mar. Res. 59, 795–812.
Machu, E., Biastoch, A., Oschlies, A., Kawamiya, M., Lutjeharms, J.R.E., Garçon, V., 2005. Phytoplankton distribution in the Agulhas system from a coupled physical-biological model. Deep Sea Res., Part I 52, 1300–1318.
Mahadevan, A., 2016. The impact of Submesoscale physics on primary production of plankton. Ann. Rev. Mar. Sci. 8, 161–184.
Mahadevan, A., Thomas, L.N., Tandon, A., 2008. Comment on "Eddy/wind interactions stimulate extraordinary mid-ocean plankton blooms". Science 320 (5875), 448.
Martin, A.P., Richards, K.J., 2001. Mechanism for vertical transport within a North Atlantic mesoscale eddy. Deep Sea Research-II 48 (4–5), 757–773.
McGillicuddy Jr., D.J., Robinson, A.R., 1997. Eddy induced nutrient supplu and new production in the Sargasso Sea. Deep Sea Research-I 44 (8), 1427–1450.
McPhaden, M.J., Cronin, M.F., McClurg, D.C., 2008. Meridional structure of the seasonally varying mixed layer temperature balance in the eastern tropical Pacific. J. Clim. 21, 3240–3260.
Mignot, A., Claustre, H., Uitz, J., Poteau, A., D'Ortenzio, F., Xing, X., 2014. Understanding the seasonal dynamics of phytoplankton biomass and the deep chlorophyll maximum in oligotrophic environments: a Bio-Argo float investigation. Global Biogeochem. Cycles 28, 856–876. https://doi.org/10.1002/2013GB004781.
Mishra, R.K., Naik, R.K., Anilkumar, N., 2015. Adaptation of phytoplankton in the Indian ocean sector of the Southern Ocean during austral summer of 1998-2014. Front. Earth Sci. 9 (4), 742–752.
Mishra, R.K., Jena, B., Anilkumar, N., Sinha, R.K., 2017. Shifting of phytoplankton community in the frontal regions of Indian Ocean sector of the Southern Ocean using in situ and satellite data. J. Appl. Remote Sens. 11 (1), 016019 https://doi.org/10.1117/1.JRS.11.016019.
Naik, R.K., George, J.V., Soares, M.A., Devi, Asha, Anilkumar, N., Roy, R., Bhaskar, P.V., Murukkesh, N., Achuthankutty, C.T., 2015. Phytoplankton community structure at the juncture of the Agulhas return front and subtropical front in the Indian ocean sector of Southern Ocean: bottom-up and top-down control. Deep-Sea Res. Part II Top. Stud. Oceanogr. 118, 233–239.
Pollard, R., Read, J., 2017. Circulation, stratification and seamounts in the southwest Indian ocean. Deep-Sea Res. Part II Top. Stud. Oceanogr. 136, 36–43.
Pollard, R., Lucas, M., Read, J., 2002. Physical controls on biogeochemical zonation in the Southern Ocean. Deep Sea Res. Part II 49, 3289–3305.
Prakash, S., Ramesh, R., Sheshshayee, M.S., Mohan, R., Sudhakar, M., 2015. Nitrogen uptake rates and f-ratios in the equatorial and southern Indian ocean. Curr. Sci. 108 (2), 239–245.
Rajkumar, A., Alagarsamy, R., Khare, N., Saraswat, R., Subramaniam, M.M., 2008. Studies on the nutrient distribution in the Southern Ocean waters along the 45°E transect. Indian J. Mar. Sci. 37 (4), 424–429.
Read, J.F., Lucas, M.I., Holley, S.E., Pollard, R.T., 2000. Phytoplankton, nutrients and hydrography in the frontal zone between the Southwest Indian Subtropical gyre and the Southern Ocean. Deep Sea Res. I 47, 2341–2368.
Sabu, P., George, J.V., Anilkumar, N., Chacko, R., Valsala, V., Achuthankutty, C.T., 2015. Observations of watermass modification by mesoscale eddies in the southern subtropical Indian Ocean. Deep-Sea Res. Part II Top. Stud. Oceanogr. 118, 152–161.
Sarmiento, J.L., Gruber, N., Brzezinski, M.A., Dunne, J.P., 2004. High-latitude controls of thermocline nutrients and low latitude biological productivity. Nature 427 (6969), 56–60.
Schlüter, L., Henriksen, P., Nielsen, T.G., Jakobsen, H.H., 2011. Phytoplankton composition and biomass across the southern Indian Ocean. Deep-Sea Res. Part I Oceanogr. Res. Pap. 58 (5), 546–556.
Zentara, S.J., Kamykowski, D., 1977. Latitudinal relationships among temperature and selected plant nutrients along the west coast of North and South America. J. Mar. Res. 35, 321–337.
Zhang, S., Curchitser, E.N., Kang, D., Stock, C.A., Dussin, R., 2018. Impacts of mesoscale eddies on the vertical nitrate flux in the Gulf stream region. J. Geophys. Res.: Oceans 123, 497–513.

Published Online on 3 May 2017

Proc Indian Natn Sci Acad **83** No. 2 June Thematic Issue 2017 pp. 377-384

DOI: 10.16943/ptinsa/2017/48961

Review Article

Indian Contributions to Chemical Studies in the Indian Sector of Southern Ocean

MELENA A SOARES* and N ANILKUMAR

National Centre for Antarctic and Ocean Research, Earth System Science Organisation, Vasco-da-Gama, Goa 403 804, India

(Received on 13 May 2016; Accepted on 01 December 2016)

Southern Ocean is a crucial oceanic regime for understanding the role of biogeochemical cycles in influencing the global climatic changes, as this is a region where signatures of global changes are more pronounced. For an Improved understanding of the link between Southern Ocean processes, biogeochemical cycles and the global climate, scientific research was commenced. Some remarkable research work has been accomplished by Indian Scientific community in the Indian sector of the Southern Ocean (ISSO). A total of six successful multi-disciplinary and multi-institutional expeditions were carried out from the year 2009 to 2015 in the ISSO, with the pilot expedition launched in the year 2004. During the last decade, an understanding of different aspects of the ocean processes has been achieved using chemical studies and proxies. Studies in the ISSO focused on shifts in the oceanic fronts, the carbon and nutrient dynamics, as well as the food web dynamics across the different fronts. The spatial-temporal variation of nutrients, dissolved oxygen, dissolved inorganic carbon and the factors regulating their distribution in the ISSO has also been addressed. Attempts were made to understand the atmosphere-ocean interaction of CO_2 and biogeochemical processes. Some experimental work have been undertaken to assess the nitrogen uptake and influence of micronutrients on phytoplankton. Similarly, stable isotope of oxygen has been used as a proxy in some early studies in the ISSO. Isotopic and molecular investigations have been commenced to understand the biogeochemical processes within the water column, as the biological pump and particulate organic matter (POM) have a major role to play in carbon sequestration and further influencing the global climate variability. Detailed studies on dissolved and particulate organic matter are being carried out to gain knowledge of the biological pump and the factors responsible for climate variability and ocean acidification.

Keywords: Indian Sector of Southern Ocean; Carbon; Oxygen Isotope; Stable Isotopes

Introduction

Southern Ocean (SO) is the largest and one of the most dynamic regions of the world Oceans. This is a regime influenced by the strongest winds and ocean currents. It is characterized by a well-defined frontal structure and supports transport and exchange of heat, salts, and other organic and inorganic components between the major ocean basins, through the Antarctic Circumpolar Current (ACC) (Jasmine *et al*., 2009; Anilkumar *et al*., 2006; Holliday and Read, 1998). The biogeochemical processes in this region have a major role in the global carbon cycle and climate change. The SO is a HNLC (High Nutrients Low Chlorophyll) region with high variability in the hydrographic and chemical characteristics (Martin *et al*., 2013). With a motive to understand this variability and the factors responsible, a pilot expedition in the Indian sector of the Southern Ocean (ISSO) was launched in the year 2004. From 2009 to 2015, six successful multi-disciplinary and multi-institutional expeditions were carried out in the ISSO. Some major national and international scientific institutions/ Universities have participated in these expeditions. With the launch of these expeditions, research in various sectors of oceanographic studies were commenced to understand the biogeochemical processes in the ISSO. Furthermore, the latitudinal variation of calcification depth of foraminifera (*G.bulloides*) was studied using stable oxygen

*Author for Correspondence: E-mail: smelena7@gmail.com

isotopes. Investigations to identify the sources and processes governing the distribution of Suspended Particulate Matter (SPM) across the different frontal zones in ISSO are also being carried out. Studies addressing the variation of $\delta^{13}C$ and $\delta^{15}N$ of particulate organic matter (POM), and the factors controlling the isotopic signatures of POM in ISSO have been initiated to achieve knowledge of the biogeochemical processes and the biological pump in the ISSO. Some of the processes studied and the findings reported by using chemical proxies in the ISSO and coastal Antarctica have been discussed in this article.

Nutrients and Dissolved Gases

Documenting and understanding the trends of nutrient and dissolved gases, especially, carbon dioxide (CO_2) and CO_2 fluxes is important for providing insights into the biogeochemical processes in the ISSO and their role in the global climate changes. SO is a region characterised by low temperatures, strong winds, surface currents and mixing velocities. The role of temperature and wind stress in the process of CO_2 uptake and variations in CO_2 fluxes is documented in the SO (Anderson *et al.*, 2009; Longinelli *et al.*, 2012; Waugh, 2014). SO has been demarcated as a major sink of atmospheric CO_2 (Caldeira and Duffy, 2000; Fletcher *et al.*, 2006). However, studies have suggested that the strength of SO as a sink is decreasing and the intensity varies seasonally across different zones (Metzl *et al.*, 1991; Metzl, 2009). A deeper understanding of the carbonate system and the processes governing CO_2 uptake is of utmost importance to ascertain whether the entire regime acts as a source or sink for atmospheric CO_2. To gain better insights in this aspect, studies on total CO_2 (tCO_2) and partial pressure of CO_2 (pCO_2) in the ISSO were initiated.

A study to address the spatio-temporal variation of pCO_2 and its relation with nutrients and biological production in the ISSO along two transects (48°E and 57°30'E) was taken up during austral summer 2009 (Shetye *et al.*, 2012). This study reported low nitrate with higher nutrient utilisation in the Sub tropical front (STF) from 41°-43°S along 48°E and 43°-46°S along 57°30'E. Vertical mixing was assumed to have a major role in the supply of higher tCO_2 to the surface waters. The pCO_2 increased southwards along both the transects and this was attributed to the lower productivity (low TOC and Chlorophyll values) in the Polar Front (PF) region from 48°S to 57°S, during the study period. Based on a correlation analysis of different factors and temperature normalised pCO_2, this study postulated biological processes to be controlling the pCO_2 along 57°30'E transect and physical processes controlling the pCO_2 variation along 48°E transect. They proposed that SO acted as a sink but the area around Crozet Island behaved as a source likely because this region is prone to upwelling. pCO_2 increased southwards mainly due to low biological productivity. This study suggested that southwards the pCO_2 exhibited an increasing trend in the last decade and is associated with the Southern Annular Mode (SAM).

To fill the existing gaps concerning the knowledge of carbon cycle and pCO_2 variability in the ISSO, Shetye *et al.* (2015) studied the physical and biological processes controlling pCO_2 in the surface mixed layer during the transition period from summer to early winter. The authors used a one dimensional model by Louanchi *et al.* (1996), and describe the mixed layer carbon cycle, using in-situ data (January 2009, February 2010, March 2012) and satellite derived data to determine the relative contribution of biological activity, mixing, thermal and air-sea fluxes on pCO_2. Significant spatial and seasonal variation was observed in surface seawater pCO_2 across the frontal zones. An average increase of ~75µatm was reported in this study, from the STF (289 µatm) to the PF (364 µatm). It was also noted that the average pCO_2 estimated in the entire study area increased from 286 µatm in January to 337 µatm in March. A transition from pCO_2saturated waters (March 2009) to under saturated waters (January 2012) was observed during the study. In the month of January, the highest biological drawdown of pCO_2 was reported. This drawdown was associated with biologicalprocesses such as primary production, respiration and calcification, and was considered as the predominant controlling factors as compared to the physical processes like thermal variability, mixing and air-sea fluxes. This study concatenates the previous study (Shetye *et al.*, 2012) which addresses ISSO as a sink. The same study also reported that the average nutrients were highest in February, however silicate was maximum in March. A deviation from the Redfield's N/P ratio (16) was displayed with a variation, from an average of 6 to 9 increasing

southwards, along the transect. The low N/P ratio indicated higher nitrate utilization. The N/P and Si/N ratios decreased from January to March.

A similar study was carried out in the Antarctic coastal waters and the Enderby basin to address the seasonal biogeochemical dynamics, pCO_2 variability and the air-sea flux through the different seasons (Shetye *et al*., 2016). They found sea-ice plays a crucial role in driving biochemical changes and pCO_2 variability in the coastal Antarctica. Sea-ice changes caused a decrease in sea surface pCO_2 during summer, while it enhances pCO_2 during winter. This study documented a higher pCO_2 in March compared to that in January and February, however, most of the study area was under saturated with pCO_2. Based on the CO_2 fluxes estimated the study inferred, Enderby basin act as a strong sink in January, but a weak sink in other two months and proposed that different factors dominate during different months. The primary productivity, nutrient availability and sea ice were dominating in January but in February temperature played a major role, followed by primary productivity and sea-ice melting. However during March, nutrients, light availability and vertical mixing along with decay of organic matter were significant factors. The study also reported that the regions east of 55°E along the coastal Antarctica acted as a source of CO_2, while the western region acted as a sink for atmospheric CO_2 and associated this deviation with vertical mixing and biological processes.

Studies on nutrient distribution and DO in ISSO waters were initiated by Rajkumar *et al*. (2008). During the pilot expedition to SO, it was reported that the trend in nutrient distribution across the frontal zones matches with the hydrographic properties. The data (nutrient and oxygen) obtained during this study also provided insights of the changes in productivity.

Recently attempts have been made to understand the nutrient variability and nutrient utilisation across the frontals zones in the ISSO using geochemical tracers such as N*(nitrate utilisation) and Si*(Silicate utilisation).

N* and Si* was calculated as follows:

$$N^* = NO_3 - 16PO_4$$

$$Si^* = Si(OH)_4 - NO_3$$ (Sarmeinto *et al.*, 2004)

It was suggested that the utilization of nitrate was high in the northern region from 39°S to 44°S; whereas the silicate utilisation was higher in the south from 45°S to 52°S (Dessai *et al*., 2011, Tech rep). The study ascertained that the nutrient dynamics across the fronts depends on the physical and biological processes.

Shetye *et al.* (2014) studied silica depletion under the Antarctic sea ice. They hypothesised that diatom bloom driven depletion of dissolved silica in the Antarctic under sea ice waters affect biomineralising organisms. They reported that surface dissolved silica (DSi) increased from subtropics towards the poles and was high all along the coast and also the dominance of diatoms resulted in high sediment organic carbon (3.5 %). They reported intense diatom dominated ice-edge plankton bloom in the Enderby basin causing severe depletion of DSi (< 5 µM) under sea ice. This was supported by the presence of small spicules of sponges under Antarctic ice, also evidence for silica depletion from penecontemperorous dissolution was observed on small style spicules and the authors attributed thelow silica concentration under Antarctic sea ice to diatom bloom which is severely affected by the silicification in sponges.

Stable Isotopic Signatures of Carbon for Understanding CO_2 Exchange

A study to identify the region of CO_2 venting over the SO was carried by Prasanna *et al*. (2015). To achieve this, the atmospheric CO_2 concentration, the $\delta^{13}C$ of atmospheric CO_2, and the $\delta^{13}C$ of DIC was estimated in the sea surface waters across the latitudes in ISSO during 2011, 2012, 2013. They used Keeling's mixing model to trace the source of CO_2. The average $\delta^{13}C$ composition of the source of CO_2 was predicted to be –9.22±0.26 ‰ in the year 2011 and 2012 whereas it was predicted to be 13.49±4.07 ‰ in the year 2013, based on measured data. The end member value for 2011, 2012 was similar but did not match with the expected value of degradation of phytoplankton, thus the authors deduced dissolution of bicarbonates in the water column to be the source of CO_2 during the study period. They also proposed the degeneration of DIC to be favoured in warmer waters. However in 2013, the source of CO_2 was inferred to be degradation of organic matter and mixing of DIC present in seawater. The Keeling's component model

identified the end member to have a composition of -36.7 ‰. Another finding from this study was that degassing of CO_2 to the atmosphere was favoured in coastal Antarctic region as this regime experience high wind speed and the surface waters have high DIC.

A recent report by Prasanna *et al*. (2016) addresses the effect of change in water mass properties with depth and latitudinal position on the incorporation of $\delta^{18}O$ and $\delta^{13}C$ in foraminifera (*G.bulloides*). The study also addressed the spatial distribution of $\delta^{13}C$ of DIC in surface waters. The $\delta^{18}O$ and $\delta^{13}C$ values of calcite at equilibrium, was calculated using the temperature and compared it with the isotopic composition of $\delta^{18}O$ and $\delta^{13}C$ in the water column. The measured $\delta^{18}O$ and $\delta^{13}C$ values were higher than the expected values by –2 ‰ and –1 ‰ respectively. They attributed the cause of disequilibrium south of 40°S to a process of mass dependent kinetic fractionation due to deeper depth habitat, partial dissolution, non-equilibrium calcification, oceanic Suess effect and genetic variability. An enrichment in $\delta^{13}C_{(DIC)}$ of surface waters was reported and this was attributed to an increase in organic matter production or its associated removal. Large inter-annual variation between the period of 2012 and 2013 was documented. They also proposed a model for production and export of organic matter. This model can be used to simulate $\delta^{13}C_{(DIC)}$ values for biologically productive regions in the SO. The model accounts for the $\delta^{13}C_{(DIC)}$ values in a given location based on the production rate of organic carbon, total organic carbon and the removal rate of organic carbon, it also demonstrates that a steady state of the carbon isotope ratio of water can be achieved in a relatively short time of ~5000 days. Beyond 50°S, the $\delta^{13}C_{(DIC)}$ values were low. The study ascertained that these $\delta^{13}C_{(DIC)}$ values are controlled by the nutrient supplied by Antarctic Bottom Water and upwelling.

Use of Stable Isotope of Oxygen ($\delta^{18}O$) and Hydrogen (δD) as a Proxy

$\delta^{18}O$ is generally used as a tracer to identify different water masses. δD values of seawater are sensitive to various processes of the hydrological cycle like evaporation, precipitation, and freezing. Therefore, study of δD and $\delta^{18}O$ along with salinity are unique and important to understand ocean surface processes.

A study was carried out by Tiwari *et al*. (2013) by coupling stable isotopes of oxygen and salinity in surface sea water to ascertain the ocean-atmospheric processes across the different fronts in the ISSO as well as to identify the water masses in this region. The study highlighted the relation between $\delta^{18}O$ and sea surface salinity pertaining to distinct water mass and confirmed the prevalence of evaporation/ precipitation. The subtropical zone was dominated by evaporation/precipitation, whereas in the Antarctic zone, ice melting-freezing is dominant. The effect of continental ice melt was noted at the southernmost location (66.73°S). Using this stable isotope proxy the Subtropical and Polar fronts were identified at 44°S and 54°S respectively. This was succeeded by a study (Tiwari *et al*., 2015) to document the $\delta^{18}O$ variability, the relation of $\delta^{18}O$ with salinity across the fronts in ISSO. The study also identified the origin, of the waters in the eddy encountered area. The slope of $\delta^{18}O$-salinity relation indicated that the warm core eddy was formed in a region dominated by evaporation and precipitation, while the waters surrounding the eddy are from a region dominated by freezing and melting. The role of eddies in the formation of intermediate waters in the SO was also explored in this study. The Antarctic Intermediate Waters (AAIW) with $\delta^{18}O$ values of 0.0 ‰ to 0.2 ‰, flowing below the Antarctic Surface waters which displayed the lowest temperature, salinity and $\delta^{18}O$ values (–0.4 ‰ to –0.2 ‰) were identified. The AAIW forms in the polar frontal waters, a region with the dominance of freezing/melting, however it was observed at a shallower depth which was possibly due to the influence of the eddy.

Experimental Work

To understand the nitrogen uptake and its role in limiting phytoplankton productivity, a few experiments have been carried out in the ISSO. Earlier studies have ascertained iron limitation in the SO and an addition of iron can increase primary productivity (Geider & Rocha, 1994; Hutchins *et al*., 1995). However the effect on different N-substrate was unknown. One such initiative was a bottle scale ^{15}N tracer iron experiment carried out by Prakash *et al*. (2010) to assess addition of iron on the N-uptake rate and f-ratio in the ISSO. It was reported that iron addition not only enhance NO_3 uptake but also showed an increase in ammonia and urea uptake with

insignificant effect on the f-ratio. The addition of iron did not enhance N-uptake based primary production at the initial stage but increased the uptake at a later stage.

Another mesocosm experiment was carried out by Dessai *et al*. (2011, Tech. Rep) to study the influence of iron and cobalt on phytoplankton community structure in the subtropical and polar front of the ISSO. It was reported that individually both the micronutrients stimulated growth when added individually but when added in combination it did not trigger much growth. It was also observed that diatom sustained longer in a cobalt enriched environment whereas the biomass was higher in the iron enriched environment.

Suspended Particulate Matter (SPM)

A study was taken up by Dessai *et al*. (2011) to gain insights into the spatial distribution of SPM and the associated trace metals and to identify its sources. The authors reported high SPM and low salinity in surface waters and also high SPM at 1000 m along with high iron and manganese in Antarctic zone. The study suggested that the particulate matter in the northern region especially the subtropical front was mainly of biogenic origin, with enrichment of calcium. It also stated that, temperature and salinity controlled primary production, has a major role in the SPM distribution of this region. Conversely, in the southern region SPM was of terrigenous origin and rich in iron and manganese. The inputs to the SPM in Southern region was proposed to be mainly from melt water and from a region with low productivity dominated by diatom. A similar study was carried out to understand the processes controlling the distribution of SPM across the frontal zones during austral summer 2010, wherein it was reported that the highest SPM was quantified in the Subantarctic zone followed by the Antarctic zone and this variability was attributed to the different biogeochemical processes dominating in the different zones of ISSO (Nayak & Noronha, Tech. rep., 2011)

Particulate Organic Matter (POM) in the Water Column

The ISSO being characterised by different oceanic fronts and influenced by eddies, this region is highly dynamic in terms of air-sea flux of CO_2 as well as the factors governing the fate of organic matter (production, remineralisation) and preservation. POM is a key component of the biological pump and it is known from earlier studies, that a major portion of POM is remineralised in the upper photic layer (Honjo *et al*., 2008; Duforet-Gauier *et al*., 2010). Therefore to understand the biogeochemical processes isotopic and molecular studies are important. The stable isotopic ratio of carbon and nitrogen of POM ($\delta^{13}C$ and $\delta^{15}N$) are often used to understand the conditions prevailing at the time of carbon fixation and to get insights of the processes related to organic matter cycling (Lourey *et al*., 2003, 2004 & references within). Recently investigations to understand the biogeochemical cycle of POM using isotopic and molecular studies have been initiated.

One such study addressed the variation of $\delta^{13}C$ and $\delta^{15}N$ of POM, and the factors controlling the isotopic signatures of POM in surface waters in the ISSO (Soares *et al*., 2015). In this study it was reported that in the ISSO, physical processes like temperature gradient and eddies as well as the biological processes contribute equally in the isotopic characterisation of POM, and these factors are responsible for the variation in $\delta^{13}C$ and $\delta^{15}N$ across the fronts in ISSO surface waters. During austral summer 2012, the $\delta^{13}C$ of POM in Subtropical front was enriched in $\delta^{13}C$ (average –22.81‰), relative to the $\delta^{13}C$ of colder Polar Front waters that displayed depleted values (average –25.82‰) similar to $\delta^{15}N$ that was enriched in the Subtropical front. It was postulated that the community structure had a major role in determining the isotopic signatures of POM with the dominance of dinoflagellates in the eddy prone, low nutrient Subtropical front waters with $\delta^{13}C$ enriched POM and diatoms dominated nutrient rich colder water displaying depleted $\delta^{13}C$ of POM.

Other Related Studies

Use of $\delta^{18}O$ as a Proxy in Planktonic Foraminifera Studies

Saraswat and Khare (2010) tried to ascertain the water depth at which the planktonic foraminiferal spp. *G. bulloides* calcifies its shell based on the stable isotopic composition of oxygen ($\delta^{18}O$) in its shells. A comparison of seawater salinity and temperature estimated from $\delta^{18}O$ of *G. bulloides* $\delta^{18}O$ show that calcification depth of *G. bulloides* varies latitudinally.

The study also stated that north of 43°S the calcification depth was deeper approximately 200 m, determined from the estimated temperature well matching the seawater temperature at 200 m. However, south of 43°S the calcification depth was shallower.

Subsequently, a study was carried out to evaluate the spatial variability of isotopic value of foraminifera across different frontal regimes (Tiwari *et al*., 2011). This study documented, planktonic foraminifera secrete their shell at isotopic equilibrium with seawater. Also, comparative analysis of $\delta^{18}O_{calcite}$ and predicted values $\delta^{18}O_{calcite}$ revealed a similar trend as that measured for the shells. They reported $\delta^{13}C$ values of plankton net samples and core top sediment samples increased southwards and attributed it to the productivity fluctuation which increase southwards due to the influx of nutrients from ice melt, since $\delta^{13}C$ variability appear to be governed mostly by primary productivity.

Recently, Mohan *et al*. (2015) demonstrated that there is a shift in the abundance of foraminifera from Subtropical Front to Polar Front and reported $\delta^{18}O$ in sediments is higher compared to towed plankton samples. The study proposed that some part of the shell precipitates in cooler deeper waters where secondary calcification occurs. This study suggested the absence of dissolution in the foraminifera from surface sediments and attributed it to low organic biomass.

Future Prospects

Although many studies have been carried out in the ISSO, the region is still understudied in terms of the biogeochemical processes. It is of utmost importance to understand the biogeochemical processes in the region as the SO have a strong global influence. Most important being the CO_2 dynamics, although studies are going on, they need to be extended on a larger scale and the system needs to be monitored to quantify the fluxes. It is essential to address Ocean acidification, which significantly influences the ocean biological community structure and other biochemical processes, consequently affecting the food web dynamics. Besides, detailed studies to understand the biological pump and processes like remineralisation within the water column are crucial, as the water masses formed in the ISSO can upwell at a different location causing degassing/flux of CO_2 to the atmosphere. As the carbon, nutrients and food web dynamics are all inter-linked and involve a complex interplay of varied physical, biological and biogeochemical processes which need to be studied in detail to understand and further predict the global climate variability.

Acknowledgement

Our sincere thanks to the Ministry of Earth Sciences for funding the Indian Southern Ocean Program. The authors would like to acknowledge Director, NCAOR for the continued support. We appreciate and thank all the authors whose contribution towards Indian Southern Ocean studies have been compiled in this article. This is ESSO-NCAOR's contribution number 40/2016.

References

Anderson R F, Ali S, Bradtmiller L I, Nielsen S H H, Fleisher M Q, Anderson B E and Burckle L H (2009) Wind-driven upwelling in the Southern Ocean and the deglacial rise in atmospheric CO2 *Science* **323** 1443-1448

Anilkumar N, Luis Alvarinho J, Somayaluju Y K, Ramesh Babu V, Dash M K, Pednekar S M, Babu K N, Sudhakar M and Pandey P C (2006) Fronts, water masses and heat content variability in the Western Indian sector of the Southern Ocean during austral summer 2004 *J Mar Syst* **63** 20-34

Caldeira K and Duffy P B (2000) The role of the Southern Ocean in uptake and storage of anthropogenic carbon dioxide *Science* **287** 620-622

Dessai D V G, Singh K T , Mohan R, Nayak G N and Sudhakar M (2011) Reading source and processes from the distribution of suspended particulate matter and its selected elemental chemistry in the Southern and Indian Oceans *Current Science* **100** 1193-1200

Dessai D R G, Bhaskar P V, Anilkumar N, Krishnan K P and Achuthankutty C T (2011) Chemical Features *Southern Ocean expedition, Technical report 2011*, pp. 10-18

Duforet-Gaurier L, Loise L, Dessailly D, Nordkvist K and Alvain

S (2010) Estimates of particulate organic carbon over the euphotic depth from in situ measurements application to satellite data over the Global Ocean *Deep Sea Research I*, **57** 351-367

Fletcher S E M, Gruber N, Jacobson A R, Doney S C, Dutkiewicz S, Gerbe M, Follows M, Joos F, Lindsay K, Menemenlis D, Mouchet A, Muller S A and Sarmiento J L (2006) Inverse estimates of anthropogenic CO2 uptake, transport, and storage by the ocean *Global Biogeochemical Cycles* **20** 2

Geider R J and Roche J La (1994) The role of iron in phytoplankton photosynthesis and the potential of iron limitation of primary productivity in the sea *Photosynth Res* **39** 275-301

Holliday N P and Read J F (1998) Surface oceanic fronts between Africa and Antarctica *Deep Sea Reearch I* **45** 217-238

Honjo S, Manganini SL, Krishfield R A and Francois R (2008) Particulate organic carbon fluxes to the ocean interior and factors controlling the biological pump: A synthesis of global sediment trap programs since 1983 *Progress in Oceanography* **76** 217-285

Hutchins D A (1995) Iron and the marine phytoplankton community *Prog Phycol Res* **11** 1-49

Jasmine P, Muraleedharan K R, Madhu N V, Asha Devi C R, Alagarsamy R, Achuthankutty C T, Jayan Z, Sanjeevan V N and Sahayak S (2009) Hydrographic and production characteristics along 45°E longitude in the southwestern Indian Ocean and Southern Ocean during austral summer 2004 *Marine Ecology Progress Series* **389** 97-116

Longinelli A, Giglio F, Langone L, Moggio L, Ori C, Selmo E and Sgavetti M (2012) Atmospheric CO_2 concentrations and delta C-13 values between New Zealand and Antarctica, 1998 to 2010: Some puzzling results *Tellus Ser B-Chem Phys Meteorol* **64** (December)

Louanchi F, Metzl N and Poisson A (1996) A modeling the monthly sea surface fCO_2 fields in the Indian Ocean *Marine Chemistry* **55** 265-280

Lourey M J, Trull T W and Sigman D M (2003) Sensitivity of ä^{15}N of nitrate, surface suspended and deep sinking particulate nitrogen to seasonal nitrate depletion in the Southern Ocean *Global Biogeochemical Cycle* **17** 1081.http://dx.doi.org/10.1029/2002GB001973

Lourey M J, Trull T W and Tilbrook B (2004) Sensitivity of ä^{13}C of Southern Ocean suspended and sinking organic matter to temperature, nutrient utilization, and atmospheric CO_2 *Deep Sea Research I* **51** 281-305

Martin P, Loeff M R, Cassar N, Vandromme P, d'Ovidio F, Stemmann L, Rengarajan R, SoaresM, González H E and Ebersbach F (2013) Iron fertilization enhanced net community production but not downward particle flux during the Southern Ocean iron fertilization experiment LOHAFEX *Global biogeochemical cycles* **27** 871-881

Metzl N (2009) Decadal increase of oceanic carbon dioxide in Southern Indian Ocean surface waters (1991–2007) *Deep Sea Research II* **56** 607-619

Metzl N, Beauverger C, Brunet C, Goyet C and Poisson A (1991) Surface water pCO_2 in the Western Indian sector of the Southern Ocean: a highly variable CO_2 source/sink region during the austral summer *Marine Chemistry* **35** 85-95

Mohan R, Shetye S S, Tiwari M and Anilkumar N (2015) Secondary calcification of planktonic Foraminifera from the Indian sector of Southern Ocean *Acta Geologica Sinica* **89** 27-37

Nayak G N and Noronha C (2011) Suspended particulate matter in the Southern Ocean:An approach to understand source and processes *Southern Ocean expedition, Technical report 2011* pp. 41-45

Prakash S, Ramesh R, SheshshayeeM S, Mohan R and Sudhakar M (2010) Effect of high level iron enrichment on potential nitrogen uptake by marine plankton in the Southern Ocean *Current Science* **99** 1400-1404

Prasanna K, Prosenjit Ghosh, Bhattacharya S K, Mohan K and Anilkumar N (2016) Isotopic disequilibrium in *Globigerina bulloides* and carbon isotope response to productivity increase in Southern Ocean *Scientific Reports* **6** 21533 doi 10.1038/srep21533

Prasanna K, Prosenjit G and Anil Kumar N (2015) Stable isotopic signature of Southern Ocean deep water CO_2 ventilation *Deep Sea Research Part II* **118** 177-185

Rajakumar A, Alagarsamy R, Khare N, Saraswat R and Subramaniam M M (2008) Studies on the nutrient distribution in the Southern Ocean waters along the 45° E transect *Indian Journal of Marine Sciences* **37** 424-429

Saraswat R and Khare N (2010) Deciphering the modern calcification depth of *Globigerina bulloides* in the Southwestern Indian Ocean from its oxygen isotopic composition *Journal of Foraminiferal Research* **40** 220-230

Sarmiento J L, Gruber N, Brzezinski M A and Dunne J P (2004) High-latitude controls of thermocline nutrients and low latitude biological productivity *Nature* **427** 56-60

Shetye S S, Jena B and Mohan R (2016) Dynamics of sea-ice biogeochemistry in the coastal Antarctica during transition from summer to winter *Geoscience Frontiers* (In press)

Shetye S S, Mohan R, Patil S, Jena B, Chacko R, George J V, Noronha S, Singh N, Priya L and Sudhakar M (2015)

Oceanic pCO_2 in the Indian sector of the Southern Ocean during the austral summer–winter transition phase *Deep Sea Research Part II* **118** 250-260

Shetye S S, Mohan R, Jafar S A, Nair A, Patil S, Jawak S, Asthana R and Gazi S (2014) Diatom burst-driven silica depletion under the Antarctic sea ice: evidence from sponge spicules *Current Science* **107** 273-277

Shetye S S, Sudhakar M, Ramesh R, Mohan R, Patil S and Laskar A (2012) Sea surface pCO_2 in the Indian Sector of the Southern Ocean during Austral summer of 2009 *Advanced Geosciences* **28** 79-92

Soares M A, Bhaskar P V, Naik R K, Dessai D, George J, Tiwari M and Anilkumar N (2015) Latitudinal ä^{13}C and ä^{15}N variations in particulate organic matter (POM) in surface waters from the Indian ocean sector of Southern Ocean and the Tropical Indian Ocean in 2012 *Deep Sea Research Part II* **118** 186-196

Tiwari M, Nagoji SS, Divya David T, Anilkumar N and Rajan S (2015) Oxygen isotope distribution at shallow to intermediate depths across different fronts of the Southern Ocean: Signatures of a warm-core eddy *Deep Sea Research Part II* **118** 170-176

Tiwari M, Nagoji S S, Kartik T, Drishya G, Parvathy R K and Rajan S (2013) Oxygen isotope–salinity relationships of discrete oceanic regions from India to Antarctica *vis-a-vis* surface hydrological processes *Journal of Marine Systems* **113-114** 88-93

Tiwari M, Mohan R, Meloth T, Naik, S S and Sudhakar M (2011) Effect of varying frontal systems on stable oxygen and carbon isotopic compositions of modern planktic foraminifera of Southern Ocean *Current Science* **100** 881-886

Waugh D W (2014) Changes in the ventilation of the southern oceans *Philos Trans R Soc A —Math Phys Eng Sci* **372** 2019.